Characterisation of TPL-2 Signalling Pathways in Innate Immunity

Olivia Mitchell

August 2015

Ph. D. Thesis

The Francis Crick Institute

Mill Hill Laboratory

The Ridgeway

London

NW7 1AA

Division of Infection and Immunity

University College London

Funding

This work was funded by a studentship from the Medical Research Council.

Declaration

I, Olivia Mitchell, confirm that the work presented in this thesis is my own. Where information has been derived from other sources I confirm that this has been indicated in the thesis.

31/07/15

Acknowledgements

Firstly, thanks to my supervisor, Dr. Steve Ley for giving me the opportunity to undertake this PhD and for his ideas throughout the project. I would particularly like to thank Dr. Bram Snijders and Dr. Helen Flynn for their expertise, advice and commitment, which made this project possible. Dr. Ana Cuenda kindly provided the *Mapk12*$^{Y185F/Y185F}$/*Mapk13*$^{-/-}$ bone marrow and valuable advice on p38γ/δ immunoprecipitation.

I am grateful to all past and present members of the Ley laboratory who have given me so much advice, support and encouragement. In particular, Dr. Matoula Papoutsopoulou and Dr. Mike Pattison who generated the transcriptomics data, Ms. Julia Janzen who generated the triple complex interactome data, and Dr. Chao-Sheng Chen who provided the purified TPL-2/ABIN-2/NFκB1 p105 complexes. I also received incredible support and guidance from my thesis committee, Dr. Jyoti Choudhary, Dr. Victor Tybulewicz and Dr. Ben Seddon.

I was incredibly lucky to have Elizabeth, Ina, Victoria, Louise, Pippa, Charlie and Ashleigh to help me keep everything in perspective. I also have the best family and friends who were understanding of my absence on so many occasions and supported me the whole way through. My final special thanks is to Caroline, who is always there for me but who I blame for everything!

Abstract

The MAP 3-kinase TPL-2 is required for activation of ERK1/2 MAP kinases in macrophages after stimulation of Toll-like receptors and the receptors for TNF and IL-1β. TPL-2 drives inflammation in a number of autoimmune and inflammatory disease models, and consequently is considered a potential anti-inflammatory drug target. Recent evidence from the Ley laboratory has indicated that TPL-2 regulates the production of the critical pro-inflammatory cytokine TNFα in an ERK1/2-independent manner. The aim of this study was to use mass spectrometry-based phosphoproteomics to investigate the signalling pathways regulated by TPL-2 in an unbiased manner to more fully understand how TPL-2 regulates innate immunity. A method for SILAC labelling of bone marrow-derived macrophages was developed and used to quantify phosphorylation changes after genetic and pharmacological perturbation of TPL-2 signalling. Across 11 pair-wise comparisons, 31,457 unique phosphosites were identified, from which a shortlist of 37 potentially TPL-2-dependent, ERK1/2-independent phosphorylations was generated. The biological consequences of the majority of these TPL-2 regulated sites remain to be determined, although bioinformatic analysis suggest that they may have roles in regulation of gene expression and the cytoskeleton. The activating residues of the MAP 2-kinases, MKK3 and MKK6 were validated as novel TPL-2 targets in LPS-stimulated macrophages and MKK6 was shown to be a direct substrate by *in vitro* kinase assays using recombinant proteins. It was also demonstrated that TPL-2 controlled the phosphorylation of the activation loop of the MAP kinase p38γ, which is a direct target of MKK3/6. These data identified a novel signalling pathway downstream of TPL-2, increasing our understanding of how TPL-2 controls inflammatory responses.

Contents

List of Figures

List of Tables

Abbreviations

ABIN-2	A20-binding inhibitor of NFκB
BMDM	Bone marrow-derived macrophages
DTT	Dithiothreitol
ERK1/2	Extracellular regulated kinase 1/2
FCS	Foetal calf serum
IKK	Inhibitor of NFκB kinase
K0R0	”Light” labelled arginine and lysine
K8R10	”Heavy” labelled arginine and lysine
LCCM	L929 cell conditioned medium
LC-MS/MS	Liquid chromatography-tandem mass spectrometry
LPS	Lipopolysaccharide
LRR	Leucine rich repeats
MAP kinase	Mitogen activated protein kinase
MEK1/2	MAPK and ERK kinase 1/2
MKK3/4/6	Mitogen activated protein kinase kinase 3/4/6
MyD88	Myeloid differentiation primary response gene 88
NFκB	Nuclear factor kappa-light-chain-enhancer of activated B cells
PBS	Phosphate buffered saline
SDS-PAGE	Sodium dodecyl sulphate-polyacrylamide gel electrophoresis
Ser (S)	Serine
SILAC	Stable isotope labelling with amino acids in cell culture
Thr (T)	Threonine
TIR	Toll-IL1R domain
TLR	Toll-like receptor
TNFα	Tumour necrosis factor-α
TPL-2	Tumour progression locus-2 (also called COT or MAP3K8)
TRIF	TIR domain-containing adapter protein inducing interferon-β
Tyr (Y)	Tyrosine

1 General Introduction

1.1 The immune response

This project focused on signalling in macrophages in response to stimulation through innate immune receptors, and these will be introduced in the following sections.

1.1.1 Innate and adaptive immunity

An invading pathogen is initially recognised through the presence of pathogen-specific molecules as well as “danger” signals, mediators released by infected or damaged cells (Iwasaki and Medzhitov, 2015). These signals are detected by tissue-resident cells of the innate immune system, the first line of defence, which react quickly and in a non-pathogen specific manner. Following pathogen recognition, these innate immune cells, which include mast cells, macrophages and innate lymphoid cells, rapidly transcribe genes, the products of which trigger an inflammatory response (Murphy et al., 2008). The responding cells also produce inflammatory factors, such as prostaglandins and histamine, which act on nearby capillaries to weaken endothelial cell contacts and induce integrin expression. This promotes fluid entry to the tissue and allows immune cells from the blood to extravasate and enter the tissue. The tissue resident innate cells release chemokines, short peptides which attract other cell types to the site. The first cell type to enter the tissue from the blood are neutrophils, innate immune cells which can kill a range of pathogens by phagocytosis, production of antimicrobial peptides/reactive oxygen species and release of neutrophil extracellular traps (Kolaczkowska and Kubes, 2013). In most cases, the neutrophil response is sufficient to eliminate the pathogen and the influx of macrophages that follows removes any debris and promotes healing of the tissue (Gilroy and De Maeyer, 2015).

In infections where the innate response is not able to clear the pathogen, a more specific adaptive immune response is induced. For this to happen, the invading pathogen must be ingested at the site of infection by professional antigen presenting cells (APCs) called dendritic cells, which degrade pathogen proteins

into short peptides (Murphy et al., 2008; Roche and Furuta, 2015). These cells then traffic to a secondary lymphoid organ, such as the lymph nodes, where they present pathogen-derived peptide antigens on their surface in association with major histocompatibility complexes (MHCs) for T cells to recognise via their antigen receptors. When a T cell encounters an APC presenting an antigen-MHC complex to which its TCR is specific, the APC provides three signals to the T cell, which help determine the subsequent fate of that T cell (Murphy et al., 2008). These are signalling through the engaged TCR itself, co-stimulation through CD80/CD86 on the APC binding to T cell CD28, and cytokines that drive the CD4+ T cell lineage decision. IFNγ and IL-12 will cause CD4+ T cells to become T helper type 1 (Th1) cells, IL-4 induces T helper type 2 (Th2) cells, IL-1β and IL-6 together with TGF-β induce differentiation into T helper type 17 (Th17) cells and TGF-β leads to differentiation of inducible regulatory T cells (iTreg) (Locksley, 2009). The T cells return to the site of infection where each T helper cell subset has a specific set of functions associated with clearance of different types of pathogen.

Like T cells, B cells are adaptive cells with hyper-variable antigen receptors. Once B cells encounter their specific antigen in peripheral lymphoid organs, they undergo a process of rapid expansion during which the affinity of the BCR for antigen is improved stochastically to create a BCR with a higher affinity for the same antigen (Wabl and Steinberg, 1996). In addition to this, antigen-stimulated B cells also rearrange their BCR constant region locus in response to T cell help through ligation of CD40 and cytokines. The use of different immunoglobulin heavy chain genes leads to production of antibodies of alternate isotypes that confer different properties. (Murphy et al., 2008). B cells then become plasma cells and produce large amount of soluble antibody which optimises pathogen killing, for example through phagocytosis by macrophages.

The immune response can become deregulated at many of these stages. Over-production of cytokines, particularly TNFα, can trigger cytokine storm as in septic shock (Apostolaki et al., 2010). In an allergic reaction, the immune sys-

tem responds aggressively to innocuous antigens. This is associated with over-activation of Th2 responses, high levels of IgE antibodies and excessive release of histamine (Licona-Limón et al., 2013). In recent years, immune responses have also been linked to seemingly unrelated diseases such as cancer. In order for a tumour to grow it must evade detection by the immune system and, to this end, some tumours induce an anti-inflammatory microenvironment around them. Furthermore, excessive inflammation over a pro-longed period can induce cancer (Wagner and Nebreda, 2009). For example, the chronic liver inflammation caused by hepatitis infection can contribute to the development of hepatocellular carcinoma by increasing levels of mutagenic free radicals in the liver, amongst other things (Aravalli, 2013). Thus whilst the immune system performs an essential role in protection from infectious diseases, if it is not tightly controlled it can cause pathology.

1.1.2 Macrophages

Macrophages are innate immune cells which specialise in sensing microorganisms and tissue damage through a wide range of receptors. Their main effector functions are to phagocytose and degrade pathogens and other particles, and to produce cytokines like TNFα to promote appropriate immune responses (Epelman et al., 2014).

Development

Macrophages are found in all tissues but vary widely in their origin, phenotype and function (Pollard, 2009). Certain macrophage populations, such as central nervous system microglia, develop from the foetal yolk sac prior to birth (Schulz et al., 2012). These populations are not commonly replenished from the periphery, but instead are largely self-renewing. Specialised tissue macrophages display many diverse phenotypes and take on particular characteristics depending on the tissue environment in which they reside. For example, liver resident macrophages, known as Kupffer cells, are highly specialised in lipid metabolism and

clearance of noxious substances (Wynn et al., 2013).

During subsequent *in utero* development, definitive haematopoiesis, which produces circulating monocytes, begins in the foetal liver (Wynn et al., 2013). After birth, foetal liver haematopoiesis declines and haematopoiesis in the bone marrow takes over generation of leukocytes. Common haematopoietic stem cells develop through myeloid committed and monocyte committed stages, and then become monoblasts under the control of monocyte colony-stimulating factor (Mosser and Edwards, 2008). Monoblasts differentiate into pro-monocytes and finally monocytes, which are released into the blood. This population replenishes certain tissue resident macrophages such as those in the skin, which are derived from both yolk sac and haematopoietic precursors (Epelman et al., 2014). In an inflammatory setting, monocytes are recruited to tissues from the blood by appropriate cytokine cues, where they differentiate into macrophages.

Function

Monocyte-derived macrophages have been sub-classified based on their functional status as classically activated, regulatory or wound-healing (figure 1.1; Mosser and Edwards, 2008). However, macrophages show a large degree of plasticity and individual cells can move between the different phenotypic classifications depending on the local tissue microenvironment. Classically activated macrophages are induced by IFN-γ and TNFα. This phenotype is associated with microbicidal functions and production of pro-inflammatory mediators. Regulatory macrophages, on the other hand, are anti-inflammatory and function to regulate the immune response through production of large amounts of IL-10. They are induced by IL-10 plus a second trigger from a diverse range of stimuli, including apoptotic cells and glucocorticoids, which may all induce slightly different subpopulations (Mosser and Edwards, 2008). Regulatory macrophages are competent in phagocytosis but may be defective in presenting antigen to T cells or specifically induce Treg or Th2 differentiation. Due to these functions, some pathogens induce regulatory macrophages to enable them to evade the immune system.

Macrophages with an alternative wound-healing phenotype are induced by the presence of IL-4 and IL-13. These macrophages are involved in tissue repair and express factors that promote remodelling of the extracellular matrix such as arginase and chitinase. In certain circumstances, such as airway remodelling in asthma, wound-healing macrophages can contribute to tissue fibrosis and disease progression (Murray and Wynn, 2011).

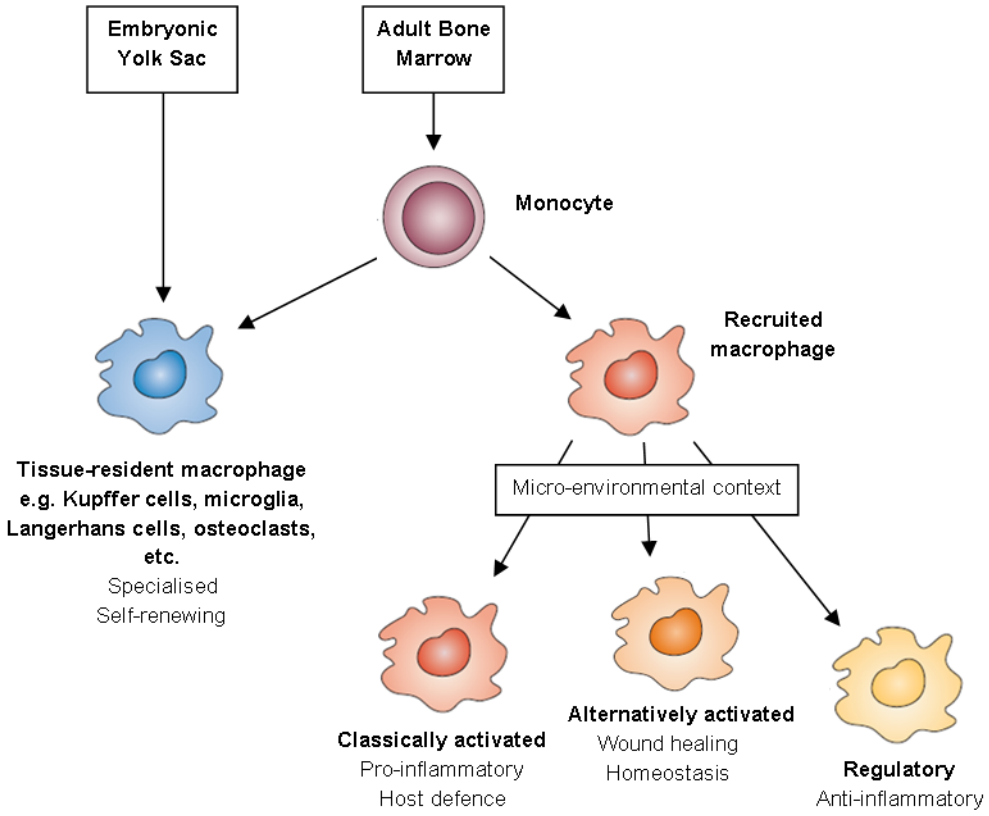

Figure 1.1: **Macrophage Heterogeneity.**
Macrophages fall broadly into either tissue resident or recruited inflammatory categories. The tissue resident macrophages can be derived either from the embryonic yolk sac or from circulating monocytes. Once in a tissue they take on highly specialised functions associated with the character of the tissue such as the bone remodelling processes of osteoclasts. Tissue resident macrophage populations are self-renewing to a greater or lesser extent. On the other hand circulating monocytes are recruited to sites of injury or infection. Depending on the signals available in the microenvironment, these macrophages can take on characteristics from one of three extremes; classically activated, alternatively activated or regulatory. The classically activated macrophages show more pro-inflammatory functions and are associated with host defence, the alternatively activated macrophages display functions which aid the wound healing process and the regulatory macrophages dampen the local immune response and protect against immunopathology.

Studies of *ex vivo* macrophage populations have supported this spectrum of activation states at the transcriptional level (Xue et al., 2014). However, this extensive heterogeneity also complicates such studies, as subpopulations may respond differently to a stimulus, leading to no clear overall phenotype for the population (Ostuni and Natoli, 2011). For this reason, macrophages derived *in vitro* from bone marrow stem cells (bone marrow-derived macrophages, BMDM) are commonly used in model studies and have the advantage of a homogeneous population that is likely to show less variability (Weischenfeldt and Porse, 2008). Recent studies using BMDMs have employed multiple "omics" approaches (e.g. transcriptomics and phosphoproteomics) and bioinformatics to investigate the biochemistry and molecular biology of macrophage responses on a systems level (Weintz et al., 2010; Dinasarapu et al., 2013).

1.1.3 Tumour necrosis factor-α

Biological functions and relevance in disease

TNFα is a key pro-inflammatory cytokine in the early immune response produced by immune cells, particularly macrophages, but also by tissue cells like keratinocytes (Papadakis and Targan, 2000). In an inflammatory setting, its release is triggered by pathogen-derived molecules and endogenous stress signals. TNFα has paracrine and autocrine actions and both the cell surface-bound and soluble forms of TNFα are biologically active.

There are two receptors for TNFα, TNFR1 and TNFR2, at least one of which is expressed on all nucleated cells, although TNFR2 is mostly limited to haematopoietic cells (Wajant et al., 2003). A further layer of complexity is added to TNFα signalling through cleavage of both receptors into soluble forms, which antagonise TNFα signalling by competing with cell surface receptors for ligand binding (Apostolaki et al., 2010). TNFR1 can be ligated by either soluble or membrane-bound TNFα. TNFR2, on the other hand, is activated more efficiently by surface-bound than soluble TNFα (Grell et al., 1995). TNFα binding to either receptor can

trigger primarily (but not exclusively) pro-inflammatory responses, inducing expression of other immune mediators, including cytokines and chemokines, as well as adhesion molecules and pro-apoptotic effectors (Bluml et al., 2012). However, these receptors have different biological functions, due to differences in their intracellular domains (MacEwan, 2002). For example, deletion of TNFR1 attenuates the inflammatory response in a model of polymicrobial septic shock, whilst TNFR2 deletion exaggerates the symptoms (Ebach et al., 2005). Therefore, TNFR1 is predominantly thought of as pro-inflammatory and TNFR2 as anti-inflammatory, although this distinction is far from absolute. As well as functions in inflammation, TNFα signalling through TNFR1 has homeostatic functions in formation of secondary lymphoid organs (Ruuls et al., 2001; Bluml et al., 2012).

TNFα is a central mediator of multiple immune disorders, including inflammatory bowel disease (IBD), rheumatoid arthritis (RA) and psoriatic arthritis (Sfikakis, 2010). Genetic over-expression of TNFα in mice leads to spontaneous development of symptoms similar to rheumatoid arthritis including joint inflammation and bone destruction (Alexopoulou et al., 1997). Rheumatoid arthritis models in rodents suggest disease development and progression can be mediated by membrane bound and soluble forms of TNFα (Palladino et al., 2003). However, in an endotoxic shock model, mice which express only the cell surface form of TNFα are resistant to immunopathology, suggesting there are functional differences between the two forms (Nowak et al., 2000).

Therapeutically targeting TNFα

In light of the role of TNFα in immunopathology, anti-TNFα biologics have become the gold standard for treatment of patients whose disease is refractory to first line therapy using disease-modifying anti-rheumatic drugs. These treatments, which include etanercept (soluble TNFR2), infliximab and adalimumab (anti-TNFα antibodies), prevent TNFα from interacting with its receptors and, in the case of the antibodies, by inducing complement-dependent and antibody-dependent cytotoxicity of cells expressing transmembrane TNFα (Sfikakis, 2010). They are effective in about 60 % of patients who did not benefit from non-biologic drugs.

However, although treatment with TNFα-blocking biologics revolutionised therapy for autoimmune diseases, less than half of those who respond achieve complete remission, so there remains a need for alternative treatments. Biologics also suffer from several important drawbacks, since they cannot be administered orally and must be injected at regular intervals. There is also strict regulation around the production of antibodies due to their batch-to-batch variation, making them expensive. For this reason, it would be advantageous if a small molecule inhibitor could be developed to target the production of TNFα, making treatment cheaper and more convenient (Palladino et al., 2003).

Synthesis and release

Deregulated TNFα expression can have many detrimental effects including septic shock following systemic bacterial infection and joint inflammation in rheumatoid arthritis. Therefore, its production is tightly controlled at every stage of its production through a range of different mechanisms (figure 1.2).

Protein expression

TNFα gene transcription is minimal in unstimulated macrophages, but is significantly enhanced by stress stimuli, such as the bacterial cell wall component lipopolysaccharide (LPS) that increases TNFα transcription 3-fold (Papadakis and Targan, 2000; Murray and Stow, 2014). The same stimulus, however, increases levels of TNFα messenger RNA (mRNA) by 50 - 100-fold indicating that further regulation is occurring at the post-transcriptional level. Indeed, the TNFα transcript is subjected to controls which alter its stability, and its half life in human monocytes is as low as 12 minutes (Papadakis and Targan, 2000). A sequence known as the AU-rich element (ARE) is present in the 3'-untranslated region of the mature TNFα mRNA. This sequence can be bound by proteins which regulate mRNA stability and inhibit translation, such as tristetraproline (TTP) (Arthur and Ley, 2013). Upon TTP binding to the TNFα message the mRNA gets targeted for degradation by RNases. TTP is phosphorylated by signalling through the p38 MAP kinase pathway, decreasing its affinity for the ARE motif and allowing HUR

to bind instead; HUR then initiates the translation of TNF mRNA. Mice in which the TNFα ARE sequence has been deleted display elevated levels of TNFα production and develop spontaneous inflammatory conditions in their joints and bowel (Kontoyiannis et al., 1999).

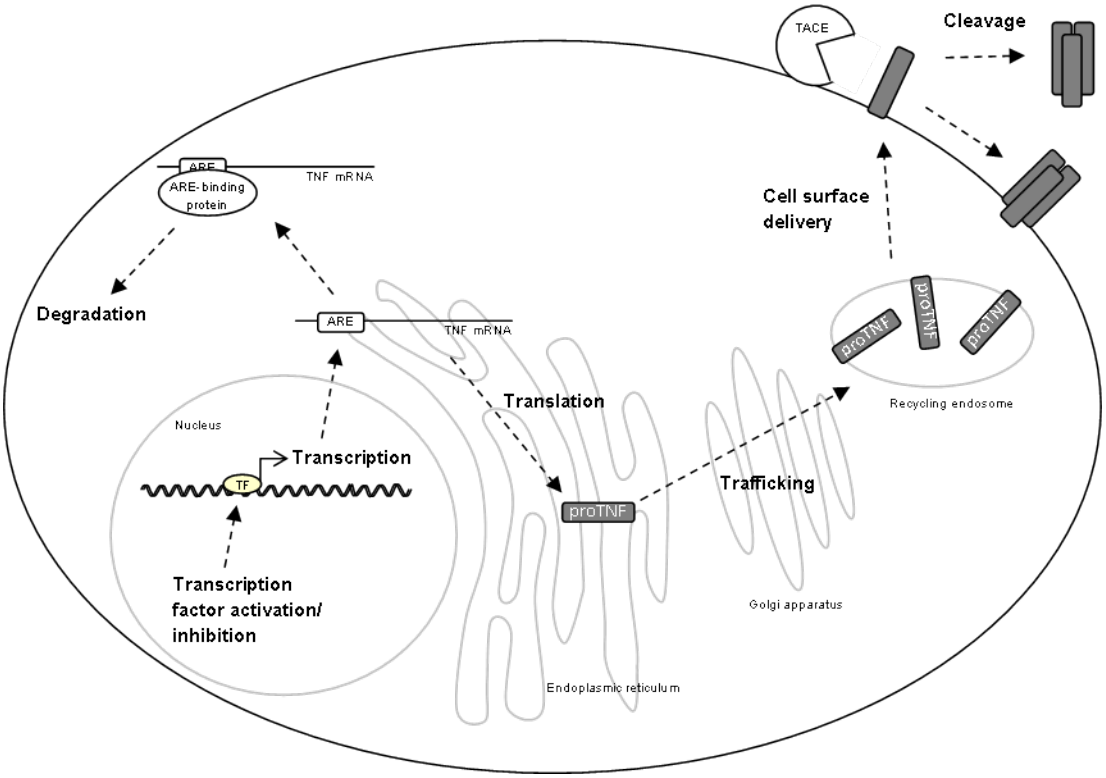

Figure 1.2: **Production, processing and secretion of TNFα**
TNFα production is regulated at multiple levels to ensure tight control of its levels. TNFα mRNA is unstable due to recognition by proteins which promote its degradation in the absence of activating signals. Once TNFα is translated to its pre-protein form, it is trafficked through the cell towards recycling endosomes, during which time its production can be regulated at many points. TNFα is finally brought to the cell surface, where eventual release of soluble TNFα is dependent on the presence of the metalloprotease TACE, whose levels of the surface of the cell can also be altered to tune soluble TNFα levels.

Trafficking

TNFα is translated as a 26 kDa, transmembrane precursor. This pro-TNFα protein is trafficked through the endoplasmic reticulum and Golgi network, where it is packaged into vesicles along with the Q-SNARE components Stx6, Stx7 and Vti1b (Murray and Stow, 2014). Vesicle exit from the Golgi is regulated by PI3Kδ and dynamin II, as well as changes in the lipid composition of the membrane

mediated by CCTα (Tian et al., 2008). After leaving the Golgi, the vesicles fuse with recycling endosomes through Q-SNARE pairing with VAMP3, the R-SNARE on the recycling endosome. TNFα reaches the plasma membrane by fusion of recycling endosomes at specific sites, determined by the location of cell surface Stx4/SNAP23 Q-SNARE complexes in cholesterol-rich lipid rafts (Kay et al., 2006). The proteins mentioned here as regulators of TNFα trafficking are all up-regulated in response to LPS stimulation to enhance TNFα production (Murray and Stow, 2014). Other proteins which have been shown to be involved in TNFα trafficking to the cell surface include the small GTPases, Rac1, Cdc42, Rab11 and Rab37. In the absence of Rac1, pro-TNFα remains sequestered in recycling endosomes rather than being delivered to the cell surface (Stanley et al., 2014).

Release

The final stage of TNFα maturation is cleavage of a 17 kDa portion from the cell surface by the metalloprotease, TNFα-converting enzyme (TACE/ADAM17) (Black et al., 1997; Moss et al., 1997). Production of soluble TNFα in response to LPS was strongly reduced in TACE-deficient macrophages compared to TACE-sufficient cells (Horiuchi et al., 2007). In order for cleavage to happen, TNFα and TACE must come into close proximity, a process which has been proposed to be regulated by partitioning into cholesterol-rich lipid rafts (Kay et al., 2006; Levine, 2008). Cholesterol depletion, which disrupts lipid rafts, leads to increased shedding of TACE substrates, implying an import role of lipid rafts in regulating TACE interaction with its substrates (Tellier et al., 2006).

TACE is itself expressed as an inactive form and requires proteolytic processing to become active (Levine, 2008). Its level on the cell surface is also augmented in response to LPS stimulation, mediated partly through ERK1/2 phosphorylation of threonine 735, which promotes TACE translocation to the plasma membrane (Soond et al., 2005; Murray and Stow, 2014). TACE activity on the cell surface is regulated by the metalloprotease inhibitor TIMP3, and, in the absence of TIMP3, levels of soluble TNFα are constitutively increased (Levine, 2008). Numerous other proteins interact with the cytoplasmic tail of TACE, including SAP97

and Eve-1, and may regulate its protease activity.

Both the membrane bound and cleaved forms of TNFα then aggregate into trimers in which conformation they can ligate their receptors (Palladino et al., 2003). The final outcome of all these levels of regulation is an increase in protein secretion of approximately 10,000-fold from macrophages in response to ligation of pattern recognition receptors (Papadakis and Targan, 2000).

1.1.4 Pattern recognition receptors

Pattern recognition receptors (PRRs) are innate immune receptors used to recognise pathogen-associated molecular patterns (PAMPs), highly conserved features of micro-organisms like components of the bacterial cell wall or the viral genome (Takeuchi and Akira, 2010). They also recognise host-derived molecules, such as heat shock proteins and crystalline uric acid, called damage-associated molecular patterns (DAMPs), which indicate injury or infection. PRRs are germline encoded and all cells express at least some of these to detect cell-intrinsic infection (Iwasaki and Medzhitov, 2015). Immune cells like macrophages and dendritic cells also detect cell-extrinsic infections and receive their initial activation stimulus through PRRs. Activation of these receptors leads to expression of genes which promote an immune response, such as cytokines like TNFα, or trigger effector mechanisms that directly target the micro-organism, like inducible nitric oxide synthase which produces nitrous oxide (Arthur and Ley, 2013).

PRRs include membrane bound Toll-like receptors (TLRs) and C-type lectin receptors (CLRs), cytosolic NOD-like receptors (NLRs) and RIG-I-like receptors, and miscellaneous others including DAI and cGAS (Unterholzner, 2013). TLRs recognise a diverse range of ligands like lipids and nucleic acids. CLRs, which contain a carbohydrate-binding domain, include Dectin-1. They recognise carbohydrates, such as fungal-derived β-glucan, and induce transcription of proinflammatory cytokines (Takeuchi and Akira, 2010). NLRs, such as NALP1, have a central nucleotide binding/oligomerisation domain and C-terminal leucine-rich repeats (LRRs) through which they respond to bacterial peptidoglycans, like

muramyl dipeptide. Upon ligand binding, NLRs oligomerize and induce release of pro-inflammatory cytokines through several mechanisms, including activation of caspase-1, which cleaves inactive pro-IL-1β into active IL-1β (Meylan et al., 2006). RLRs, such as MDA5, have a central helicase/ATPase domain, a regulatory C-terminus and two N-terminal CARD domains through which they interact with their downstream adaptor, MAVS. They recognise viral double stranded RNA and induce type I interferons through NFκB and IRF3 and IRF7.

Thus many cells will have both extracellular and intracellular sensors for the same common pathogen features, allowing the immune system to determine the location of the micro-organism. For example, LPS is recognised by TLR4 on the cell surface and by the caspase 4 (murine caspase 11) inflammasome in the cytosol (Shi et al., 2014). The micro-environment induced by PRR signalling provides context to antigen-recognition by adaptive immune cells, as well as information on micro-organism viability and pathogenicity, leading to an appropriate immune response (Iwasaki and Medzhitov, 2015).

This study focused on signalling pathways initiated via TLRs, particularly TLR4, which will be described in detail in the next section.

Toll-like receptor signalling

The TLRs are the most intensively studied of the PRRs (table 1.1). There are 10 in human and 12 in mice, present either on the surface of the cell or inside endosomes (Takeuchi and Akira, 2010). They play vital roles in immune responses and immunopathology in instances where the innate immune system is over-activated. For example, TLR4 is essential for protection in *Salmonella* Typhimurium infection (Talbot et al., 2009) but also for LPS-induced endotoxic shock. Wild type mice injected with LPS succumb to endotoxic shock in 18 - 48 hours whereas in the absence of TLR4, LPS injection is not lethal in the absence of priming stimuli (Hagar et al., 2013).

Table 1.1: **Toll-like receptors and their ligands.**

Receptor	Subcellular location	Physiological ligands	Species
TLR1/2	Cell surface	Triacylated lipopeptides	Mouse/human
TLR2	Cell surface	Peptidoglycan, phospholipomannan, tGPI-mucins, haemagglutinin, porins, lipoarabinomannan, glucuronoxylomannan, HMGB1	Mouse/human
TLR2/6	Cell surface	Diacylated lipopeptides, lipoteichoic acid, zymosan	Mouse/human
TLR3	Endosome	Double stranded RNA	Mouse/human
TLR4	Cell surface	LPS, VSV glycoprotein G, RSV fusion protein, MMTV envelope protein, mannan, glucuronoxylomannan, glycosylinositolphospholipids, HSP60, HSP70, fibrinogen, nickel, HMGB1	Mouse/human
TLR4/6	Cell surface	Oxidised low density lipoprotein, amyloid-β fibrils	Mouse/human
TLR5	Cell surface	Flagellin	Mouse/human
TLR6	Cell surface	Diacyl lipoprotein	Mouse/human
TLR7	Cell surface	Single stranded RNA	Mouse/human
TLR8	Endosome	Single stranded RNA	Mouse/human
TLR9	Endosome	DNA, haemozoin	Mouse/human
TLR10	Endosome	Unknown	Human
TLR11	Cell surface	Profilin	Mouse
TLR12	Unknown	Profilin	Mouse
TLR13	Endosome	Bacterial ribosomal RNA	Mouse

HMGB1 = high-mobility group box 1 protein; VSV, vesicular stomatitis virus; RSV = respiratory syncytial virus; MMTV, mouse mammary tumour virus; HSP = heat-shock protein; tGPI-mucin = *Trypanosoma cruzi* glycosylphosphatidylinositol-anchored mucin-like glycoprotein. [Table adapted from Takeuchi and Akira (2010) and Kawai and Akira (2010)]

TLRs are type I transmembrane proteins. The extracellular portion has a number of LRRs through which they engage their ligands (Takeuchi and Akira, 2010). Their intracellular portion contains a Toll-IL-1 receptor (TIR) domain, which is necessary for transducing downstream signals. All TLRs signal via one of two adaptor proteins upon ligand binding; most use MyD88 (myeloid differentiation primary response gene 88) except for TLR3 which uses TRIF (TIR domain-

containing adapter protein inducing IFN-β, or TICAM-1). TLR4 is exceptional in that it can transduce signals via both of the adaptors, MyD88 and TRIF.

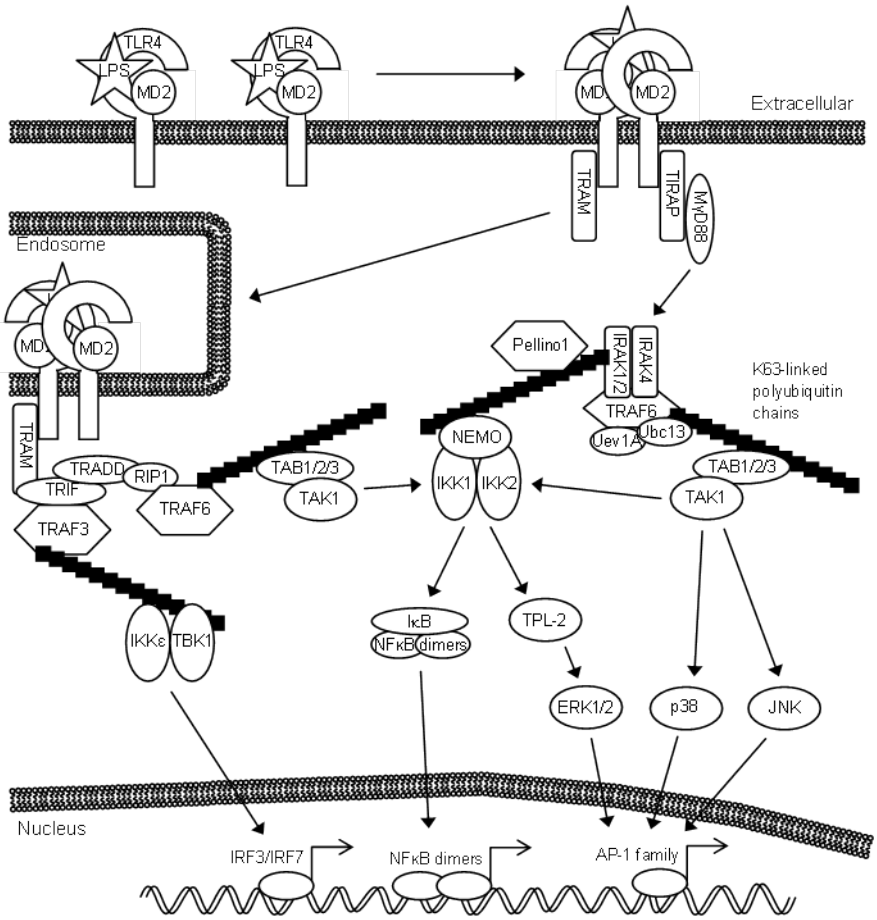

Figure 1.3: **Signalling pathways activated following TLR4 ligation with LPS.** Extracellular LPS is sensed by TLR4 on the cell surface leading to formation of TLR4 dimers. These dimers transduce signals into the cell through two pathways, MyD88 and TRIF. Signalling through the MyD88 adaptor leads to activation of the canonical IKK complex and MAP kinase pathways. TRIF mediated signalling leads to activation of the non-canonical IKKs, IKKε and TBK1. Through these three pathways TLR4 ligation leads to activation of three groups of transcription factors, NFκB, AP-1 and IRF3.

TLR4 on the cell surface is bound to the co-receptor, MD2, and as a complex they function as the main LPS-binding receptor (Kawai and Akira, 2010). *In vivo* the plasma protein, LPS-binding protein (LBP), is also important for capturing LPS in the blood. LBP bound to LPS is delivered to the TLR4-MD2 complex by a LRR-containing, glycosylphosphatidylinositol-linked co-receptor called CD14. LPS binding induces dimerisation of two TLR4-MD2-LPS complexes (figure 1.3; Takeuchi and Akira, 2010).

MyD88 activated pathways

TLR4 is somewhat unusual in that it uses another adaptor, TIRAP, to recruit MyD88 and trigger intracellular signalling. MyD88 interacts with the serine/threonine kinase IRAK4, that then activates IRAKs 1 and 2 (Wesche et al., 1997; Kawagoe et al., 2008). At this stage, the IRAKs dissociate from MyD88 and subsequently interact with TRAF6. TRAF6 is an E3 ubiquitin ligase, which, together with the E2 ubiquitin-conjugating complex of Uev1A and Ubc13, synthesises K63-linked polyubiquitin chains anchored on TRAF6 (Lamothe et al., 2006). The poly-ubiquitin chains enable TAB1, TAB2 and TAB3 to recruit the kinase TAK1, which becomes active, phosphorylates MAP 2-kinases and initiates MAP kinase cascades (Wang et al., 2001). IRAK1 also phosphorylates another E3 ligase, Pellino1, which catalyses formation of K63-linked polyubiquitin chains on IRAK1 (Goh et al., 2012). NEMO, the regulatory subunit of the canonical IKK complex, is also brought into close proximity with TAK1 by binding to these ubiquitin chains (Conze et al., 2008). This enables TAK1 to phosphorylate IKK2, which then phosphorylates IκB proteins, inducing their proteolysis by the proteasome. This releases NFκB transcription factors to translocate to the nucleus, as well as activating the kinase TPL-2 and subsequently the ERK1/2 MAP kinase pathway (see below).

TRIF activated pathways

After ligand binding, TLR4 becomes internalised to endosomes, and it is from this location that the TRIF pathway is activated (Kawai and Akira, 2010). Unlike TLR3, TLR4 requires the adaptor TRAM to interact with TRIF (Yamamoto et al., 2002). TRIF recruits TRAF3, which undergoes auto-ubiquitination and activates the non-canonical inhibitor of NFκB kinases (IKKs), IKKε and TBK1 (Häcker et al., 2006; Oganesyan et al., 2006). IKKε and TBK1 phosphorylate IRF3 and IRF7 leading to induction of type I interferons. TRIF also uses another adaptor, TRADD, to recruit RIP1 and TRAF6 (Cusson-Hermance, 2005; Ermolaeva et al., 2008; Pobezinskaya et al., 2008). TRAF6 catalyses synthesis of polyubiquitin chains which bring TAB1/2/3 and TAK1 together, enabling activation of the canon-

ical IKK complex of NEMO, IKK1 and IKK2. Activation of IKK1 and IKK2 leads to a second wave of activation of NFκB transcription factors and the ERK1/2 MAP kinase pathway.

The major downstream outputs of TLR4 signalling pathways are activation of NFκB and IRF transcription factors and MAP kinase pathways (discussed in detail below).

1.2 Mitogen-activated protein kinase pathways

Mitogen-activated protein (MAP) kinases are protein kinases. These are enzymes that catalyse the addition of a phosphate group on serine, threonine or tyrosine residues. This modification can lead to functional changes in the ability of the target to interact with other proteins or catalyse other reactions, amongst other things. Protein kinases have a highly conserved active site (Cohen, 2002). Key residues within the active site, such as the DFG (aspartate-phenylalanine-glycine) motif, bind ATP, the phosphate donor, in complex with a metal ion cofactor, commonly Mg^{2+}. Such residues orientate the ATP-metal ion complex towards the substrate to allow the phosphate transfer (Adams, 2001).

The MAP kinase subgroup of protein kinases are activated when macrophages sense changes in the extracellular environment, such as pathogen infection, cytokine stimulation and osmotic stress, and initiate cellular programmes that enable the cell to respond in an appropriate manner (e.g. through proliferation or growth). MAP kinase signalling pathways consist of conserved three-tiered kinase cascades. At the top of these cascades, a serine/threonine MAP 3-kinase phosphorylates the activation loop of the downstream dual-specificity protein kinase (MAP 2-kinase). The activated MAP 2-kinase, in turn, phosphorylates the threonine-X-tyrosine (T-X-Y, where X is any amino acid) motif in the activation loop of a MAP kinase, which then phosphorylates a number of target proteins (figure 1.4). Recognition of a specific MAP kinase by MAP 2-kinases, mediated via MAP kinase-docking domains, ensures specificity of signal transmission via a particular MAP kinase pathway (Arthur and Ley, 2013). Specificity, amplitude

and duration of MAP kinase cascade interactions is also regulated through scaffold proteins (e.g. JNK-interacting protein 1, JIP1) that link the different members of the cascade into complexes (Langeberg and Scott, 2015).

MAP kinases are proline directed kinases, preferentially phosphorylating serine/threonine residues to the N-terminal side of a proline residue. Many MAP kinase substrates also contain D-domains and DEF-domains, which allow them to be recognised by the MAP kinase (Roux and Blenis, 2004). Activated MAP kinases ultimately phosphorylate a range of effectors directly. These include cytoskeletal proteins and transcription factors, particularly NFκB and AP-1 transcription factors (e.g. c-Fos, c-Jun, ATF) through which they induce the transcription of "immediate-early" genes, the products of which trigger a programme of cellular changes in response to stimulation (O'Donnell et al., 2012). Many of the effects of MAP kinases are mediated by phosphorylation of downstream MAP kinase-activated protein kinases (MAPKAPKs). These include RSKs (1, 2, 3 and 4), MKs (2, 3 and 5), MSKs (1 and 2) and MNKs (1 and 2) which can be activated by ERK1/2 and/or p38 MAP kinases (Roux and Blenis, 2004). Through the phosphorylation of these substrates, MAP kinases regulate multiple cellular processes involved in innate immunity including phagocytosis, cell migration and production of cytokines.

Termination of MAP kinase signalling is largely controlled by dual-specificity phosphatases (DUSPs, also known as MAP kinase phosphatases). These enzymes can dephosphorylate both the threonine and tyrosine residues of the MAP kinase activation loop and inactivate them (Caunt and Keyse, 2013). DUSP mRNA expression is induced by MAP kinases signalling downstream of PRR activation, creating a negative feedback loop. Signalling through MAP kinase pathways is also terminated by ubiquitin-mediated degradation of components of the MAP kinase pathways, including MAP 2-kinases and MAP 3-kinases (Chen and Thorner, 2007). Furthermore, post-translational modifications or protein interactions can disrupt associations between pathway components and prevent continued signalling.

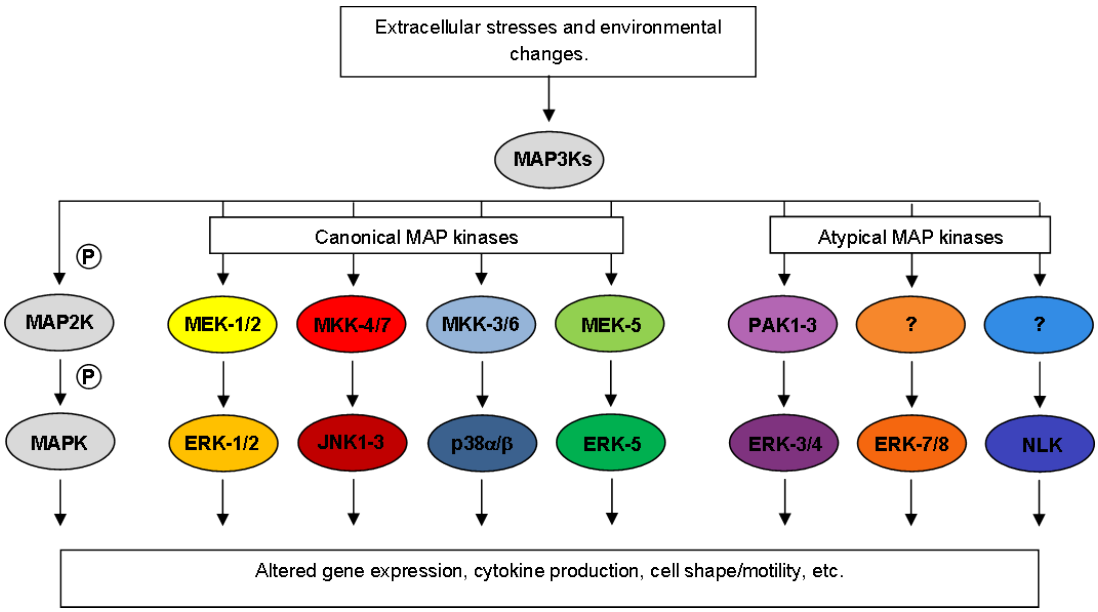

Figure 1.4: **Mitogen-activated protein kinase pathways.** Changes in the extracellular environment, including the presence of microorganisms and other stresses, trigger activation of the MAP kinase pathways. These three tiered kinase cascades consist of upstream MAP 3-kinases (MAP3K), which phosphorylate and activate a MAP 2-kinase (MAP2K), which then phosphorylates and activates the MAP kinase (MAPK). Active MAPKs phosphorylate multiple substrate proteins with a variety of functions, resulting in altered gene expression as well as a host of other intracellular changes in response to the extracellular change.

Due to the important role of MAP kinase pathways in triggering immune responses downstream of PRR ligation, pathogens have developed ways to disrupt them, thereby avoiding elimination by the immune response. For example, *Vibrio parahaemolyticus* VopA protein acetylates lysine in the ATP-binding site of MAP kinases, blocking its signalling by preventing ATP binding (Trosky et al., 2007). Similarly *Yersinia pestis* YopJ protein acetylates MAP kinase activation loop serine and threonine residues blocking their phosphorylation and kinase activation (Mukherjee et al., 2006).

1.2.1 The atypical MAP kinases

Very little is known about the atypical MAP kinases ERK3/4, ERK7 and NLK in immune responses, owing partly to the absence of chemical inhibitors of these kinases (Arthur and Ley, 2013). Their classification as “atypical” is based on two

characteristics (Coulombe and Meloche, 2007). ERK3/4 has a different activation loop sequence to the canonical MAP kinase T-X-Y, consisting instead of a serine-glutamate-glycine motif. NLK also has only a single phosphorylation site in its activation loop motif of threonine-glutamine-glutamate, as well as unusual extensions on both the N- and C-terminals. ERK7 is also atypical because of its extended C-terminal that is not present in the canonical MAP kinases.

NLK can be activated by cytokines, such as IL-6 and TGF-β, and Wnts, like Wnt-1 and Wnt-5a (Kanei-Ishii et al., 2004; Ohkawara et al., 2004). It has been shown that the MAP 3-kinase TAK1 can activate NLK but the identity of any intermediate MAP 2-kinases are not known. Several transcription factor substrates of NLK have been identified, including STAT3 (Kojima et al., 2005). For ERK7, the MAP 2-kinase involved in its activation is currently not known in spite of it having the canonical activation loop sequence, T-X-Y. ERK7 is known to phosphorylate some of the same substrates as classical MAP kinases, namely myelin basic protein, c-Fos and c-Myc (Abe et al., 1999) and to regulate cell proliferation, as well as the response to glucocorticoids and oestrogens (Cargnello and Roux, 2011).

Although it is not known what stimuli activate the ERK3/4 pathway, Deleris et al. (2011) showed that the MAP 2-kinase family responsible are the PAKs. The only known substrate of ERK3/4 is MK5, although ERK3 has been shown to be important in immunity through a role in T cell activation. Marquis et al. (2014) showed that ERK3-deficient T cells secreted decreased amounts of cytokines and showed impaired proliferation in response to TCR-stimulation *in vitro*.

1.2.2 Canonical MAP kinase pathways

The p38 and JNK pathways

The p38 and JNK MAP kinases are also known as stress-activated protein kinases due to their predominant role in transduction of danger signals after PRR engagement. These pathways can also be activated by diverse environmental stimuli such as osmotic stress and ultraviolet light (Rosette and Karin, 1996; Aggeli et al., 2002). Based largely on experiments with knockout fibroblasts, multiple MAP 3-

kinases have been shown to activate p38 pathways including TAK1, ASK1, DLK1 and TAO1 (Matsuzawa et al., 2005; Cuadrado and Nebreda, 2010; Sakurai, 2012). Similarly, the MAP 3-kinases TAK1, MLK1, and MEKK1 have been implicated in JNK activation (Davis, 2000; Sakurai, 2012). However, the MAP 3-kinase used by TLR4 for activation of p38 and JNK pathways in innate immune cells has yet to be determined (Arthur and Ley, 2013).

The MAP 2-kinases responsible for activation of p38 and JNK MAP kinases are much better defined as they have a more restricted substrate specificity and show less context dependence. The canonical p38α pathway is activated by the MAP 2-kinases MKK3 and MKK6 and current knowledge suggests these MAP 2-kinases exclusively activate p38 isoforms (Remy et al., 2010). JNK MAP kinases are activated by the MAP 2-kinases MKK4 and MKK7 (Lawler et al., 1998). MKK4 and MKK7 appear to show a preference for the activation loop tyrosine and threonine, respectively, and co-operate to induce maximal JNK activation following stress stimulation (Fleming et al., 2000). However, inflammatory stimuli like IL-1β and TNFα have been shown to activate JNK through MKK7 alone (Tournier et al., 2001).

Some of the downstream targets of p38 and JNK pathways regulate transcriptional changes. In addition, JNK can control many other targets in a variety of cellular pathways. For example, adaptor proteins like IRS-1, that can alter how other signalling pathways are integrated, Bcl2 family members, that promote cell survival, and paxillin, a protein involved in focal adhesions through which JNK is thought to regulate cell movement (Bogoyevitch and Kobe, 2006). JNK signalling has been linked to development of insulin resistance in mice fed a high-fat diet (Han et al., 2013). JNK deletion in myeloid cells correlates with reduced numbers of macrophages in adipose tissue and impaired polarisation of macrophages to an inflammatory phenotype.

p38α also regulates gene expression at the post-transcriptional level, regulating mRNA stability through control of the RNA binding protein tristetraprolin (TTP). A key target for TTP is the mRNA of cytokines, such as TNFα, which are

targeted for degradation by TTP binding. p38α activates its substrate, MK2, which phosphorylates TTP, decreasing TTP affinity for the mRNA ARE motif. This allows HUR to bind the mRNA instead and initiate translation (Tiedje et al., 2012). Through control of this pathway, p38α promotes production of cytokines and has been associated with inflammatory diseases. In support of this, p38α/β inhibitors have been shown to be protective in animal models of inflammatory and autoimmune diseases like rheumatoid arthritis (Cohen, 2009). Clinical trials of p38α/β inhibitors in immune diseases have suffered from problems of toxicity and an absence of long-term efficacy (Zhang et al., 2007; Arthur and Ley, 2013). A possible explanation for these problems comes from the fact that p38α inhibition blocks negative feedback pathways and results in increased inflammation. For example, p38α phosphorylation of TAB1 and/or TAB3 leads to inhibition of TAK1. In the absence of p38α activity, this feedback loop is inactive, resulting in elevated TAK1 activation and greater activation of NFκB, JNK and ERK1/2 pathways (Cheung et al., 2003).

The ERK5 pathway

Although its kinase domain shares 51 % amino acid identity with ERK2 (Cargnello and Roux, 2011), ERK5 has a unique structure amongst the canonical MAP kinases due to its large C-terminal domain. ERK5 is activated by extracellular stimuli, including growth factors like VEGF, cytokines like IL-6 and environmental stresses like hypoxia (Nithianandarajah-Jones et al., 2012). These stimuli induce the activation of the MAP 3-kinases MEKK2/3, which then activate the only MAP 2-kinase for ERK5, MEK5 (Cargnello and Roux, 2011). ERK5 activation induces phosphorylation of a number of proteins, the best characterised of which are MEF2A, MEF2C and MEF2D transcription factors that are positively regulated by ERK5.

In the immune system, ERK5 negatively regulates expression of the macrophage colony stimulating factor receptor (M-CSFR) in human acute myeloid leukemia cells, preventing their differentiation into macrophages (Wang et al., 2015).

ERK5 also promotes B cell survival in response to BAFF stimulation and therefore maintenance of mature B cell numbers (Jacque et al., 2015).

The MEK1/2/ERK1/2 pathway

One of the key MAP kinase pathways is the MEK1/2/ERK1/2 pathway, which can be activated by a variety of exogenous and endogenous stimuli, such as growth factor signalling via tyrosine kinase receptors, and PAMP signalling via TLRs.

ERK1/2 signalling controls cellular function at transcriptional and post-transcriptional levels. Its role at the transcriptional level is fairly well understood (O'Donnell et al., 2012). However, the functions of other ERK1/2 substrates have not been fully elucidated. This was illustrated by a recent study in which use of an "analog-sensitive" ERK2 kinase identified 80 ERK2 substrates, of which only 13 were previously known (Carlson et al., 2011). The majority of these were not directly related to transcriptional control and suggested functions for ERK1/2 signalling in mRNA processing, cytoskeletal organisation and protein transport.

ERK1/2 has a role in many cancers (e.g. melanoma, ovarian and colon cancer) through promotion of cell growth and survival (Davies et al., 2002). In this instance, ERK1/2 activation is often the result of activating mutations in Raf isoforms, the MAP 3-kinases which activate ERK1/2 in response to growth factor stimulation, or Ras, the small GTPase upstream of Raf. Fortunately, it is possible to inhibit Raf without blocking the important immune functions of ERK1/2 because immune stimuli use the alternative MAP 3-kinase, TPL-2, which is the main focus of this study. Similarly, this could eventually allow selective blockade of immunological ERK1/2 activation through TPL-2 inhibition, meaning inflammatory diseases could be treated without the side effects of MEK1/2 or ERK1/2 inhibition on growth factor signalling.

1.3 Tumour progression locus-2

The ERK1/2 MAP 3-kinase tumour progression locus 2 (TPL-2, also known as COT or MAP3K8) has been characterised primarily as a regulator of MAP kinase signalling in macrophages.

It was first identified as an oncogene in a human thyroid carcinoma cell line and in Moloney murine leukaemia virus-induced T cell lymphomas (Miyoshi et al., 1991; Patriotis et al., 1993). Pro-virus insertion into the final intron of the TPL-2 gene, between exons 7 and 8, produces a C-terminally truncated protein with transforming potential (Ceci et al., 1997; Uren et al., 2005). Furthermore, the Catalogue of Somatic Mutations in Cancer (COSMIC) database shows 83 unique mutations in the *Map3k8* gene in human cancer (http://cancer.sanger.ac.uk/cosmic, accessed 5/11/15; Forbes et al., 2015).

TPL-2 is a serine/threonine protein kinase, expressed as two isoforms: M1 (467 amino acids, 58 kDa) and M30 (437 amino acids, 52 kDa), differing at their N-terminal due to initiation of translation from either methionine 1 or methionine 30, respectively (Aoki et al., 1993). Both isoforms are cytoplasmic, but M1 has a longer half-life than M30 suggesting they are regulated differently (Cho and Tsichlis, 2005), although the functional consequences of this difference have not been investigated. The TPL-2 kinase domain extends between residues 146 and 386 (M1 isoform).

1.3.1 Regulation of TPL-2

The majority of TPL-2 in a cell is sequestered in a complex with NFκB1 p105 and ABIN-2 (figure 1.5). Interaction with both these proteins is essential for optimal stability of TPL-2, whose steady-state levels are very low in cells lacking either NFκB1 p105 or ABIN-2 (Waterfield et al., 2003; Lang et al., 2004; Papoutsopoulou et al., 2006).

Other than maintaining steady-state levels of TPL-2, the function of ABIN-2 is not yet known. However, by retroviral expression of TPL-2 in *Tnip2*$^{-/-}$ (ABIN-2 “knock-out”) macrophages, it has been established that ABIN-2 is not required for

TPL-2 activation and phosphorylation of MEK1/2 (Papoutsopoulou et al., 2006). Degradation of NFκB1 p105 releases ABIN-2, in addition to TPL-2, and it is possible that ABIN-2 mediates its signalling function once released from the TPL-2 complex. ABIN-2 binds to linear and K63-linked poly-ubiquitin chains through its conserved UBAN domain. However, the importance of the UBAN domain in ABIN-2 function, and the polyubiquitinated proteins to which ABIN-2 binds under physiological conditions have yet to be determined.

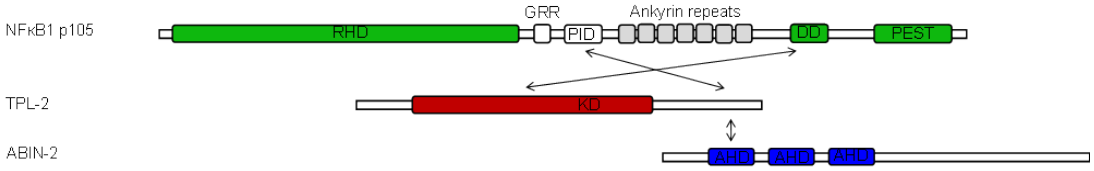

Figure 1.5: **Interactions between TPL-2, NFκB1 p105 and ABIN-2.** In unstimulated cells, TPL-2 is held in a complex with NFκB1 p105 and ABIN-2. The C-terminus of TPL-2 (residues 398-467) interacts with part of the processing inhibitory domain (PID) of NFκB1 p105 (residues 497-539), masking the TPL-2 degron sequence. In addition, the kinase domain (KD) of TPL-2 interacts with the death domain (DD) of NFκB1 p105, inhibiting TPL-2 MEK-kinase activity and forming a very strong association between the two proteins. The TPL-2 C-terminus also associates with ABIN-2 through a region (residues 194-250) containing one of the ABIN homology domains (AHD). The N-terminal half of ABIN-2 also associates with NFκB1 p105. RHD = Rel homology domain, GRR = glycine-rich region, PEST = domain rich in proline (P), glutamate (E), serine (S) and threonine (T). [Adapted from Gantke et al. (2011)]

NFκB1 p105 functions as a cytoplasmic inhibitor of NFκB (IκB), preventing NFκB transcription factors, particularly p50 homodimers and the p50-containing heterodimers p50-cRel and p50-RelA, entering the nucleus in the absence of stimulation (Sriskantharajah et al., 2009). NFκB1 p105 is also constitutively processed by the proteasome into the mature transcription factor p50. This processing is regulated by the E3 ubiquitin ligase, KPC1 (Kravtsova-Ivantsiv et al., 2015).

Following receptor activation, NFκB1 p105 is phosphorylated in its PEST region on serines 927 and 932 by IKK2 (Orian et al., 2000; Salmerón et al., 2001; Lang et al., 2003). These modifications allow recognition by the E3 ligase $SCF^{\beta TrCP}$, which catalyses K48-linked polyubiquitination of NFκB1 p105 triggering

predominantly complete degradation by the proteasome rather than processing to p50 (Belich et al., 1999; Heissmeyer et al., 2001; Lang et al., 2003). This releases associated NF-κB dimers to translocate into the nucleus and modulate gene transcription. TPL-2 forms a strong stoichiometric association with NFκB1 p105 through 2 interactions (figure 1.5); the C-terminal of TPL-2 binds to a region of NFκB1 p105 adjacent to the ankyrin repeats, and the kinase domain of TPL-2 binds to the NFκB1 p105 death domain (Belich et al., 1999; Beinke et al., 2003). The association with NFκB1 p105 maintains TPL-2 stability by masking a degron sequence, which lies between residues 435 and 457 (Gándara et al., 2003). When in the complex, TPL-2 is incapable of phosphorylating MEK1 because access to the kinase domain is prevented by the interaction with the NFκB1 p105 death domain. In contrast, the intrinsic kinase activity of TPL-2 is not inhibited by NFκB1 p105 association, as evidenced by the ability of TPL-2 to phosphorylate associated NFκB1 p105 (Babu et al., 2006b; Robinson et al., 2007). Activation of the MEK1/2 kinase activity, following stimulation of receptors such as TLR4, requires release of a fraction of TPL-2 from NFκB1 p105, triggered by IKK2-induced NFκB1 p105 proteolysis (figure 1.6). Interestingly, this suggests a possible functional link between NFκB and MAP kinase pathways.

Intra-molecular interactions are also important for the regulation of TPL-2 activity. Oncogenic mutants of TPL-2 are always truncated at the C-terminus (TPL-2ΔC), indicating an important regulatory role for the C-terminal in the full-length protein (Gantke et al., 2012). The isolated C-terminus has been shown to interact with the kinase domain of TPL-2, reducing its catalytic activity (Ceci et al., 1997; Gándara et al., 2003). Based on these data, it has been suggested that the C-terminal end of TPL-2 (residues 425-467) forms intra-molecular interactions with its kinase domain, preventing phosphorylation of substrates in unstimulated cells. TPL-2ΔC is more stable, with a half life of 95 mins versus 35 mins for full length human TPL-2, and expressed at increased levels than the full length protein, probably due to absence of the C-terminal degron motif (Gándara et al., 2003). Truncation may also increase the specific activity of the oncogenic form of TPL-2 by

removing the auto-inhibitory interaction and also blocking negative regulation by NFκB1 p105 which partly relies on the TPL-2 C-terminus (figure 1.5).

A key phosphorylated residue is serine 400 (S400) in the C-terminal tail of TPL-2 which is a target site for IKK2 after LPS-stimulation (Roget et al., 2012). Expression of TPL-2 in *Nfκb1*$^{-/-}$ macrophages has shown that stimulation-induced phosphorylation of S400 is required in addition to release from NFκB1 p105 to induce TPL-2 signalling (Robinson et al., 2007). Phosphorylation at S400 is essential for intracellular MEK1/2 kinase activity in LPS-stimulated macrophages. S400 phosphorylation triggers TPL-2 signalling by promoting the interaction between TPL-2 and 14-3-3 dimers, increasing TPL-2 kinase activity (Ben-Addi et al., 2014). The TPL-2 auto-phosphorylation at serine 443 is also required for optimal 14-3-3 interaction in addition to S400 trans-phosphorylation by IKK2. C-terminal deletion may trigger the oncogenic potential of TPL-2 by rendering its kinase activity independent of 14-3-3 binding.

Table 1.2: **Phosphorylation sites in the TPL-2 protein**

Site	Method	Notes	References
S62	pAb, MS	Required for maximal activation	Stafford et al. (2006)
T80	MS	-	Black et al. (2007)
S125	MS	-	Stafford et al. (2006)
S141	MS	Present prior to stimulation	Stafford et al. (2006) Weintz et al. (2010)
T290	pAb	Required for MEK1/2 kinase activity, regulates NFκB1 p105 binding	Stafford et al. (2006)
S334	MS	-	Stafford et al. (2006)
S400	pAb, KA, MS	Phosphorylated by IKK2. Required for 14-3-3 binding and intracellular MEK1/2 kinase activity	Robinson et al. (2007); Ben-Addi et al. (2014)
S413	KA	-	Robinson et al. (2007)
S443	pAb, MS	Autophosphorylation. Required for optimal 14-3-3 binding	Ben-Addi et al. (2014)

pAb = phospho-specific antibody, MS = mass spectrometry, KA = *in vitro* kinase assay

Mass spectrometry has identified multiple other phosphorylated residues on TPL-2 (table 1.2) (Luciano et al., 2004; Stafford et al., 2006; Black et al., 2007). Of these, only one has been shown to be functionally important. Phosphorylation of threonine 290 (T290) within the activation loop is essential for TPL-2 kinase activity (Luciano et al., 2004; Stafford et al., 2006) and LPS-induced MEK1/2 phosphorylation is blocked in TPL-2 knock-out macrophages retrovirally expressing TPL-2^{T290A} (Cho and Tsichlis, 2005). T290 phosphorylation may activate TPL-2 both by reducing its affinity for its inhibitor NFκB1 p105 and promoting interaction with MEK1/2. There is also contention over the kinase responsible for phosphorylating T290. High concentrations of the IKK2 inhibitor, PS1145, were reported to block its phosphorylation (Cho et al., 2005), however this was refuted by a subsequent study using lower concentrations (Stafford et al., 2006). Serine 62 phosphorylation has also been reported as an autophosphorylation required for maximal activation of TPL-2 following IL-1 stimulation of IL-1R-expressing HEK293 cells (Stafford et al., 2006). However, phosphorylation of this residue is not important for LPS activation of TPL-2 in macrophages (Roget et al., 2012).

The availability of nutrients appears to be important for regulating TPL-2 activation by phosphorylation (Mieulet et al., 2010). When macrophages are deprived of arginine, the interaction between TPL-2 and protein phosphatase 2A is enhanced, leading to dephosphorylation of TPL-2 residues T290 and S400 and abrogation of kinase activity towards substrates following LPS stimulation.

Thus in response to stimulation through receptors like TLR4 and IL-1R, TPL-2 transduction of signals to its downstream targets is regulated by post-translational modification, intra-molecular interactions and protein-protein interactions.

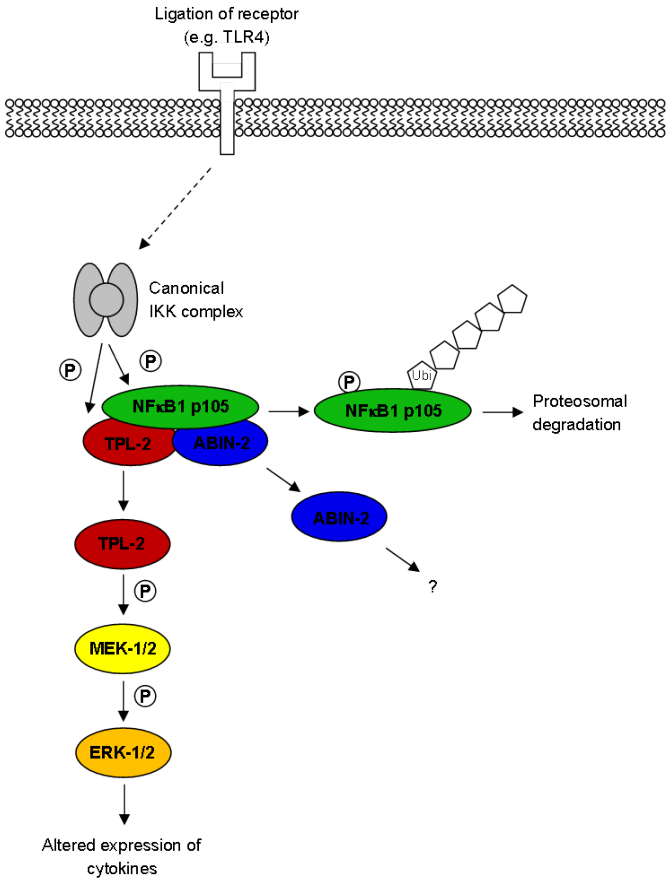

Figure 1.6: **Regulation and signalling of TPL-2.**
Ligation of receptors such as TLR4 or TNFR1 activates the canonical IKK complex. The IKK complex then phosphorylates NFκB1 p105, leading to its K48-linked polyubiquitination followed by degradation by the proteasome and release of TPL-2. The IKK complex also directly phosphorylates the C-terminus of TPL-2 inducing 14-3-3 binding. Once released from the NFκB1 p105 complex, TPL-2 can phosphorylate MEK1/2, resulting in changes in cytokine and chemokine expression. ABIN-2 is also released from TPL-2 following NFκB1 p105 degradation, but its function remains unknown. [Adapted from Gantke et al. (2011)]

1.3.2 TPL-2 MAP 3-kinase in immune responses and disease

TPL-2 functions as a MAP 3-kinase, activated by TIR domain-containing receptors from the Toll-like receptor/IL-1 receptor family, and the TNF receptor superfamily (Gantke et al., 2011). TPL-2 is essential for activation of the MEK1/2/ERK1/2 pathway in macrophages stimulated via TLRs, TNFR1 and IL-1R. ERK1/2 activation in B cells stimulated through CD40 and TLR4 is also mediated via TPL-2 (Eliopoulos et al., 2003; Gantke et al., 2012).

In vitro evidence

TPL-2 has roles in both the innate and adaptive arms of the immune system. In innate immune responses, signalling through TPL-2 leads to changes in expression of inflammatory mediators such as COX2 and cytokines (Eliopoulos et al., 2002b). TPL-2 signalling positively regulates TNFα, IL-1β, IL-10 and IL-23 production by macrophages (Dumitru et al., 2000; Mielke et al., 2009; Kakimoto et al., 2010), whereas IFNβ and IL-12p70 are negatively regulated, independent of the autocrine effects of increased IL-10 release (Kaiser et al., 2009; Yang et al., 2011). The effects of TPL-2 on cytokine expression are largely mediated at the transcriptional level (e.g. IL-1β and IL-10). However, levels of TNFα mRNA and pre-TNFα protein in *Map3k8*$^{-/-}$ BMDM are normal, but mature TNFα secretion is substantially reduced compared to wild type (Dumitru et al., 2000). TPL-2 therefore regulates TNFα production at a post-translational level (figure 1.2). It has been suggested that TPL-2 deficiency in macrophages reduces transport of pro-TNFα to the cell surface in response to TLR stimulation (Rousseau et al., 2008). However, MEK1/2 inhibition does not effect pro-TNFα trafficking from the Golgi to the plasma membrane in LPS-stimulated RAW264.7 macrophages. Rather, ERK1/2 phosphorylates TACE at Thr735, thereby regulating the levels of mature TACE at the cell surface (Soond et al., 2005). TACE may facilitate transport of pre-TNFα to the cell surface for subsequent TACE-mediated proteolysis (Rousseau et al., 2008).

TPL-2 also regulates the movement of innate immune cells by controlling the production of and response to chemokines. For example, the mRNA levels of the chemokines CCL2, CCL7, CXCL2 and CXCL3 are reduced in LPS-stimulated *Map3k8*$^{-/-}$ BMDM compared to wild type, whereas CCL5, CCL8, CXCL9, CXCL10 and CXCL13 are increased (Bandow et al., 2012). TPL-2-deficient macrophages also express lower levels of the chemokine receptor CCR1 than wild type cells after LPS stimulation and are impaired in trafficking to the peritoneal cavity after thioglycollate injection (Rowley et al., 2014). In addition to regulating macrophage trafficking, TPL-2 regulates their phagocytic function. Phagocytosis of beads by

peritoneal macrophages stimulated *ex vivo* with adiponectin is reduced in the absence of TPL-2 (Sanz-Garcia et al., 2014). Therefore it seems that TPL-2 is important for a range of functions in innate immune cells.

In vivo evidence

Consistent with these *in vitro* experiments, analyses of *Map3k8*$^{-/-}$ mice have also established important roles for TPL-2 regulation of inflammation. For example, *Map3k8*$^{-/-}$ mice are protected in a model of endotoxic shock induced by LPS and D-galactosamine due to the critical role of TPL-2 in regulating TNFα production by macrophages (Dumitru et al., 2000). TPL-2 deficient mice are also protected from experimental autoimmune encephalomyelitis (EAE), a model of multiple sclerosis (Sriskantharajah et al., 2014). Similarly, Kontoyiannis et al. (2002) found that, in the TNF$^{\Delta ARE/\Delta ARE}$ mouse model of Crohn's-like inflammatory bowel disease (IBD), *Map3k8*$^{-/-}$ mice show attenuated intestinal pathology, with later onset and reduced inflammation. TPL-2 has also been linked to this disease in patients by a genome wide association study that showed an association between a *Map3k8* single nucleotide polymorphism and IBD (Jostins et al., 2012).

TPL-2 expression in T cells is required for efficient differentiation of CD4+ T cells into Th1 effector cells. TPL-2-deficient CD4+ T cells have a reduced capacity to induce the transcription factors, T-bet and Stat4, which drive optimal Th1 polarisation. In line with these observations, TPL-2 is required for a normal immune response to the Th1-inducing parasite *Toxoplasma gondii* due to compromised IFN-γ production. Furthermore, transplantation of *Rag2*$^{-/-}$ mice with T cells confirmed a T cell-intrinsic role for TPL-2 in resistance to *T. gondii* infection (Watford et al., 2008). *Map3k8*$^{-/-}$ mice are also more susceptible to *Mycobacterium tuberculosis* and *Listeria monocytogenes* due to the increased production of IFNβ by innate immune cells that is detrimental in this infection (McNab et al., 2013).

However, the majority of studies into TPL-2 immune function use TPL-2-deficient macrophages/mice which also have substantially reduced amounts of ABIN-2 protein compared to wild type (Sriskantharajah et al., 2014). Therefore,

until these results are confirmed in TPL-2 kinase-inactive macrophages/mice, where presence of the kinase-inactive TPL-2 protein acts as a scaffold to stabilise ABIN-2, it cannot be ruled out that some of these effects could be dependent on ABIN-2.

1.3.3 TPL-2 signalling in cancer

Oncogenic functions of TPL-2

TPL-2 was initially identified by several laboratories by virtue of its transforming activity when its C-terminus is deleted. However, there is only one reported example of TPL-2 truncation occurring in human cancer. Clark et al. (2004) found TPL-2 truncated at residue 421 in a human lung adenocarcinoma. There are also two cancers in which mutation of residues within the C-terminus might contribute to carcinogenesis; an alanine to threonine mutation at residue 387 in a patient with glioblastoma multiforme (Parsons et al., 2008) and a proline to leucine mutation was found at residue 461 in breast cancer and metastasis samples from a patient (Ding et al., 2010). It is possible that these mutations impair the interaction of TPL-2 with its inhibitor NFκB1 p105, thereby augmenting TPL-2 signalling.

There is clearer evidence linking TPL-2 over-expression to cancer development. Studies by Sourvinos et al. (1999) and Christoforidou et al. (2004) implicated elevated levels of TPL-2 in breast tumours and large granular lymphocyte proliferative disorders, respectively. Higher TPL-2 expression may augment ERK1/2 activation, a key survival signal in cancers driven by Ras and Raf mutations (Vougioukalaki et al., 2011). Indeed, increased TPL-2 expression can drive the acquisition of B-Raf inhibitor drug-resistance in melanoma patients who have constitutively activating B-Raf mutations (Johannessen et al., 2010; Monsma et al., 2015). Furthermore, TPL-2 constitutively activates ERK1/2 in anaplastic large-cell lymphoma (ALCL), and TPL-2 inhibition reduces ALCL cell proliferation *in vitro* (Fernández et al., 2011).

Other studies which have linked TPL-2 with advanced and invasive cancer include Lee et al. (2013) who showed that lung metastasis in animals given a

renal cell carcinoma (RCC) xenograft was reduced in the absence of TPL-2. The same study also found that RNAi “knock-down” of TPL-2 in RCC cell lines impaired their proliferation, migration and invasion capabilities. An alternative role for TPL-2 in cancer could be through co-operating in signalling deregulated by activation of a separate oncogene. For example, the Epstein-Barr virus protein, LMP-1 that has transforming capacity, can induce kinase activity of co-transfected TPL-2 (Eliopoulos et al., 2002a). Similarly, after human T cell leukaemia virus type I transformation of human leukaemia cell lines, TPL-2 disassociates from NFκB1 p105 and becomes constitutively active (Babu et al., 2006a).

In addition to these cell-intrinsic roles in cancer, Hope et al. (2014) showed a non-cell-intrinsic role for TPL-2 in a genetic murine model of myeloma. During disease progression, wild type myeloma-associated macrophages switch towards an inflammatory phenotype associated with tumour progression. This switch was blocked in the absence of TPL-2, resulting in delayed disease development.

Tumour suppressor functions of TPL-2

Several studies with *Map3k8*$^{-/-}$ mice suggest that TPL-2 can act as a tumour suppressor in certain contexts. *Map3k8*$^{-/-}$ mice crossed onto a transgenic MHC Class I-restricted T-cell receptor background, develop T-cell lymphomas as a result of excessive activation of CD8+ T cells after TCR stimulation (Tsatsanis et al., 2008). TPL-2 also limits the generation of adenocarcinomas in the urethane-model of lung cancer, possibly via cell intrinsic regulation of JNK activation (Gkirtzimanaki et al., 2013). *Map3k8*$^{-/-}$ mice also have a higher incidence of skin tumours than wild type in a two-stage skin carcinogenesis model. However, in this case, TPL-2 signalling inhibits carcinogenesis by regulating the inflammatory mileau in which cancer cells develop (DeCicco-Skinner et al., 2011). Similarly, using the Apc^{min} genetic model of intestinal cancer crossed with *Map3k8*$^{-/-}$ mice, Serebrennikova et al. (2012) showed that the absence of TPL-2 results in an increase in intestinal adenomas, which correlates with higher inflammation.

However, as mentioned previously, the majority of studies use TPL-2-

deficient macrophages/mice which are also ABIN-2 deficient at the protein level (Sriskantharajah et al., 2014). Therefore, these studies may be looking at ABIN-2 signalling defects rather than TPL-2, and this will have to be addressed using TPL-2 kinase-inactive mutants.

1.3.4 TPL-2 as a drug target

Due to its importance in production of TNFα by TLR/IL-1/TNFR1 stimulated macrophages, and apparent role in disease models, TPL-2 is considered a potential therapeutic target for treating conditions such as inflammatory bowel disease and rheumatoid arthritis.

Homozygous *Map3k8*^{D270A} "knock-in" mutation results in viable mice lacking any catalytically active TPL-2 (Sriskantharajah et al., 2014). Consequently, it would be expected that small molecule TPL-2 inhibitors should be tolerated and not cause any developmental defects, although immune function might be substantially reduced. However, studies suggesting TPL-2-deficiency exacerbates models of asthma or promotes tumour progression (detailed above) call this into question.

The kinase domain of TPL-2 displays marked differences to other kinases, sharing only 35 % identity with its closest homolog, MST4. Furthermore, TPL-2 has a proline (P154) in place of the first glycine in the conserved glycine-rich loop that contributes to ATP binding and enables the phosphoryl transfer reaction. Computer modelling of this residue suggested it would confer important differences to the ATP binding pocket (Gantke et al., 2012). This was recently confirmed by Gutmann et al. (2015), who determined the crystal structure of human TPL-2$^{66-395}$ and TPL-2$^{30-404}$ in combination with ATP-competitive inhibitors and found the TPL-2 kinase domain has a unique, flexible structure. The unusual features of TPL-2 make development of highly specific inhibitors more likely. TPL-2 may also be easier to inhibit pharmacologically than other kinases due to its high Michaelis-Menten constant (K_m) for ATP (Cohen, 2002). The K_m, determined *in vitro* with the cofactor Mg^{2+} using TPL-2$^{30-397}$ purified from insect cells, was greater

than 300 μM (Jia et al., 2005). This implies that high concentrations of ATP are needed to reach maximum activity, and therefore the potency of ATP-competitive inhibitors needed to out-compete this *in vivo* is lower. Several inhibitors have already been developed which are highly selective for TPL-2 and exhibit low IC_{50}s *in vitro,* meaning they are very potent as the amount needed to reduce the kinase activity to half its maximum is low. These compounds are effective at inhibiting LPS-induced production of TNFα in primary human macrophages, whole human blood and mice (Hall et al., 2007; George et al., 2008; Hu et al., 2011). However, so far TPL-2 inhibitors have not been tested in clinical trials. Work in the Ley laboratory (unpublished data) has suggested that this could be due to the poor aqueous solubility of at least one of these potent inhibitors from Wyeth (now part of Pfizer, USA). Additionally these inhibitors have been developed using a peptide substrate based on the activation loop of MEK1/2 insect cell-purified TPL-2^{30-397} which is known to partially aggregate and associate with chaperone proteins (Jia et al., 2005). Inhibitors developed in this way may not be optimal for inhibiting the biologically active form and work in the Ley laboratory is currently focused on optimising the method for screening compound libraries to identify more promising leads.

1.3.5 Downstream targets of TPL-2

MAP 2-kinases are currently the only established substrates of TPL-2. The most prominent of these in myeloid cells are MEK1 and 2, which are phosphorylated on residues S217/S221 and S218/S222, respectively, resulting in their activation and subsequent phosphorylation and activation of ERK1/2 MAP kinases. Analyses of *Map3k8*$^{-/-}$ macrophages has shown that TPL-2 regulates the activation of ERK1/2 after ligation of TLRs, IL-1R and TNFR1 (Gantke et al., 2012). There are also reports of TPL-2 phosphorylating other MAP 2-kinases, for example immunoprecipitated TPL-2 can phosphorylate the MAP 2-kinase MKK4 *in vitro* (Salmeron et al., 1996). Similarly, over-expressed TPL-2 can directly phosphorylate and activate MEK5 leading to ERK5 activation (Chiariello et al., 2000). Analyses of *Map3k8*$^{-/-}$

fibroblasts have also suggested that TPL-2 can regulate JNK activation via phosphorylation of MKK4 following TNFα and IL-1β stimulation (Das et al., 2005).

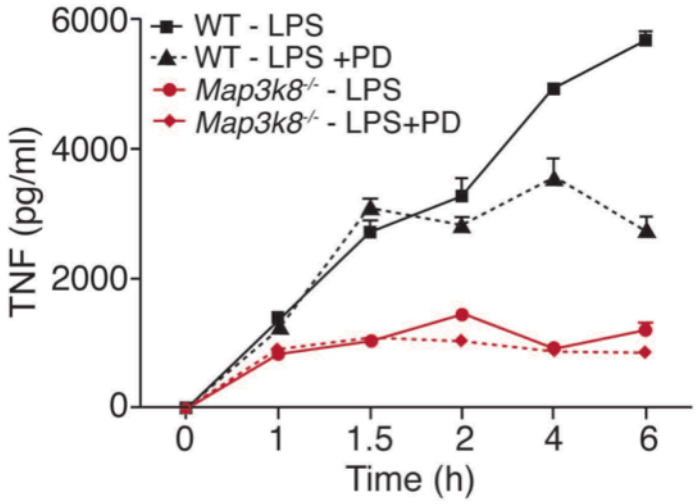

Figure 1.7: **TPL-2 regulates TNFα production by BMDM independently of ERK1/2.**
During the first 2 hours of LPS stimulation, treatment with a MEK1/2 inhibitor does not effect the amount of TNFα produced by wild type (WT) BMDM. From 1.5 hours to 6 hours pre-treatment with the MEK1/2 inhibitor reduces the amount of TNFα produced. However TNFα production in the presence of MEK1/2 inhibitor is higher than that of *Map3k8*$^{-/-}$ BMDM at all time points. PD = PD184352, MEK1/2 inhibitor. [Reproduced from Yang et al. (2012)]

It was widely thought that most TPL-2 functions were regulated through ERK1/2, including the post-translational regulation of TNFα. However, recently the Ley Laboratory published several lines of evidence that TPL-2 induces TNFα production in LPS-stimulated macrophages independently of ERK1/2 activation (Yang et al., 2012). Firstly, when wild type BMDM were stimulated with LPS, experiments with MEK1/2 inhibitor indicated that the early release of TNFα was independent of ERK1/2 signalling (figure 1.7). Pharmacological blockade of ERK1/2 activation only reduced TNFα production over 2 hours after LPS stimulation. In contrast, TPL-2 was required for TNFα production as early as 1 hour after LPS stimulation. These results suggest that TPL-2 regulated the early release of TNFα independently of its activation of ERK1/2 and that regulation of TNFα production by ERK1/2 was a late and potentially secondary effect.

Analyses of BMDM from the *Nfκb1*$^{SSAA/SSAA}$ mice, in which the IKK2 phosphorylation sites on NFκB1 p105 are mutated to alanine, have also indicated that TPL-2 can induce TNFα production independently of ERK1/2 activation. *Nfκb1*^{SSAA} mutation prevents IKK2-induced degradation of NFκB1 p105 and release of TPL-2, blocking ERK1/2 activation following LPS stimulation. However, the production of TNFα after LPS stimulation is comparable between wild type and *Nfκb1*$^{SSAA/SSAA}$ BMDM (figure 1.8). However, *Nfκb1*^{SSAA} mutation does not affect the TPL-2 dependence of TNFα production as demonstrated by experiments with LPS-stimulated *Nfκb1*$^{SSAA/SSAA}$, *Map3k8*$^{-/-}$ or *Nfκb1*$^{SSAA/SSAA}$*Map3k8*$^{D270A/D270A}$ macrophages. These results suggest that TPL-2 is able to regulate TNFα production when bound in the ternary complex with NFκB1 p105 and ABIN-2, independently of its ability to activate the ERK1/2 MAP kinase pathway.

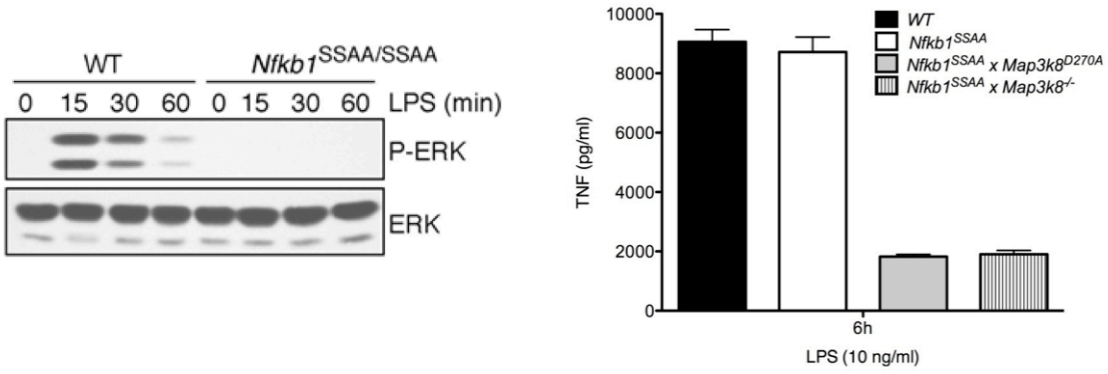

Figure 1.8: **TPL-2 regulates production of TNFα when bound in the ternary complex.**
Nfκb1^{SSAA} mutation prevents activation of ERK1/2 in LPS-stimulated macrophages (left hand panel) but does not impair TNFα production (right hand panel). However, production of TNFα is abrogated in *Nfκb1*^{SSAA}*/Map3k8*^{D270A} and *Nfκb1*^{SSAA}*/Map3k8*$^{-/-}$ compound mutant macrophages showing that TPL-2 is still required to stimulate TNFα production in the *Nfκb1*$^{SSAA/SSAA}$ mutant background. *Map3k8*^{D270A} = TPL-2 kinase-inactive BMDM, *Map3k8*$^{-/-}$ = TPL-2 knock out BMDM. [Reproduced from Yang et al. (2012)]

Additional evidence of ERK1/2-independent TPL-2 signalling comes from RNA sequencing experiments conducted in the Ley laboratory. Of the genes which are dependent on TPL-2 kinase activity, a large proportion are regulated independently of ERK1/2 activation (unpublished data).

Moreover, TPL-2 has been demonstrated to phosphorylate a number of non-MAP 2-kinase substrates (table 1.3) *in vitro* or after over-expression. However, it remains to be determined if any of these are physiologically relevant using TPL-2 kinase-inactive cells. It is also important to note that many of the studies were not conducted in macrophages and did not test the effect of inhibiting MEK1/2 to ensure that the TPL-2-dependent phosphorylation was not mediated via ERK1/2.

In order to fully understand its functions in immune responses and cancer, it is essential to have a complete understanding of the proteins endogenous TPL-2 phosphorylates in cells. This is also important to predict potential side-effects from therapeutic TPL-2 inhibition. Therefore this project will address the lack of knowledge of TPL-2 downstream signalling in order to better understand its role in innate immune responses. To achieve this goal, it is necessary to employ an unbiased method for identifying physiological kinase substrates *in situ*.

1.4 Hypothesis

As discussed earlier, recent studies by the Ley laboratory have indicated that TPL-2 regulation of innate immunity is partly mediated independently of ERK1/2. Therefore the specific aim of this study was to identify ERK1/2-independent signalling pathways regulated by TPL-2. To do this, it was first necessary to develop a system whereby global phosphorylation could be monitored in an unbiased, site-specific and quantifiable way. The overall aim was to generate a list of ERK1/2-independent TPL-2 regulated phosphoproteins and then to test whether any of these were direct TPL-2 targets. A final aim was to understand how novel TPL-2 substrates identified contribute to the function of TPL-2 in innate immune responses.

Table 1.3: **Published substrates of TPL-2, excluding MAP 2-kinases.**

Protein	Residue(s)	Limitations	Reference
PLCβ3	S537	Retrovirally reconstituted immortalised MEFs. Overexpression. *In vitro* kinase assay.	Hatziapostolou et al. (2011)
Nfκb1 p105	ND	Cell lines. *In vitro* kinase assay.	Babu et al. (2006b)
Histone H3	S10	Cell lines. *In vitro* interaction and kinase assays. Overexpression.	Choi et al. (2008)
Tvl-1	ND	Cell lines. *In vitro* kinase assay.	Patriotis et al. (2001)
NPM	T199	Cell lines. *In vitro* kinase assay.	Kanellis et al. (2014)
p70S6K	T389	MEK1/2 inhibition blocks phosphorylation.	Lopez-Pelaez et al. (2011)
Akt1	S473	MEK1/2 inhibition blocks phosphorylation.	Lopez-Pelaez et al. (2011)
Pin1	S16	Cell lines. *In vitro* kinase assay. Overexpression.	Kim et al. (2015)
PLK1	S137	Peptide substrate screen. Cell lines. *In vitro* kinase assay. Overexpression.	Wu et al. (2009)
Histone H2B	S33	Peptide substrate screen. Not validated.	Wu et al. (2009)
Chk1	S345	Peptide substrate screen. Not validated.	Wu et al. (2009)
Eif4ebp1	T70	Peptide substrate screen. Not validated.	Wu et al. (2009)
Abl1	T735	Peptide substrate screen. Not validated.	Wu et al. (2009)
CDK1	T161	Peptide substrate screen. Not validated.	Wu et al. (2009)
CREB1	S133	Peptide substrate screen. Not validated.	Wu et al. (2009)
Eif4g1	S1147	Peptide substrate screen. Not validated.	Wu et al. (2009)
Moesin / Ezrin / Radixin	T558 / T567 / T564	Peptide substrate screen. Not validated.	Wu et al. (2009)

ND = not determined

2 Introduction to Kinase Substrate Identification

Protein phosphorylation by kinases is a central mechanism by which protein function is regulated and controls multiple aspects of cell physiology. Methods for the systematic identification of kinase substrates are vital for a complete understanding of kinase function. However, this is not a trivial problem, since there are over 500 protein kinases in the human genome, which are responsible for phosphorylating an estimated 30 % of proteins. Consequently, linking the responsible kinases to each substrate clearly poses a major challenge (Cohen, 2000; Ubersax and Ferrell Jr, 2007; Duong-Ly and Peterson, 2013). This is made more difficult still by the structural similarity of kinases, which limits the specificity of inhibitors, and potential for functional redundancy, which can confound results from genetic elimination of kinase function (Elphick et al., 2007). Furthermore the deletion of one kinase can disrupt expression or stability of others or alter cell development, making interpretation of knock-out mutant cells lacking specific kinases more complex than it initially appears.

Identification of kinase substrates was previously dependent on low throughput *in vitro* assays, such as incubation of a purified kinase with a predicted substrate and assessing incorporation of radioactive phosphate into the target protein. Edman degradation was used to determine the site(s) of phosphorylation by monitoring when the radiolabel was released (Elphick et al., 2007). This approach demonstrates a direct kinase-substrate relationship but requires optimisation for individual proteins and pre-existing knowledge to identify candidate substrates.

One way to circumvent the need to predict individual kinase-substrate relationships is through the use of libraries of potential protein substrates. For example it is possible to identify proteins which interact specifically with a particular kinase domain by yeast two-hybrid assay (Municio et al., 1995). Alternatively, purified potential substrates can be adsorbed onto slides to generate protein arrays that can be screened for phosphorylation by the selected kinase (MacBeath and Schreiber, 2000; Zhu et al., 2001). Another method is KESTREL (kinase substrate tracking and elucidation), in which cell extracts are subjected to ion exchange chromatography and aliquots of the fractions collected are incubated with

radioactive magnesium-ATP in presence and absence of closely related protein kinases, such as different p38 isoforms (Cohen and Knebel, 2006). The aim is to detect proteins that are phosphorylated selectively by just one of these kinase isoforms, minimising the possibility of false positives.

All of the methods outlined thus far are limited by the artificial environment in which the kinase and candidate substrates interact; temporal and spatial constraints, as well as the role of accessory proteins, are ignored and amounts of both kinase and substrate can be significantly higher than those *in vivo* (Elphick et al., 2007). The potential for artefact is considerable.

2.1 Analysis of phosphopeptides by mass spectrometry

With advances in mass spectrometry (MS) techniques, it has become possible to vastly increase coverage and quantification accuracy of the physiological phosphoproteome. In a single experiment a huge number of phosphorylation sites can be identified and quantified from a complex mixture such as cell lysate, allowing a greater proportion of a specific kinase's potential substrates to be investigated simultaneously.

Analysis of phosphopeptides uses tandem MS (MS/MS), which involves two rounds of MS, termed MS1 and MS2. The most abundant peptides, as determined by quantification of the relative intensity of the signals in MS1, are subjected to further fragmentation prior to MS2 (Palumbo et al., 2011). The masses of the resulting fragment ions are used to identify the original peptide as well as the phosphorylated residue by comparison with predicted spectra from *in silico* digestion of the proteome. Common fragmentation techniques used include collision induced dissociation (CID), multistage activation (MSA) and higher-energy collisional dissociation (HCD). These different methods result in different fragment ions. For example CID is efficient in removal of the phosphate group but not fragmentation of the backbone (Palumbo et al., 2011), whereas HCD provides better disruption of the peptide backbone and therefore more sequence information (Olsen et al., 2007).

2.2 Enrichment of phosphopeptides

Signalling proteins are commonly expressed at low levels and phosphorylation of these proteins is often sub-stoichiometric, with as little as 1 % of the total protein being modified (Villen and Gygi, 2008). This makes the study of global phosphorylation changes inefficient from complex mixtures, with a bias towards detection of abundant proteins. To overcome this, early MS methods fractionated cell lysates, for example by two-dimensional gel electrophoresis with or without phosphatase treatment, to identify phosphorylated proteins. These were then excised and identified by MS (Mann and Jensen, 2003). However this approach lacked resolution and accuracy and has been superseded by introduction of specific phospho-enrichment techniques. These fall into two categories, chemical methods and affinity methods. Chemical methods include the chemical replacement of the phosphate group on a serine or threonine with an affinity tag (Oda et al., 2001). However, such strategies suffer from side reactions which increase complexity of the sample and complicate data analysis.

Affinity enrichment using phospho-specific antibodies has been used to enrich phosphopeptides but has give variable results due to use of different immunogens to raise the antibodies (Wang, 1988; Gronborg, 2002). Consequently the most common affinity based techniques are based on physicochemical differences between phosphopeptides and their non-phosphorylated counterparts. Strong cation exchange (SCX) chromatography for example uses a negatively charged resin to retain non-phosphorylated peptides slightly better than phosphorylated ones (Zhou et al., 2011). This is because trypsin cleaves proteins at the basic amino acids arginine and lysine so, at low pH, each peptide will have two positive charges, one on its amino terminus and one on the arginine or lysine (the carboxy terminus is neutral at low pH). Phosphopeptides are less positively charged than non-phosphorylated peptides due to the addition of the negatively charged phosphate group. Another common method for enriching phosphopeptides is using titanium dioxide beads that bind phosphopeptides specifically via their attached phosphate groups (Pinkse et al., 2004; Sano and Nakamura, 2004).

Various studies have suggested that the enrichment protocol can significantly influence the type of phosphopeptides (e.g. singly or multiply phosphorylated) that are subsequently detected (Bodenmiller et al., 2007; Li et al., 2009; Zarei et al., 2011). As each of these methods are reliant on small differences in peptide properties, contaminating peptides are usually co-purified. For example, acidic peptides can also bind titanium dioxide although this can be reduced by addition of certain acids (Jensen and Larsen, 2007; Wu et al., 2007). For SCX, phosphopeptides with basic residues like histidine can mimic un-phosphorylated peptides in their interaction with the anionic resin (Zhou et al., 2011). Moreover multiply phosphorylated peptides have a net neutral or even negative charge and will not bind the SCX matrix so that they are lost in the flow-through. Affinity enrichment techniques are therefore most powerful when used in combination (e.g. SCX fractionation followed by titanium dioxide enrichment of phosphopeptides from the fractions) .

2.3 Use of labelling techniques

In spite of the accuracy that can be achieved with MS, it is not inherently suitable for quantification because of errors introduced through liquid handling steps and changes in chromatographic conditions over time (Mann, 2006). For this reason label free techniques such as iBAQ (Schwanhäusser et al., 2011), which uses the number of observed peptides for each protein as a surrogate for its abundance, are not generally applied to studies of global phosphorylation. To compensate for such errors, methods for peptide labelling have been introduced into MS workflows.

2.3.1 *In vitro* labelling

A number of methods for labelling peptides *in vitro* during or following trypsinisation have been developed, including ^{18}O (Ye et al., 2009) or iTRAQ (Wiese et al., 2007). Once the peptides in each lysate are labelled, they can be combined for subsequent steps of the enrichment and analysis procedure thus reducing the impact of errors. A relative quantification between the labelled and unlabelled forms

is determined from the MS signals obtained. However, *in vitro* labelling involves enzymatic or chemical steps, which can have variable labelling efficiency and the possibility of side reactions, as well as errors introduced in steps prior to labelling (Mann, 2006).

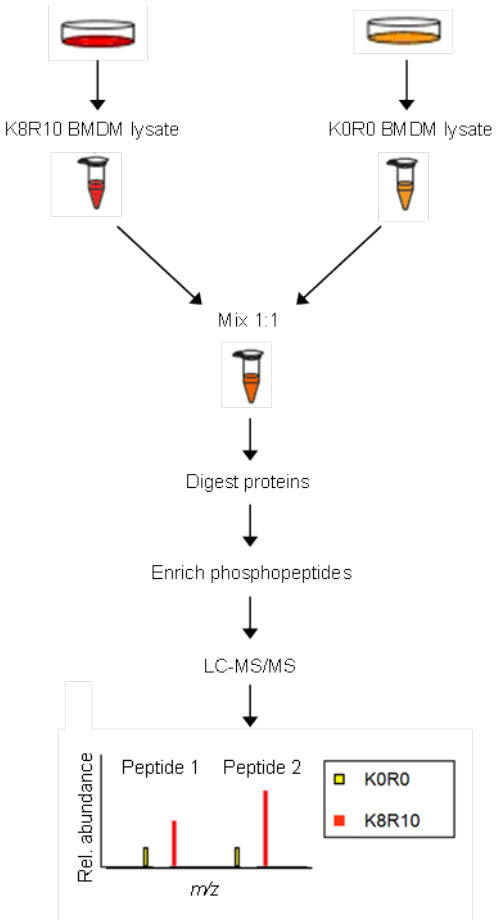

Figure 2.1: **SILAC labelling and subsequent analysis by mass spectrometry.** Amino acids labelled with stable isotopes are added to culture medium and incorporated into proteins by cells through their normal metabolic processes. Differential labelling in this way allows proteins to be pooled directly following lysis of the cells. Any errors introduced during subsequent steps of trypsin digestion, phosphopeptide enrichment and LC-MS/MS analysis will effect both samples identically and therefore the relative abundance of phosphopeptides will not be altered. Upon LC-MS/MS analysis of the mixtures, peptides from the labelled culture will have a greater mass than their unlabelled counterparts, meaning the two signals can be distinguished and a ratio corresponding to their relative abundance can be calculated. [Adapted from Weintz et al. (2010)]

2.3.2 Stable isotope labelling with amino acids in cell culture

Stable isotope labelling with amino acids in cell culture (SILAC) is a metabolic labelling technique whereby cultured cells take up and incorporate a label into their proteins through their normal metabolic processes (Jiang and English, 2002; Ong et al., 2002; Zhu et al., 2002). Relative quantification of two differentially labelled conditions is achieved by comparing the relative signal intensity between conditions for each peptide. The label consists of the amino acids arginine and lysine containing ”heavy” isotopes of hydrogen, carbon and nitrogen that are added into the culture media and can be used by the cells in the synthesis of new proteins.

Arginine and lysine are ideal for this for several reasons. Most importantly these residues are exclusively recognised and cleaved by trypsin meaning that, when proteins are digested, every resulting peptide will carry exactly one label (assuming 100 % cleavage efficiency). Therefore all peptides (except the most C-terminal) will be quantifiable and have a predictable mass shift, which simplifies analysis of the peaks (Ong et al., 2003; Olsen, 2004; Ong, 2012). Arginine and lysine are essential amino acids not produced by cells. This is beneficial for labelling because if cells could produce unlabelled arginine or lysine it would lead to incomplete labelling. However, some cell types have been shown to convert proline to arginine, and *vice versa* (Mann, 2006). In addition to introducing unlabelled arginine, this could result in the presence of labelled proline and hence peptides with two labels. This would cause errors in peptide quantification by making it harder to identify which peaks correspond to a particular peptide.

SILAC has become the gold standard labelling technique for proteomic studies and has been used to identify substrates for a variety of kinases, for example Grb10 as a substrate of mTORC1 in fibroblasts (Yu et al., 2011) and AEG-1 as a substrate of IKKβ in MCF-7 breast cancer cells (Krishnan et al., 2015).

The main drawback of MS-based phosphoproteomics, regardless of the labelling method used, is that it does not only identify direct substrates but also secondary phosphorylation events resulting from activation of downstream kinases.

Table 2.1: **Strengths and weaknesses of the standard SILAC approach.**

Strengths	Weaknesses
Proteins should have normal functions and post-translational modifications.	Biology of cells may be altered by the culture conditions.
Eliminates variability in sample preparation.	Labelling efficiency is not 100 %.
Labelled peptides have the same physico-chemical properties and behave the same in the mass spectrometer, reducing variability in analysis.	No more than 3 conditions can be compared at one time.
Predictable mass shifts between labels.	Complexity of the mixture is increased.

2.4 Analogue-sensitive kinases

To address the issue of direct phosphorylations, another technology developed specifically to identify kinase substrates is the use of "analogue-sensitive" kinases. This requires an engineered form of the kinase of interest in which the "gatekeeper" residue in the kinase domain is mutated to allow use of an unnatural ATP analogue with a bulky side group (Shah et al., 1997). By using an analogue where the γ-phosphate (which a kinase transfers to a substrate) has been replaced by a thiol, only direct substrates of the kinase will be labelled with the thiol group and these can be isolated before being identified and quantified by MS (Carlson et al., 2011).

Analogue-sensitive kinases can increase the identification of specific substrates because, in theory, other kinases cannot use the unnatural ATP analogue. It is also an effective method for establishing causal relationships between a kinase and its substrates on a large scale. However this is not universally applicable with about 30 % of kinases intolerant of the gatekeeper mutation and potentially requiring further mutations to rescue kinase activity (Zhang et al., 2005). Furthermore, the assay currently has to be done *in vitro* using cell lysates as the ATP analogues are not cell permeant. Consequently, the subcellular context is

lost and phosphorylations detected using this method may not be physiological.

Of the available technologies, SILAC labelling and MS currently provide the highest accuracy data and the most widely applicable methodology, so this approach will be implemented in the current study.

3 Materials and Methods

3.1 Buffers

ACK Buffer (0.2 µm filter sterilised)		
Ingredient	**Supplier**	**Final Concentration**
Ammonium chloride	Sigma-Aldrich, USA	155 mM
EDTA	Sigma-Aldrich, USA	100 µM
Potassium bicarbonate	Sigma-Aldrich, USA	10 mM
Water	-	To 1 L

S-Lysis Buffer		
Ingredient	**Supplier**	**Final Concentration**
Tris/HCl	Sigma-Aldrich, USA	50 mM
Sodium chloride	Sigma-Aldrich, USA	150 mM
EDTA	Sigma-Aldrich, USA	2 mM
Sodium fluoride	Sigma-Aldrich, USA	50 mM
Sodium pyrophosphate	Sigma-Aldrich, USA	2 mM
Igepal*	Sigma-Aldrich, USA	1 %
cOmplete, EDTA-free protease inhibitor mix*	Roche, Switzerland	1 x
Sodium orthovanadate*	Sigma-Aldrich, USA	1 mM

*Ingredients added immediately prior to use.

Detergent Free Lysis Buffer		
Ingredient	**Supplier**	**Final Concentration**
Urea	Sigma-Aldrich, USA	8 M
Tris/HCl pH 8.2	Sigma-Aldrich, USA	50 mM
Glycerol 2-phosphate	Sigma-Aldrich, USA	10 mM
Sodium fluoride	Sigma-Aldrich, USA	50 mM
Sodium pyrophosphate	Sigma-Aldrich, USA	5 mM
EDTA	Sigma-Aldrich, USA	1 mM
Sodium orthovanadate*	Sigma-Aldrich, USA	1 mM
Dithiothreitol*	Sigma-Aldrich, USA	1 mM
Phenylmethylsulfonyl fluoride*	Sigma-Aldrich, USA	1 mM
Aprotinin*	Merck Millipore, USA	153 nM
Leupeptin*	Chemicon, Japan	2 µM
Okadaic acid*	Enzo Life Sciences, USA	100 nM
MilliQ water	-	To 500 ml

*Ingredients added immediately prior to use.

HEPES Lysis Buffer		
Ingredient	**Supplier**	**Final Concentration**
Hepes	Sigma-Aldrich, USA	50 mM
Sodium chloride	Sigma-Aldrich, USA	100 mM
Sodium fluoride	Sigma-Aldrich, USA	50 mM
Glycerol 2-phosphate	Sigma-Aldrich, USA	50 mM
EDTA	Sigma-Aldrich, USA	2 mM
EGTA	Sigma-Aldrich, USA	2 mM
Glycerol	Sigma-Aldrich, USA	10 %
Igepal*	Sigma-Aldrich, USA	1 %
cOmplete, EDTA-free protease inhibitor mix*	Roche, Switzerland	1 x
Sodium orthovanadate*	Sigma-Aldrich, USA	1 mM
Okadaic acid*	Enzo Life Sciences, USA	100 nM

*Ingredients added immediately prior to use.

Lysis Buffer A (Risco et al., 2012)		
Ingredient	**Supplier**	**Final Concentration**
Tris/HCl (pH7.5)	Sigma-Aldrich, USA	50 mM
EDTA	Sigma-Aldrich, USA	1 mM
EGTA	Sigma-Aldrich, USA	1 mM
Sodium pyrophosphate	Sigma-Aldrich, USA	5 mM
Glycerol 2-phosphate	Sigma-Aldrich, USA	50 mM
2-mercaptoethanol	Sigma-Aldrich, USA	0.1 %
Sodium chloride	Sigma-Aldrich, USA	150 mM
Sodium fluoride	Sigma-Aldrich, USA	10 mM
Sucrose	Sigma-Aldrich, USA	270 mM
cOmplete, EDTA-free protease inhibitor mix*	Roche, Switzerland	1 x
Phenylmethylsulfonyl fluoride*	Sigma-Aldrich, USA	0.1 mM
Sodium orthovanadate*	Sigma-Aldrich, USA	1 mM
Triton-X100*	Sigma-Aldrich, USA	1 %

*Ingredients added immediately prior to use.

Laemmli Buffer		
Ingredient	**Supplier**	**Final Concentration**
Glycerol	Sigma-Aldrich, USA	20 %
Sodium dodecyl sulphate	Sigma-Aldrich, USA	4 % (w/v)
Tris/HCl pH 6.8	Sigma-Aldrich, USA	120 mM
Bromophenol blue	Sigma-Aldrich, USA	0.02 % (w/v)
Distilled H_20	-	To 50 ml
+/- 2-Mercaptoethanol	Sigma-Aldrich, USA	10 %

Strong Cation Exchange Buffers		
Ingredient	**Buffer A**	**Buffer B**
Ammonium formate	10 mM	500 mM
Acetonitrile	25 %	25 %
pH	3.0	6.8

LC-MS/MS Buffers		
Ingredient	**Buffer A**	**Buffer B**
Formic acid	0.1 %	0.1 %
DMSO	5 %	5 %
Acetonitrile	-	77.5 %
Water	95 %	17.5 %

Kinase Buffer		
Ingredient	**Supplier**	**Final Concentration**
HEPES pH 7.4	Sigma-Aldrich, USA	50 mM
$MnCl_2$	Sigma-Aldrich, USA	10 mM
TCEP	Sigma-Aldrich, USA	1 mM
Brij 35	Sigma-Aldrich, USA	0.03 %
Bovine serum albumin	Sigma-Aldrich, USA	0.01 %

3.2 Cell culture media

All foetal calf serum (FCS) was heat inactivated by incubation at 56 ºC for 30 mins.

SILAC RAW264.7 Medium			
Ingredient	**Supplier**	**K0R0 Final Concentration**	**K8R10 Final Concentration**
RPMI without arginine or lysine	NIMR Media Kitchen	To 500 ml	
5 kDa MWCO dialysed FCS	Dundee Cell Products, UK	10 %	
$^{12}C_6{}^{14}N_4$ L-arginine	Sigma-Aldrich, USA	482 µM	-
$^{12}C_6{}^{14}N_2$ L-lysine	Sigma-Aldrich, USA	799 µM	-
$^{13}C_6{}^{15}N_4$ L-arginine	Sigma-Aldrich, USA	-	482 µM
$^{13}C_6{}^{15}N_2$ L-lysine	Cambridge Isotope Laboratories Inc., USA	-	799 µM
Proline	Sigma-Aldrich, USA	261 µM	261 µM

Standard BMDM Medium			
Ingredient	**Supplier**	**Differentiation Medium**	**Starvation Medium**
		Final Concentration	
RPMI 1640	Sigma-Aldrich, USA	To 500 ml	To 500 ml
Foetal calf serum	Biosera, France	10 %	1 %
L929-cell conditioned media	NIMR Media Kitchen	20%	-
Sodium pyruvate	Sigma-Aldrich, USA	1 mM	1 mM
HEPES	Sigma-Aldrich, USA	10 mM	10 mM
L-glutamine PenStrep	Sigma-Aldrich, USA	1/500	1/500
Non-essential amino acids	Life Technologies, USA	1 x	1 x
2-Mercaptoethanol	Life Technologies, USA	50 µM	50 µM

Weintz et al. BMDM Medium			
Ingredient	**Supplier**	**Non-Differentiating Medium**	**Differentiating Medium**
DMEM without arginine or lysine	NIMR Media Kitchen	To 500 ml	
5 kDa MWCO dialysed FCS	Dundee Cell Products, UK	10 %	
Sodium pyruvate	Sigma-Aldrich, USA	1 mM	
HEPES	Sigma-Aldrich, USA	10 mM	
L-glutamine PenStrep	Sigma-Aldrich, USA	1/500	
Non-essential amino acids	Life Technologies, USA	1 x	
2-Mercaptoethanol	Life Technologies, USA	50 µM	
IL-3	Insight Biotechnology, UK	20 ng/ml	-
IL-6	Insight Biotechnology, UK	50 ng/ml	-
SCF	Insight Biotechnology, UK	50 ng/ml	-
M-CSF	Life Technologies, USA	40 ng/ml	40 ng/ml
$^{12}C_6{}^{14}N_4$ L-arginine	Sigma-Aldrich, USA	482 µM	482 µM
$^{12}C_6{}^{14}N_2$ L-lysine	Sigma-Aldrich, USA	799 µM	799 µM

Ley Laboratory SILAC BMDM Medium					
Ingredient	**Supplier**	**Differentiation Medium**		**Starvation Medium**	
		Final K0R0 Concentration	**Final K8R10 Concentration**	**Final K0R0 Concentration**	**Final K8R10 Concentration**
RPMI without arginine or lysine	NIMR Media Kitchen	To 500 ml		To 500 ml	
1 kDa MWCO dialysed FCS	Dundee Cell Products, UK	10 %		1 %	
2 kDa MWCO dialysed L929-cell conditioned media	NIMR Media Kitchen, dialysed by CRUK Cell Services	20%		-	
Sodium pyruvate	Sigma-Aldrich, USA	1 mM		1 mM	
HEPES	Sigma-Aldrich, USA	10 mM		10 mM	
L-glutamine PenStrep	Sigma-Aldrich, USA	1/500		1/500	
Non-essential amino acids	Life Technologies, USA	1 x		1 x	
2-Mercaptoethanol	Life Technologies, USA	50 µM		50 µM	
$^{12}C_6{}^{14}N_4$ L-arginine	Sigma-Aldrich, USA	482 µM	-	482 µM	-
$^{12}C_6{}^{14}N_2$ L-lysine	Sigma-Aldrich, USA	799 µM	-	799 µM	-
$^{13}C_6{}^{15}N_4$ L-arginine	Sigma-Aldrich, USA	-	482 µM	-	482 µM
$^{13}C_6{}^{15}N_2$ L-lysine	Cambridge Isotope Laboratories Inc., USA	-	799 µM	-	799 µM
Methionine	Sigma-Aldrich, USA	201 µM		201 µM	

3.3 Cell culture

3.3.1 Generation of bone marrow-derived macrophages (BMDM)

Protocol adapted from Weintz et al. (2010)

All work was done in compliance with the United Kingdom Home Office regulations. Mouse strains were bred in specific pathogen-free environments at The

Francis Crick Institute, Mill Hill Laboratory. All experimental mice were fully backcrossed onto the C57BL/6 background and genotyped to ensure they carried the correct mutations. On day 0, stem cells were harvested from male mice aged 8-12 weeks by flushing femurs and tibias with media. The stem cells were centrifuged (277 x g, 5 mins) and resuspended in 1 ml ACK buffer for 1 minute to lyse erythrocytes, before blank media was added to stop the hypotonic lysis. The stem cells were centrifuged as before, washed with blank media and finally resuspended in media. Cell numbers were determined using a CASY® Technology Cell Counter (Roche, Switzerland). Cells were plated at 5 x 10^6 on 9 cm Sterilin bacteriological dishes (Thermo Fisher Scientific, USA) in 10 ml Weintz et al. (2010) BMDM Medium without cytokines and rested overnight to allow differentiated bone marrow resident macrophages to adhere to the dish. The following day non-adherent cells were collected and adherent cells were discarded. Non-adherent cells were centrifuged (277 x g, 5 mins) and resuspended in 1 ml Weintz et al. (2010) BMDM Non-Differentiating Medium. Cells were plated in triplicate at 1 x 10^7 cells per 9 cm bacteriological dish in Weintz et al. (2010) BMDM Non-Differentiating Medium.

On days 4, 7 and 10 the non-adherent cells were collected and placed on ice. Adherent cells were detached by incubating at 37 ºC for 15 mins using 4 ml accutase (Sigma-Aldrich, USA) diluted 1:4 with PBS and scraping. Cells were then centrifuged (277 x g, 5 mins), resuspended with the non-adherent cells plus fresh Weintz et al. (2010) BMDM Non-Differentiating Medium and replated on Sterilin bacteriological dishes. On day 13 adherent and non-adherent cells were collected as above, washed with PBS, then replated on bacteriological plates in Weintz et al. (2010) BMDM Differentiating Medium. On day 16 non-adherent cells were discarded and adherent cells were collected and centrifuged at 277 x g for 5 mins. The cells were resuspended in Weintz et al. (2010) BMDM Medium with only 1 % FCS and without cytokines, plated at 25 x 10^6 cells per 14 cm Nunc™ tissue culture treated dish (Thermo Fisher Scientific, USA), and rested overnight to reduce background signalling levels.

Ley laboratory protocol for generation of BMDM

Stem cells were harvested and processed as detailed above then 8 x 10^6cells were plated in 20 ml Standard BMDM Differentiation Medium on 14 cm bacteriological dishes. On day 4, an additional 20 ml fresh media was added. On day 7 the cells were detached by incubating for 10 mins at 37 ºC with Dulbecco's PBS (Life Technologies, USA) supplemented with 5 % FCS (Biosera, France) and 2.5 mM EDTA (Life Technologies, USA). The cells were centrifuged at 277 x g for 5 mins and then counted using the CASY® Technology Cell Counter. Finally cells were re-plated at 12 x 10^6cells on 14 cm tissue culture treated dishes in Standard BMDM Starvation Medium and rested overnight.

Ley laboratory protocol for SILAC BMDM

To generate K0R0 unlabelled or K8R10 labelled SILAC BMDM, stem cells were harvested and processed as detailed above then 8 x 10^6cells were plated per 14 cm Sterilin bacteriological dish in 25 ml K0R0 or K8R10 Ley Laboratory SILAC BMDM Differentiation Medium. The same mice were used to produce both K0R0 and K8R10 lysates for each condition by dividing the precursor cells in half prior to culture. The cells from each mouse were cultured and treated separately. On day 4, the media was removed and cells still in suspension were collected by centrifugation at 277 x g for 5 mins. The cells were re-suspended in 25 ml fresh K0R0 or K8R10 Ley Laboratory SILAC BMDM Differentiation Medium per plate and then returned to the original plates. On day 6, the adherent cells were detached from the dishes by incubating with Dulbecco's PBS/2.5 mM EDTA for 10 mins at 37 ºC, collected by centrifugation at 277 x g for 5 mins and then counted using the CASY® Technology Cell Counter. 12 x 10^6cells were plated per 14 cm Nunc™ tissue culture treated dish in K8R10 Ley Laboratory SILAC BMDM Starvation Medium and rested overnight.

To establish the length of time required to achieve sufficient incorporation of labelled amino acids, parallel cultures were set up in Ley Laboratory SILAC BMDM Differentiation Medium. In this instance, the media were also changed a second

time on day 7. Cells were lysed every second day up to 10 days; on days 2 and 4 this included collection and lysis of the non-adherent as well as adherent cells. However at later time points only adherent cells were lysed because macrophages should have differentiated and attached by this stage.

Stimulation in SILAC lysates was checked individually by immunoblotting to ensure that activation of the NFκB1 p105/TPL-2/ERK1/2 pathway and other MAP kinase pathways was in line with what we expect from the stimulation, inhibition and mutant conditions (Appendix A). Finally the lysates were combined in protein ratios of 1:1 according to the mixes shown in the experimental design table (table 5.1). Only stimulated cell lysates were compared.

3.3.2 RAW264.7 cell culture

SILAC labelling

RAW264.7 cells, obtained from Dundee University (UK), were cultured in SILAC RAW264.7 media (section 3.2). The cells were split every 3 days by detaching with Dulbecco's PBS/2.5 mM EDTA and seeded in tissue culture treated flasks. After 6 passages, cells were lysed to check SILAC incorporation was greater than 90 % and stocks of the labelled RAW264.7 cells were frozen in FCS with 10 % DMSO. The cells were then expanded and the spike-in lysate produced in 3 equal batches over 7 days. In preparation for stimulation the cells were plated in SILAC RAW264.7 Medium without FCS. Cells were either stimulated with 100 ng/ml LPS from *Salmonella minnesota R595* (Enzo Life Sciences Inc., USA) for 15 mins or left unstimulated. On ice the medium was removed and the cells were washed with ice cold Dulbecco's PBS and lysed in Detergent Free Lysis Buffer by scraping the plates. Lysates were collected and clarified by centrifugation at 21,100 x g for 15 mins, followed by snap freezing in liquid nitrogen for storage at -70 ºC. All K8R10 SILAC labelled lysates from the stimulated and unstimulated RAW264.7 cells were combined to produce a spike-in lysate which contained as many relevant phosphopeptides as possible. This spike-in lysate was then combined in a 1:1 protein ratio with 2.5 mg of the unlabelled BMDM lysate.

3.4 Cell treatments, lysis and protein extraction

Cells were stimulated with 100 ng/ml LPS from *Salmonella minnesota R595* (Enzo Life Sciences Inc., USA) for 15 mins or left unstimulated. 15 mins was chosen as the peak of ERK1/2 activation and a time point where secondary effects of protein production and release of autocrine signals should be minimal. MEK1/2 inhibitor treated cells were pre-treated with 0.1 μM PD0325901 (University of Dundee, UK) for 10 mins (Bain et al., 2007). To block IKK2 catalytic activity, cells were pre-treated with 10 μM BI605906 (University of Dundee, UK) for 1 hour (Clark et al., 2011). Mock-treatment with similarly diluted DMSO was used to control for use of the use of inhibitors.

After stimulation, tissue culture plates were placed on ice, medium was removed and cells were washed with ice cold Dulbecco's PBS. Cells were lysed by scraping the plates in appropriate lysis buffer. For western blotting, cells were lysed in S-Lysis Buffer, while those for mass spectrometry were lysed in Detergent Free Lysis Buffer. For MKK3, MKK4 and MKK6 immunoprecipitation, cells were lysed in HEPES Lysis Buffer. Cells for p38γ/δ immunoprecipitation were stimulated with 100 ng/ml LPS for 30 mins, as the peak of p38 activation occurs later than ERK1/2, and lysed in Lysis Buffer A (Risco et al., 2012). Lysates were collected and clarified by centrifugation at 21,100 x g for 15 mins, followed by storage at -20 ºC or snap freezing in liquid nitrogen for storage at -70 ºC. Protein concentrations were measured by Pierce™ reducing agent-compatible BCA assay (Thermo Fisher Scientific, USA), according to the manufacturer's instructions.

3.5 Immunoblotting and antibodies

For immunoblotting cells were lysed standard lysis buffer. Equal amounts of protein were separated by SDS-PAGE and transferred to PVDF membranes (Bio-Rad, USA). Non-specific binding was prevented by incubating the membranes in PBS/0.05 % Tween/5 % milk for 1 hour. Membranes were incubated with primary antibody overnight, followed by incubation with an appropriate secondary antibody for approximately 2 hours. Bound antibody was visualised using ECL (enhanced

chemiluminescence; GE Healthcare, UK) and exposing an X-ray film. Quantification of relative signal levels was performed by densitometry using a Bio-Rad (USA) GS-800 densitometer and the QuantityOne software v4.6.9 (Bio-Rad, USA).

Primary antibodies used were: ERK1/2 (#44654, lot 913234A), phospho-T185/Y187 ERK1/2 (#44680, lot 1440090A), and phospho-T183/Y185 JNK (#44682 lot 290218D), all from Life Technologies (USA); phospho-S933 NFκB1 p105 (#4806 lot 4), phospho-S217/221 MEK1/2 (#9121 lot 31), phospho-T180/Y182 p38 (#4511 lot 5), p38 (#9212 lot 20), phospho-S176/180 IKKα/β (#2697 lot 16), phospho-S257/T261 MKK4 (#9156 lot 2), phospho-S189/207 MKK3/6 (#9236 lot 5 and #9231 lot 9), MKK3 (#5674 lot 1), MKK6 (#9264 lot 2), eEF2 (#2332 lot 5), phospho-T56 eEF2 (#2331 lot 7), RSK2 (#9340 lot 1), phospho-S380 p90RSK (#9341 lot 8) and phospho-T573 p90RSK (#9346 lot 4) all from Cell Signaling Technology (USA); MEK1/2 (9G3) (#sc-81504 lot E0911), TPL-2 (H-7) (#sc-373677 lot F1112), and MKK4 (#sc-837 lot E077), all from Santa Cruz Biotechnology (USA); α-tubulin (produced in-house from a clone kindly provided by Keith Gull, University of Oxford, UK) was used as a loading control protein for whole cell lysates. Secondary antibodies used were goat anti-rabbit and goat anti-mouse (#4050-05 and #1010-05 respectively, Southern Biotech, USA) conjugated to horse radish peroxidase.

3.6 Flow cytometry

On day 7 of culture SILAC labelled and unlabelled BMDM were collected from culture dishes by incubating with Dulbecco's PBS/2.5 mM EDTA for 10 mins at 37 ºC. They were then counted using the CASY® Technology Cell Counter. Approximately 5 x 10^6 BMDM cells per condition were washed with PBS/3 mM sodium azide/1 % FCS. They were then incubated in 100 µl 24G2 Fc receptor blocker (in house) diluted 1/10 in PBS Azide/1 % FCS for 15 mins on ice in order to block the Fc receptors on the cell surface. The Fc receptor blocker was washed off and then the cells were incubated with 100 µl anti-F4/80 antibody coupled to the fluorophore APC (#17-4801 lot, E07285-1634) from eBioscience (USA) which had

been diluted 1/200 in PBS Azide/1 % FCS on ice with protection from light. After incubating for at least 20 mins the antibody was washed off and the cells were resuspended in 300 µl 7-amino-actinomycin D (7-AAD, in house) diluted 1/200 in PBS Azide/1 % FCS. Levels of F4/80 on the cell surface were measured on the FACSCalibur™ (BD Biosciences, USA) and analysed using FlowJo v8.8.7 (USA). Dead cells were excluded based on forward scatter and presence of 7-AAD staining.

3.7 Sample preparation for mass spectrometry

Carried out by Dr. Helen Flynn and Dr. Bram Snijders at The Francis Crick Institute, Clare Hall Laboratory.

3.7.1 Protein digestion

Lysates were reduced with 7 µl 1 M dithiothreitol (DTT) for 25 mins at 56 °C and then alkylated in the dark with 14 µl 1 M iodoacetamide for 30 mins at room temperature. This reaction was quenched with a further 7 µl 1 M DTT. Lysates were diluted with 6 ml 50 mM ammonium bicarbonate (pH 8) to reduce the urea concentration to 2 M. To digest proteins into peptides, sequencing grade porcine trypsin (#V5280, Promega, USA) was added at 1:50 (based on protein concentrations) and incubated overnight at 37 °C. 24 µl trifluoroacetic acid (TFA) was then added to give a final concentration of 0.4 % and samples were centrifuged for 5 mins at 3,220 x g. Supernatants were filtered through 0.22 µm filters.

To desalt samples, C18 Sep Pak Lite columns with 130 mg bed volume (Waters, USA) were used with a vacuum manifold set at -1 psi to pass each solution slowly through the solid phase extraction cartridge. Columns were washed with 3.2 ml acetonitrile, conditioned with 1.1 ml 50 % acetonitrile, 0.5 % acetic acid and then equilibrated using 3.2 ml 0.1 % TFA. Loaded samples were desalted using 3.2 ml 0.1 % TFA followed by washing with 325 µl 0.5 % acetic acid. 1.8 ml 50 % acetonitrile, 0.5 % acetic acid (vacuum pressures up to -5 psi) was used to elute samples. A 10 µl aliquot of each eluate was used to evaluate the efficiency of the

digest by liquid chromatography-tandem mass spectrometry (LC-MS/MS) and the remainder was dried by vacuum centrifugation.

Dried samples were then resuspended by adding 50 µl 50 mM ammonium bicarbonate, 10 % acetonitrile and sonicating. A further 100 µl of 50 mM ammonium bicarbonate, 10 % acetonitrile containing 5 µg of Lys-C (#V1671, Promega, USA) was added to the samples, which were then mixed vigorously and incubated for 2 hours at 37 °C. Sequencing grade porcine trypsin (#V5280, Promega, USA) was added to each and incubated overnight at 37 °C. 1.75 ml 0.5 % TFA was added to the digested samples which were then vortexed and sonicated before centrifugation at 20,817 x g. Supernatants were then filtered through 0.22 µm filters and then desalted using C18 Sep-Pak® Lite columns with 130 mg bed volume with a vacuum manifold, as described above. As previously, 10 µl aliquots were taken to evaluate the digest by LC-MS/MS and the remaining samples were dried by vacuum centrifugation.

3.7.2 Phosphopeptide enrichment

Strong cation exchange fractionation

Samples were fractionated by strong cation exchange (SCX) to reduce the complexity of each fraction. This was done using an Agilent Technologies (USA) liquid chromatography system with a PolySULFOETHYL A™ column (100 x 4.6 mm, average particle size 5 µm, average pore size 200 Å) (Poly LC, USA). Samples were resuspended in 110 µl SCX buffer A, sonicated for 15 mins and then centrifuged at 20,817 x g for 5 mins prior to injection. Samples were separated over a 10 min gradient to 80 % SCX buffer B with a flow rate of 1 ml/min. Six fractions of 2 ml were collected, starting 1 min after injection. Between each sample, the column was washed with 100 % buffer B and re-equilibrated for 15 mins. All fractions were dried by vacuum centrifugation.

Titanium dioxide enrichment

SCX fractions were solubilised in 1 ml 80 % acetonitrile, 5 % TFA, 1 M glycolic acid and sonicated for 10 mins. Each fraction was then added to 5 mg of titanium dioxide beads (GL Sciences, Japan) and mixed thoroughly to resuspend. Peptide samples and beads were incubated for 10 mins with shaking at 1400 rpm on the thermomixer at room temperature to allow phospho-peptides to bind to the beads. Beads were pelleted by centrifugation at 1,000 x g for 1 min. Supernatants containing non-phosphorylated peptides were carefully aspirated without disturbing the beads.

For the first wash step, 150 µl 80 % acetonitrile, 5 % TFA, 1 M glycolic acid was added to the beads and samples were incubated for 10 mins with shaking at room temperature. Beads were pelleted by centrifugation at 1,000 x g for 1 min and the supernatant discarded. 150 µl of 80 % acetonitrile, 1 % TFA was added to the beads for the second wash step and samples were incubated for 10 mins with shaking at room temperature. Beads were pelleted by centrifugation at 1,000 x g for 1 min and the supernatant discarded. 150 µl of 10 % acetonitrile, 0.2 % TFA was added to the beads for the third wash step. Samples were incubated for 10 mins with shaking at room temperature, the beads pelleted by centrifugation at 1,000 x g for 1 min and supernatant discarded. Any remaining supernatant was removed by drying in a vacuum centrifuge.

In order to elute the phosphopeptides 100 µl 1 % ammonium hydroxide was added followed by incubation for 10 mins with shaking at room temperature. Eluate was removed and transferred to a fresh tube. A second elution was then done using 100 µl 5 % ammonium hydroxide and incubating for 10 mins with shaking at room temperature. Eluate was collected and combined with that from the first elution. The combined eluate was then filtered through C8 material to remove any remaining beads. The C8 material was washed with 50 µl 60 % acetonitrile which was collected ensure good recovery of peptides. Finally, samples were dried by vacuum centrifugation.

Sample clean-up

200 µl tips packed with an Empore C18 membrane (3M, USA) were washed with 100 µl methanol and centrifuged for 2 mins (425 - 1700 x g). 200 µl 1 % TFA was then used to equilibrate the C18 tips followed by centrifugation for 3 mins. The enriched phosphopeptides were resuspended in 100 µl 1 % TFA by sonicating for 15 mins and loaded onto the C18 tips by centrifugation (3 mins). C18 tips were washed 4 times by addition of 300 µl 1 % TFA and centrifugation (4 mins). Phosphopeptides were eluted with 50 µl 80 % acetonitrile, 5 % TFA by centrifugation at for 2 mins and dried by vacuum centrifugation.

3.7.3 Liquid chromatography-tandem mass spectrometry

Each phosphopeptide fraction was resuspended in 35 µl 1 % TFA and sonicated for 15 mins. 10 µl of each sample was injected onto a PepMap™ 100 C18 pre-column (5 mm x 300 µm, average particle size 5 µm and pore size 100 Å; Thermo Fisher Scientific, USA) followed by an EASY-Spray™ PepMap RSLC C18 analytical column (50 cm x 75 µm, average particle size 2 µm and pore size 100 Å; Thermo Fisher Scientific, USA). Phosphopeptides were eluted over a 3 hour multi-step gradient using LC-MS/MS buffers A and B increasing from 2 % to 90 % buffer B. Samples were injected onto an LTQ-Orbitrap Velos™ mass spectrometer (Thermo Fisher Scientific, USA) in triplicate using a different activation method (collision induced dissociation - CID, multi-stage activation - MSA or higher energy collisional dissociation - HCD) for each replicate. In each case the top 10 most abundant phosphopeptides were fragmented for identification.

3.8 Phosphoproteomic data processing and analysis

3.8.1 Spike-in SILAC

The raw mass spectrometry files were analysed using MaxQuant v1.3.0.5 software (Cox and Mann, 2008) to identify and quantify the phosphopeptides present. The obtained spectra were searched against mouse (*Mus musculus*) proteome

sequences obtained from the UniProt database (Magrane and Consortium, 2011, accessed 14/3/11) concatenated with a list of common contaminants. In addition, the spectra were searched against a decoy database of reverse peptide sequences to gauge the number of false positive identifications present in the dataset. The list of identified phosphopeptides was truncated using a 1 % false discovery rate (FDR) cutoff (determined by matches in the reverse sequence decoy database). For sites found on multi-phosphorylated peptides, the least modified peptide ratio was reported. From the MaxQuant output, the "Phospho (STY)Sites" table was uploaded into the Perseus v1.2 analysis program (Cox and Mann, 2012). The ratios were logarithmically transformed with a base of 2 in order to distribute the ratios between zero and 1 evenly with those of 1 and greater. The log ratios for the RAW264.7 vs TPL-2^{D270A} were then subtracted from the log ratios for RAW264.7 vs PD0325901-treated wild type in order to produce a ratio-of-ratios, the values of which represent the relative phosphopeptide level between wild type and TPL-2^{D270A}. The intensities were logarithmically transformed with a base of 10.

The identified phospho-sites were annotated with further information including Gene Ontology protein annotations (Ashburner et al., 2000, v1.2, accessed 22/9/11), known phosphorylation sites and regulatory kinases downloaded from the PhosphoSitePlus® database (www.phosphosite.org, Hornbeck et al., 2012 accessed 9/6/12), and information on whether the site conforms to the known sequence motifs of various kinases. In order to identify proteins that were likely to be regulated by TPL-2, the built-in Perseus test, Significance B was used with a p-value cutoff of 0.05. This test is based on z-statistics for identifying outliers from the mean in a normal distribution. A posterior error probability (PEP) cutoff of 1 x $10^{-5}$was used to remove poor quality peptide identifications.

3.8.2 Standard SILAC

The raw mass spectrometry data were processed using MaxQuant v1.3.0.5 and Perseus v1.4.0.2 software (Cox and Mann, 2008, 2012). A 1 % FDR cutoff and 1 x

10^{-5} PEP cutoff were used and the least modified peptide ratio was reported. For one member of each pair of label reversal mixes the ratios were inverted in order to simplify what changes in each direction mean for the level of phosphorylation of a particular site; this was achieved by dividing 1 by the ratio for each phosphosite. The ratios were logarithmically transformed with a base of 2 in order to distribute the ratios between zero and 1 evenly with those of 1 and greater. The intensities were logarithmically transformed with a base of 10.

The identified phosphosites were annotated with further information including Gene Ontology (GO) Slim annotations (Ashburner et al., 2000, v1.2, accessed 22/9/11), known phosphorylation sites and regulatory kinases downloaded from the PhosphoSitePlus® database (www.phosphosite.org, Hornbeck et al., 2012 accessed 3/6/13 and 25/11/13 respectively), and information on whether the site conforms to the known sequence motifs of various kinases. In addition, consensus motifs for TPL-2 were added (Ley Laboratory, unpublished data and Parikh et al., 2009). The built in Perseus test, Significance B, was used to identify significant outliers with a p-value of 0.01 in each of the mixes. Phosphosites that were B significant in both mixes of a label reversal pair (e.g. heavy-labelled wild type versus light-labelled mutant and heavy-labelled mutant versus light-labelled wild type) and were showing a consistent (positive or negative) response between the mixes were considered to be likely candidates for TPL-2-dependent phosphorylation sites.

3.8.3 Bioinformatics analysis

To determine significantly enriched GO cell compartment Slim terms, annotations in the phosphoproteomics dataset were compared against the annotations of all genes expressed by mouse BMDM (Ley laboratory, unpublished data) using the Chi2 test with p value cut-off of 0.05. Enrichment of GO biological process terms was determined by comparison with the entire dataset of phosphopeptides identified in this study, using the DAVID bioinformatics resource functional annotation enrichment tool (Huang et al., 2008, 2009) with a p-value cut-off of 0.02.

3.9 Immunoprecipitation

3.9.1 MKK3, MKK4 and MKK6

Cells were lysed in 500 µl HEPES Lysis Buffer per 14 cm dish. Lysates were clarified by centrifugation at 21,100 x g for 15 mins and protein concentrations determined by Pierce™ BCA assay. Lysate concentrations were equalised to 2 mg/ml by addition of lysis buffer and 1 mg of protein lysate from each condition was added to 10 µl packed Protein A Sepharose™ 4 Fast Flow beads (GE Healthcare, UK) covalently coupled to antibodies against either MKK3, MKK4 or MKK6 (#9238 lot 1, #9152 lot 3 and #8550 lot 1 respectively, Cell Signaling Technology, USA) which had been washed in HEPES Lysis Buffer. The beads and lysate were incubated for 3 hrs at 4 ºC with shaking at 1,000 rpm. The beads were pelleted by centrifugation at 100 x g for 5 mins and the supernatant collected for western blotting. The beads were then washed 3 times with 500 µl of HEPES Lysis Buffer followed by elution of bound protein using 1 bead volume of non-reducing Laemmli buffer.

3.9.2 p38γ/δ

p38γ (SAPK3) and p38δ (SAPK4) were immunoprecipitated from BMDM following a method described in Risco et al. (2012) with minor modifications. 120 x 10^6 cells per condition were lysed in Lysis Buffer A. The protein concentration in the lysates was determined by Pierce™ reducing agent-compatible BCA assay and concentrations were adjusted to 3.75 mg/ml with the lysis buffer. 10 µl of Protein G Sepharose™ 4 Fast Flow beads (GE Healthcare, UK) were coupled to 10 µg of antibody per condition by shaking for 30 min at 4 ºC. The antibodies were anti-SAPK3 (352-367) S476 2nd bleed and anti-SAPK4 (353-365) S580 2nd bleed (Dundee University, UK). 15 mg of protein per condition was added to 10 µl of anti-p38γ coupled beads and incubated on a rotor for 2 hours at 4 ºC. The supernatant from the first immunoprecipitation was added to 10 µl of anti-p38δ coupled beads and incubated on a rotor for a further 2 hours at 4 ºC. All beads were washed twice in Lysis Buffer A with 0.5 M NaCl and twice with Lysis Buffer A alone. Proteins were

eluted by boiling in 1 bead volume of Laemmli buffer without 2-mercaptoethanol.

3.10 *In vitro* kinase assays

Unactive recombinant MBP-MKK6 and inactive GST-MEK1 was obtained from Dundee University (UK). Recombinant NFκB1 p105/ABIN-2/TPL-2 and NFκB1 p105ΔDD/ABIN-2/TPL-2 complexes were produced in the Ley laboratory. 4 nM TPL-2 complex ± NFκB1 p105DD, 200 nM MBP-MKK6 or GST-MEK1 and 200 μM ATP were mixed in a final reaction volume of 40 μl using Kinase Assay Buffer (section 3.1). The reactions were incubated at room temperature for 1 hour to allow phosphorylation to proceed. Identical control reactions were incubated on ice. Reaction mixtures were resolved by SDS-PAGE and western blotted for phospho/total-MKK6 or phospho/total-MEK1/2.

4 Development of Phosphoproteomics for Primary Macrophages

4.1 Introduction

To identify TPL-2 regulated signalling pathways, a suitable cellular system was needed. As TPL-2 is essential for TLR activation of the ERK1/2 MAP kinase pathway and induction of the pro-inflammatory cytokine TNFα in macrophages, we chose to use *in vitro* cultured bone marrow-derived macrophages (BMDM) for all experiments. This widely used model system has the added advantage of providing a large quantity of homogeneous cells, a requirement for biochemical studies. In addition, genetic and pharmacological tools allowed the selective manipulation of TPL-2 and ERK1/2 signalling in this cell type.

4.1.1 *Map3k8*$^{D270A/D270A}$ mice

As discussed earlier, TPL-2 forms a complex with NFκB1 p105 and ABIN-2 in unstimulated cells and this is essential for maintenance of TPL-2 stability (Beinke et al., 2003; Papoutsopoulou et al., 2006). BMDM from TPL-2-deficient also have substantially reduced ABIN-2 levels suggesting a reciprocal relationship where TPL-2 stabilises ABIN-2 (Sriskantharajah et al., 2014). Although no function has yet been attributed to ABIN-2, TPL-2 "kinase dead" (*Map3k8*$^{D270A/D270A}$) mice were generated in the Ley laboratory to eliminate any possible confounding effects of altered ABIN-2 levels. These mice express TPL-2 and ABIN-2 at levels similar to the wild type (Sriskantharajah et al., 2014) but the mutation of aspartate (D) 270 to alanine (A) renders TPL-2 catalytically inactive (Salmeron et al., 1996). Asp270 lies in the conserved aspartate-phenylalanine-glycine (DFG) motif in the TPL-2 kinase domain and its mutation disrupts binding of the metal cofactor necessary for catalytic activity, preventing phosphorylation of substrates (Kornev et al., 2006; Duong-Ly and Peterson, 2013).

4.1.2 PD0325901 inhibitor

A small molecule inhibitor developed by Pfizer (USA), PD0325901, was the most potent MEK1/2 inhibitor available at the time of this study (Barrett et al., 2008). This compound is a non-ATP-competitive inhibitor which binds the inactive form

of MEK1/2 and prevents its activation, similar to the earlier MEK1/2 inhibitor, PD98059 from which it was derived. The IC_{50} for inhibition of MEK1 by this compound *in vitro* has been shown to be close to 1 μM and even lower in cells (Bain et al., 2007). Activation of ERK1/2 (as a read out of MEK1/2 activity) is inhibited using concentrations of PD0325901 as low as 25 nM in EGF-stimulated HeLa cells with minimal effects on other kinases at these sub-μM concentrations.

To test the effects of these tools on TPL-2 signalling pathways in an unbiased manner, it was decided to use mass spectrometry-based phosphoproteomic analysis of BMDM. It was first necessary to establish a method by which different conditions could be relatively quantified to yield the most reliable and accurate data. To this end, the use of SILAC labelling was investigated which allows direct comparison of two conditions in a physiological setting.

4.2 Can primary bone marrow derived macrophages be SILAC labelled?

Due to the strengths of SILAC labelling for accurate relative quantification of phosphopeptides (detailed above), a SILAC/mass spectrometry approach was taken for this study. SILAC labelling and phosphoproteomic analysis of BMDM was first published by the group of Prof. Matthias Mann (Weintz et al., 2010). In this study, a cocktail of cytokines was used to maintain bone marrow stem cells in an undifferentiated state for 13 days, to allow them to undergo multiple cell divisions and incorporate labelled amino acids, prior to differentiation using L929-cell conditioned medium (LCCM) for 3 days. Using this method, incorporation levels of 90 - 95 % could be achieved. Initially this protocol was implemented as described. However, it soon became apparent that bone marrow precursors were not surviving under these altered culture conditions. The most likely explanation for this was the use of FCS dialysed at 5 kDa MWCO, which lacked unlabelled amino acids but also potentially other low molecular weight components required to maintain cell viability. Comparison of cell numbers throughout the culture protocol confirmed that supplementation of medium with dialysed FCS could not support cell

expansion, in contrast to whole serum control (figure 4.1).

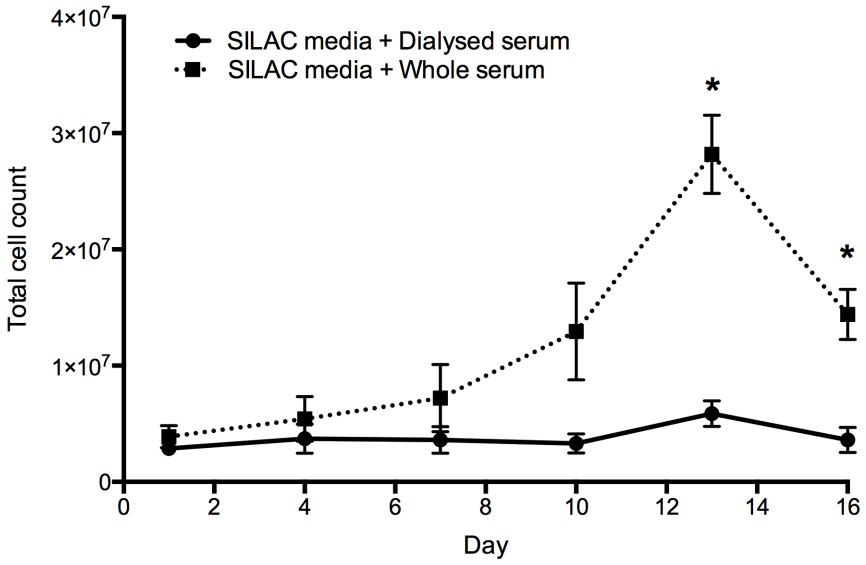

Figure 4.1: **FCS dialysed at a MWCO of 5,000 Da does not support the expansion of bone marrow precursors into bone marrow derived macrophages.** Bone marrow cells were cultured in SILAC media supplemented with either whole or 5,000 Da MWCO dialysed FCS. Cells were subcultured and counted every 3 days. Two independent experiments, significance determined by multiple t-tests with multiple comparison testing by the Holm-Sidak method, * = $p < 0.05$.

4.3 Is there an alternative if BMDM cannot be labelled?

4.3.1 Spike-in SILAC

Spike-in SILAC is a variation on the SILAC labelling technology which is particularly useful for samples that are difficult or impossible to label such as non-dividing primary cells or human tissue samples including cancer samples (Geiger et al., 2010). Spike-in SILAC uses metabolic labelling of a cell line to produce internal standards for the whole proteome of a cell population (Geiger et al., 2011). A cell line similar to the target cells of interest is labelled with stable carbon and nitrogen isotopes using SILAC and a pool of lysate is generated from this cell line (figure 4.2). This pool of lysate is then “spiked” into unlabelled test cell lysates. As long as the same spike-in lysate is used for all test conditions, the test cell

phosphoproteomes can be compared by calculating a ratio-of-ratios. Generating a ratio-of-ratios effectively eliminates the contribution of the spike-in values leaving a value for the relative expression between the different test conditions.

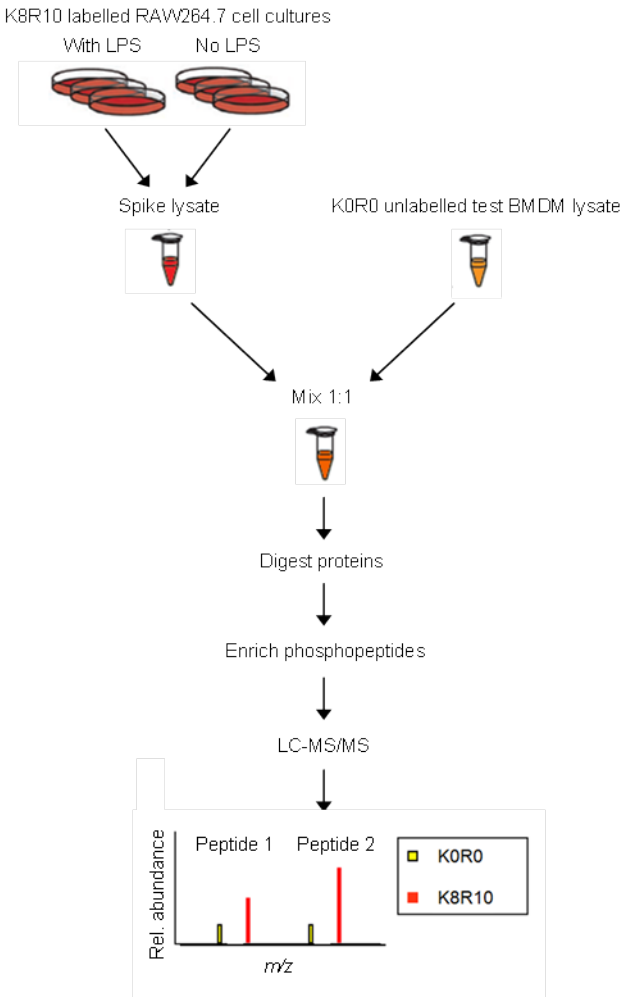

Figure 4.2: **The spike-in SILAC approach.**
A cell line (e.g. RAW264.7 macrophages) similar to the cells of interest is labelled by SILAC, expanded, left unstimulated or stimulated with LPS and then lysed to give a mixture of ”heavy”-labelled proteins, compositionally similar to the proteome of the cells to be investigated. This labelled “spike” lysate, from the 50:50 mixture of LPS stimulated and unstimulated ”heavy”-labelled RAW264.7 cells, can then be mixed with lysates from unlabelled test cells (e.g. BMDM from wild type or TPL-2^{D270A}), to provide the SILAC pairs for relative quantification of peptide levels in the test lysate. For each phosphopeptide, a ratio is calculated between the test condition and the spike lysate that allows comparison of phosphopeptide levels between different test conditions. [Adapted from Monetti et al. (2011)]

Table 4.1: **Strengths and weaknesses of the spike-in SILAC approach.**

Strengths	Weaknesses
Test cells are not labelled; their biology is normal and comparable to previous experiments.	Calculating a ratio-of-ratios compounds errors.
Possible to compare many conditions if sufficient spike-in lysate.	Protein sequences must be identical between the spike-in and the test cells.
Can be used for in vivo samples, non-dividing cells or those which are sensitive to SILAC culture conditions.	Missing data are common as peptides must be found in 2 different mixes to give one ratio-of-ratios.

RAW264.7 cell line

The RAW264.7 cell line is a macrophage cell line, which was derived in 1978 from a Abelson murine leukaemia virus-transformed tumour in a male BAB/14 mouse (Raschke et al., 1978) and is commonly used to study macrophage biology. Although the strain differs from that used here for generation of BMDM (C57BL/6), it is likely that the characteristics of RAW264.7 cells will be sufficiently similar to BMDM to allow quantification of the majority of the phosphopeptides of interest. Furthermore RAW264.7 cells have previously been SILAC-labelled by Clark et al. (2012) to investigate the biology of macrophages by phosphoproteomic analysis. Consistent with this, the RAW264.7 cells used here were successfully labelled to roughly 98 % incorporation.

Can RAW264.7 cells be used to quantify BMDM peptides?

To quantify all of the phospho-peptides present in BMDM, RAW264.7 cells must contain all the same phospho-peptides. For this reason, the response of unlabelled and SILAC-labelled RAW264.7 cells to LPS stimulation was checked (figure 4.3). LPS activation of ERK1/2 and JNK MAP kinases was found to be normal in SILAC-labelled RAW264.7 cells compared to unlabelled cells. Furthermore, LPS induction of these phosphorylations in SILAC labelled RAW264.7 cells was similar to that of unlabelled BMDM stimulated with LPS (Beinke et al., 2004).

Having confirmed that known TPL-2-dependent phosphorylations in ERK1/2 were also present in RAW264.7 cells, it was possible to use these cells for the spike-in lysate to enable quantification of different conditions in BMDM. To fully maximise the coverage of the primary BMDM phosphoproteome, both stimulated and unstimulated RAW264.7 cell lysates were included in the spike-in lysate.

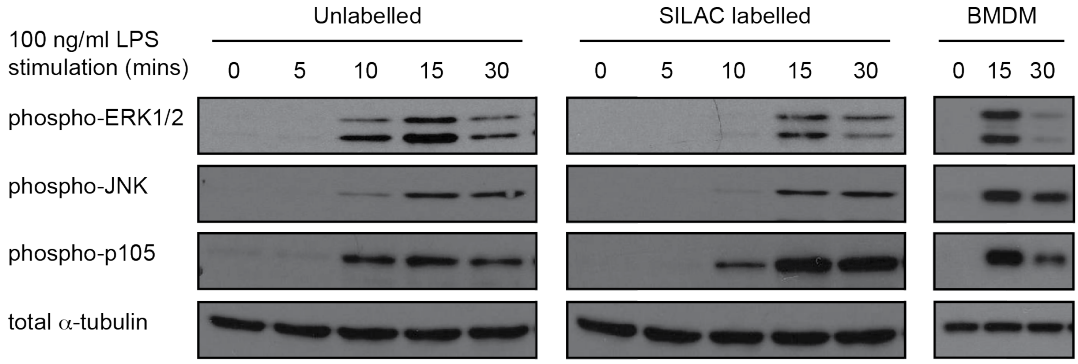

Figure 4.3: **Unlabelled and SILAC labelled RAW264.7 cell responses to LPS are comparable and similar to those of BMDM.**
RAW264.7 cells were SILAC labelled or left unlabelled, wild type BMDM were generated under unlabelled culture conditions. Cells were left unstimulated or stimulated with 100 ng/ml LPS for the indicated times before lysis. Proteins were separated by gel electrophoresis and transferred to PVDF membranes, followed by immunoblotting with the indicated antibodies. Representative of 3 independent experiments.

4.3.2 Can TPL-2-dependent phosphorylations be identified by spike-in SILAC?

A single spike in lysate was created from heavy-labelled RAW264.7 cells stimulated and lysed in 3 equal batches over 7 days. Using this one spike-in lysate, phosphoproteomics experiments were done using test lysates from a pool of 3 mice each for wild type, MEK1/2 inhibitor-treated and TPL-2 kinase dead BMDM. These conditions allowed comparison of the absence of TPL-2 activity with the absence of ERK1/2 activity from which TPL-2-dependent, ERK1/2-independent phosphorylations could be inferred. These interventions could also be compared with the control situation in wild type macrophages to ensure the phosphorylation was being affected specifically by the applied perturbation.

In order to assess the spike-in SILAC method, we first looked at the distribution of phosphopeptide ratios in the data. From ratio versus intensity scatterplots, it could be seen that the RAW264.7 and BMDM phosphoproteomes overlapped substantially as a ratio was found for large numbers of peptides (8,149 for RAW264.7 versus wild type, 9,022 for RAW264.7 versus PD0325901-treated wild type, 9,971 for RAW264.7 versus *Map3k8*$^{D270A/D270A}$). Thus, through the presence of the same peptides in both RAW264.7 and BMDM lysates, many phosphopeptides from the different BMDM conditions could be compared (figure 4.4). The RAW264.7 and wild type BMDM proteins do however display a large degree of variability in their phosphorylation status as seen through the wide distribution along the x-axis in figure 4.4A. However, after calculating the ratio-of-ratios, the consensus between phosphorylation status in the different BMDM phosphoproteomes was shown to be greater than with the RAW264.7 cells as indicated by a much narrower distribution for the ratios of ratios along the x-axis of figure 4.4B; this illustrates how the spike-in SILAC approach can work by cancelling out the contribution of the RAW264.7 peptides.

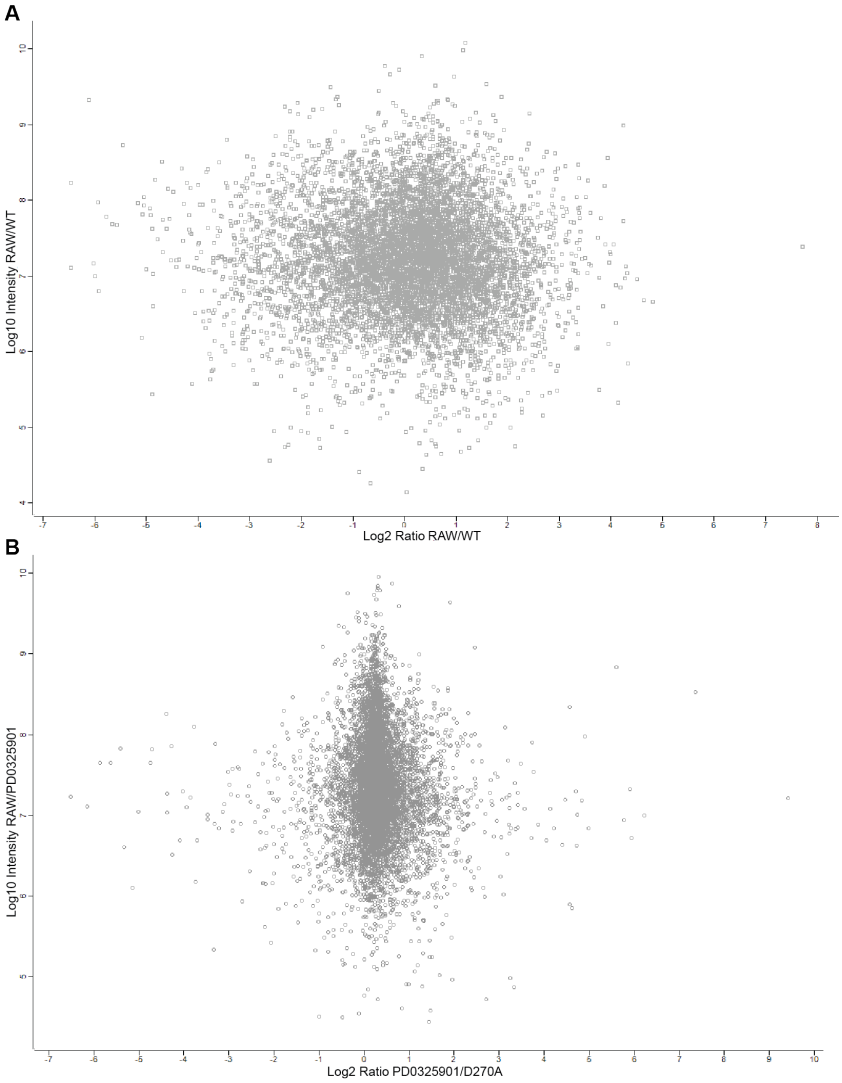

Figure 4.4: **Comparison of the phosphoproteomes of RAW264.7 cells and BMDM.**
A: Unlabelled WT and K8R10 SILAC-labelled RAW264.7 lysates were compared by mass spectrometry. X-axis shows Log_2 ratio comparing RAW264.7 cell lysates with wild type BMDM lysates; y-axis shows Log_{10} intensity for each identified phosphopeptide in this comparison. B: Ratio-of-ratios was calculated from 2 BMDM versus RAW264.7 comparisons to give a relative quantification between PD0325901-treated WT and *Map3k8*$^{D270A/D270A}$ BMDM. X-axis shows the ratio-of-ratios comparing MEK1/2 inhibitor-treated wild type with *Map3k8*$^{D270A/D270A}$ BMDM; y-axis shows Log_{10} intensity for each identified phosphopeptide in the RAW264.7 versus MEK1/2 inhibitor-treated wild type BMDM. BMDM lysates generated from a pool of 3 individual mice per condition. WT = wild type, RAW = RAW264.7 cells, PD0325901 = MEK1/2 inhibitor treated wild type BMDM, D270A = *Map3k8*$^{D270A/D270A}$ BMDM.

Potential TPL-2-regulated phosphorylations were identified as significant outliers using z-statistics, which allows identification of points which deviate from the mean value of a normal distribution (figure 4.5). This identified 1,042 pos-

sible TPL-2-dependent, ERK1/2-independent phosphorylation sites, which was reduced to 839 sites by removing those for which the protein had a low identification score (PEP > 1 x 10^{-5}). The behaviour of the known TPL-2-dependent phosphorylations in the activation loops of MEK1/2 and ERK1/2 was used to verify that the detected phosphosites were behaving as expected (figure 4.6). MEK1/2 can be phosphorylated on its activating sites in the presence of the MEK1/2 inhibitor, but not in the absence of TPL-2 kinase activity, and a MEK1/2 activation loop phosphorylation was visible by its presence as a significant outlier to the left hand side in the distribution of ratio-of-ratios ($p = 2.80 \times 10^{-20}$). It was also present in the top 10 largest ratio-of-ratios that show TPL-2 dependence (table 4.2). Phosphorylation of ERK1/2 activating sites on the other hand was not expected to be induced in either MEK1/2 inhibitor-treated or TPL-2 kinase dead conditions; therefore these sites should not have varied from the mean of the distribution, where unchanging phosphorylations (the majority of sites) fell. The data did follow this trend, although there was a slight deviation towards lower ratios for two of the three ERK1/2 activating sites. This may be because the block in ERK1/2 phosphorylation was incomplete using the small molecule inhibitor whereas the genetic blockade was complete.

Overall, analysis of the MEK1/2 and ERK1/2 internal controls confirmed that the spike-in SILAC technique could identify regulated phosphorylation sites. There is however a drawback with this comparison in that off-target effects of the MEK1/2 inhibitor were not controlled for and, due to their presence in only one side of the comparison, could potentially be false positives in the TPL-2-regulated sites. These off-target effects have been shown to include inhibition of JAK activity by experiments at GlaxoSmithKline (Dr. David Powell, personal communication).

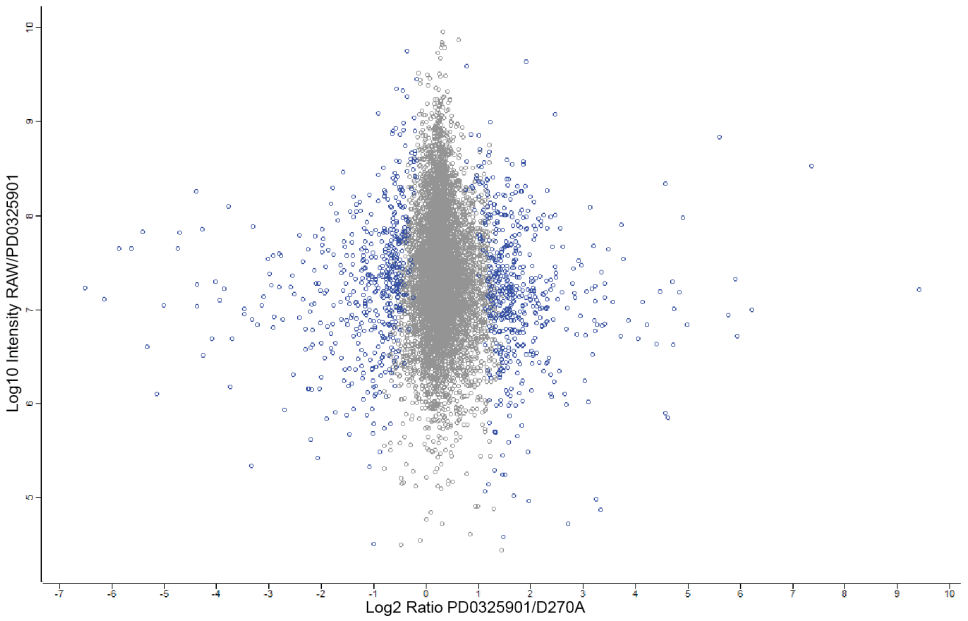

Figure 4.5: **Phosphosites showing significant deviation from the average ratio.**
A ratio-of-ratios was calculated from 2 BMDM versus RAW264.7 comparisons to give a relative quantification between PD0325901-treated WT and *Map3k8*$^{D270A/D270A}$ BMDM lysates. The Perseus algorithm, "B significance", based on z-statistics for identifying outliers from a normal distribution, was used to identify significant outliers in the comparison of PD0325901-treated wild type and *Map3k8*$^{D270A/D270A}$ BMDM. Outliers significant at $p < 0.01$ are highlighted. X-axis shows the ratio-of-ratios comparing MEK1/2 inhibitor-treated wild type with *Map3k8*$^{D270A/D270A}$ BMDM; y-axis shows Log_{10} intensity of phosphopeptides in the RAW264.7 comparison with MEK1/2 inhibitor-treated wild type BMDM. BMDM lysates generated from a pool of 3 individual mice per condition. RAW = RAW264.7 cells, PD0325901 = MEK1/2 inhibitor-treated wild type BMDM, D270A = *Map3k8*$^{D270A/D270A}$ BMDM.

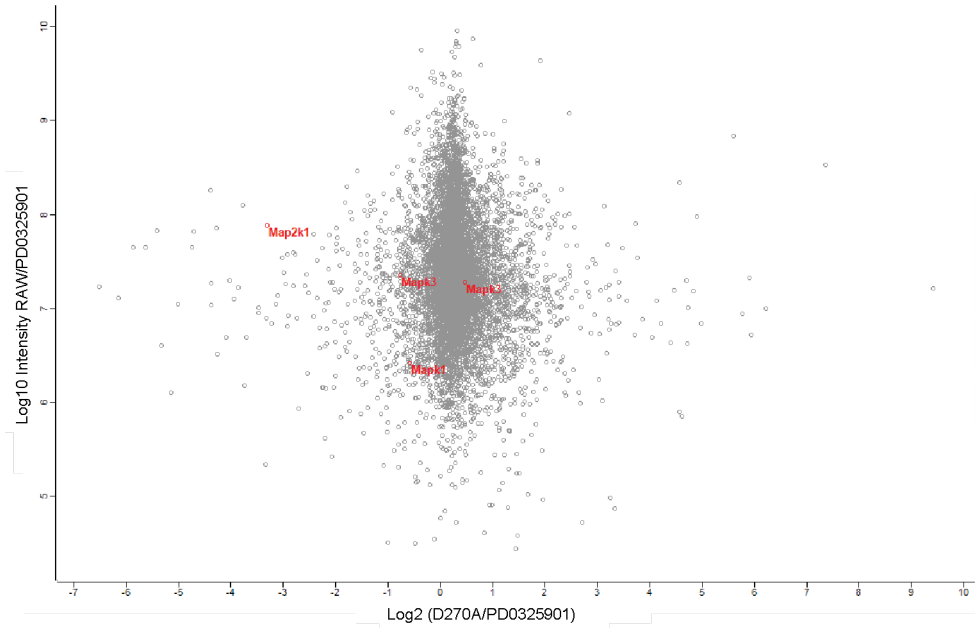

Figure 4.6: **The activation loop phosphorylations of MEK1/2 and ERK1/2 act as internal controls.**
A ratio-of-ratios was calculated from 2 BMDM versus RAW264.7 comparisons to give a relative quantification between PD0325901-treated WT and *Map3k8*$^{D270A/D270A}$ BMDM. Activation loop phosphorylations from MEK1/2 (Map2k1 - S222) and ERK1/2 (Mapk3 - T203/Y205 - and Mapk1 - T183/Y185 - respectively) are highlighted. X-axis shows the ratio-of-ratios comparing MEK1/2 inhibitor-treated wild type with *Map3k8*$^{D270A/D270A}$ BMDM; y-axis shows Log_{10} intensity of phosphopeptides in the RAW264.7 comparison with MEK1/2 inhibitor-treated wild type BMDM. BMDM lysates generated from a pool of 3 individual mice per condition. RAW = RAW264.7 cells, PD0325901 = MEK1/2 inhibitor-treated wild type BMDM, D270A = *Map3k8*$^{D270A/D270A}$ BMDM.

From the 839 phosphorylation sites, only the 403 sites with a negative ratio-of-ratios were taken for subsequent analysis because these were reduced in the absence of TPL-2 kinase activity and consequently more likely to be direct TPL-2 substrates. At this stage, it became clear that a complication with interpreting the data arose from the quantification of ratios where changes could have been occurring in either the numerator or the denominator values. To establish whether it was the PD0325901-treated wild type or the *Map3k8*$^{D270A/D270A}$ cells which were showing a change in phosphorylation for each peptide, the original RAW264.7/BMDM ratios were taken into account. This drastically reduced the list to 74 potentially interesting phosphorylation sites, the top 15 of which are shown in table 4.2. In addition, this list should be free from the risk of false positives res-

ulting from the MEK1/2 inhibitor treatment mentioned above. Unfortunately this analysis highlighted another difficulty with using spike-in SILAC to identify TPL-2 regulated pathways; there were 107 phosphosites from the list of 403 for which it was not possible to say whether the changes were in the *Map3k8*$^{D270A/D270A}$ or the PD0325901 inhibitor-treated wild type cells. These phosphopeptides had not been detected in the RAW264.7 versus wild type experiment and therefore did not have a measurement representing the unperturbed state against which to compare the effect of the perturbations. This was indicative of a much wider problem with the spike-in SILAC approach where, due to the need to calculate the ratio-of-ratios from identification of the same peptide in two different BMDM versus RAW264.7 comparisons, a large amount of data was being lost. As a further illustration, from a total of 12,726 quantified sites across all conditions in this study, only 7,273 sites could be compared between the *Map3k8*$^{D270A/D270A}$ and the MEK1/2 inhibitor-treated conditions, clearly limiting the amount of useful data that could be obtained with this approach (figure 4.7). Calculating this ratio-of-ratios had the added drawback of compounding errors, making quantification less accurate. This contrasted with standard SILAC where the comparison is made within one sample and is thus more accurate and less susceptible to loss of data. Although the spike-in SILAC yielded some useful results, this approach was not taken further due to the problem of compounding errors as well as the loss of useful data.

Table 4.2: **Phosphosites with the greatest reduction in the absence of TPL-2 activity.**

Protein names	Position	PD0325901/ D270A ratio-of-ratios	RAW264.7/ WT ratio	RAW264.7/ PD0325901 ratio	RAW264.7/ D270A ratio	Significance B p-value
Integrator complex subunit 12	S352	-6.52	-4.12	-4.72	1.80	5.34E-65
Src kinase-associated phosphoprotein 2	Y260	-6.14	-3.33	-4.40	1.75	1.92E-32
MAP2K1/2	S222	-3.30	0.78	-0.15	3.16	2.80E-20
Desmoyokin	S5101	-2.92	-2.06	-2.88	0.04	2.67E-10
AP-3 complex subunit delta-1	S755	-2.78	-1.62	-2.55	0.23	2.30E-15
TBC1 domain family member 2B	S959	-2.56	-1.65	-1.91	0.64	1.61E-13
DENN domain-containing protein 1A	S522	-2.55	-2.21	-2.97	-0.42	2.43E-12
Phosphatidylinositol 4,5-bisphosphate 3-kinase catalytic subunit β isoform	S318	-2.14	-1.77	-2.44	-0.30	2.30E-09
DENN domain-containing protein 1A	S523	-2.00	-2.21	-2.83	-0.83	1.84E-08
Uncharacterized protein KIAA0930 homolog	S351	-1.79	-0.29	0.11	1.89	3.59E-09
Vesicle-associated membrane protein 3	S15	-1.62	-0.90	-0.97	0.65	3.09E-06
Protein capicua homolog	S2275	-1.58	0.72	-0.02	1.56	3.89E-07
ATP-binding cassette sub-family F member 1	S194	-1.58	2.39	1.76	3.34	1.67E-09
Dolichyl-diphosphooligosaccharide–protein glycosyltransferase subunit STT3B	S29	-1.52	2.04	1.56	3.09	1.10E-03
Leucine-rich repeat and calponin homology domain-containing protein 3	S415	-1.47	-1.87	-2.15	-0.67	5.24E-04

Fifteen phosphosites with largest PD0325901/*Map3k8*$^{D270A/D270A}$ ratio-of-ratios shown from sites significantly down-regulated in absence of TPL-2 activity. Measured using spike-in SILAC methodology. PD0325901 = MEK1/2 inhibitor, D270A = TPL-2 kinase dead, WT =wild type.

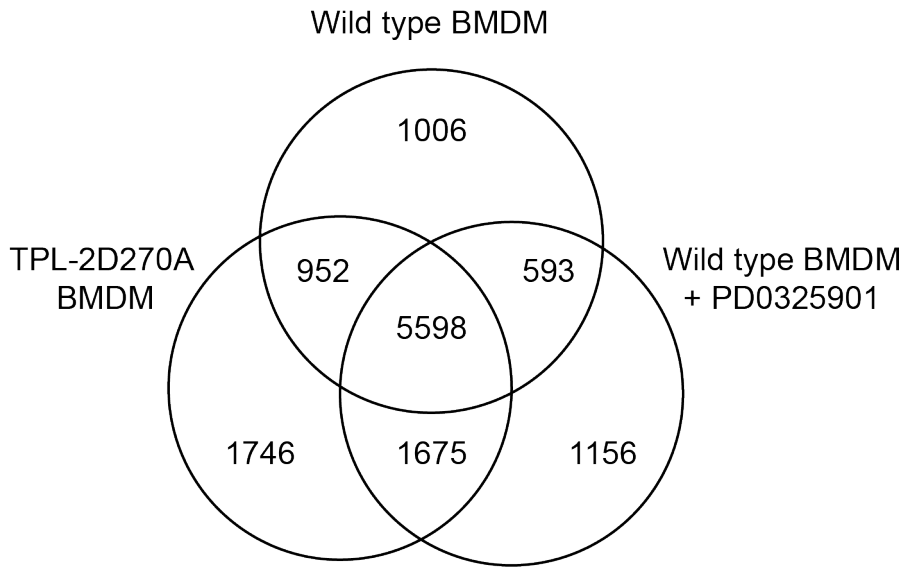

Figure 4.7: **The spike-in SILAC method leads to loss of data due to limited overlap between mass spectrometry runs.**
Three different unlabelled BMDM conditions were each compared with K8R10 SILAC-labelled RAW264.7 lysates by mass spectrometry. The overlap between each of these comparisons is shown. TPL-2D270A = TPL-2 kinase dead, PD0325901 = MEK1/2 inhibitor.

4.4 Optimisation of BMDM SILAC labelling

4.4.1 Can the Ley laboratory BMDM culture protocol be adapted for SILAC labelling?

Due to the limitations with the spike-in SILAC protocol, we attempted to adapt the standard Ley laboratory BMDM protocol for SILAC labelling. This 7 day protocol is well established and reliably produces large numbers of differentiated BMDM. In order to make it appropriate for SILAC labelling, both the FCS and the L929-cell conditioned media (LCCM) were dialysed with a low molecular weight cut-off (1 kDa and 2 kDa respectively). This lower cut-off should have removed amino acids, yet retained more low molecular weight factors to promote BMDM generation than 5 kDa dialysis. Arginine and lysine were omitted from the basal media and labelled versions were supplemented. Using this protocol, incorporation of SILAC amino acids was tested over 10 days of culture to find the optimum culture length for greatest incorporation (figure 4.8). This showed that BMDM were

successfully labelled to over 90 % after 6 days of culture, which was sufficient to achieve good coverage in a phosphoproteomics experiment. A high degree of incorporation is important to avoid skewing of the quantification between light-labelled and heavy-labelled test conditions. After 6 days, the incorporation level unexpectedly began to decline. This was difficult to explain because there was no obvious source of unlabelled amino acids; media was changed rather than added to when cells were fed in order to prevent re-incorporation. Additionally, from inspection of the incorporation check mass spectrometry data, there was no evidence of partial incorporation within individual peptides (Dr. Helen Flynn, personal communication).

Based on these results, BMDM will be cultured under SILAC conditions for 6 days but not longer to ensure the maximum degree of labelling is achieved.

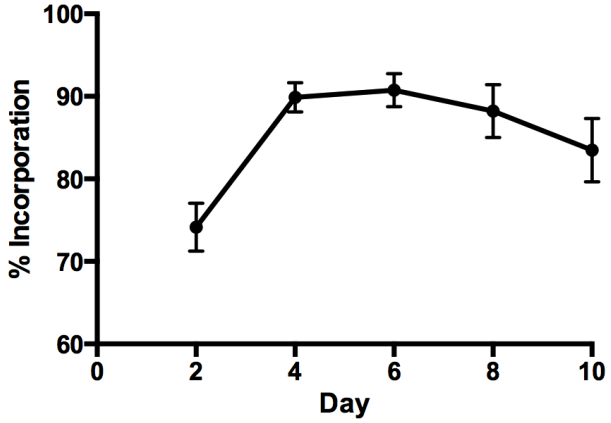

Figure 4.8: **BMDM can incorporate SILAC amino acids to over 90 %.** BMDM were cultured under SILAC conditions using FCS dialysed at 1,000 Da MWCO. Parallel cultures were lysed every 2 days and their percentage incorporation of “heavy” amino acids determined by mass spectrometry. Mean and standard deviation of all identified peptides from 4 separate cultures in 2 independent experiments.

4.4.2 Are SILAC-labelled cells comparable to unlabelled BMDM?

As the culture conditions for SILAC were non-standard, it was necessary to ensure that the biology of the cells was comparable to BMDM produced using the normal

Ley laboratory methodology. As mentioned above, the medium is supplemented with 2 kDa dialysed LCCM which contains a mixture of growth factors which drive differentiation of stem cells towards a macrophage phenotype. However, dialysis could have removed low molecular weight factors necessary for normal BMDM differentiation. Flow cytometric analysis determined that the percentage of cells expressing the macrophage marker, F4/80, was comparable between the standard culture protocol and the SILAC culture protocol (figure 4.9) suggesting that the majority of cells being analysed were indeed macrophages. Another important measure of normal biology was pathway activation in response to LPS stimulation. SILAC "heavy"-labelled wild type BMDM showed similar activation of IKK2 and phosphorylation of NFκB1 p105, known to be upstream of TPL-2/MEK1/2/ERK1/2 pathway activation, to unlabelled BMDM (figure 4.10). Activation of ERK1/2, p38α and JNK MAP kinases were also comparable between labelled and unlabelled cells. Furthermore, TPL-2 expression was normal after SILAC labelling wild type BMDM. Therefore, in terms of differentiation and response to stimulation, SILAC BMDM were comparable to unlabelled BMDM and could be used for phosphoproteomic comparisons to identify TPL-2-regulated signalling pathways.

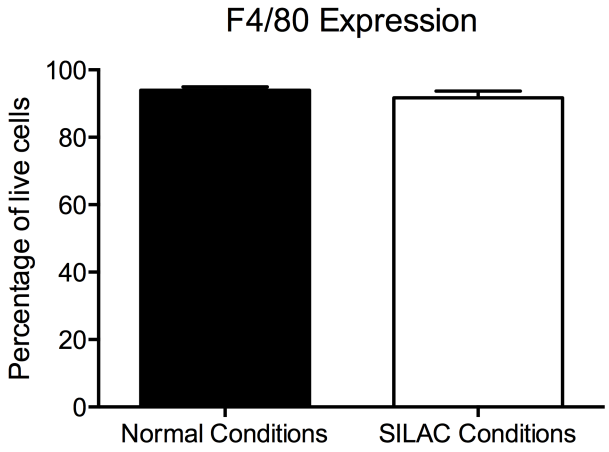

Figure 4.9: **Differentiation of BMDM is normal in SILAC conditions.** BMDM were cultured for 6 days under normal or K8R10 SILAC conditions. Cells were detached using Dulbecco's PBS/2.5 mM EDTA and stained with APC-conjugated anti-F4/80 antibodies and 7-amino-actinomycin D. Cells were analysed by flow cytometry. Dead cells were excluded based on forward scatter and presence of 7-AAD staining. Mean and standard deviation of 6-9 replicate cultures from 3 independent experiments.

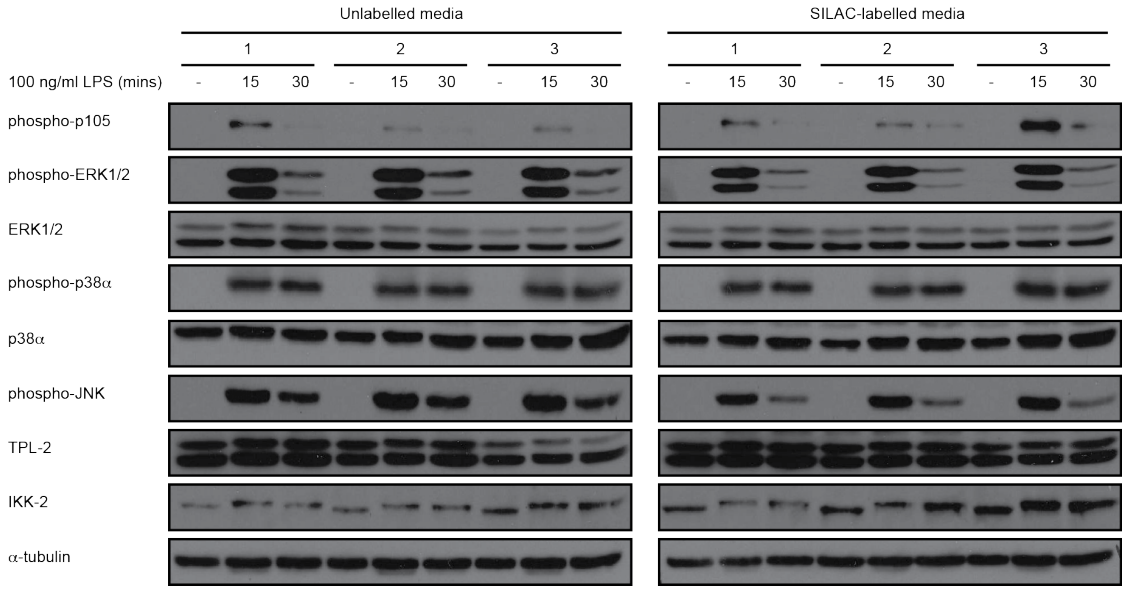

Figure 4.10: **Unlabelled and SILAC labelled BMDM show similar responses to LPS stimulation.**
BMDM were cultured for 6 days under either unlabelled conditions or K8R10 SILAC conditions with 1,000 Da MWCO dialysed FCS. Cells were left unstimulated or stimulated with 100 ng/ml LPS for 15 or 30 minutes before lysis. Proteins were separated by gel electrophoresis and transferred to PVDF membranes, followed by immunoblotting with the indicated antibodies. Three technical replicates shown; representative of 6 replicate cultures over 2 independent experiments.

4.5 Summary

To identify TPL-2-dependent signalling pathways, we developed a method to analyse the phosphoproteome of BMDM by mass spectrometry and SILAC labelling. Initial experiments using a published SILAC labelling protocol for BMDM did not support the differentiation and expansion of macrophages from bone marrow stem cells, due to the use of FCS dialysed at 5 kDa. Subsequently, an alternative spike-in SILAC approach was evaluated in a pilot experiment, as it has the advantage of labelling an established macrophage cell line, leaving the BMDM biology unaltered. Using RAW264.7 cell lysate as the spike-in standard, a comparison was made between MEK1/2 inhibitor-treated wild type and TPL-2 kinase dead BMDM producing a large number of potentially TPL-2-regulated phosphorylations. This

method was validated using the known TPL-2-dependent phosphosites in MEK1/2 and ERK1/2. However, there were limitations; in particular the loss of data vastly reduced coverage of the phosphoproteome and subsequently the chances of identifying TPL-2-regulated pathways. This could be overcome to some extent by increasing the lysate fractionation during phosphopeptide enrichment and/or increasing the mass spectrometry run time to identify as many phosphopeptides as possible. However, we concluded that it was unlikely this would solve the problem completely given that mass spectrometric analyses only sampling a fraction of the phosphoproteome (Boekhorst et al., 2011).

Having established that the use of 5 kDa dialysed FCS was a limiting factor in the primary BMDM culture, a method for SILAC labelling was devised using 1 kDa dialysed FCS and a simpler culture protocol. In spite of reports that SILAC conditions can alter cell biology (Imami et al., 2010), wild type BMDM appeared to have normal biology after culture under SILAC conditions. However, it is not possible to rule out that SILAC labelling subtly altered BMDM physiology. Using this newly developed method for SILAC labelling of BMDM, it was now possible to carry out mass spectrometric phosphoproteome analyses to identify TPL-2 regulated pathways.

5 Characterisation of the TPL-2 regulated phosphoproteome

5.1 Introduction

Once a system for ensuring accurate relative quantification between different BMDM lysates using SILAC had been established, TPL-2-regulated pathways could be identified by mass spectrometry-based phosphoproteomics (table 5.1). Pairwise comparisons between different perturbations to TPL-2 signalling were made to identify regulated phosphorylation sites. For each pair of conditions, two comparisons were made: a forward comparison and a label reversal comparison, where the condition which was “heavy”-labelled in the forward experiment was instead “light”-labelled and vice versa. This controlled for any phosphorylations that were altered by the presence of the “heavy”-labelled amino acids, as well as providing a biological replicate.

Each condition consisted of a pool of BMDM lysate from 6-7 mice which were cultured in 2-3 separate groups. This method of controlling for biological variation was chosen in preference to carrying out multiple mass spectrometry runs with lysates from individual mice. Due to the stochastic nature of phosphopeptide sampling, the degree of overlap between replicate mass spectrometry analyses of the same sample can be as low as 50 % (Gauci et al., 2009). Prior to pooling, all lysates were checked individually by immunoblotting to confirm ERK1/2 MAP kinase activation in response to LPS stimulation. In addition, mass spectrometry determined the percentage incorporation of labelled amino acids and conversion between proline and arginine, as these factors can affect phosphopeptide quantification. All heavy-labelled BMDM lysates had incorporation greater than 89 % and low arginine/proline conversion.

Table 5.1: **Phosphoproteomics experimental design table**

		K8R10 SILAC labelled						
		WT	WT + PD0325901	$TPL2^{D270A}$	$NF\kappa B1^{SSAA}$	$TPL2^{D270A}$ $NF\kappa B1^{SSAA}$	$TPL2^{D270A}$ + PD0325901	RAW264.7
K0R0 SILAC labelled	WT	Control						
	WT + PD0325901							
	$TPL2^{D270A}$							
	$NF\kappa B1^{SSAA}$							
	$TPL2^{D270A}$ $NF\kappa B1^{SSAA}$							
	$TPL2^{D270A}$ + PD0325901							

Comparisons highlighted blue were made in the spike-in SILAC experiment, those in red were compared in the standard SILAC experiment. K0R0 = ”light” label, K8R10 = ”heavy” label, PD0325901 = MEK1/2 inhibitor.

5.2 Identification of TPL-2-dependent phosphorylations and indirect removal of ERK1/2-dependent sites

5.2.1 Internal variation in the SILAC-labelled BMDM system

In order to gauge the intrinsic variation in the system, a comparison was first made between “light”-labelled and “heavy”-labelled wild type BMDM. The narrow distribution of the phosphopeptides identified in this comparison showed that few phosphorylations differed between the labelled and unlabelled conditions, as expected in these equivalent conditions (figure 5.1). Only a small fraction of phosphosites showed variation from the mean ratio suggesting the impact of incompletely labelled low turnover proteins or changes in biology caused by the SILAC amino acids was low. This was promising as it made it possible to detect smaller differences between the test conditions. A slight deviation of the mean away from zero, towards negative ratios, suggested a bias for phosphopeptides to be present at higher levels in the ”light”-labelled wild type BMDM. Although this could suggest that the labelled amino acids reduced overall phosphorylation levels in the cells, it is more likely that this was the result of label incorporation levels being between

89 - 94 % and therefore incomplete. Whilst this prevented the value being used for exact quantification of the difference between the compared conditions, it was still possible to identify TPL-2 dependent phosphorylations by their variation from the tight cluster of unregulated sites around this experimental mean.

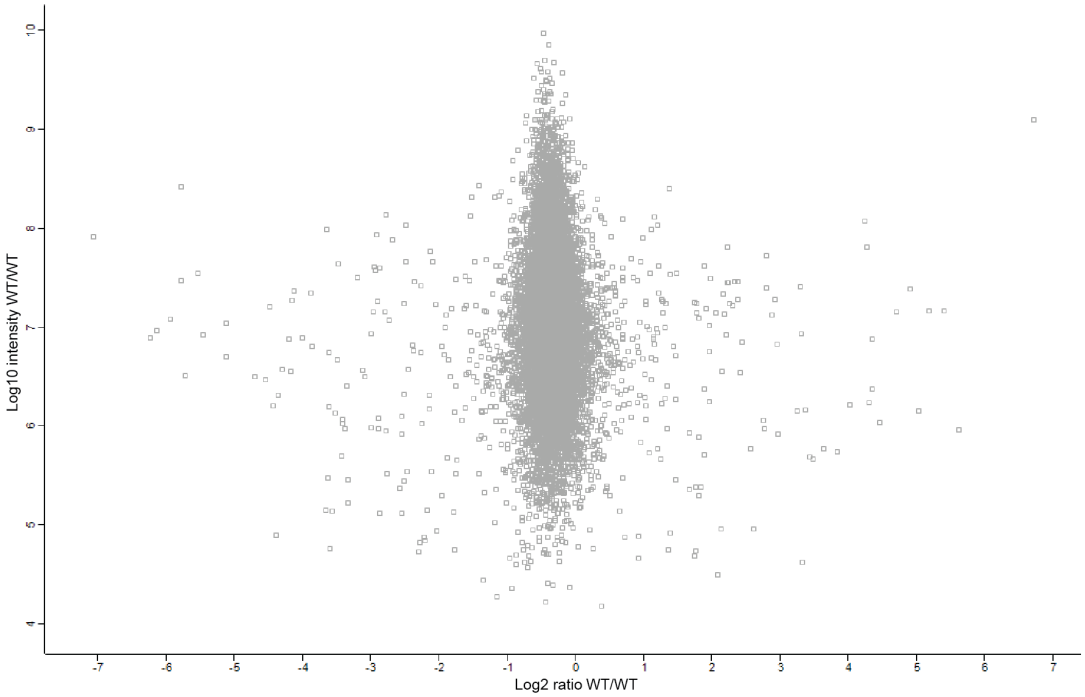

Figure 5.1: **Internal variation in the SILAC-labelled BMDM system.** Lysates from K0R0 SILAC-labelled WT and K8R10 SILAC-labelled WT, stimulated with 100 ng/ml LPS for 15 mins, were compared by mass spectrometry. X-axis shows Log_2 ratio comparing ”light”-labelled with ”heavy”-labelled wild type BMDM; y-axis shows Log_{10} intensity of phosphopeptides in this comparison. Pearson correlation factor = -0.026. WT = wild type BMDM.

5.2.2 Identification of TPL-2-dependent phosphorylations

To identify all the phosphorylations which were dependent on TPL-2 kinase activity, a comparison was made between wild type and *Map3k8*$^{D270A/D270A}$ BMDM, which express kinase-inactive TPL-2. In this and all subsequent comparisons, a positive Log_2 ratio value indicated that the phosphorylation was potentially TPL-2-dependent.

Internal controls

An initial check of the known TPL-2 target phosphorylations, MEK1/2 and ERK1/2 activation loop residues, showed that these phosphorylations were outliers and therefore differentially present between wild type and *Map3k8*$^{D270A/D270A}$ samples, as expected (figure 5.2). This demonstrated that it was possible to identify TPL-2-dependent phosphorylations from the global phosphoproteome.

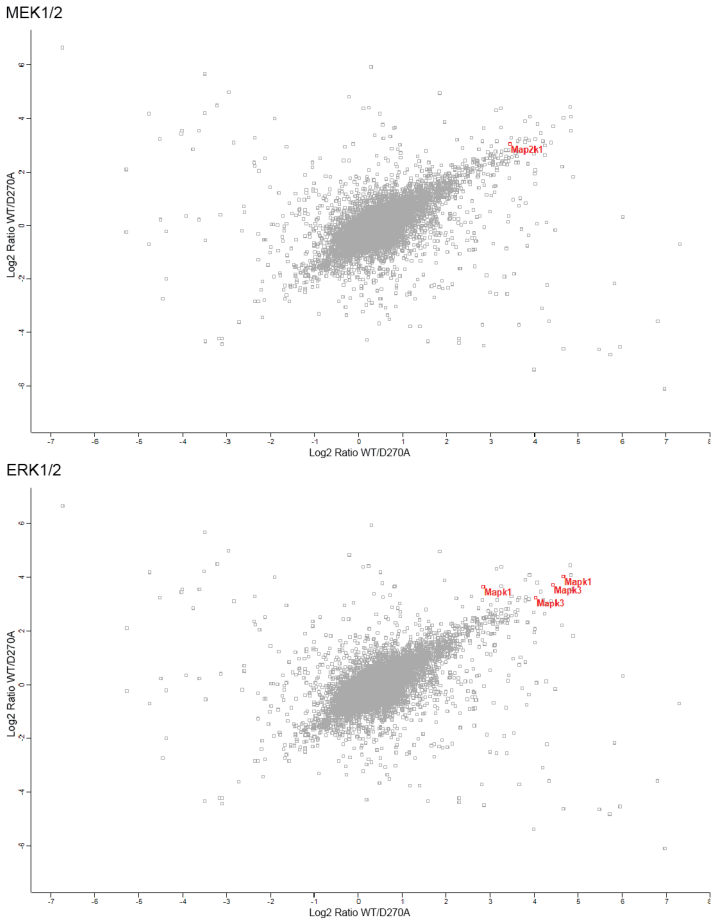

Figure 5.2: ***Map3k8***$^{D270A/D270A}$ **mutation reduces activation loop phosphorylation of MEK1/2 and ERK1/2.**
Lysates from SILAC-labelled WT and *Map3k8*$^{D270A/D270A}$, stimulated with 100 ng/ml LPS for 15 mins, were compared by mass spectrometry in label reversal experiments. Activation loop phosphorylations from MEK1/2 (Map2k1 - S222) and ERK1/2 (Mapk3 - T203/Y205 - and Mapk1 - T183/Y185 - respectively) are highlighted. X-axis shows Log_2 ratio comparing wild type with *Map3k8*$^{D270A/D270A}$ BMDM, y-axis shows the label reversal experiment of x-axis. Pearson correlation factor = 0.43. Lysates generated from a pool of 6 individual mice per condition. WT = wild type BMDM, D270A = TPL-2 kinase-inactive BMDM.

Mass spectrometric analyses of other published TPL-2 substrates

Several other TPL-2 substrates have been identified, largely be candidate-base approaches (summarised in table 1.3). We next determined whether any of these putative TPL-2 substrates were identified using our unbiased, mass spectrometry approach. The previously reported target sites in eIF4BP1 and PLCβ3 were present in the mass spectrometry dataset, but did not display TPL-2-dependent regulation (figure 5.3). Other phosphopeptides for each of these proteins also showed no TPL-2-dependent regulation. These results suggest that these proteins are not regulated by TPL-2 catalytic activity in LPS-stimulated BMDM. The phosphorylation sites were not determined in the original report showing TPL-2 phosphorylation of NFκB1 p105 so all identified phosphosites were analysed for this protein. Residues Ser949 and Ser953 did show TPL-2-dependent regulation (figure 5.4) which was consistent with previous reports indicating that TPL-2 can phosphorylate NFκB1 p105 with which it is associated (Babu et al., 2006b; Robinson et al., 2007). As only LPS-stimulated samples were analysed, it was not clear whether these phosphorylations were constitutive or inducible, or whether TPL-2 was phosphorylating these residues directly or indirectly via ERK1/2. Since these phosphorylation sites on NFκB1 p105 are not known to be functionally important, these possibilities were not investigated further.

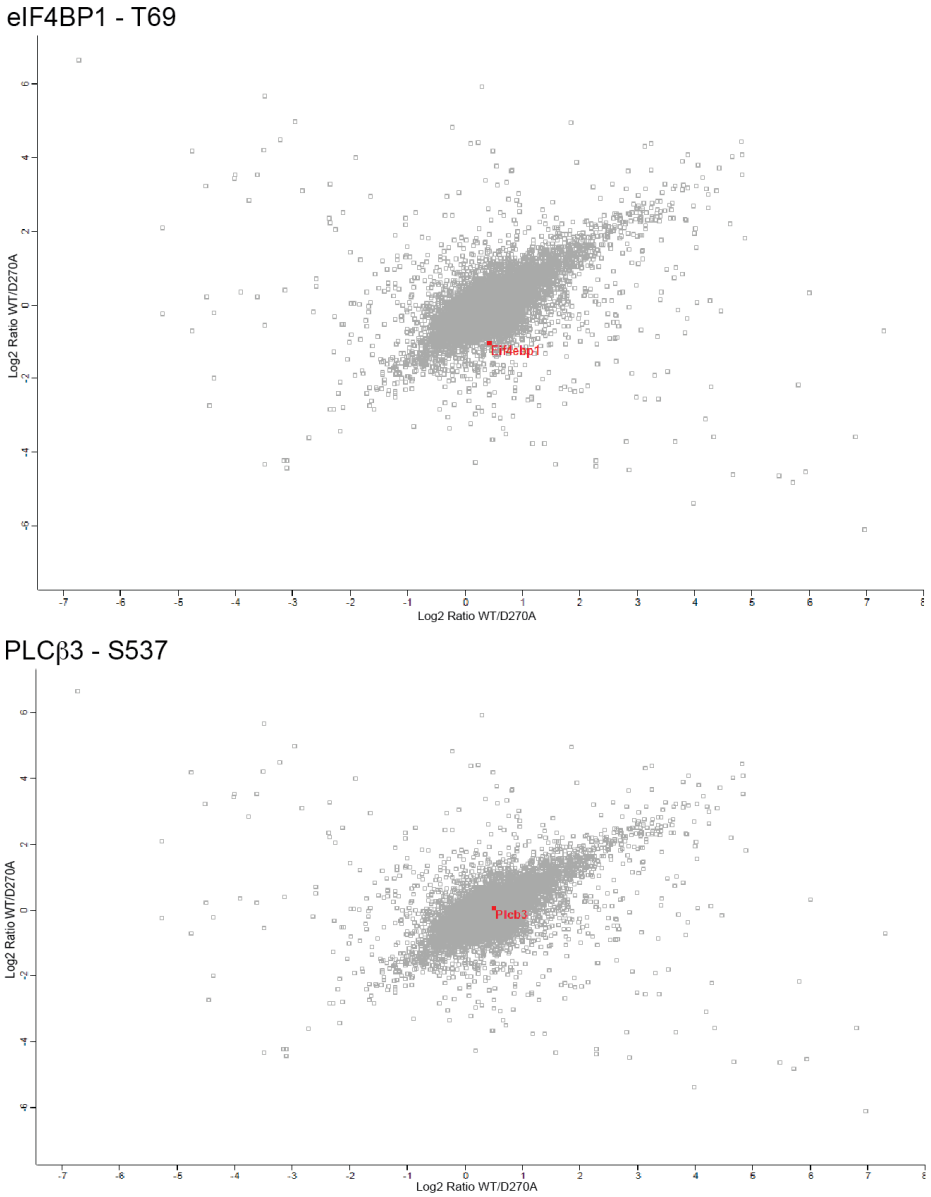

Figure 5.3: **Phosphorylation of published TPL-2 target phosphosites in wild type versus *Map3k8*$^{D270A/D270A}$ BMDM - localised sites.**
Lysates from SILAC-labelled WT and *Map3k8*$^{D270A/D270A}$ BMDM, stimulated with 100 ng/ml LPS for 15 mins, were compared by mass spectrometry in label reversal experiments. The published TPL-2 target sites in eIF4BP1 and PLCβ3 are highlighted. X-axis shows Log_2 ratio comparing wild type with *Map3k8*$^{D270A/D270A}$ BMDM; y-axis shows the Log_2 ratio of the label reversal experiment. WT = wild type BMDM, D270A = TPL-2 kinase-inactive BMDM.

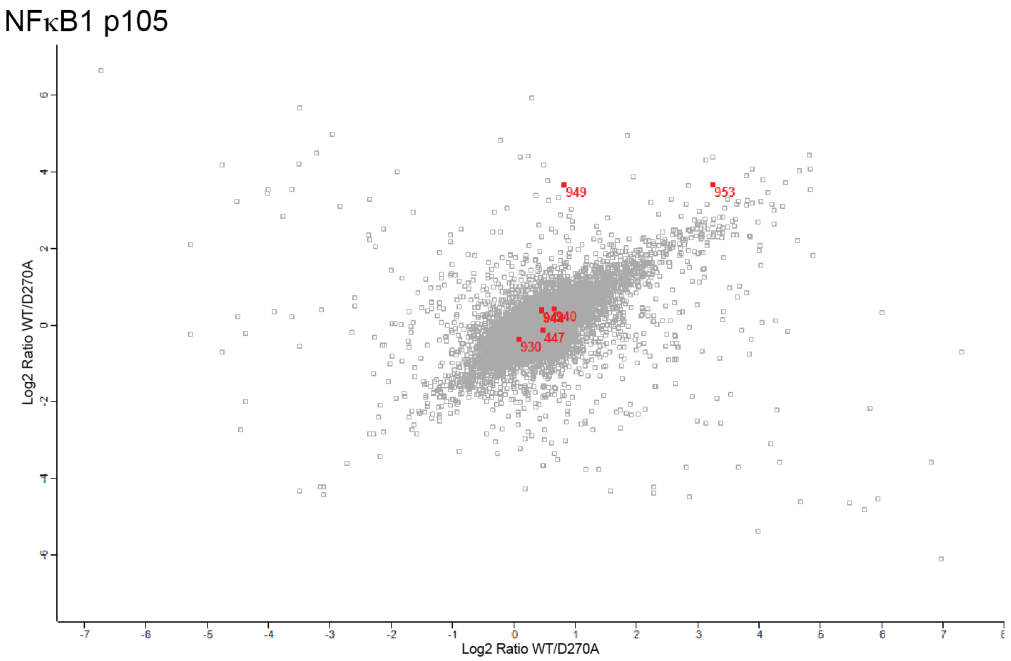

Figure 5.4: **Phosphorylation of published TPL-2 target proteins in wild type versus *Map3k8*$^{D270A/D270A}$ BMDM - non-localised sites.**
Lysates from SILAC-labelled WT and *Map3k8*$^{D270A/D270A}$ BMDM, stimulated with 100 ng/ml LPS for 15 mins, were compared by mass spectrometry in label reversal experiments. All phosphorylation sites in NFκB1 p105 are highlighted. X-axis shows Log_2 ratio comparing wild type with *Map3k8*$^{D270A/D270A}$ BMDM; y-axis shows the Log_2 ratio of the label reversal experiment. WT = wild type BMDM, D270A = TPL-2 kinase-inactive BMDM.

Identification of TPL-2 regulated phosphoproteins

In order to systematically identify TPL-2 regulated phosphorylations, z-statistics was used to establish a list of significant outliers. This resulted in a total of 469 outlier phosphopeptides, which could be directly phosphorylated by TPL-2 or an intermediate downstream kinase. Since this was a large number of proteins, it was necessary to incorporate other data to shorten the list. A number of bioinformatic approaches were taken, as detailed below:

- The Ley laboratory has previously shown that TPL-2 controls TNFα production independently of ERK1/2 via some unknown substrate (Yang et al., 2012). The list of outliers was searched for proteins annotated with Gene Ontology (GO) terms (Ashburner et al., 2000, accessed 22/9/11) related to

the production and release of TNFα; however none of the identified phosphoproteins were annotated with these terms.

- The consensus motif for TPL-2 has previously been determined in the Ley laboratory (unpublished data) and this, along with a published TPL-2 consensus sequence determined by another group (Parikh et al., 2009), was used to search the sequences of the identified phosphopeptides. These sequences were only matched in very few of the 16,769 identified phosphosites; 137 sites contained the loosest combination of preferred residues determined in the Ley laboratory and 55 matched to the motif determined by (Parikh et al., 2009). Sites that matched the TPL-2 sequence motif were not enriched in the significant outliers compared to the background data (Chi2 $p = 0.37$) and in fact only one of the matched sites was a significant outlier in both wild type versus TPL-2 kinase dead comparisons (from the protein Ahnak). The use of TPL-2 consensus motifs, therefore, did not suggest any direct targets for TPL-2.

- The Ley laboratory has generated an interactome dataset for the TPL-2/ABIN-2/NFκB1 p105 complex when over-expressed in HEK293 cells (unpublished data). Proteins from the phosphoproteomics dataset that are associated with TPL-2 are more likely to be direct substrates. Cross-referencing this list with the 469 outliers from the current study found 12 matches (Ahnak, Bag3, CDK14, Crebbp, Ep300, Map2k3/Map2k6, NFκB1, NFκB2, Sec16A, TNRC6B, Vim, YBX1). Although this comparison may ultimately help to identify direct TPL-2 substrates, these proteins were not followed up at this stage because we did not want to exclude indirect phosphorylations that may indicate biological processes regulated by TPL-2.

- RNA sequencing experiments have identified TPL-2 regulated genes in LPS-stimulated BMDM (Ley laboratory, unpublished data). Transcription factor enrichment analysis on these data has identified a number of transcription factors that are likely to be activated after 30 minutes of LPS stim-

ulation. Of the 7 suggested transcription factors, only 2 were found in the phosphoproteome dataset (CREB1 and SRF), but neither showed regulation of the detected sites. However, few transcription factors were identified in the TPL-2-dependent phosphoproteome as a whole, probably due to their low abundance.

Ultimately, given the length of the list and absence of leads from current information about TPL-2 biology, it was not possible to gain any further insights on the downstream signalling of TPL-2 from bioinformatic analyses of this dataset alone.

5.2.3 Indirect identification of TPL-2-dependent phosphorylations independent of ERK1/2 activation

Our major aim was to identify ERK1/2-independent TPL-2 signalling pathways. We first determined ERK1/2-dependent phosphorylations by a comparative mass spectrometric analysis of LPS-stimulated wild type macrophages with LPS-stimulated wild type macrophages treated with a small molecule MEK1/2 inhibitor, PD0325901.

Internal controls

As before, the activation loop phosphorylation sites of MEK1/2 and ERK1/2 were used as internal controls (figure 5.5). PD0325901 treatment reduced ERK1/2 phosphorylations as expected. MEK1/2 phosphorylation was not reduced in this comparison, consistent with the action of the PD0325901 compound in inhibiting the active form of MEK1/2 which has already been phosphorylated (Bain et al., 2007). Indeed, serine 222 phosphorylation was slightly increased by PD0325901 treatment, as could be seen from the negative Log_2 ratios in the wild type versus PD0325901-treated wild type comparison. Immunoblotting confirmed an increase in MEK1/2 phosphorylation in the presence of the MEK1/2 inhibitor compared to vehicle control (figure 5.6). PD0325901 also blocked the decrease in electrophoretic mobility of MEK1/2 detected after LPS stimulation in vehicle control cells. This

may be indicative of negative feedback pathways downstream of MEK1/2/ERK1/2 which are being blocked by the inhibitor (Caunt and Keyse, 2013).

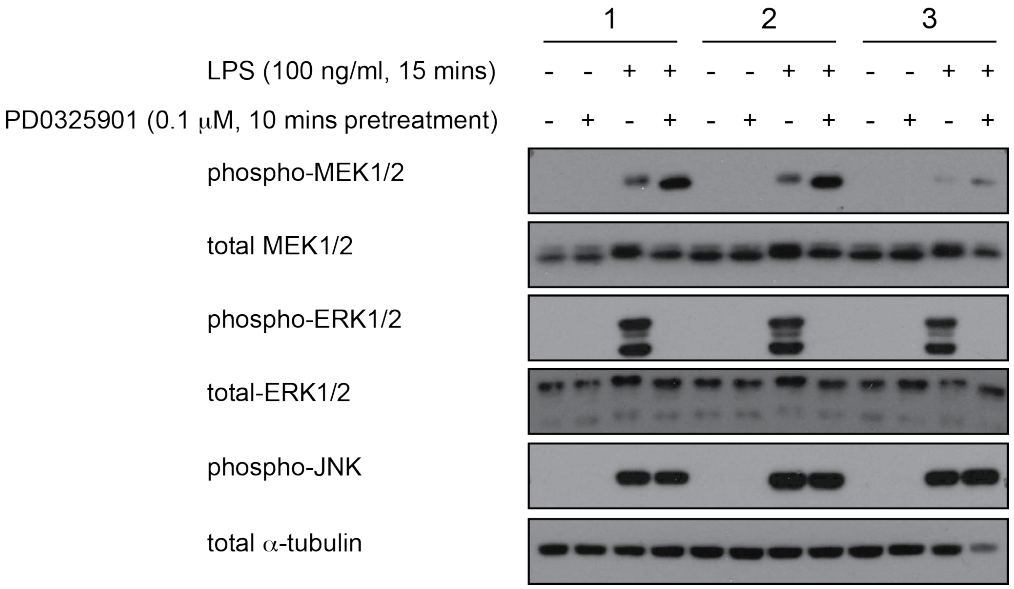

Figure 5.6: **MEK1/2 activation loop phosphorylation is increased in the presence of a small molecule MEK1/2 inhibitor.**
Wild type BMDM were left untreated, or treated with 0.1 μM PD0325901 and/or 100ng/ml LPS prior to lysis. Proteins were separated by gel electrophoresis and transferred to PVDF membranes, and immunoblotted with the indicated antibodies. Three technical replicates shown; representative of 3 independent experiments.

Identification of interesting hits

By combining the results of this wild type versus MEK1/2 inhibitor comparison with those from the previous wild type versus *Map3k8*$^{D270A/D270A}$ comparison, it was possible to subtract the ERK1/2-dependent phosphorylation from the list of TPL-2 regulated phosphorylations. To do this, phosphosites which were significant outliers in the wild type versus PD0325901 comparison were subtracted from the list of 469 significant outliers from the wild type versus *Map3k8*$^{D270A/D270A}$ comparison, leaving 123 outliers. Although this list was a much more manageable size, there were limitations with this approach. Due to the stochastic nature of peptide

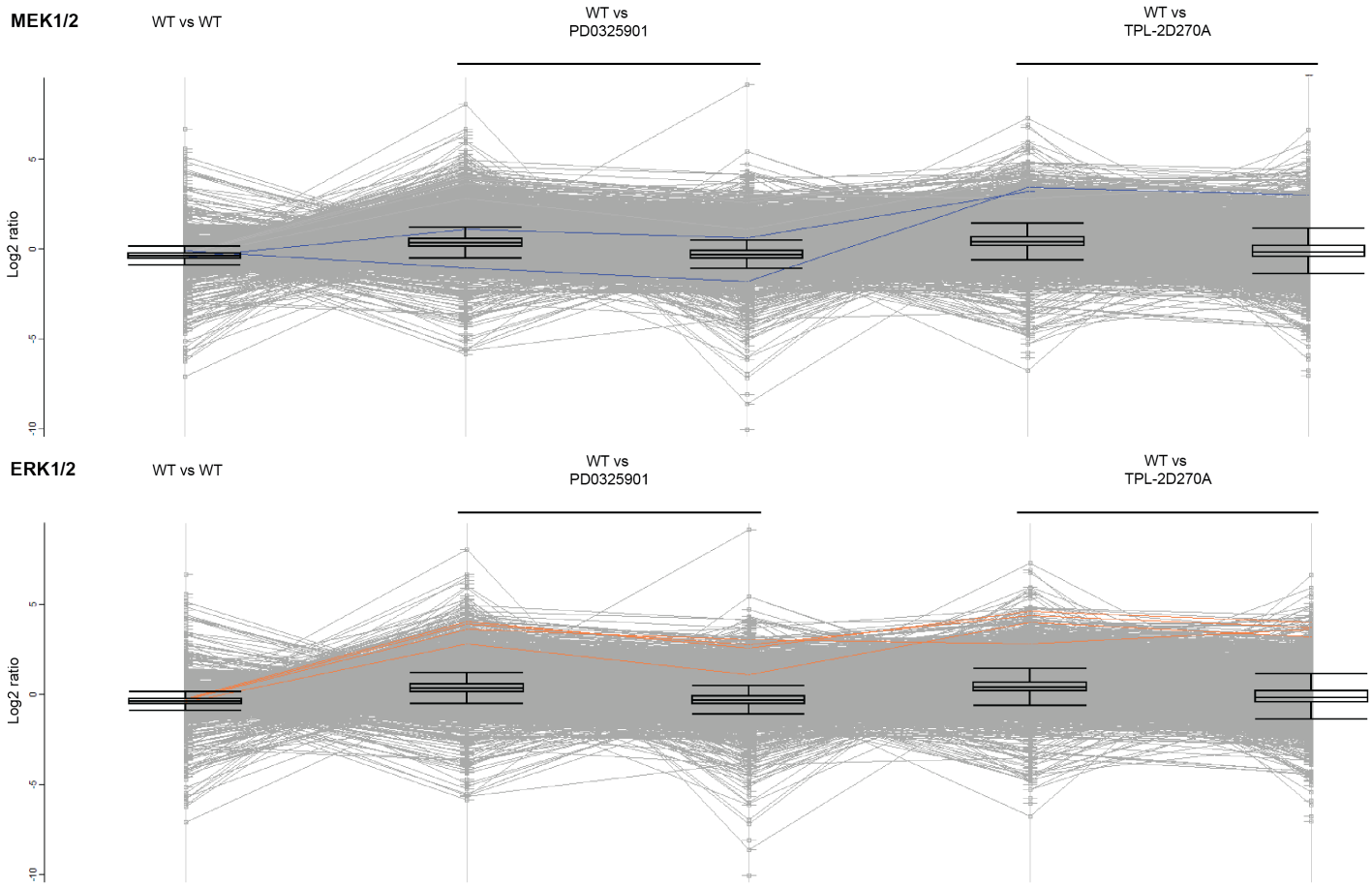

Figure 5.5: **Behaviour of the MEK1/2 and ERK1/2 activating phosphorylations in comparisons of LPS activated BMDM.** Lysates from different SILAC-labelled BMDM conditions, stimulated with 100 ng/ml LPS for 15 mins, were compared by mass spectrometry in label reversal experiments. Activation loop phosphorylations from MEK1/2 (S222) and ERK1/2 (T203/Y205 and T183/Y185 respectively) are highlighted. WT = wild type BMDM, TPL-2D270A = TPL-2 kinase-inactive BMDM.

detection by mass spectrometry, there may have been ERK1/2-dependent phosphosites in the wild type versus TPL-2 kinase dead comparison which were not found in the wild type versus MEK1/2 inhibitor comparison. These would score as false positives in the list of 123 phosphosites. Furthermore, it was possible that PD0325901 had off-target effects independent of MEK1/2 inhibition, confounding the results. In light of these two points, a more valid way to identify ERK1/2-independent TPL-2-regulated phosphorylations was sought.

5.3 Genetic inhibition of TPL-2-dependent ERK1/2 activation

In light of the problems with indirectly determining which of the outliers are ERK1/2-independent we decided to take a more direct approach and block ERK1/2 activation genetically.

5.3.1 *Nfκb1*$^{SSAA/SSAA}$ mutation inhibition of ERK1/2 activation by TPL-2

The *Nfκb1*$^{SSAA/SSAA}$ mice were previously generated in the Ley laboratory (Sriskantharajah et al., 2009). These mice carry serine to alanine mutations of the two residues in the PEST region of NFκB1 p105 (Ser930 and Ser935) which are phosphorylated by IKK2 upon agonist stimulation (Lang et al., 2003). If NFκB1 p105 is not phosphorylated it cannot be recognised or K48-ubiquitinated by the E3 ligase SCF$^{\beta TrCP}$ and is therefore not targeted for proteosome-mediated degradation (Lang et al., 2003). Constitutive processing of the mutant p105 to p50 is partially inhibited, although it is unclear why as stimulus induced phosphorylation is not required for recognition by KPC1, which controls this partial proteolysis (Yang et al., 2012; Kravtsova-Ivantsiv et al., 2015). Although generation of p50 is not altered this mutation disrupts NFκB signalling through the other function of NFκB1 p105 as an IκB (inhibitor of NFκB). Due to inhibition of stimulus induced NFκB1 p105 proteolysis, NFκB subunits (p50 homodimers and heterodimers with c-Rel and RelA) are not released and consequently are retained in the cytoplasm bound to with NFκB1 p105 (Sriskantharajah et al., 2009). Genes which depend on these NFκB subunits for their expression are therefore presumably expressed

at lower levels in the *Nfκb1*$^{SSAA/SSAA}$ mice compared to wild type.

Earlier work by the Ley laboratory established that *Nfκb1*$^{SSAA/SSAA}$ mutation blocks LPS activation of ERK1/2 in macrophages. Mutant NFκB1 p105$^{SSAA/SSAA}$ is resistant to signal-induced proteolysis and consequently TPL-2 remains associated with its inhibitor, NFκB1 p105, when *Nfκb1*$^{SSAA/SSAA}$ macrophages are stimulated with LPS. This prevents TPL-2 phosphorylation of MEK1/2 (figure 5.7 and Yang et al., 2012). Blocking ERK1/2 activation genetically has the advantage of avoiding off-target effects of inhibitor treatment which are particularly difficult to control for in MS proteomics experiments where large numbers of phosphorylations are sampled with high accuracy. For this reason it was predicted that a phosphoproteomic comparison between *Nfκb1*$^{SSAA/SSAA}$ and *Nfκb1*$^{SSAA/SSAA}$*Map3k8*$^{D270A/D270A}$ macrophages would identify TPL-2-regulated phosphorylations that were independent of ERK1/2 activation.

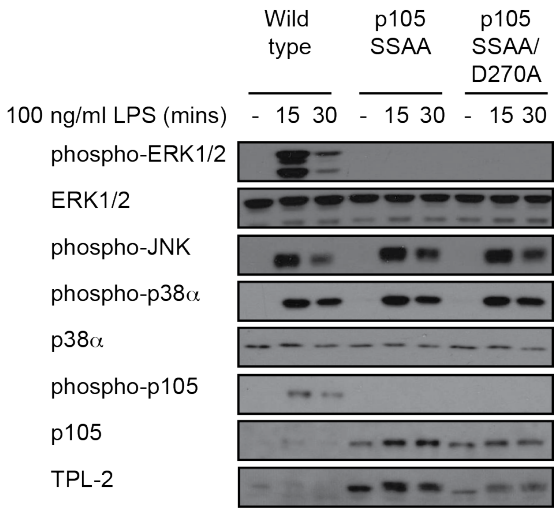

Figure 5.7: **Phosphorylation of ERK1/2 activation loop phosphorylations in response to LPS stimulation is absent in BMDM from *NFκB1*$^{SSAA/SSAA}$ mice.** Lysates from wild type, *NFκB1*$^{SSAA/SSAA}$ and *NFκB1*$^{SSAA/SSAA}$*Map3k8*$^{D270A/D270A}$ BMDM unstimulated or stimulated with 100 ng/ml LPS for 15 or 30 minutes were compared by mass spectrometry in label reversal experiments. Representative of 3 independent experiments.

5.3.2 *Nfκb1*$^{SSAA/SSAA}$ mutation does not block LPS-induced phosphorylation of MEK1/2 by TPL-2 in SILAC-labelled macrophages

Activation loop phosphorylations of MEK1/2 and ERK1/2 were monitored by mass spectrometry to determine whether *Nfκb1*$^{SSAA/SSAA}$ mutation blocked TPL-2 activation of MEK1/2/ERK1/2 as expected. Surprisingly, however, the level of phospho-ERK1/2 was reduced by *Map3k8*$^{D270A/D270A}$ mutation even in the *Nfκb1*$^{SSAA/SSAA}$ background (figure 5.8). This was contrary to previous immunoblotting results and implied that *Nfκb1*$^{SSAA/SSAA}$ mutation did not completely block TPL-2 activation of ERK1/2 activation loop phosphorylation. However, as the data were expressed as ratios, it was not possible to distinguish which component was changing. One possibility was that the mass spectrometric analysis was more sensitive than immunoblotting. Consequently, the levels of ERK1/2 phosphorylation detected in *Nfκb1*$^{SSAA/SSAA}$ may have been very low (too low to detect by immunoblotting), but when compared to the complete absence of ERK1/2 phosphorylation in *Nfκb1*$^{SSAA/SSAA}$*Map3k8*$^{D270A/D270A}$, the difference between these conditions resulted in a ratio that deviated from zero.

To understand these results better, a mass spectrometry comparison was made between *Nfκb1*$^{SSAA/SSAA}$ and wild type macrophages, in which the difference in ERK1/2 activation loop phosphorylation between genotypes was expected to be much greater based on immunoblotting experiments (Yang et al., 2012). Phosphopeptide enrichment for this experiment was done using titanium dioxide batch enrichment alone because these sites were very abundant in all previous comparisons. This comparison confirmed that the level of ERK1/2 phosphorylation was decreased by *Nfκb1*$^{SSAA/SSAA}$ mutation compared to wild type as these sites were outliers in this comparison (figure 5.9).

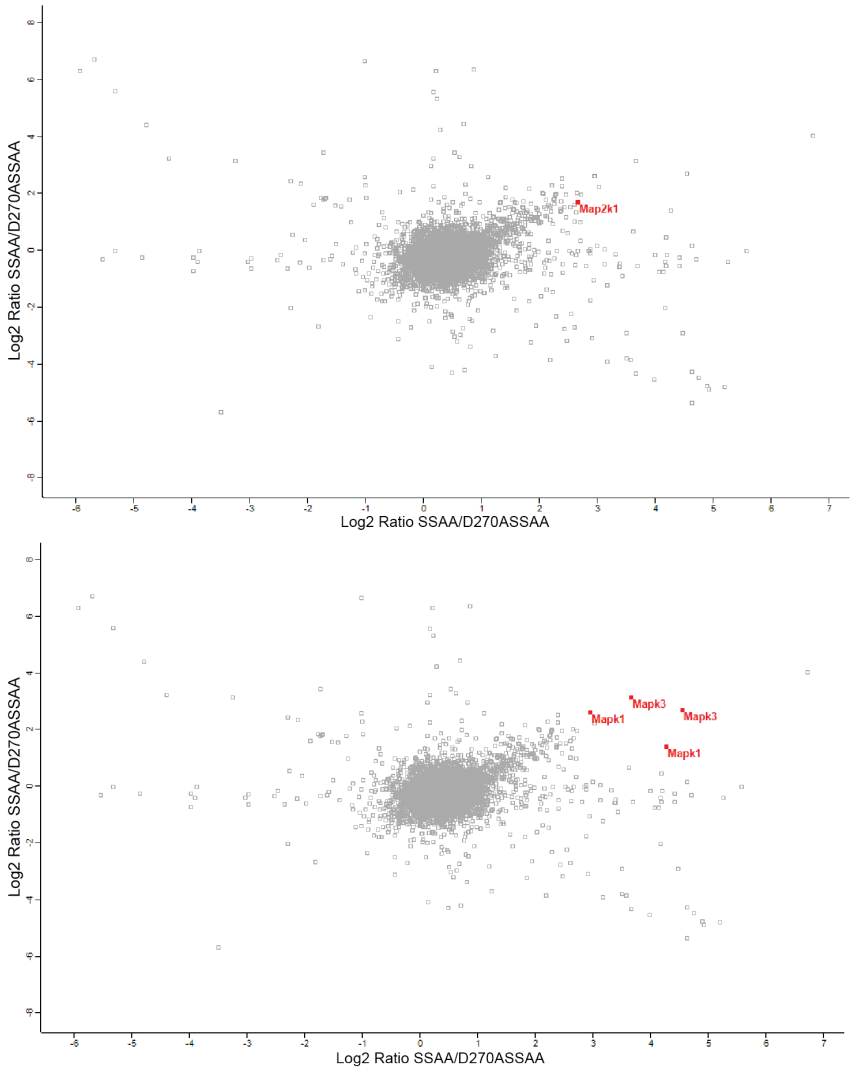

Figure 5.8: **ERK1/2 activation loop phosphorylations are differentially phosphorylated between *Nfκb1*$^{SSAA/SSAA}$ and *Nfκb1*$^{SSAA/SSAA}$ *Map3k8*$^{D270A/D270A}$ BMDM.**
Lysates from SILAC-labelled *Nfκb1*$^{SSAA/SSAA}$ BMDM and *Nfκb1*$^{SSAA/SSAA}$ *Map3k8*$^{D270A/D270A}$ BMDM, stimulated with 100 ng/ml LPS for 15 mins, were compared by mass spectrometry in label reversal experiments. Activation loop phosphorylations from MEK1/2 (Map2k1 - S222 - upper panel) and ERK1/2 (Mapk3 - T203/Y205 - and Mapk1 - T183/Y185 - respectively, lower panel) are highlighted. X-axis shows Log_2 ratio comparing *Nfκb1*$^{SSAA/SSAA}$ and *Nfκb1*$^{SSAA/SSAA}$ *Map3k8*$^{D270A/D270A}$ BMDM; y-axis shows the Log_2 ratio of the label reversal experiment. SSAA = *Nfκb1*$^{SSAA/SSAA}$ BMDM, D270ASSAA = *Nfκb1*$^{SSAA/SSAA}$ *Map3k8*$^{D270A/D270A}$ BMDM.

When looking at the ratio values for the four ERK1/2 activation loop phosphorylation sites there was evidence of a pattern which could explain the mass spectrometry results from the comparison of *Nfκb1*$^{SSAA/SSAA}$ and *Nfκb1*$^{SSAA/SSAA}$*Map3k8*$^{D270A/D270A}$ macrophages (table 5.2). The wild type versus

Map3k8$^{D270A/D270A}$ comparison had the maximum possible ratios for these phosphopeptides because they were present at wild type levels on one side of the comparison, and completely absent from the other. The *Nfκb1*$^{SSAA/SSAA}$ versus *Nfκb1*$^{SSAA/SSAA}$*Map3k8*$^{D270A/D270A}$ comparison had slightly smaller ratios for these phosphopeptides because they were present at low levels in *Nfκb1*$^{SSAA/SSAA}$ cells and completely absent in *Nfκb1*$^{SSAA/SSAA}$*Map3k8*$^{D270A/D270A}$ cells. These phosphopeptide ratios could theoretically take values of infinity in both these comparisons because the phosphopeptide is completely absent in one side of the comparison. However, in practise, the mass spectrometry signal is not linear and ratio suppression prevents the ratios exceeding certain limits (Dr. Bram Snijders, personal communication). Consequently, the ratios do not reach infinity and the difference between ERK1/2 activation loop phosphopeptides in wild type and *Nfκb1*$^{SSAA/SSAA}$ can be seen. Finally, the smallest ratios were seen in the wild type versus *Nfκb1*$^{SSAA/SSAA}$ comparison because the phosphopeptides were present in both conditions so the difference between two measurable values was being determined.

One important caveat with this analysis is that the ratios cannot be taken as exact measures of the difference because they can be affected by many errors, not least by different labelling levels between samples. However, from these data we concluded that there was a gradient of ERK1/2 phosphorylation levels across these genotypes, with wild type cells having the highest levels followed by *Nfκb1*$^{SSAA/SSAA}$, and *Nfκb1*$^{SSAA/SSAA}$*Map3k8*$^{D270A/D270A}$ with the lowest levels.

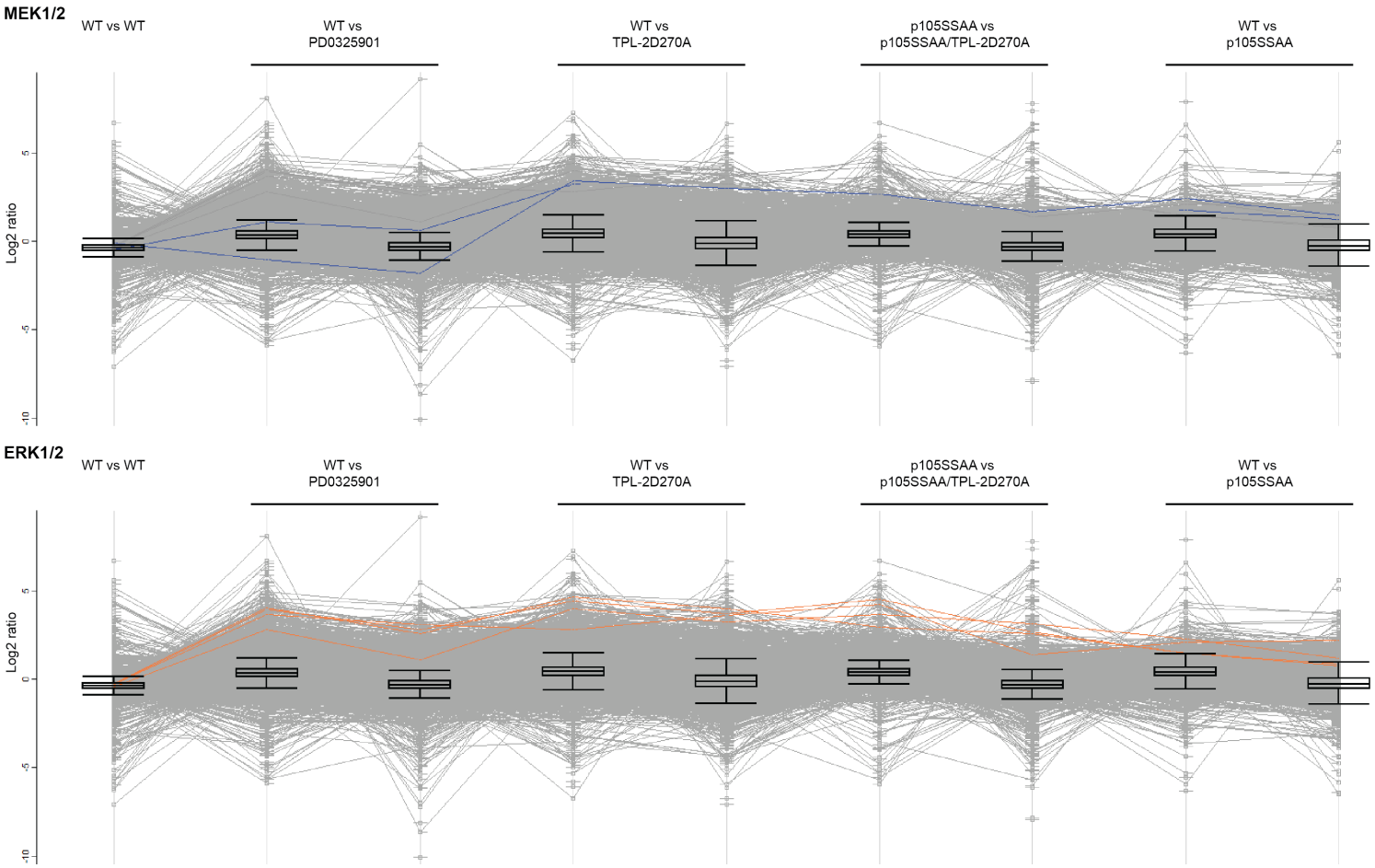

Figure 5.9: **Behaviour of MEK1/2 and ERK1/2 activation residue phosphorylations in phosphoproteomic comparisons.** Lysates from different SILAC-labelled BMDM conditions, stimulated with 100 ng/ml LPS for 15 mins, were compared by mass spectrometry in label reversal experiments. Activation loop phosphorylations from MEK1/2 (S222) and ERK1/2 (T203/Y205 and T183/Y185 respectively) are highlighted. WT = wild type BMDM, TPL-2D270A = TPL-2 kinase-inactive BMDM, p105SSAA = *Nfκb1*$^{SSAA/SSAA}$ BMDM.

Table 5.2: **Ratios of ERK1/2 activation loop phosphorylations from SILAC comparisons.**

	ERK1 T203	ERK1 Y205	ERK2 T183	ERK2 Y185
WT vs WT	-0.40	-0.27	-0.28	-0.23
WT vs PD0325901	2.85	3.96	3.66	4.08
	1.14	2.81	3.10	2.59
WT vs TPL-2D270A	4.03	4.43	2.85	4.66
	3.24	3.73	3.64	4.03
NFkB1SSAA vs NFkB1SSAA/TPL-2D270A	3.66	4.55	4.27	2.95
	3.14	2.69	1.39	2.59
WT vs NFkB1SSAA	2.32	1.51	2.12	1.48
	1.19	0.79	2.20	0.90

Colour indicates Log_2 ratio magnitude, from lowest ratio (lightest colour) to highest ratio (darkest colour). WT = wild type, PD0325901 = MEK1/2 inhibitor-treated wild type.

5.3.3 SILAC conditions altered signalling through the IKK2/NFκB1 p105/TPL-2/ERK1/2 pathway in *Nfκb1*$^{SSAA/SSAA}$ BMDM

This gradient of ERK1/2 phosphorylation detected by mass spectrometry was not expected from earlier immunoblotting analyses of BMDM lysates, which indicated that *Nfκb1*$^{SSAA/SSAA}$ mutation completely blocked ERK1/2 activation loop phosphorylation (Yang et al., 2012). One possible explanation for this was that the SILAC culture conditions altered the behaviour of the signalling pathways in the BMDM. This hypothesis was tested by comparing wild type, *Nfκb1*$^{SSAA/SSAA}$ and *Nfκb1*$^{SSAA/SSAA}$*Map3k8*$^{D270A/D270A}$ macrophages grown in standard, "light"-labelled SILAC or "heavy"-labelled SILAC conditions. It was clear from immunoblotting of cell lysates that culturing BMDM in SILAC conditions led to LPS-inducible ERK1/2 phosphorylation in the *Nfκb1*$^{SSAA/SSAA}$ cells which was not evident under normal culture conditions (figure 5.10). This phosphorylation was dependent on TPL-2 kinase activity because it was absent from cultures of *Nfκb1*$^{SSAA/SSAA}$*Map3k8*$^{D270A/D270A}$ macrophages under SILAC conditions. This did not appear to be due to the presence of the labelled amino acids because a low level of ERK1/2 phosphorylation could be seen in both the K0R0 "light" label and the K8R10 "heavy" label conditions. It was more likely that this resulted from one

of the other changes compared to standard culture conditions, such as the use of dialysed FCS, which has previously been reported to alter phosphorylation patterns compared to whole FCS (Imami et al., 2010).

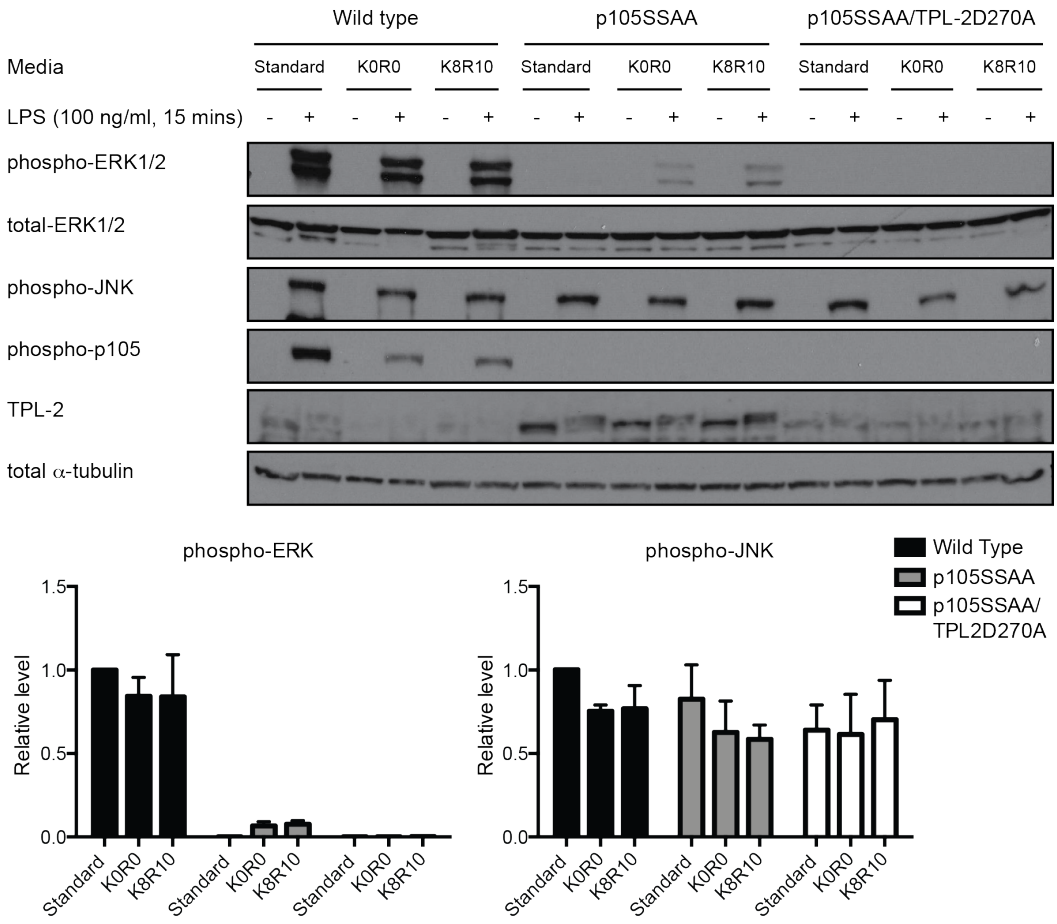

Figure 5.10: **SILAC culture conditions lead to altered signalling in BMDM from *Nfκb1*$^{SSAA/SSAA}$ mice.**
BMDM were cultured for 6 days under normal conditions, K0R0 SILAC conditions or K8R10 SILAC conditions. Cells were left unstimulated or stimulated with 100 ng/ml LPS for 15 mins and lysed. Proteins were separated by gel electrophoresis and transferred to PVDF membranes, prior to immunoblotting with the indicated antibodies. Relative phosphorylation levels were quantified from immunoblots by densitometry. Phosphorylation of ERK1/2 was normalised against total ERK1/2 levels, JNK phosphorylation was normalised against total α-tubulin levels; both were expressed relative to the signal in stimulated unlabelled BMDM. Standard = normal conditions, K0R0 = ”light”-labelled SILAC conditions, K8R10 = ”heavy”-labelled SILAC conditions.

These results validate the presence of a gradient of ERK1/2 phosphorylation predicted by the mass spectrometry results. Unfortunately this meant that the results from the *Nfκb1*$^{SSAA/SSAA}$ and *Nfκb1*$^{SSAA/SSAA}$*Map3k8*$^{D270A/D270A}$ comparison

could not be used because there were still ERK1/2 dependent phosphorylations present in *Nfκb1*$^{SSAA/SSAA}$ that would be extremely hard or impossible to identify and remove. One possible way to overcome this would be to use a different type of labelling, such as *in vitro* iTRAQ labelling (Wiese et al., 2007), or to use an alternative approach to directly analyse the TPL-2-dependent, ERK1/2-independent phosphorylations.

5.4 Alternative approaches to removing ERK1/2 activation

Due to problems with SILAC labelling *Nfκb1*$^{SSAA/SSAA}$ BMDM, an alternative approach was taken to directly identify the ERK1/2-independent TPL-2 targets using a small molecule inhibitor to block ERK1/2 activation. To do this, a final mass spectrometry comparison was made where the MEK1/2 inhibitor, PD0325901, was added to both wild type and *Map3k8*$^{D270A/D270A}$ BMDM, ensuring that the difference being compared was the presence or absence of TPL-2 activity in a background of no ERK1/2 signalling.

5.4.1 Whole dataset summary statistics

This study has thus produced data from a total of 11 different SILAC comparisons. Across all 11 mass spectrometry comparisons made throughout this work, there were 31,457 phosphosites identified representing 4,721 proteins, making this a comparatively large phosphoproteomics dataset. The composition of the phosphorylated residues was ~ 2 % tyrosine, 21 % threonine, 77 % serine (figure 5.11) which is consistent with previous estimates of the phosphoproteome which have put the proportions in the range of < 1 - 4 % tyrosine, 10 - 17 % threonine and 80 - 90 % serine (Hunter and Sefton, 1980; Weintz et al., 2010). This suggests that the phosphopeptide enrichment protocol used in this study did not lead to a bias in the phosphorylated residues which were detected.

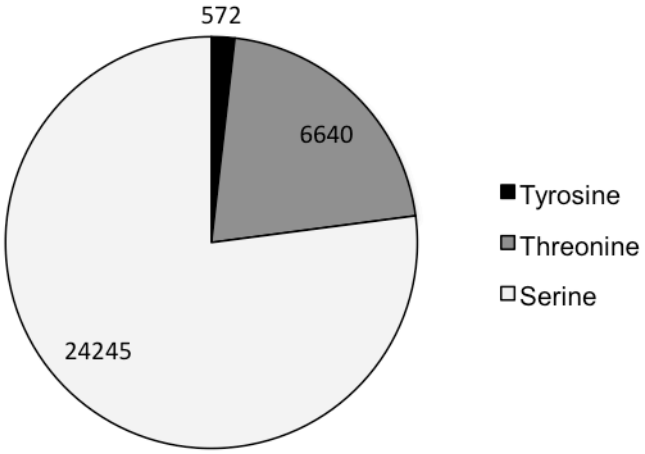

Figure 5.11: **Distribution of phosphorylation sites across serine, threonine and tyrosine residues.**
Lysates from various SILAC-labelled BMDM, stimulated with 100 ng/ml LPS for 15 mins, were compared by mass spectrometry. Number of phosphorylations on each type of residue were calculated. Absolute number of phosphosites are indicated.

In the comparison between MEK1/2 inhibitor-treated wild type and MEK1/2 inhibitor-treated *Map3k8*$^{D270A/D270A}$ there were a total of 16,353 unique phosphosites identified representing 2,655 proteins. Of these, 7,143 phosphosites were also found in the wild type versus wild type, wild type versus PD0325901 and wild type versus *Map3k8*$^{D270A/D270A}$. This has to be viewed in the context of the whole (phospho-)proteome which currently stands at 45,188 proteins in the UniProt *Mus musculus* proteome on (Consortium, 2015, accessed 11/3/15) and over 250,000 non-redundant phosphorylation sites in the PhosphoSitePlus® database (www.phosphosite.org, Hornbeck et al., 2012, accessed 11/3/15).

From this point onwards, only the 7 comparisons consisting of wild type versus wild type, wild type versus PD0325901-treated wild type, wild type versus *Map3k8*$^{D270A/D270A}$ and PD0325901-treated wild type versus PD0325901-treated *Map3k8*$^{D270A/D270A}$ were considered, as these provided the most valid and useful information about potential TPL-2 substrates (total and ERK1/2-independent). GO cellular compartment slim annotations (Ashburner et al., 2000, accessed 22/9/11)

of all identified phosphoproteins were compared with those of all genes expressed in murine BMDM, as determined by RNA sequencing (Ley laboratory, unpublished data), to identify whether any subcellular locations were over- or under-represented. Proteins from all the major subcellular compartments were found in the current dataset. There was a significant enrichment of proteins annotated as macromolecular complex (figure 5.12) which is in line with the function of phosphorylation in providing docking sites for formation of multi-protein signalling complexes (Cohen, 2000). On the other hand, terms which were significantly under-represented included several which indicate a membrane or membrane-bound compartment e.g. membrane, vesicle, endomembrane system. This may be due to the increased difficulty of extracting proteins from lipid membranes and their increased tendency to aggregate (Smith, 2011). Unsurprisingly there was also an under-representation of extracellular proteins in the phosphoprotein data as cell lysates and not culture supernatants were analysed.

5.4.2 Identifying ERK1/2-independent TPL-2 substrates

As before, we first checked for the behaviour of the internal control phosphorylations from the ERK1/2 activation loop. For both ERK1 and ERK2, the threonine (Thr203/183 respectively) phosphosite was not found in the PD0325901-treated wild type comparison with PD0325901-treated *Map3k8*$^{D270A/D270A}$ cells which suggested, as expected, that these residues were not being phosphorylated in either of the conditions. These phosphopeptides were otherwise very abundant in comparisons including wild type cells without PD0325901 (table 5.3). Activation loop phosphorylation of ERK2 Tyr185 was found in one of the two label reversal repeats but the ratio suggested it did not differ between wild type and *Map3k8*$^{D270A/D270A}$ in the presence of the MEK1/2 inhibitor; again this was as expected. However phosphorylation of Tyr203 in the activation loop of ERK1 was regulated by TPL-2 even in the presence of PD0325901 (wild type and *Map3k8*$^{D270A/D270A}$ plus MEK1/2 inhibitor comparison). This could have been due to incomplete MEK1/2 inhibition by

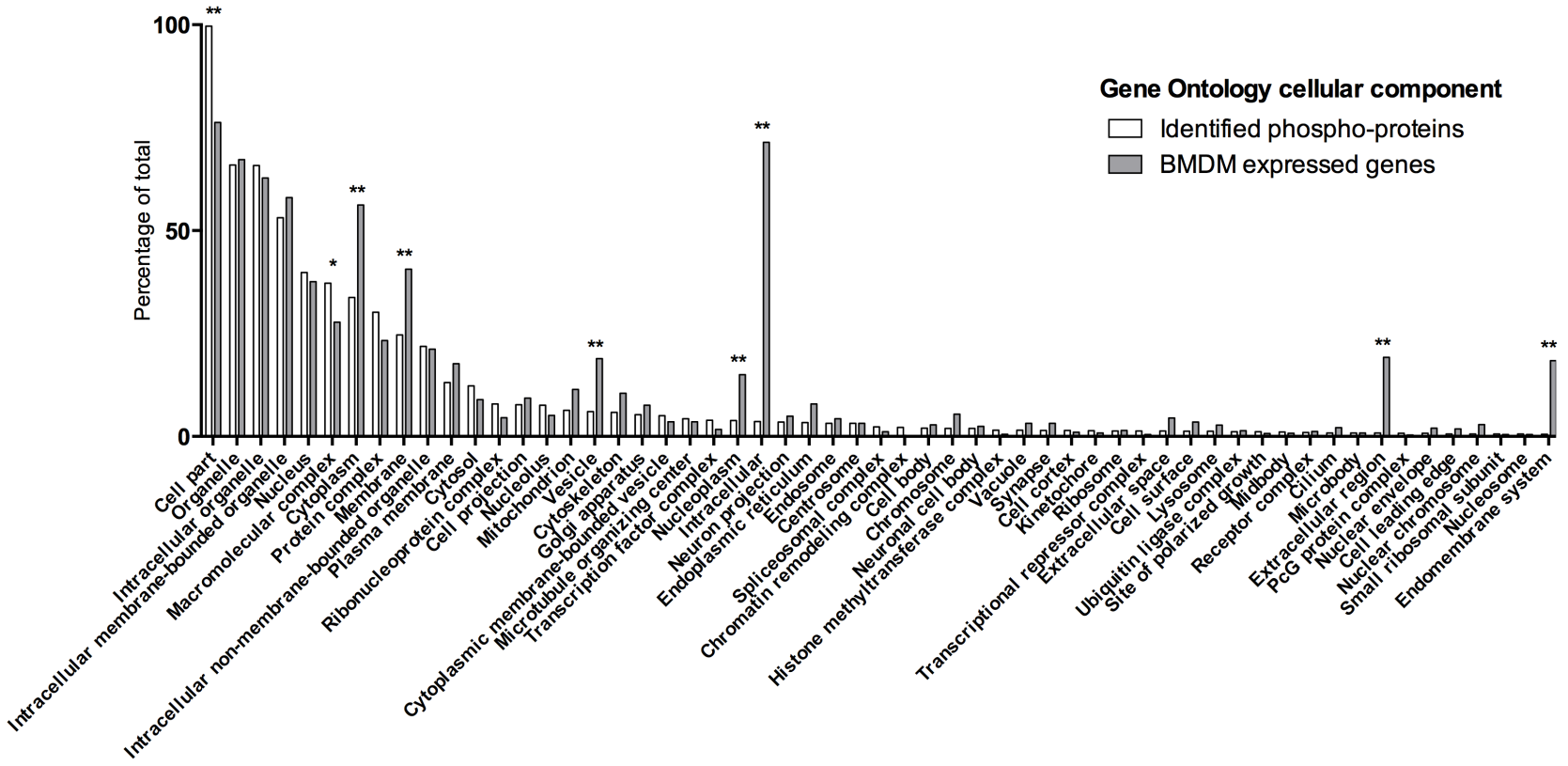

Figure 5.12: **Enrichment of GOCC terms in all identified phosphoproteins.**
GO cellular compartment annotations of proteins identified in the phosphoproteomics dataset were compared against those of all the genes expressed in BMDM as determined by RNA sequencing. Analysed by Chi2. * < 0.05, ** <0.01. All significantly different terms had odds ratios > 1.3 or < 0.76.

PD0325901, allowing some inducible phosphorylation to continue. Alternatively, it could be that MEK1/2 phosphorylation is blocked but the rate of removal of baseline activation loop phosphorylation (i.e. present before inhibitor added) differs; if this ERK1 tyrosine residue were de-phosphorylated more slowly than the other activation loop residues then its phosphorylation would persist for longer. As the inhibitor treatment only provides an acute block, whereas the genetic block is long term, this would result in differential levels of the phosphorylation between these conditions for a period of time. In support of this conclusion, differential regulation of the two activation loop residues of ERK1/2 has been shown previously (Robbins et al., 1993). The same study found that ERK1/2 was partially active and able to auto-phosphorylate when phosphorylated at only the tyrosine activation loop residue. However, phosphorylation on both residues was necessary for stable binding of the substrate, myelin-basic protein (Prowse et al., 2001). Moreover, we could be sure that the phosphorylation in the presence of PD0325901 was reduced relative to the level of fully active ERK1 because, when wild type BMDM were compared with PD0325901-treated wild type BMDM, all the ERK1/2 activating residues were differentially regulated (see above and table 5.3). Therefore, it is likely that ERK1/2 downstream signalling is also much reduced.

Table 5.3: **Behaviour of ERK1/2 activation loop phosphorylations in the phosphoproteomic comparison of PD0325901-treated wild type and *Map3k8*$^{D270A/D270A}$ macrophages.**

Comparison	ERK1 T203	ERK1 Y205	ERK2 T183	ERK2 Y185
WT vs WT	-0.40	-0.27	-0.28	-0.23
WT vs PD0325901	2.85	3.96	3.66	4.08
	1.14	2.81	3.10	2.59
WT vs TPL-2^{D270A}	4.03	4.43	2.85	4.66
	3.24	3.73	3.64	4.03
WT+PD0325901 vs TPL-2^{D270A}+PD0325901	X	3.53	X	0.40
	X	2.54	X	X

X = not found, WT = wild type, PD0325901 = MEK1/2 inhibitor-treated wild type.

Using z-statistics to determine significant deviation from the mean in the wild type versus *Map3k8*$^{D270A/D270A}$ comparison in the presence of the MEK1/2 inhibitor, resulted in a list of 145 outliers at significance of p = 0.01. These outliers were

assessed using the DAVID resource (Huang et al., 2008, 2009) for enrichment of GO biological process slim terms relative to all proteins found in the current phosphoproteomics data. This was chosen as the background dataset, rather than the whole mouse genome, because not all genes will be expressed in BMDM. Additionally, aspects of the methodology (e.g. chromatographic separation, ionisation) may prevent identification of certain proteins so their inclusion could skew the background population against any terms which are enriched in the regulated proteins. Predictably most of the enriched terms were related to phosphorylation and intracellular signalling, including MAP kinase pathways (table 5.4). Other terms which were present were “nucleosome positioning”, which had the highest fold enrichment, “locomotion” and “cell projection organisation” as well as several related to synthesis of steroids; with current knowledge it is hard to interpret these terms in relation to TPL-2 biology. However one term which could be equated with our understanding of TPL-2 biology is “regulation of transcription factor activity” because a recent RNA sequencing study in the Ley laboratory found TPL-2 regulated expression of 51 genes independently of ERK1/2, compared with 43 genes which were dependent on both TPL-2 and ERK1/2 (unpublished data).

The list of 145 significant outliers was further narrowed down by looking at the behaviour of the sites across multiple comparisons to include more information on the likely regulation of each site. To qualify as an ERK1/2-independent TPL-2 regulated site, the expected pattern of behaviour was such that was unregulated in the wild type versus wild type control and the wild type plus/minus MEK1/2 inhibitor but regulated in the wild type versus *Map3k8*$^{D270A/D270A}$. This analysis identified two groups of phosphosites (figure 5.13, table 5.5 and table 5.6); one group of 11 sites which were likely to be TPL-2-dependent, ERK-independent substrates based on a large divergence from the mean Log_2 ratio and mostly complete data across all the conditions, and a further 32 sites which were possible TPL-2-dependent, ERK-independent substrates. It is harder to draw conclusions about the regulation of this second group of possible substrates due to their smaller divergence from the mean Log_2 ratio and/or missing data, making it more likely that

these were false positives. It may also be more difficult to detect any real difference by other assays (e.g. immunoblotting) due to the need for greater sensitivity to detect a small difference.

Table 5.4: **Enriched GO biological process slim terms in all significant outliers found in the comparisons between PD0325901-treated wild type and PD0325901-treated *Map3k8*$^{D270A/D270A}$ BMDM.**

GOBP Slim term	P value	Fold enrichment
Protein amino acid phosphorylation	1.61E-05	2.97
Phosphorylation	3.31E-05	2.83
Phosphorus metabolic process	2.54E-04	2.44
Phosphate metabolic process	2.54E-04	2.44
Biopolymer modification	5.55E-04	2.05
Protein modification process	6.48E-04	2.08
Post-translational protein modification	7.03E-04	2.13
Signal transduction	1.67E-03	1.94
Nucleosome positioning	1.72E-03	40.58
Response to stimulus	2.64E-03	1.88
Regulation of cell communication	4.24E-03	2.28
Regulation of MAP kinase activity	5.48E-03	6.76
Sterol biosynthetic process	5.57E-03	24.35
Cholesterol biosynthetic process	5.57E-03	24.35
Regulation of signal transduction	6.56E-03	2.26
Positive regulation of molecular function	7.16E-03	3.45
Steroid biosynthetic process	8.22E-03	20.29
Activation of MAPK activity	8.67E-03	9.02
Regulation of molecular function	8.69E-03	2.41
Locomotion	9.61E-03	3.74
Positive regulation of MAP kinase activity	1.17E-02	8.12
Regulation of phosphorylation	1.22E-02	3.12
Protein kinase cascade	1.29E-02	3.09
Cell projection organization	1.37E-02	3.46
Regulation of transcription factor activity	1.53E-02	7.38
MAPKKK cascade	1.66E-02	4.95
Regulation of phosphorus metabolic process	1.71E-02	2.93
Regulation of phosphate metabolic process	1.71E-02	2.93
Protein metabolic process	1.80E-02	1.49
Multicellular organismal process	1.81E-02	1.53

Analysed using DAVID functional annotation enrichment tool (Huang et al., 2008, 2009). Background dataset for comparison was all identified phosphoproteins, cutoff $p < 0.02$.

The list was next filtered to remove those sites for which the confidence of protein identification, as assessed by the posterior error probability (PEP), was

higher than 1 x 10^{-5}. Low scoring localisation of the phosphorylation was not used as grounds to remove a hit because at this stage as the main aim was to find substrate proteins and the site of modification could be identified in future if necessary. Finally, the list was compared against the results of the digestion and mixing check to give an indication as to whether the total protein level was changing for a particular hit. This check was not a comprehensive proteomic analysis, so the total number of proteins represented was low, however peptides were found for Map2k1/Map2k2, Luc7l2, Hist1h1c and Fermt3 and did not show much variation across the 7 comparisons (Appendix B). Arg1 on the other hand had 20 peptides showing a deviation from a Log_2 ratio of zero in the comparisons between wild type and *Map3k8*$^{D270A/D270A}$ in the presence of the MEK1/2 inhibitor. Hsp90b1 also showed changes at the protein level in several of the conditions compared. This suggested that the changes in phosphopeptide level could be due to changes in total protein level rather than changing phosphorylation status. Arg1 and Hsp90b1 were therefore excluded from further analysis leaving a final list of 37 sites from 21 proteins.

Table 5.5: **Likely ERK1/2-independent TPL-2 regulated sites.**

Gene names	Protein names	Positions within proteins	Protein information	In absence of TPL-2 kinase activity	Comments
Map2k1/Map2k2	MEK1/MEK2	S218/S222; S222/S226	MAP2K for ERK1/2; activating site	Decreased	Good scores for protein identification and site localisation
Ece2	Endothelin-converting enzyme 2	S9	Membrane protease	Decreased	Good scores for protein identification and site localisation
Crebbp	CREB-binding protein	S2064	Protein acetyltransferase that transcriptionally activates histones	Increased	Good scores for protein identification and site localisation
Map3k8	TPL-2	S141	Possible autophosphorylation	Decreased	Good scores for protein identification and site localisation
Map2k3/ Map2k6	MKK3/MKK6	S218/S207	MAP kinase for p38 pathway; activating site	Decreased	Good scores for protein identification and site localisation
Top2b	DNA topoisomerase 2-β	S1330	Controls topological states of DNA	Increased	Good scores for protein identification and site localisation
Iws1	Protein IWS1 homolog	S384; S386	Pol II transcription elongation factor	Decreased	Good scores for protein identification and site localisations
Vav1	Proto-oncogene vav	T550	Proto-oncogenic GEF for Rho family	Increased	Poor score for protein identification, will not be included in further analyses
Pdlim2	PDZ and LIM domain protein 2	T142	Probable adapter protein	Decreased	Good scores for protein identification and site localisation

Well localised phosphorylations have score of > 0.75, confidently identified proteins have posterior error probability score < 1×10^{-5}.

Table 5.6: **Possible ERK1/2-independent TPL-2 regulated sites.**

Gene Names	Protein Names	Positions within proteins	Protein Information	In absence of TPL-2 kinase activity	Comments
Mndal	Myeloid cell nuclear differentiation antigen-like protein	S111	Cell growth	Increased	Good scores for protein identification and site localisation
Steap3	Metalloreductase STEAP3	S17	Exocytosis	Decreased	Good scores for protein identification and site localisation
Tbc1d4	TBC1 domain family member 4	S651	Exocytosis	Increased	Good scores for protein identification and site localisation
Mark2	Serine/threonine-protein kinase MARK2	S47	Cell growth	Decreased	Good scores for protein identification and site localisation
Luc7l2	Putative RNA-binding protein Luc7-like 2	S18	RNA processing	Increased	Good scores for protein identification and site localisation
Chd4	Chromodomain-helicase- DNA-binding protein 4	S1301	Transcription/DNA metabolism	Increased	Good scores for protein identification and site localisation
Hsp90b1	Endoplasmin	S42	Protein processing	Decreased	Good scores for protein identification and site localisation
Spp1	Osteopontin	S234; S238	Cell adhesion	Increased	Good score for protein identification and localisation of S234, S238 poorly localised
Hist1h1 c/e/b/d	Histone H1.2/H1.4/H1.5/H1.3	S102; S104	Transcription/DNA metabolism	Increased	Good scores for protein identification and site localisations
Fermt3	Fermitin family homolog 3	S345	Cell adhesion	Increased	Good scores for protein identification and site localisation
Prkaa1/2	5'-AMP-activated protein kinase catalytic subunit alpha-1/2	T183; S184	Energy sensing, T183 is an activating site	Increased	Good scores for protein identification and site localisations
Arg1	Arginase-1	S7	Amino acid metabolism	Increased	Good scores for protein identification and site localisation
Sqstm1	Sequestosome-1	S178; S182	Ubiquitin binding/adaptor	Decreased	Good score for protein identification and site localisation at S178, poor identification score for S182 so will not be included in further analysis
Nes	Nestin	S484; S485; S728; S841; S919; S1021; S1114; S1213; S1216; S1246; S1380; S1541	Cytoskeleton	Increased	Good scores for protein identification and site localisation, several sites showing similar behaviour but many others not changing
Dnajb11	DnaJ homolog subfamily B member 11	S37	Protein processing	Decreased	Poor score for protein identification, will not be included in further analyses
Skor2	SKI family transcriptional corepressor 2	T914	Transcription/DNA metabolism	Decreased	Poor score for protein identification, will not be included in further analyses
Sept6	Septin-6	T418	Cytoskeleton	Increased	Good scores for protein identification and site localisation

Well localised phosphorylations have score of > 0.75, confidently identified proteins have posterior error probability score < 1×10^{-5}.

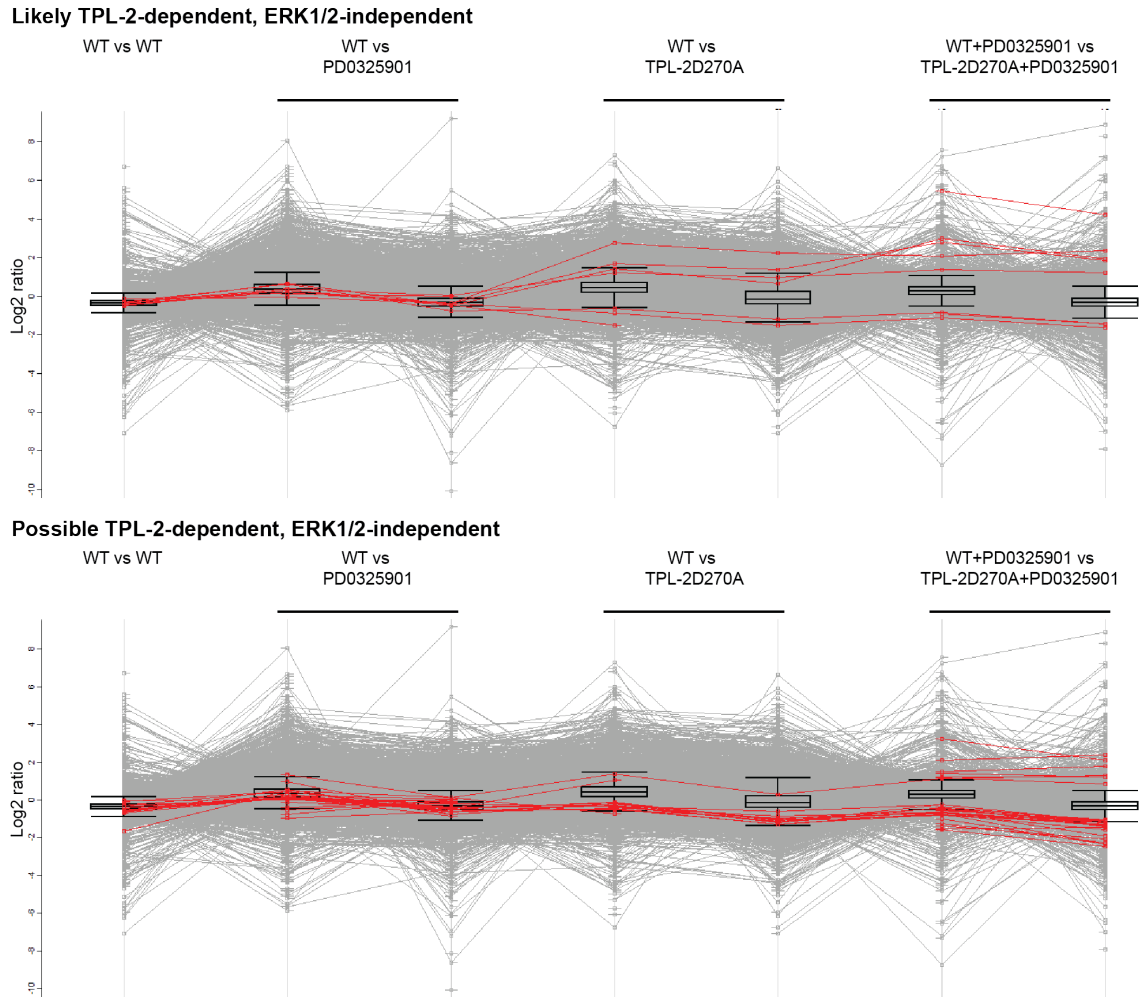

Figure 5.13: **Phosphosite profiles across the phosphoproteomic data reveal TPL-2-dependent phosphorylations.**
Lysates from SILAC-labelled BMDM, stimulated with 100 ng/ml LPS for 15 mins, were compared by mass spectrometry. Likely TPL-2-dependent phosphosites are highlighted in the upper panel and possible TPL-2-dependent phosphosites are highlighted in the lower panel. WT = wild type BMDM, PD0325901 = MEK1/2 inhibitor-treated BMDM, TPL-2D270A = TPL-2 kinase-inactive BMDM.

The resulting shortlist of proteins with likely and possible TPL-2-regulated phosphorylations were classified according to their functions based on UniProt annotation (Consortium, 2015, accessed 11/3/15), Gene Ontology terms (Ashburner et al., 2000, accessed 11/3/15) and literature review (figure 5.14). Consistent with the GOBP enrichment analysis discussed above, the most common function was "transcription/DNA metabolism". This category included proteins involved in DNA topology and histone modification which could play a role in the ERK-independent changes in gene expression which have been observed in TPL-2 kinase dead

mice by RNA sequencing (Ley laboratory, unpublished data). The second largest groups included proteins related to “cytoskeleton” and “MAPK signalling” which have been demonstrated to be key outcomes in the macrophage response to LPS by a previous phosphoproteomic study (Weintz et al., 2010). However due to the low numbers of proteins in the list it is difficult to draw conclusions about the function of TPL-2 regulated pathways from this analysis.

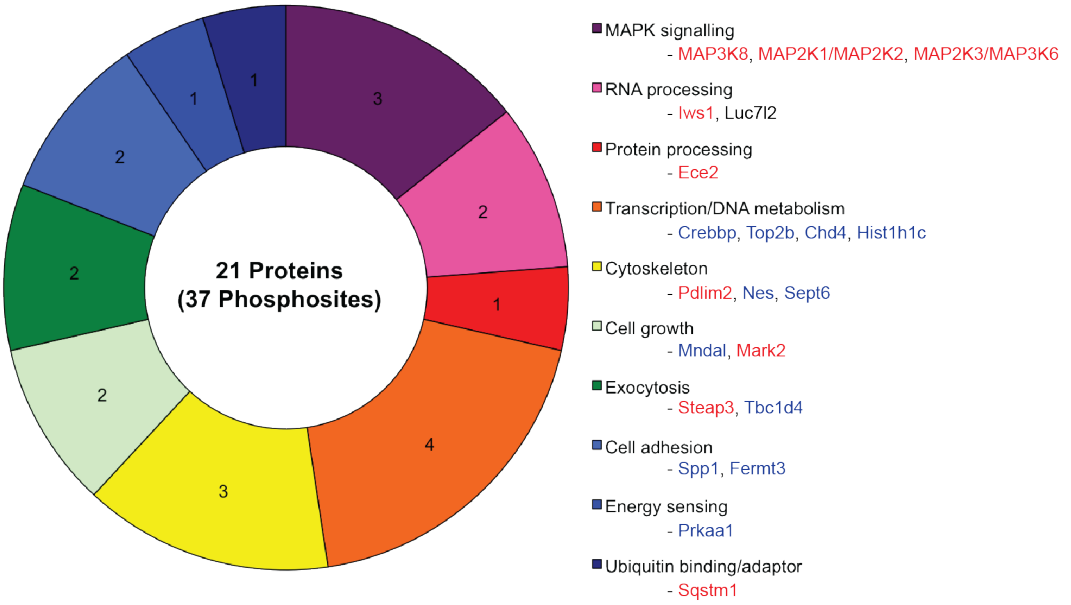

Figure 5.14: **Biological functions of proteins with likely and possible TPL-2-dependent, ERK1/2-independent phosphorylations.**
Proteins with identified phosphosites showing regulation by TPL-2, independent of ERK1/2, were grouped according to biological function determined using information from GO terms, Uniprot and literature review. Gene names of proteins in each category are shown; highlighted in red are phosphorylations decreased in the absence of TPL-2 kinase activity, those highlighted in blue are increased without TPL-2 kinase activity. Absolute numbers of proteins in each category are shown.

As no confirmed ERK1/2-independent TPL-2 targets are known, it was not possible to establish whether the process outlined above would be able to segregate the ERK1/2-dependent and -independent TPL-2 targets. Therefore, a known ERK1/2 target, RSK1/2/3, was used to illustrate that these sites could be discriminated by comparing the conditions that have been used in this study. The activating residues of the 3 isoforms RSK1/2/3, S380 and T573, were found in

the phosphoproteomics data (figure 5.15). These sites were not regulated when both conditions in the comparison had been treated with PD0325901, which on its own could suggest either that the site is not regulated by TPL-2 kinase activity or that the site is regulated by TPL-2 in an ERK1/2-dependent manner. By including the information from the wild type versus MEK1/2 inhibitor-treated and wild type versus *Map3k8*$^{D270A/D270A}$ comparisons it became evident that the latter of these two scenarios was the more likely because the sites showed differential regulation in both these comparisons. This demonstrated that ERK1/2-dependent TPL-2 targets could be distinguished from the ERK1/2-independent ones with which this study is concerned.

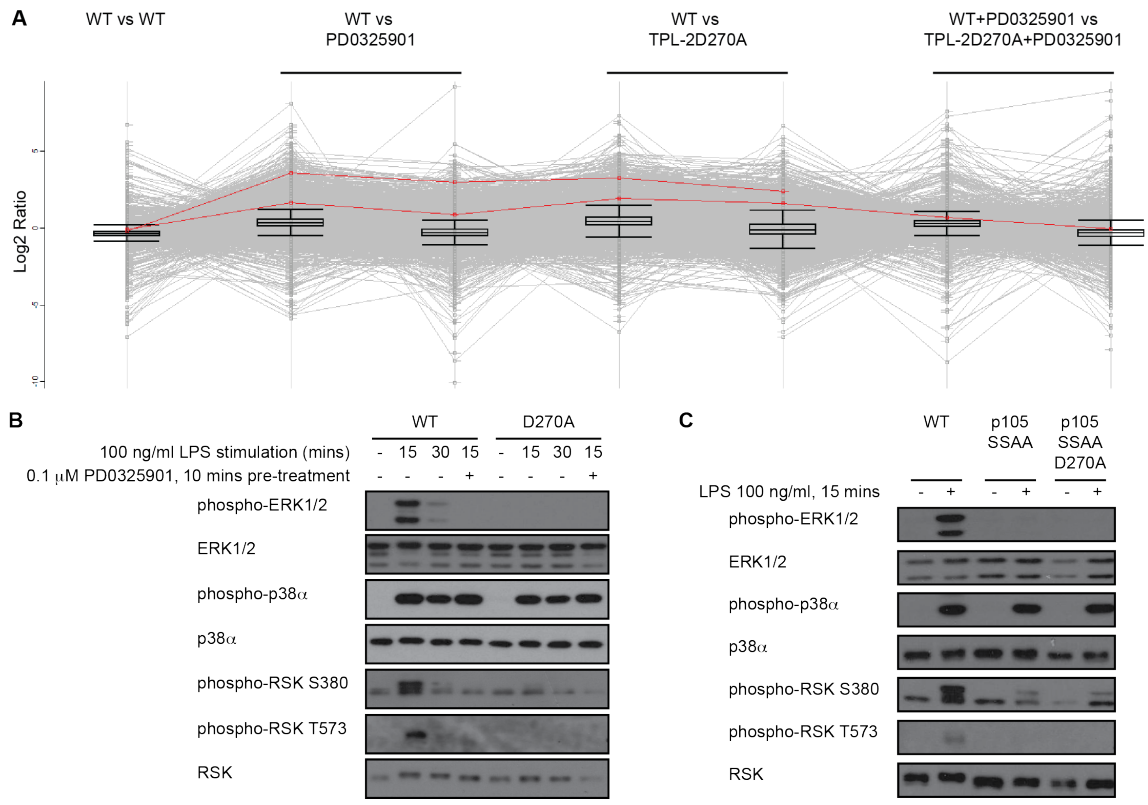

Figure 5.15: **ERK1/2-dependent phosphorylations could be distinguished from ERK1/2-independent sites using the comparisons.**
A: Lysates from SILAC-labelled BMDM, stimulated with 100 ng/ml LPS for 15 mins, were compared by mass spectrometry. RSK1/2/3 phosphorylation sites (Ser380 and Thr573) are highlighted. B: wild type, and *Map3k8*$^{D270A/D270A}$ BMDM were left untreated or treated with PD0325901 and 100 ng/ml LPS for the indicated times. C: wild type, *Nfκb1*$^{SSAA/SSAA}$ and *Nfκb1*$^{SSAA/SSAA}$*Map3k8*$^{D270A/D270A}$ BMDM were left untreated or stimulated with 100 ng/ml LPS for 15 mins. Cells were lysed, proteins separated by gel electrophoresis and transferred to PVDF membranes. The indicated antibodies were used for immunoblotting. Immunoblots are representative of 3 independent experiments. WT = wild type BMDM, PD0325901 = MEK1/2-inhibitor treated wild type BMDM, D270A = TPL-2 kinase-inactive BMDM.

5.4.3 Identifying ERK1/2 targets in LPS-stimulated macrophages

A second interesting question which could be investigated with this dataset was which ERK1/2 targets were becoming phosphorylated in LPS-stimulated BMDM? Starting in this case with the 681 significant outliers from the wild type versus MEK1/2 inhibitor-treated wild type comparison and considering the mass spectrometry data from across the different comparisons we could again narrow down the phosphosites which behave most like ERK1/2-dependent targets (figure 5.16).

This gave a list of 318 phosphorylations in 219 proteins after filtering by PEP (Appendix C). Of these sites, 236 were decreased when TPL-2 or MEK1/2 activity was blocked and 82 were increased. Interestingly, only 13 had been previously identified as ERK1/2 downstream targets (Carlson et al., 2011; Courcelles et al., 2013). These included RSK1 and RSK3, which are MAPKAPKs, key effector kinases activated by canonical MAP kinase pathways.

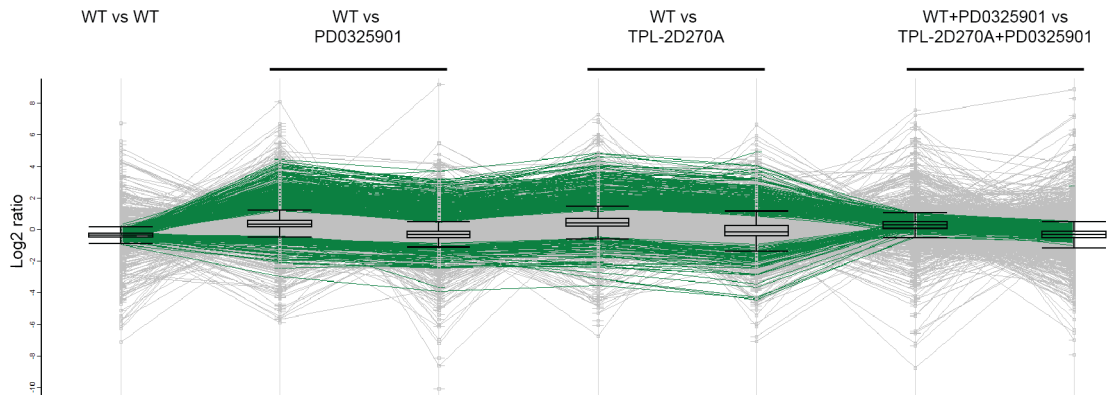

Figure 5.16: **Behaviour across the phosphoproteomic comparisons reveals ERK1/2-dependent phosphorylations.**
Lysates from SILAC-labelled BMDM, stimulated with 100 ng/ml LPS for 15 mins, were compared by mass spectrometry. ERK1/2-dependent phosphosites are highlighted. WT = wild type BMDM, PD0325901 = MEK1/2 inhibitor treated; TPL-2D270A = TPL-2 kinase-inactive BMDM.

The biological functions of proteins phosphorylated by TPL-2/ERK1/2 signalling after LPS stimulation of BMDM are shown in figure 5.17. Consistent with previous studies of the substrates of ERK2 (Carlson et al., 2011; Courcelles et al., 2013), this analysis suggested that ERK1/2 controlled changes in cell shape and/or motility ("Cytoskeleton" and "GTPase regulator"). This was also consistent with the large numbers of cytoskeletal and actin binding proteins previously shown to be regulated as a major outcome of LPS activation of BMDM (Weintz et al., 2010). Other key processes suggested by this data to be regulated by TPL-2/ERK1/2 were gene expression ("Transcription/DNA metabolism") and RNA processing, including translation which is also consistent with these previous studies.

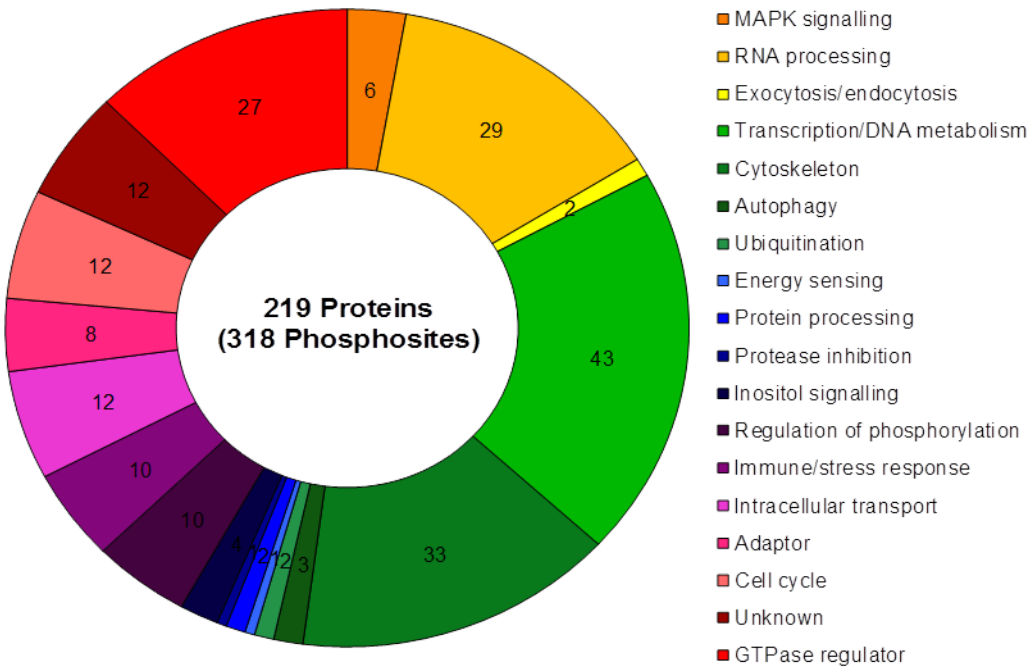

Figure 5.17: **Biological functions of proteins with TPL-2/ERK1/2 regulated phosphorylations.**
Proteins with identified phosphosites showing regulation by ERK1/2-dependent TPL-2 signalling were grouped according to biological function determined using information from GO terms, Uniprot and literature review. Absolute numbers of proteins in each category are shown.

5.5 Summary

By combining the information from 4 different comparisons to build a description of phosphorylation site behaviour across conditions, it was possible to narrow down a list containing thousands of phosphorylation sites to 37 that are worthy of further investigation. However, it should be noted that these phosphorylations have yet to be validated and this will be a critical next step in this project.

A selection of ERK1/2-independent TPL-2 regulated phosphoproteins are discussed below:

TPL-2 Ser141

One of the likely TPL-2-dependent, ERK-independent sites was TPL-2 (Map3k8) Ser141 (table 5.5). Although this phosphorylation site was previously identified, it was not known how it is regulated or if it has functional consequences

(Stafford et al., 2006). Its behaviour in the current study suggests that it is likely to be an autophosphorylation as it is not dependent on the MEK1/2/ERK1/2 known downstream pathway of TPL-2. However the possibility remains that it could be a feedback mechanism induced by unidentified TPL-2 pathways and this would require further study once novel pathways have been established.

Ece2

Ece2 phosphorylation was decreased in the absence of TPL-2 kinase activity. As a metalloprotease, Ece2 belongs to the same family as TACE (ADAM17), the cell surface enzyme responsible for cleavage of soluble TNFα from the membrane bound form which has been shown to be regulated by ERK1/2 signalling in LPS-stimulated macrophages. Ece2 is localised to intracellular vesicles and processes co-expressed big endothelin to produce endothelin-1 (Emoto and Yanagisawa, 1995; Russell and Davenport, 1999). Interestingly, Hinsley et al. (2012) found that endothelin-1 stimulated release of soluble bioactive molecules from fibroblasts. This was shown to be ADAM17-dependent using a small molecule inhibitor and siRNA knock-down of ADAM17. It is possible that a similar mechanism could be contributing to the TPL-2-dependent release of TNFα from macrophages, whereby TPL-2 phosphorylation of Ece2 leads to release of endothelin and promotion of TACE activity.

Pdlim2 and osteopontin

Two members of the list of ERK1/2-independent TPL-2-regulated proteins, Pdlim2 and osteopontin (OPN), are known to functionally interact with one another. OPN expression is essential for the Ser137 phosphorylation and activation of Pdlim2 which polyubiquitinates STAT1, leading to its degradation and termination of STAT1 signalling (Guo et al., 2010). In the present study Pdlim2 phosphorylation at Thr142 was decreased in the absence of TPL-2 kinase activity, indicating that TPL-2 promotes Pdlim2 phosphorylation at a site close to the activating residue. It will be important in future studies to determine whether Thr142 phosphorylation is required for Pdlim2 activation. Pdlim2 has also been reported to negatively regulate RelA activity, again by acting as an E3 ubiquitin ligase

(Tanaka et al., 2007). This may provide a mechanism by which TPL-2-dependent genes are regulated, as transcription factor enrichment analysis of these genes identified RelA as a possible regulator (Ley laboratory, unpublished data).

OPN is found in both extracellular soluble, and intracellular forms and has separate effects on inflammatory signalling in each context. In the secreted form it functions like a cytokine, driving Th1 skewed T cell responses over Th2 responses, whereas in the intracellular form it can function as part of the signal transduction complex in IFNα induction in TLR9 stimulated plasmacytoid dendritic cells (Cao, Wei and Liu, Yong-Jun, 2006; Shinohara et al., 2006). TPL-2 has been shown to negatively regulate IFNβ production (Kaiser et al., 2009). The phosphorylation of OPN is increased in the absence of TPL-2 kinase activity, raising the possibility that TPL-2 signalling might suppress IFNβ induction via down-regulation of OPN phosphorylation.

Crebbp

Crebbp was previously found by mass spectrometry to interact with over-expressed TPL-2/ABIN-2/NFκB1 p105 triple complex immunoprecipitated from HEK293 cells (Ley laboratory, unpublished data). Therefore, it is a likely candidate for direct phosphorylation by TPL-2, although this will need to be confirmed by kinase assays.

TPL-2-regulated phosphorylation of Crebbp may also be linked to RelA-dependent transcriptional regulation. The transcriptional coactivator, Crebbp, associates with RelA and promotes efficient transcription of a subset of RelA target genes (Zhong et al., 1998). This suggests an alternative way that TPL-2 may regulate transcription of certain RelA target genes, by altering the interaction between RelA and Crebbp.

Prkaa1

The current study identified two sites in Prkaa1 (AMPK) which appeared to be phosphorylated in a TPL-2-dependent manner, one of which was the activating residue (Thr183) (Lizcano et al., 2004; Shaw et al., 2004). AMPK is a negative regulator of inflammatory signalling in macrophages and is down-regulated as

a consequence of dephosphorylation as early as 10 minutes after LPS stimulation (Sag et al., 2008; Yang et al., 2010). The data in the current study showed phosphorylation of both AMPK sites increased in the absence of TPL-2 kinase activity. These data suggested that LPS-induced dephosphorylation of AMPK, which blocks its inhibition of inflammatory signalling, could be regulated by TPL-2. Moreover, reducing AMPK signalling using a dominant negative AMPK or short hairpin RNA AMPK knock-down increased the amount of TNFα produced following LPS stimulation in RAW264.7 macrophages or BMDM respectively (Sag et al., 2008; Yang et al., 2010). However, this increase was apparent at both the mRNA and protein levels and therefore does not correlate with TPL-2 regulation of TNFα which is predominantly mediated at the protein level.

Yang et al. (2010) also showed that activation of AMPK inhibited NFκB activity on a luciferase reporter and also RelA binding to target genes. TPL-2 signalling may induce NFκB-dependent gene expression by increasing RelA activity as a consequence of AMPK inhibition. Other key roles of AMPK include energy sensing and homeostatic changes in anabolic and catabolic pathways, and, whilst some reports have implicated TPL-2 in similar processes such as obesity, its role in such settings remains to be clarified (Perfield et al., 2011; Lancaster et al., 2012). The proposed modification of AMPK activity by TPL-2 must be indirect as AMPK phosphorylation is increased in *Map3k8*$^{D270A/D270A}$ compared to wild type. This suggests that TPL-2 may phosphorylate and activate an AMPK phosphatase. Alternatively TPL-2 may phosphorylate and inactivate an AMPK kinase. Many kinases have been reported to phosphorylate AMPK at this site and it will be important in future experiments to determine whether any of these are negatively regulated by TPL-2.

This study has shown that SILAC labelling alters signalling in *Nfκb1*$^{SSAA/SSAA}$ BMDM . In order for phosphorylation of ERK1/2 to remain in this mutant either NFκB1 p105 is being targeted for degradation in another way, thus enabling free TPL-2 to phosphorylate MEK1/2 as in wild type cells, or release is no longer necessary for TPL-2 to activate MEK1/2. This latter possibility is consistent with

previous findings that TPL-2 is still active in the triple complex. The presence of NFκB1 p105 prevents TPL-2 from accessing MEK1/2 in an all-or-nothing manner in cells whereas *in vitro* TPL-2 remains able to phosphorylate substrates; the efficiency of this phosphorylation is dependent on which NFκB1 p105 domains are present (Babu et al., 2006b; Robinson et al., 2007 and Ley laboratory, unpublished data). The results presented do raise the possibility that labelling cells from any genotype can change their signalling patterns compared to the physiological state. Although MAP kinase pathway activation was normal in wild type BMDM in this study it cannot be ruled out that other pathways were not, and this could lead to false positives or negatives in the phosphoproteomic dataset. This highlights the need to validate leads in unlabelled cells. Furthermore, these data have not been corrected for changes in protein expression. Although the label incorporation check, performed on digested whole cell lysate, indicated that overall expression level changes were minimal, it cannot be excluded that expression levels of specific substrates were changed and explain differences in phosphopeptide levels.

As well as ERK1/2-independent TPL-2 regulated targets, the data generated in the current study allowed identification of targets downstream of TPL-2/ERK1/2 signalling in LPS stimulated macrophages, which have not been looked at specifically on a large scale before. A far greater number of phosphopeptides fitted the expected behaviour of an ERK1/2 regulated site than a ERK1/2-independent TPL-2 regulated site, demonstrating the central role of ERK1/2 in orchestrating responses to external stimuli. This was further supported by analysis of the biological functions of TPL-2/ERK1/2 signalling which reflected the major responses of BMDM to LPS determined by Weintz et al. (2010). As these sites have been identified using a small molecule inhibitor, they would ideally be validated using a structurally unrelated MEK1/2 inhibitor, such as trametanib. Under standard cell culture conditions, it would also be possible to compare wild type with *Nfκb1*$^{SSAA/SSAA}$ macrophages, in which activation of ERK1/2 is blocked (Yang et al., 2012) in order to rule out off-target effects.

The most likely direct target of TPL-2 identified by the phosphoproteomics ex-

periments in this study were MKK3 and MKK6, since TPL-2 is known to be a MAP 3-kinase (Salmeron et al., 1996). MKK3/6 has also been found to specifically associate with the TPL-2/ABIN-2/NFκB1 p105 triple complex by mass spectrometric analyses of immunoprecipitates from transiently transfected HEK293 cells (Ley laboratory, unpublished data). Together, these data indicate that the link between TPL-2 and MKK3/6 phosphorylation is worthy of further investigation. The identification of TPL-2-dependent, ERK1/2-independent targets indicated that the SILAC/mass spectrometric methodology used in the current study worked and is likely to contribute to the increased understanding of downstream signalling pathways regulated by TPL-2.

6 Delineating the TPL-2/MKK3/6 pathway

6.1 Introduction

As detailed in Chapter 4, mass spectrometry identified MKK3/6 activation loop residues (Ser218/Ser207) as a TPL-2-dependent phosphorylation in LPS-stimulated BMDM (table 5.5). These phosphosites stood out as interesting because TPL-2 can contribute to p38 activation in LPS or CpG-treated dendritic cells, and canonical activation of this pathway is via MKK3/6 (Kaiser et al., 2009). Furthermore, MAP kinase signalling was over-represented in the regulated phosphorylation sites (table 5.4). Combined with the presence of MKK3/6 in the TPL-2/ABIN-2/NFκB1 p105 triple complex interactome, MKK3/6 regulation by TPL-2 was worthy of further investigation.

MKK3 and MKK6

MKK3/6 are the canonical MAP 2-kinases for the p38 MAP kinase pathway (figure 6.1). They are known to be exclusively able to phosphorylate p38 isoforms and do not show cross-talk with the other MAP kinase pathways (Cuenda and Rousseau, 2007). MKK3 and MKK6 share about 80 % homology.

Deletion of both MKK3 and MKK6 results in embryonic lethality whereas deletion of either alone is viable in mice, suggesting overlapping functionality and compensation by the remaining isoform (Cuenda and Rousseau, 2007). Their actions are not entirely redundant however, with differences in the importance of each isoform varying in a cell type and stimulus specific manner. For example, MKK6 was found to be necessary for deletion of double positive thymocytes whereas MKK3 was not. Instead, *Mkk3*$^{-/-}$ CD4+ T cells were resistant to T cell death upon TCR activation or cytokine removal, neither of which were affected by absence of MKK6 (Tanaka et al., 2002). There is also evidence that MKK3 and MKK6 activation can be regulated separately in certain circumstances, as protein kinase R (PKR) has been shown to activate MKK6, but not MKK3, in response to double-stranded RNA stimulation (Silva et al., 2004).

MKK4

In contrast to the single MKK3 or MKK6 “knock-outs”, constitutive deletion of MKK4 in mice is embryonic lethal (Abell et al., 2005). MKK4 shares roughly 50 % identity with MKK3 and about 60 % identity with MKK6. MKK4 and MKK7 are the canonical MAP 2-kinases for the JNK MAP kinase pathway. However, *in vitro* studies suggested that MKK4 could also contribute to p38 MAP kinase activation (Dérijard et al., 1995; Doza et al., 1995; Lin et al., 1995). Analyses of MKK4-deficient murine embryonic fibroblasts (MEFs) have subsequently demonstrated that MKK4 contributes to the activation of p38α by ultraviolet light but not TNFα in whole cells (Brancho et al., 2003).

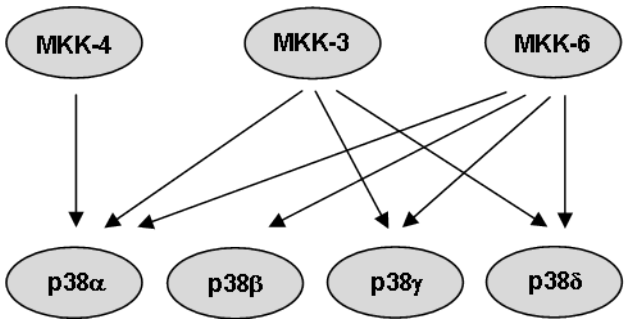

Figure 6.1: **p38 MAPK pathways.**
The four p38 isoforms show different patterns of activation by MKK3, MKK4 and MKK6. Unlike the other isoforms, p38α can be activated by MKK4. All four p38 isoforms can be activated by MKK6, whilst MKK3 activates all except p38β. MAP 2-kinase - MAP kinase pairing shows cell type and stimulus specificity.

6.1.1 Validation of MKK3/6 phosphorylation as an ERK1/2-independent, TPL-2 regulated site

The phosphorylated residues from MKK3/6 found in this study were compared with those listed in the Uniprot (Consortium, 2015, accessed 8/5/15) and PhosphoSitePlus® databases (www.phosphosite.org, Hornbeck et al., 2012, accessed 8/5/15). This study found three phosphorylated sites in MKK3 of which one, S7, was previously unknown (figure 6.2). For the site responsible for activation of MKK3/6 kinase activity it was not possible to determine whether the identified

peptide came from MKK3 (S218) or MKK6 (S207). Only this site was found to be changing upon perturbation of the system, supporting the assumption that it is a change in phosphorylation status and not protein level. Immunoblotting confirmed this phosphorylation was dependent on TPL-2 kinase activity, because it was absent in *Map3k8*$^{D270A/D270A}$ cells, and independent of ERK1/2 activity, because it was not affected by treatment of wild type cells with a MEK1/2 inhibitor (figure 6.3). Furthermore, it was shown to be dependent on NFκB1 p105 phosphorylation using the *Nfκb1*$^{SSAA/SSAA}$ and *Nfκb1*$^{SSAA/SSAA}$*Map3k8*$^{D270A/D270A}$ mutants.

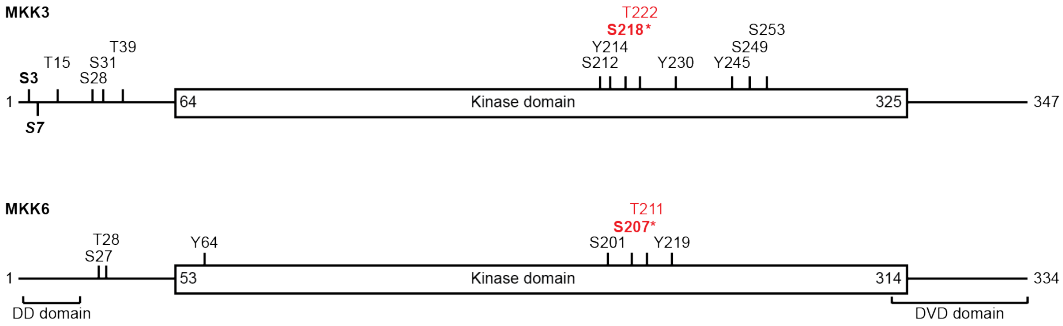

Figure 6.2: **Known MKK3 and MKK6 phosphorylation sites.**
Sites highlighted in red are the activating residues. Sites shown in bold were identified in this study, of which those in italics were newly identified. * indicates sites found to be regulated by TPL-2. The MKK6 D domain, which mediates binding to the MAPK substrate, and DVD domain, which mediates MAP3K binding, are predicted by similarity. Information was collated from Uniprot and PhosphoSitePlus® databases (Consortium, 2015, accessed 8/5/15; www.phosphosite.org, Hornbeck et al., 2012, accessed 8/5/15).

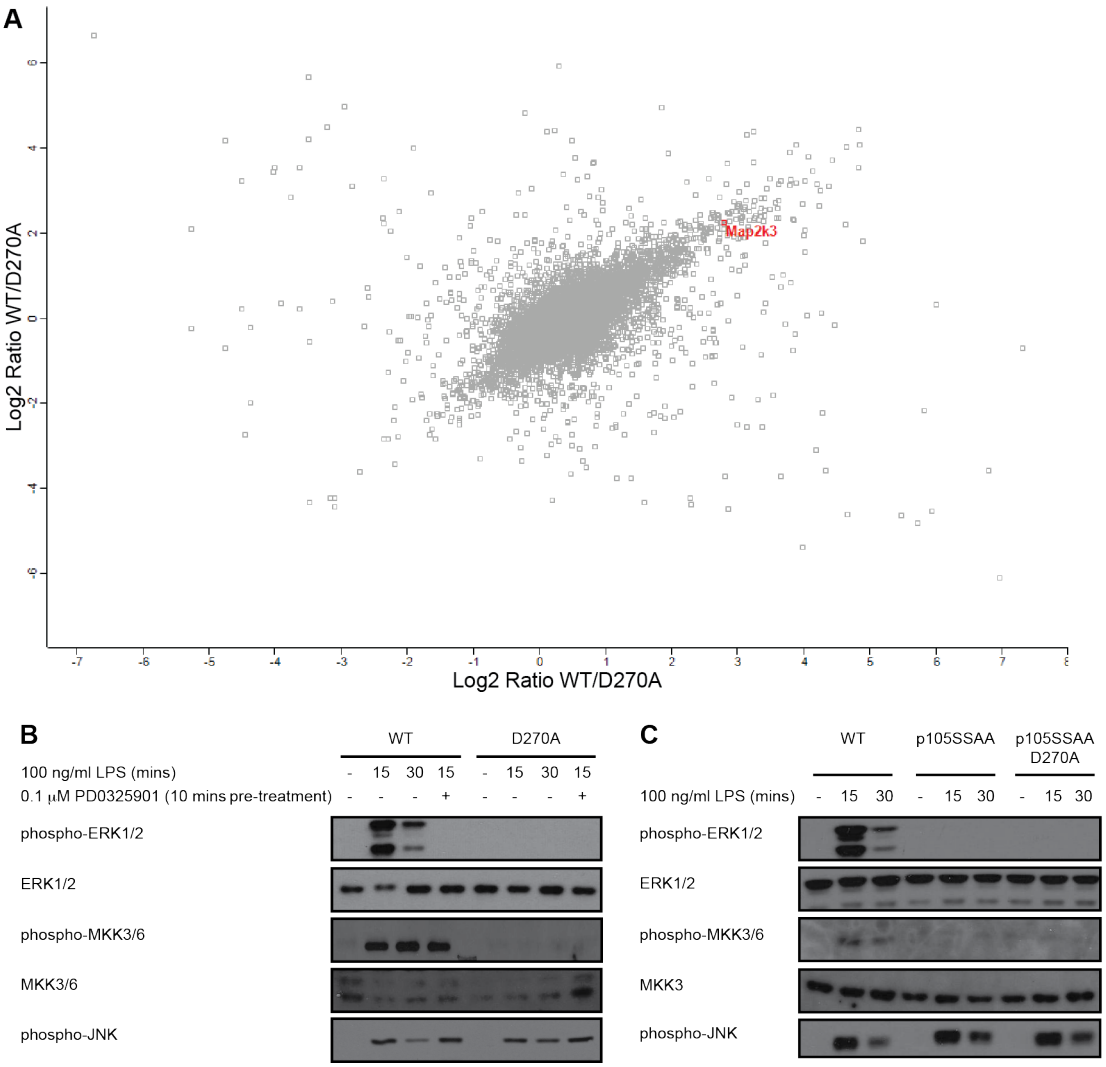

Figure 6.3: **MKK3/6 activation loop phosphorylation is regulated by TPL-2.** A: Lysates from SILAC-labelled BMDM, stimulated with 100 ng/ml LPS for 15 mins, were compared by mass spectrometry. The MKK3 (Map2k3) and/or MKK6 activation loop phosphopeptide (S218/S207 respectively) is highlighted. Graph axes show Log_2 ratio comparing wild type with *Map3k8*$^{D270A/D270A}$ BMDM; x-axis shows the label reversal experiment of the y-axis. B: wild type, and *Map3k8*$^{D270A/D270A}$ BMDM were left untreated or treated with PD0325901 and 100 ng/ml LPS for the indicated times. C: wild type, *Nfκb1*$^{SSAA/SSAA}$ and *Nfκb1*$^{SSAA/SSAA}$*Map3k8*$^{D270A/D270A}$ BMDM were left untreated or stimulated with 100 ng/ml LPS for the indicated times. Cells were lysed, proteins separated by gel electrophoresis and transferred to PVDF membranes. The indicated antibodies were used for immunoblotting. Immunoblots are representative of 3 independent experiments. WT = wild type BMDM, PD0325901 = MEK1/2 inhibitor treated BMDM. D270A = TPL-2 kinase-inactive BMDM.

6.2 Which MKK isoforms are regulated by TPL-2?

Due to sequence identity in their activation loop sequences, it was not possible to distinguish between MKK3 and MKK6 activating site phosphorylations in the phosphoproteomics data. These kinases are often co-regulated, however there are reports of differential isoform activation (e.g. PKR activates MKK6 but not MKK3 in response to double-stranded RNA stimulation), meaning the detected phosphopeptides might have originated from both or just one of the two isoforms (Silva et al., 2004; Zhang et al., 2007). Interrogation of the phosphoproteomics data also indicated that the activating residues of MKK4 were not being regulated by TPL-2 (figure 6.4). However, it is thought that TPL-2 can contribute to the regulation of JNK activation via MKK4 in fibroblasts following TNFα and IL-1β stimulation, as well as p38 activation, presumably via MKK3 and MKK6, in dendritic cells treated with LPS or CpG (Das et al., 2005; Kaiser et al., 2009). Therefore, in order to understand more completely which isoforms were being regulated by TPL-2, each isoform was immunoprecipitated individually and probed for activation loop phosphorylation by immunoblotting.

MKK3 and MKK6 separately immunoprecipitated from wild type BMDM showed LPS-inducible phosphorylation of their activation loops, which was not blocked by the presence of the MEK1/2 inhibitor, PD0325901. However, MKK3 and MKK6 phosphorylation was blocked by *Map3k8*$^{D270A/D270A}$ mutation. In contrast MKK4 showed LPS-inducible phosphorylation when immunoprecipitated from wild type, PD0325901-treated wild type or *Map3k8*$^{D270A/D270A}$ BMDM (figure 6.5). These results demonstrated that TPL-2 catalytic activity regulated the activation of both MKK3 and MKK6 after LPS stimulation. In contrast, TPL-2 catalytic activity was dispensable for LPS activation of MKK4.

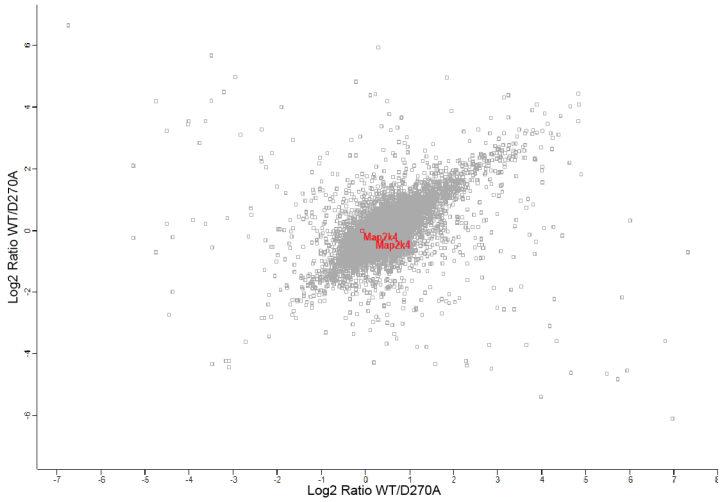

Figure 6.4: **MKK4 activating phosphorylations do not appear to be regulated by TPL-2.**
MKK4 (Map2k4) activation loop phosphopeptides (Ser255 and Thr259) are highlighted. Lysates from SILAC-labelled WT and *Map3k8*$^{D270A/D270A}$ BMDM, stimulated with 100 ng/ml LPS were compared by mass spectrometry. Graph axes show $\log_2$ ratio comparing wild type with TPL-2^{D270A} BMDM; the x-axis shows the label reversal mix of the y-axis. WT = wild type BMDM, D270A = TPL-2 kinase-inactive BMDM.

Earlier research by the Ley laboratory established that TPL-2 activation of MEK1/2 was dependent on IKK2 phosphorylation of its inhibitor, NFκB1 p105 (Babu et al., 2006b). To investigate whether this IKK2 regulated step was also required for TPL-2-dependent phosphorylation of MKK3 and MKK6, each kinase was immunoprecipitated from *Nfκb1*$^{SSAA/SSAA}$ BMDM, in which the IKK2 phosphorylation serines, 930 and 935, in the PEST region of NFκB1 p105 are mutated to alanine. *Nfκb1*$^{SSAA/SSAA}$ mutation blocked LPS-induced phosphorylation of both MKK3 and MKK6, while MKK4 phosphorylation was unaffected (figure 6.6). Consistent with this, LPS-induced phosphorylation of MKK3 and MKK6, but not MKK4, was blocked by pre-treatment of cells with a small molecule inhibitor of IKK2, BI605906 (Clark et al., 2011). Together, these results indicated that TPL-2 regulation of MKK3 and MKK6 phosphorylation was dependent on IKK2 activity and NFκB1 p105 phosphorylation, similar to MEK1/2.

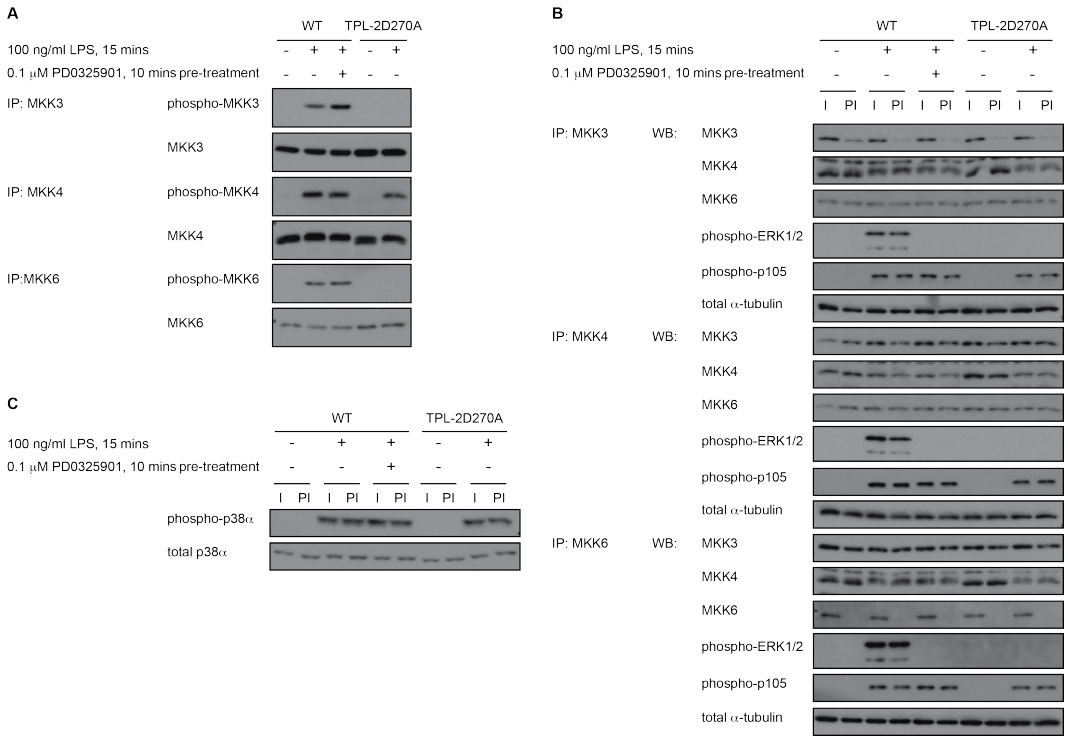

Figure 6.5: **Phosphorylation of MKK3 and MKK6, but not MKK4, is dependent on TPL-2 kinase activity but not ERK1/2 activation.**
MKK3, MKK4 and MKK6 were individually immunoprecipitated from wild type, PD0325901-treated wild type and *Map3k8*$^{D270A/D270A}$ BMDM, left unstimulated or stimulated with 100 ng/ml LPS for 15 mins. Eluates (A) or whole cell lysates (B and C) were separated by gel electrophoresis and transferred to PVDF membranes, followed by immunoblotting with the indicated antibodies. Representative of three independent experiments. WT = wild type BMDM, I = immunoprecipitation input, PI = post-immunoprecipitation.

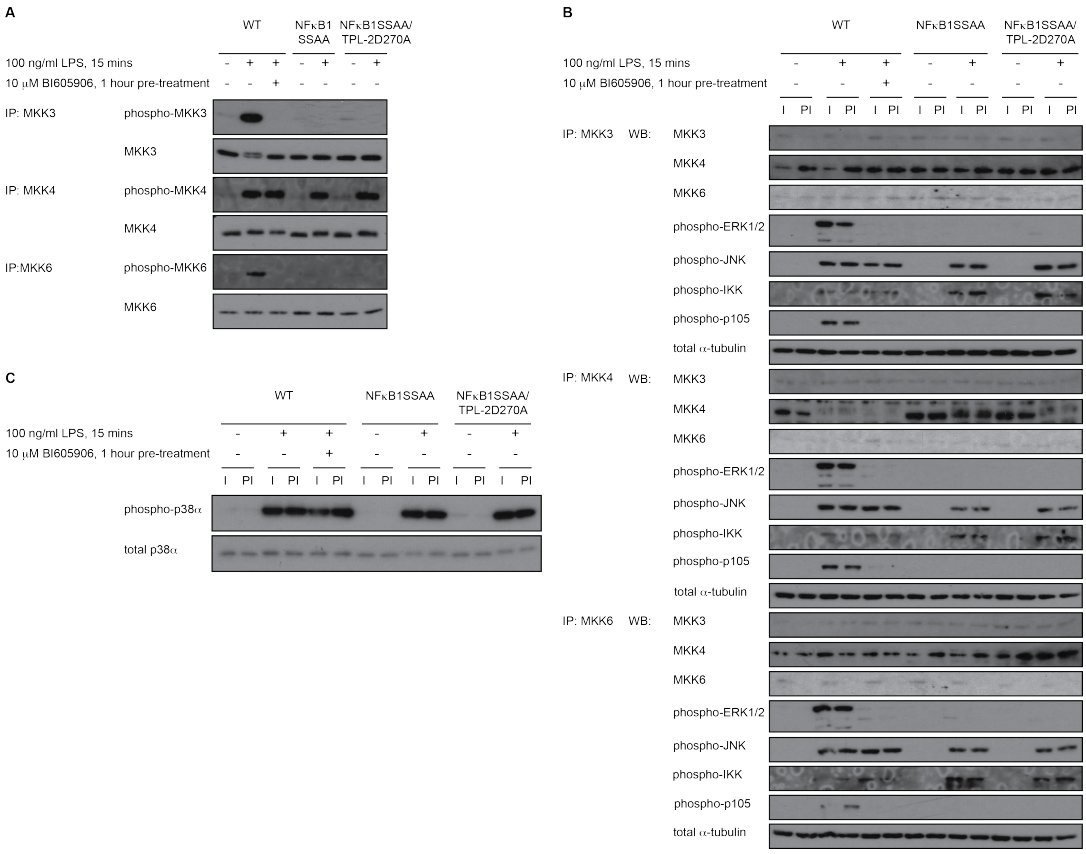

Figure 6.6: **Phosphorylation of MKK3 and MKK6, but not MKK4, is dependent on IKK2 activity and NFκB1 p105 phosphorylation.**
MKK3, MKK4 and MKK6 were individually immunoprecipitated from wild type, *Nfκb1*$^{SSAA/SSAA}$ and *Nfκb1*$^{SSAA/SSAA}$*Map3k8*$^{D270A/D270A}$ BMDM, left untreated or treated with BI605906 and/or 100 ng/ml LPS for 15 mins. Eluates (A) or whole cell lysates (B and C) were separated by gel electrophoresis and transferred to PVDF membranes, followed by immunoblotting with the indicated antibodies. Representative of three independent experiments. WT = wild type BMDM, I = immunoprecipitation input, PI = post-immunoprecipitation.

6.2.1 Can TPL-2 directly phosphorylate MKK3 and MKK6?

The experiments in the previous section clearly established that TPL-2 catalytic activity controlled the phosphorylation of MKK3/6 in primary LPS-stimulated macrophages. However, it was not clear whether this reflected the direct phosphorylation of MKK3 and MKK6 by TPL-2 or was mediated via an intermediate downstream kinase. It is not possible to isolate soluble active TPL-2 without co-expression with NFκB1 p105 and ABIN-2, as it is completely insoluble. M30-TPL-2$^{30-397}$ is partially soluble and active, but can only be purified to approximately 40

% (Jia et al., 2005). To circumvent these problems, *in vitro* kinase assays were performed using highly purified recombinant TPL-2/ABIN-2/NFκB1 p105 complex (Gantke et al., 2013), generated in the Ley laboratory. As earlier experiments had demonstrated that TPL-2 phosphorylation of MEK1 is inhibited by the NFκB1 p105 death domain (DD) (Babu et al., 2006b), *in vitro* kinase assays were also carried out using recombinant TPL-2/ABIN-2/NFκB1 p105ΔDD. Recombinant purified MKK6 protein was used as a substrate and phosphorylation on the activation loop was monitored by immunoblotting. Purified MEK1 protein was included in assays as a control.

These assays demonstrated that TPL-2/ABIN-2/NFκB1 p105 complex phosphorylated the activation loop of MKK6 (figure 6.7). In line with earlier experiments using MEK1 as a substrate, the ability of TPL-2 to phosphorylate MKK6 was regulated by NFκB1 p105DD, and MKK6 phosphorylation was stronger with TPL-2/ABIN-2/NFκB1 p105ΔDD than the wild type complex. It will be important to test whether TPL-2-dependent regulation of MKK3 phosphorylation in LPS-stimulated macrophages is also a result of direct MKK3 phosphorylation. This is very likely because of the high degree of similarity between the two MKK isoforms. In addition, it will be necessary to determine whether endogenous TPL-2, immunoprecipitated from LPS-stimulated primary macrophage lysates, phosphorylates MKK3 and MKK6 *in vitro*.

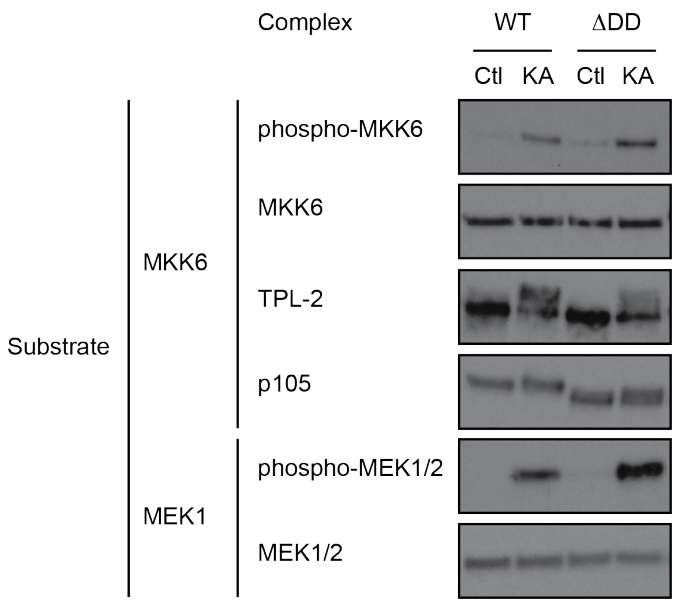

Figure 6.7: **Complexed TPL-2 directly phosphorylates MKK6 *in vitro*.** Recombinant TPL-2/ABIN-2/NFκB1 p105 triple complex with or without the NFκB1 p105 death domain was incubated with either recombinant MKK6 or recombinant MEK1 for 60 mins. Reaction mixtures were separated by gel electrophoresis and transferred to PVDF membranes, before immunoblotting with the indicated antibodies. Representative of 3 technical replicates. WT = wild type TPL-2/ABIN-2/NFκB1 p105 complex, ΔDD = TPL-2/ABIN-2/NFκB1 p105ΔDD complex, Ctl = control reaction on ice, KA = kinase reaction at room temperature.

6.3 What are the downstream targets of TPL-2/MKK3/6 signalling?

6.3.1 p38 isoforms

Four p38 isoforms exist, α, β, γ and δ. These can be separated broadly into two groups based on homology, sensitivity to inhibitors and substrate specificity; α and β, which share 75 % identity, and γ and δ, which are about 70 % identical to each other but only about 60 % identical to α and β (Cuenda and Rousseau, 2007). The four isoforms have over 90 % identity in the kinase domains (Coulthard et al., 2009). At low concentrations, only p38α and p38β are sensitive to the pyridinyl imidazole inhibitors, although others such as the allosteric inhibitor BIRB-796 are capable of inhibiting all four isoforms (Zhang et al., 2007; González-Terán et al., 2013). Expression patterns also vary between the different isoforms. Whilst

p38α is ubiquitously high, p38β, p38γ and p38δ show more restricted expression patterns with p38β most abundant in brain, p38γ in skeletal muscle, and p38δ in endocrine glands (Tortorella et al., 2003; Risco and Cuenda, 2012).

Substrates and downstream functions

Some substrates are shared between all four p38 isoforms, such as transcription factors like Elk-1 and Elk-4. There are also isoform specific substrates, such as MAPKAP-K2 and MAPKAP-K3 that are phosphorylated by p38α/β, but not p38γ/δ (Cuenda et al., 1997; Goedert et al., 1997). Several splice variants exist for p38α in humans, including Exip, Mxi2 and CSBP1. Exip, which has a different C-terminus and cannot be phosphorylated by classical p38 activating treatments, has been reported to regulate NFκB signalling (Yagasaki et al., 2004). Mxi2 also has an alternate C-terminus and reduced binding to, and subsequent phosphorylation of, classical p38α substrates, but instead regulates nuclear import of ERK1/2 (Casar et al., 2007). The third variant, CSBP1, differs at an internal sequence of 25 amino acids; its role in signalling is not yet understood (Lee et al., 1994).

Unique amongst the p38 MAP kinases, p38γ contains a PDZ binding domain which facilitates interaction with specific substrates. These include the cytoskeletal scaffold protein α1-syntrophin, which localises p38γ to the neuromuscular junction in skeletal muscle (Hasegawa et al., 1999). Although not containing a PDZ domain, p38δ has also been reported to regulate the cytoskeleton via phosphorylation of stathmin (Parker et al., 1998). SAP97 function in cell adaptation to osmotic stress is regulated by p38γ, independently of its kinase activity, by displacing interacting proteins such as PSF, a regulator of transcription and pre-mRNA processing (Sabio et al., 2005, 2010). Another example of the kinase-independent functions is the stabilisation of TPL-2 by p38γ/δ in macrophages (Risco et al., 2012). Although the substrate specificities of the different p38 isoforms have not been systematically investigated, present knowledge indicates differences in isoform substrate specificity and implies distinct functional

roles. As the most widely expressed and extensively studied isoform, p38α has been implicated in processes including mRNA stability, apoptosis, cell migration and senescence (Cuadrado and Nebreda, 2010; Risco and Cuenda, 2012). The strength and duration of signalling are thought to determine the final outcome, with strong signalling in response to stress signals more likely to cause apoptosis and weaker/shorter activation associated with homeostatic functions (Dolado and Nebreda, 2008). It has been suggested that p38α is involved in pathologies ranging from inflammatory/immunological disease to cancer and neurodegenerative disease (Cuadrado and Nebreda, 2010). A chemical genetic approach, in which either p38α or p38β were mutated to be resistant to most commonly used p38 inhibitors, showed that blockade of TLR-induced TNFα release and protection from antibody-induced arthritis by these inhibitors is largely the result of p38α inhibition (O'Keefe et al., 2007). This implies that p38β is largely dispensable for inflammatory signalling. p38δ is thought to be involved in cytoskeletal remodelling and insulin secretion (Risco and Cuenda, 2012). p38γ and p38δ have jointly been implicated in cancer, immune disorders such as rheumatoid arthritis and metabolic disorders (Coulthard et al., 2009; Cuadrado and Nebreda, 2010). Biological functions ascribed to p38γ include skeletal muscle differentiation and senescence, although through a different mechanism to p38α (Risco and Cuenda, 2012).

Regulation of p38 activation

The major pathway of p38 activation involves phosphorylation by MAP 2-kinases MKK3 and MKK6 on the threonine and tyrosine residues of the Thr-Gly-Tyr (TGY) motif in the p38 activation loop (figure 6.1). Although MKK3/6 are the primary activators of all p38 isoforms, MKK4 has also been shown to phosphorylate and activate p38α in MEFs exposed to ultraviolet light (Brancho et al., 2003). Alternative mechanisms of activation that do not require a MAP 2-kinase have also been proposed for p38α. These include p38α interaction with TAB1, which promotes p38α auto-phosphorylation and activation (Ge et al., 2002). In T cells activated through the T cell receptor, p38α activation has been reported to involve phosphorylation

of a non-canonical activating residue, Tyr323. This phosphorylation induces p38α activity, possibly by altering the structural conformation, allowing phosphorylation of both the canonical activating TGY motif residues and substrates (Salvador et al., 2005). However, these MAP 2-kinase-independent mechanisms have not been confirmed in cells lacking MKK3, 4 and 6.

The mechanism by which p38 signalling is down-regulated is less well described than its activation. De-phosphorylation of p38α by multiple phosphatases, including protein serine/threonine phosphatases, protein tyrosine phosphatases and dual-specificity phosphatases has been described (Cuadrado and Nebreda, 2010; Risco and Cuenda, 2012). The PDZ binding motif of p38γ allows it to interact with and be dephosphorylated by the protein tyrosine phosphatase, PTPH1 (Risco and Cuenda, 2012). In contrast, p38α, which lacks a PDZ domain, is not dephosphorylated by PTPH1.

Peregrin et al. (2006) also demonstrated a role for phosphorylation in the inactivation of p38α. Phosphorylation of threonine 123 reduces the ability of p38α to interact with both its MAP 2-kinase MKK6 and its substrates decreasing its ability to transduce signals. It is unclear whether other p38 isoforms are subject to a similar type of regulation.

6.3.2 Does TPL-2 control p38 MAPK pathway activation

MKK3 and MKK6 are considered to be the canonical MAP 2-kinases for the p38α signalling pathway. However, my immunoblotting and phosphoproteomic data showed that although TPL-2 catalytic activity was required for activation of MKK3 and MKK6 in LPS-stimulated macrophages, the phosphorylation of p38α was TPL-2 independent (figure 6.8). Experiments in MEFs have previously shown that MKK4 can activate p38α (Brancho et al., 2003). Together these results suggest that LPS activation of p38α in macrophages is largely mediated via MKK4, rather than MKK3/6.

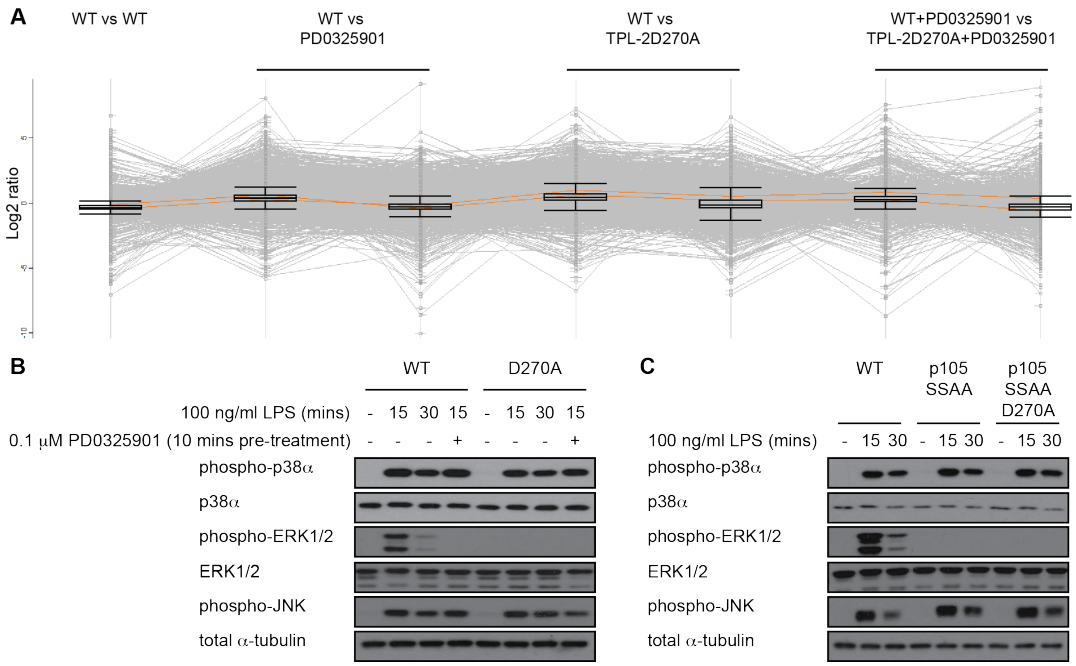

Figure 6.8: **p38α phosphorylation is not regulated by TPL-2.**
A: Lysates from SILAC-labelled BMDM, stimulated with 100 ng/ml LPS for 15 mins, were compared by mass spectrometry. The p38α activation loop phosphopeptides (Thr180 and Tyr182) are highlighted. B: wild type and *Map3k8*$^{D270A/D270A}$ BMDM were left untreated or treated with PD0325901 and/or 100 ng/ml LPS for the indicated times. C: wild type, *Nfκb1*$^{SSAA/SSAA}$ and *Nfκb1*$^{SSAA/SSAA}$*Map3k8*$^{D270A/D270A}$ BMDM were left untreated or stimulated with 100 ng/ml LPS for the indicated times. Cells were lysed, proteins separated by gel electrophoresis and transferred to PVDF membranes, followed by immunoblotting with the indicated antibodies. Immunoblots are representative of 3 independent experiments. WT = wild type BMDM, PD0325901 = MEK1/2 inhibitor treated BMDM, D270A = TPL-2 kinase-inactive BMDM.

Although the results of the current study clearly demonstrated TPL-2 regulated the activation of MKK3 and MKK6 in LPS-stimulated macrophages, the biological significance of this signalling pathway remained unclear. One possibility was the TPL-2 specifically regulated the activation of p38 isoforms other than p38α. A surprising link between TPL-2 signalling and p38γ and p38δ was recently reported by the group of Dr. Ana Cuenda. Cells lacking expression of p38γ and p38δ were found to be profoundly deficient in both TPL-2 and ABIN-2 protein, although levels of mRNA encoding these proteins were not affected (Risco et al., 2012). The stability of TPL-2 and/or ABIN-2 therefore are regulated by p38γ/δ, and consequently TPL-2 signalling is impaired in p38γ/δ-deficient cells. These results were remin-

iscent of an earlier study showing that the stability of p38α was dependent on the expression of one of its substrates, MK2 (Ronkina et al., 2007). This raised the possibility that TPL-2 might function upstream of p38γ and p38δ, which are specifically phosphorylated by MKK3 and MKK6.

Analysis of the phosphoproteomics data revealed that no p38γ/δ phosphorylation sites had been identified, likely due to their very low abundance in BMDM (Risco et al., 2012). Therefore, immunoprecipitation was used to enrich p38γ and p38δ consecutively from 15 mg BMDM whole cell lysate prior to immunoblotting for activation loop phosphorylation. In wild type cells, phosphorylation of the activating residues of p38γ was clearly induced by stimulation with 100 ng/ml LPS for 30 minutes. However, LPS did not induce p38γ phosphorylation in *Map3k8*$^{D270A/D270A}$ BMDM, showing that p38γ activation was regulated by TPL-2 catalytic activity (figure 6.9). Pre-treatment of wild type cells with a MEK1/2 inhibitor did not affect LPS induction of p38γ phosphorylation, in agreement with earlier results showing that MKK3/6 phosphorylation in LPS-stimulated macrophages was independent of ERK1/2 signalling. Phosphorylation of p38δ could not be detected even after immunoprecipitation. This may reflect the low levels of this kinase or be the result of non-specific losses during the sequential immunoprecipitation methodology in which p38γ was isolated before p38δ.

To investigate indirectly whether TPL-2 regulated p38δ activation, the phosphorylation of a reported p38δ downstream target, eEF2 Thr56, was assessed by immunoblotting. p38δ phosphorylates eEF2K at Ser359 which results in eEF2K inactivation. This in turn prevents phosphorylation of eEF2 at the inhibitory site T56 and results in a reduction in its phosphorylation when p38δ is active (Knebel et al., 2001; González-Terán et al., 2013). Reduced phosphorylation at Thr56 allows eEF2 to catalyse extension of nascent proteins at the ribosome (Ryazanov et al., 1988; Carlberg et al., 1990). In line with this, wild type BMDM phosphorylation of eEF2 was clearly reduced by LPS stimulation. However, this reduction was substantially blunted in *Map3k8*$^{D270A/D270A}$ BMDM (figure 6.10). p38γ is not able to activate this pathway (Knebel et al., 2001; Cohen and Knebel, 2006) giving

support to the hypothesis that TPL-2 is necessary for activation of p38δ as well as p38γ. The reduction was also partially abrogated in wild type cells treated with the MEK1/2 inhibitor, suggesting the ERK1/2 MAP kinase pathway also contributes to this response, although this could alternatively be due to off-target effects of the inhibitor.

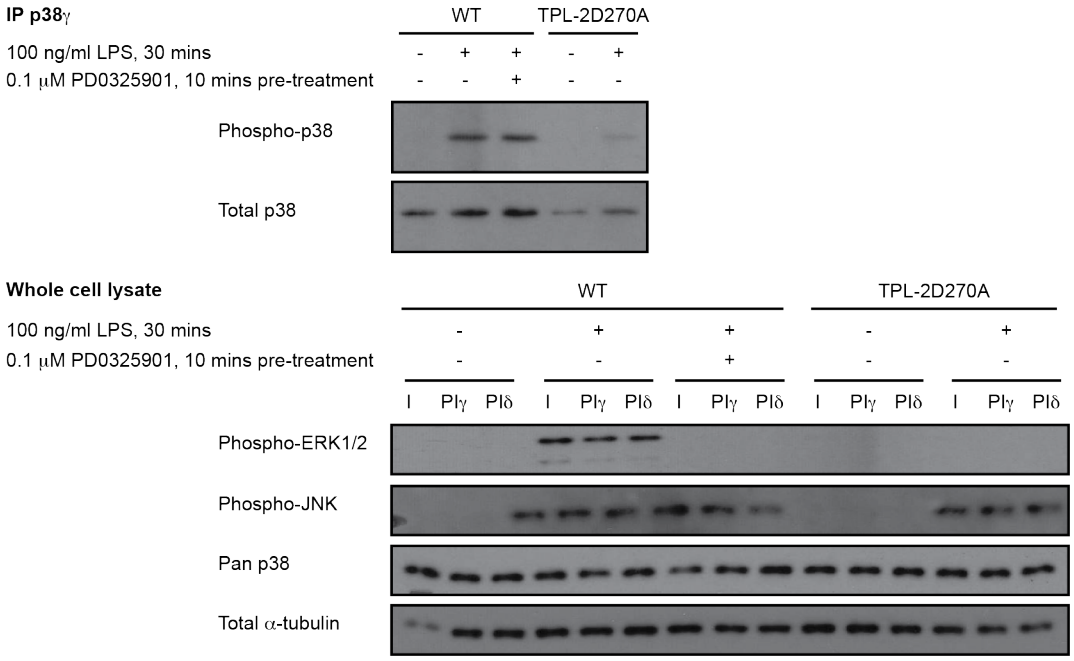

Figure 6.9: **Phosphorylation of p38γ activation loop residues is dependent on TPL-2 kinase activity.**
p38γ was immunoprecipitated from lysates of unstimulated or LPS-stimulated wild type, PD0325901-treated wild type or *Map3k8*$^{D270A/D270A}$ BMDM. Eluates (upper panel) or whole cell lysates (lower panel) were separated by gel electrophoresis and transferred to PVDF membranes, followed by immunoblotting with the indicated antibodies. Representative of 3 independent experiments, each using 6 wild type and 3 *Map3k8*$^{D270A/D270A}$ mice. WT = wild type, IP = immunoprecipitation, I = immunoprecipitation input, PIγ = post-immunoprecipitation of p38γ, PIδ = post-immunoprecipitation of p38δ.

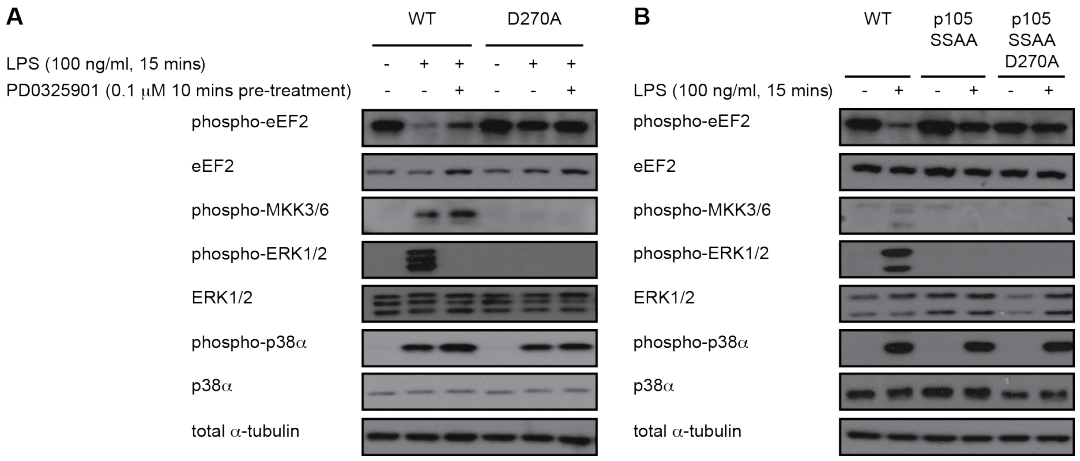

Figure 6.10: **Phosphorylation of eEF2, a downstream target of p38γ/δ, is altered by disruption of the TPL-2 pathway.**
A: wild type and *Map3k8*$^{D270A/D270A}$ were left untreated or treated with PD0325901 and/or 100 ng/ml LPS for 15 mins. B: wild type, *Nfκb1*$^{SSAA/SSAA}$ and *Nfκb1*$^{SSAA/SSAA}$*Map3k8*$^{D270A/D270A}$ were left unstimulated or stimulated with 100 ng/ml LPS for 15 mins. Cell were lysed, proteins separated by gel electrophoresis and transferred to PVDF membranes. The indicated antibodies were used for immunoblotting. Representative of 3 independent experiments. WT = wild type BMDM, D270A = TPL-2 kinase-inactive BMDM.

6.4 TPL-2 protein levels and ERK1/2 phosphorylation are normal in *Mapk12*$^{Y185F/Y185F}$/*Mapk13*$^{-/-}$ BMDM

The laboratory of our collaborator, Dr. Ana Cuenda, generated a *Mapk12*$^{Y185F/Y185F}$/*Mapk13*$^{-/-}$ mouse strain that expresses catalytically inactive p38γ and no p38δ. Generation of BMDM from these mice demonstrated that expression of kinase-inactive p38γ allowed normal expression of TPL-2 protein in BMDM and rescued LPS-induced activation of ERK1/2 (figure 6.11). These results suggested that p38γ functioned as a scaffold to stabilise TPL-2 and indicated that p38γ catalytic activity was not required for TPL-2-dependent activation of MEK1/2 and subsequent activation of ERK1/2. Cells from these mice will be useful in future experiments for investigating the specific functions of the TPL-2/MKK3/6/p38γ/δ signalling pathway identified by this study.

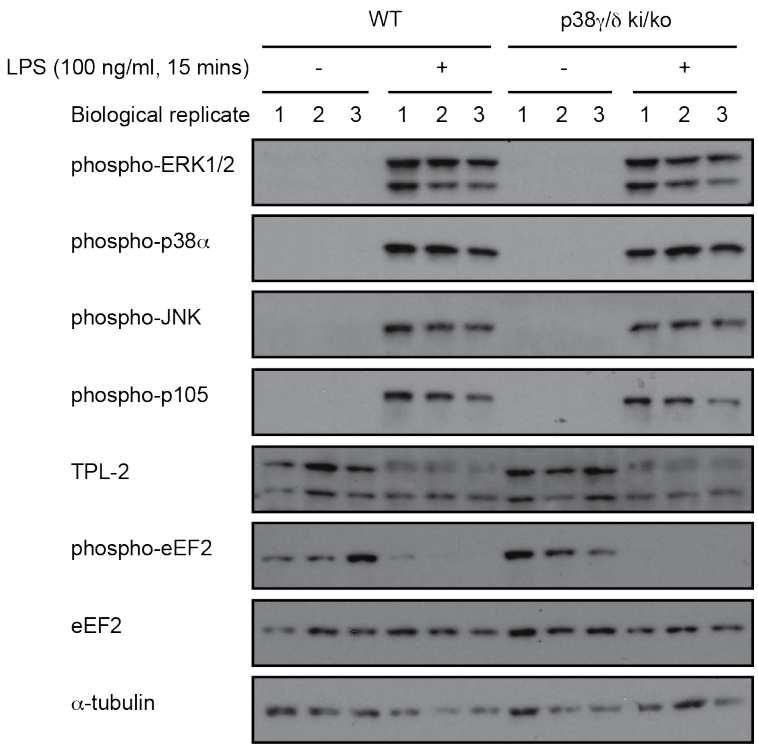

Figure 6.11: ***Mapk12$^{Y185F/Y185F}$/Mapk13$^{-/-}$* BMDM have normal levels of TPL-2 and phosphorylation of ERK1/2 activation loop residues upon LPS stimulation.**
BMDM generated from wild type or *Mapk12$^{Y185F/Y185F}$/Mapk13$^{-/-}$* mice were left unstimulated or stimulated with 100 ng/ml LPS for 15 mins. Cells were lysed, proteins separated by gel electrophoresis and transferred to PVDF membranes. The indicated antibodies were used for immunoblotting. Shown are replicates from parallel cultures of three different mice. WT = wild type BMDM, p38γ/δ = kinase-inactive p38γ/p38δ deficient BMDM.

6.5 Summary

The current study has validated MKK3/6 activation loop residues, identified by SILAC/mass spectrometry, as TPL-2-dependent, ERK1/2-independent phosphorylations by immunoblotting in unlabelled BMDM plus/minus LPS stimulation. It was subsequently shown, using immunoprecipitation-immunoblotting, that TPL-2 phosphorylates MKK3 and MKK6, but not MKK4, on their activating residues. Using small molecule inhibitors, this was found to be independent of ERK1/2 kinase activity but dependent on IKK2 kinase activity. The phosphorylation of MKK3 and MKK6 is also dependent on NFκB1 p105 phosphorylation by IKK2, as shown using NFκB1 p105 macrophages. TPL-2 phosphorylation of MKK6 was

found to be direct using recombinant TPL-2 in an *in vitro* kinase assay. However, it will be necessary to confirm that this phosphorylation is the result of TPL-2 activity using the specific inhibitor, C34 (Green et al., 2007), as well as repeating these experiments using kinase-inactive MKK6 that was not available at the time of this study. Furthermore, proof that endogenous TPL-2 can also directly phosphorylate MKK6 by doing immunoprecipitation-kinase assays from LPS stimulated wild type and TPL-2 kinase dead BMDM will be vital. It has subsequently been shown that TPL-2-dependent MKK3/6 phosphorylation results in the phosphorylation of p38γ. In order to show that p38δ regulation is the same as p38γ it will be necessary to repeat the immunoprecipitations of p38δ from fresh lysates. We have, however, provided indirect evidence for the activation of p38δ by showing defective dephosphorylation of eEF2, a downstream target of p38δ that associates with the TPL-2/ABIN-2/NFκB1 p105 complex in HEK293 cells (Ley laboratory, unpublished data), in the absence of TPL-2 kinase activity.

Although it has not been formally investigated here, it is likely that, given the proven ability of MKK4 to regulate p38α phosphorylation, the p38α pathway is activated through MKK4 in LPS stimulated macrophages independently of TPL-2. This would need to be tested using a macrophage specific MKK4 knock-out because the full knock out has an embryonic lethal phenotype (Abell et al., 2005).

Published targets of p38γ/δ give some indication of what TPL-2 could be regulating though this novel pathway. All four p38 isoforms are known to activate the transcription factors Elk1, Elk3 (SAP2) and Elk4 (SAP1) (Goedert et al., 1997; O'Callaghan et al., 2014) which belong to the SRF-TCF family of transcription factors, members of which were suggested as regulators of TPL-2-dependent, ERK1/2-independent genes by transcription factor enrichment analysis following RNA sequencing (Ley laboratory, unpublished data). Control of p38γ/δ may also provide the mechanism by which TPL-2 regulates TNFα. A recent study by González-Terán et al. (2013) found that absence of p38γ/δ in macrophages was protective against an LPS and D-galactosamine-induced murine model of liver disease. This protection was mediated by a reduction in TNFα production which

was shown to result from a block in eEF2-dependent translation of TNFα mRNA. This is a striking parallel with the phenotype of *Map3k8*$^{D270A/D270A}$ macrophages which seem to have fairly normal levels of TNFα mRNA but produce very little TNFα protein. Alternatively, p38γ could regulate TACE-dependent TNFα cleavage through its substrate, SAP97, which can interact with the cytoplasmic tail of TACE (Levine, 2008).

With the newly available p38γ/δ knock-in/knock-out mice it will be interesting to test more fully how BMDM from these mice compare to those from the TPL-2 kinase dead. As well as ELISAs for production of TNFα and other key cytokines, this could include RNA sequencing to identify genes overlapping with the TPL-2 transcriptome recently generated in the Ley laboratory (unpublished data). A large proportion of TPL-2 regulated genes (51 out of 94 genes) were shown to be independent of ERK1/2 and these, or a proportion thereof, could be regulated instead by p38γ/δ. By identifying the link between TPL-2 and p38γ/δ it will now be possible to use the p38γ/δ knock-in/knock-out mice to understand more completely how TPL-2 regulates innate immune responses.

7 Discussion

7.1 Impact

In this study, BMDM have been SILAC labelled and used to generate an unbiased phosphoproteomics dataset of sites present in LPS stimulated cells. By making pairwise comparisons between different genetic and chemical perturbations, it has been possible to determine which phosphosites were regulated *in vivo* by endogenous TPL-2 independent of ERK1/2 signalling. This allowed identification of the activation loop residue of MKK3 and MKK6 as TPL-2 substrates in LPS-stimulated BMDM, which was confirmed by immunoblotting with phospho-specific antibodies. Furthermore, TPL-2 was shown to be required for phosphorylation of the MKK3/6 substrate p38γ. These data define a novel TPL-2/MKK3/6/p38γ MAP kinase pathway that is activated in LPS-stimulated macrophages. Interestingly, TPL-2 suppression of the HGF/c-Met pathway in intestinal myofibroblasts is mediated independently of any effects on ERK1/2 and p38α activation (Koliaraki et al., 2012). It is possible that TPL-2 regulates this pathway via activation of p38γ. It will be important in future studies to determine whether TPL-2 also regulates the activation of p38δ in LPS-stimulated macrophages and whether TPL-2 regulates p38γ/δ activation after stimulation with other TLR ligands and in other cell types.

Although relatively few substrates of p38γ/δ are known, they could shed light on how TPL-2 regulates its ERK1/2-independent functions. Known p38γ substrates include SAP97 (Risco and Cuenda, 2012), which interacts with the cytoplasmic tail of TACE (Levine, 2008) and could explain how TPL-2 regulates release of TNFα. Proteins regulated by p38δ include eEF2K and its substrate eEF2 (Risco and Cuenda, 2012). eEF2 phosphorylation was shown in the current study to be regulated by TPL-2 kinase activity, and eEF2 was previously found to associate with the TPL-2/ABIN-2/NFκB1 p105 triple complex in HEK392 cells (Ley laboratory, unpublished data). eEF2 promotes translation (Ryazanov et al., 1988), indicating another level, in addition to transcriptional and post-translational modification levels, at which TPL-2 may control cell function. González-Terán et al. (2013) have shown that eEF2 is important for the translation of TNFα mRNA, providing an alternative possible link between TPL-2 and TNFα production.

The results of this study may explain seemingly conflicting results in mutant mice. Deletion of either MKK3 or MKK6 was protective in antibody transfer models of arthritis, however, deletion of p38α in myeloid cells was not (Guma et al., 2012). The results of the current study suggest that the reason for this discrepancy may be that MKK3/6 are controlling p38γ/δ in this model rather than p38α. Currently most p38 inhibitors do not block p38γ/δ and there are no specific inhibitors for these isoforms, therefore TPL-2 inhibitors may prove an effective way to block p38γ/δ activation until specific inhibitors become available.

In spite of the limited knowledge of p38γ/δ substrates, some studies have demonstrated their role in models of inflammatory conditions. For example, Criado et al. (2014) found that mice deficient in both p38γ and p38δ were protected from collagen-induced arthritis. Similarly, p38γ/δ-deficient mice were protected from an inflammation-associated colon cancer model induced by azoxymethane and dextran sodium sulphate (del Reino et al., 2014). These mice had reduced recruitment of neutrophils and macrophages as well as lower levels of pro-inflammatory cytokines and chemokines than the wild type. The current study has indicated that p38γ may contribute to immune functions of TPL-2 and the autoimmune and inflammatory diseases in which TPL-2 is implicated (e.g. IBD). Therefore, direct comparison of the effects of *Map3k8*$^{D270A/D270A}$ and *Mapk12*$^{Y185F/Y185F}$/*Mapk13*$^{-/-}$ in disease models will be important to determine whether the effects of TPL-2 in inflammation are mediated via p38γ/δ.

None of the published substrates of TPL-2 were found to be regulated in the current study, except for NFκB1 p105. This could be the result of differences in the cell type and/or stimulus used. For example, PLCβ3 was found to be a TPL-2 target in fibroblasts stimulated through G-protein coupled receptors (Hatziapostolou et al., 2011) and the signalling could be substantially different in the TLR-activated macrophages tested in this study. Alternatively these phosphorylations may have been artefacts of the non-physiological methods used by many of the studies.

This study identified a major limitation with the SILAC methodology as both K0R0 and K8R10 SILAC labelling altered the activation of ERK1/2 in response

to LPS stimulation in *Nfκb1*$^{SSAA/SSAA}$ macrophages. This did not appear to be dependent on the presence of carbon/nitrogen/hydrogen isotopes in the amino acids, but may have been due to dialysis of the FCS or LCCM used. Changes in MAP kinase pathways were not evident for all genotypes, so it is possible that only certain genotypes are affected. However, as all genotypes experience the same culture conditions it seems likely that other signalling pathways may also be affected compared to unlabelled cells. Therefore, SILAC labelling could have impacted the phosphorylations which were identified as TPL-2 regulated in this study, hence the need for independent validation of each phosphosite. To enable future MS-based phosphoproteomics studies of *Nfκb1*$^{SSAA/SSAA}$ and *Nfκb1*$^{SSAA/SSAA}$ *Map3k8*$^{D270A/D270A}$ macrophages alternative methods will be needed such as *in vitro* labelling after cell lysis using iTRAQ (Wiese et al., 2007).

In spite of these problems, the ability to SILAC label BMDM will be valuable in combination with other studies. For example, in studies with an analogue-sensitive TPL-2 mutant being developed by the Ley laboratory, SILAC labelling will help to reduce false-positives (Shah et al., 1997; Carlson et al., 2011). A SILAC-labelled cell lysate incubated with the analogue-sensitive TPL-2 would be compared with an unlabelled lysate incubated without the mutant kinase, allowing any background use of the ATP analogue by other kinases to be removed from the results. It would also be interesting to develop analogue-sensitive mutants of p38γ and p38δ as there is currently very little known about what these p38 isoforms do. None of the TPL-2-dependent phosphorylations identified in this study are known p38γ/δ substrates, however, using analogue-sensitive p38γ/δ isoforms to identify their substrates on a large scale may change this.

This study also identified over 200 ERK1/2 regulated proteins. A large proportion of these were suggested to be involved in gene expression and RNA processing, including translation, key processes for activation of macrophages. Other highly represented protein categories were components of the cytoskeleton and regulators of small GTPases. Such proteins contribute to actin rearrangement, an important process in the phagocytic and chemotactic functions of activated mac-

rophages during the innate immune response. This suggests that ERK1/2 may play a role in regulating these processes in pathogen clearance.

7.2 Future work

Further characterisation of MKK3/6 as TPL-2 substrates, including determination of Michaelis-Menten parameters (K_m, V_{max} and K_{cat}), will allow a detailed comparison with MEK1/2 which could indicate how these two pathways might be coordinately regulated by TPL-2 in cells and whether there might be competition for TPL-2 phosphorylation between MEK1/2 and MKK3/6. Further studies will be necessary to show that regulation of MKK3/6 phosphorylation by TPL-2 is dependent, not only on NFκB1 p105 phosphorylation by IKK2 as has been shown here, but also on TPL-2 release from the triple complex. It will also be interesting to determine whether 14-3-3 binding to the TPL-2 C-terminus is required for phosphorylation of MKK3/6, similar to MEK1/2 (Ben-Addi et al., 2014).

In addition to further biochemical characterisation, it will be important to understand how the TPL-2/MKK3/6/p38γ/δ pathway contributes to macrophage functions in innate immune responses. Whether p38γ/δ control TNFα production will need to be tested in *Mapk12*$^{Y185F/Y185F}$/*Mapk13*$^{-/-}$ macrophages. As shown in the current study, the *Mapk12*$^{Y185F/Y185F}$/*Mapk13*$^{-/-}$ mutation does not affect TPL-2 signalling via ERK1/2 but selectively blocks p38γ/δ signalling, enabling specific investigation of this pathway in TNFα production. If there is an effect on TNFα production, further experiments, such as retroviral replacement of p38γ or p38δ in p38γ/δ-deficient cells, will be needed to determine which isoform is responsible. Similarly, it will be necessary to determine by RNA sequencing experiments, using *Mapk12*$^{Y185F/Y185F}$/*Mapk13*$^{-/-}$ macrophages, whether p38γ/δ control the ERK1/2-independent fraction of TPL-2 regulated genes identified by RNA sequencing (Ley laboratory, unpublished data). In particular, transcription factors from the SRF-TCF family can be activated by both p38γ and p38δ (Goedert et al., 1997; O'Callaghan et al., 2014) and were suggested as regulators of TPL-2-dependent, ERK1/2-independent genes by transcription factor enrichment analysis.

As the list of TPL-2-dependent, ERK1/2-independent sites is not extensive it would be feasible to take a medium throughput approach to investigate whether these sites are important in TPL-2 regulated innate immune functions. Knock-down of targets using genome-wide perturbation methods like RNA interference (RNAi) has historically been more challenging in macrophages than in other cell types like fibroblasts because of highly sensitive induction of non-specific immune responses to both dsRNA and transfection reagents (Judge et al., 2005; Cekaite et al., 2007; Lacaze et al., 2009). Recently, a protocol for achieving this using small interfering RNA (siRNA) in the RAW264.7 and THP1 macrophage cell lines was published by Li et al. (2015). By testing hundreds of transfection conditions, the authors identified combinations of siRNA and transfection lipids that resulted in minimal induction of type I interferons while maintaining efficient target gene silencing. Their optimised transfection system would be useful for conducting a secondary siRNA screen of the most interesting phosphorylated proteins identified in the current study. Readouts which could be applied in this secondary screen to assess similarity of each "knock-down" to the effects of *Map3k8*$^{D270A/D270A}$ mutation include cytokine release using a multiplexed assay such as Luminex® (Life Technologies, USA). Furthermore, GO analysis of TPL-2 regulated phosphoproteins in the current study has suggested that TPL-2 may regulate cell movement, the actin cytoskeleton, intracellular transport and steroid metabolism. It will be interesting to determine the importance of TPL-2 signalling in regulating these processes by determining the effects of *Map3k8*$^{D270A/D270A}$ mutation in LPS-stimulated macrophages. If these experiments are positive, the role of specific TPL-2 regulated phospho-proteins could be determined by siRNA knockdown.

Proteins identified by the secondary screen as relevant to macrophage function could then be mutated at the TPL-2 phosphorylation site in an alternative system already established in the Ley laboratory to show that the phosphorylation is important. Using the Hoxb8 oncogene under control of the oestrogen receptor, primary myeloid progenitors can be immortalised then differentiated with cytokines to produce macrophages (Wang et al., 2006). As these cells can be maintained

indefinitely, CRISPR (clustered regularly interspaced palindromic repeats) could be used to create point mutations in the genes of interest (Cong et al., 2013; Mali et al., 2013) and then the determined read-outs used to test if the phosphorylation is functional. CRISPR uses a guide RNA to target a DNA endonuclease to a corresponding gene sequence, where it introduces a double-strand break. By introducing a template DNA strand, non-homologous end joining can be harnessed to introduce a mutation when repairing the break (Shalem et al., 2015).

Proteins found to be phosphorylated in a TPL-2-dependent manner will be tested as substrates in *in vitro* kinase assays using immunoprecipitated wild type or kinase-inactive TPL-2 to establish whether they are direct TPL-2 substrates or if an intermediate kinase is required. Finally, validated proteins could be mutated in mice to allow a more detailed investigation of their physiological relevance in immune responses and autoimmune or inflammatory diseases.

The importance of ERK1/2-regulated phosphoproteins in different aspects of macrophage function could also be validated and investigated using the approach outlined above, in combination with MEK1/2 inhibitors. As this study suggested that ERK1/2 regulated proteins linked to cytoskeletal rearrangement, macrophage functions like phagocytosis, migration and chemotaxis could be tested using MEK1/2 inhibitors to identify which processes involving ERK1/2 activity. This would provide the read-out with which to interpret the siRNA and CRISPR screens as well as suggesting a mechanism through which TPL-2/ERK1/2 signalling could contribute to macrophage function in the innate immune response.

The SILAC/MS experiments identified very few transcription factors that were regulated by TPL-2 so it is difficult to assess directly how TPL-2 signalling might regulate gene expression. To focus the investigation on transcription factors, which are generally of low abundance, it will be necessary to repeat the phosphoproteomic comparisons with a greater degree of fractionation prior to LC-MS/MS analysis. This could be achieved by bulk purification of nuclei prior to lysis. This might introduce quantification errors but would mean that only nuclear proteins will be analysed. Alternatively, more fractions could be collected during strong

cation exchange, which would significantly increase the time necessary for phosphopeptide enrichment and analysis. If one of these approaches works, it should be possible to determine which transcription factors are phosphorylated in a TPL-2 dependent fashion, and whether these are controlled via ERK1/2-dependent or -independent pathways. This is particularly interesting as RNA sequencing experiments carried out by the Ley laboratory have demonstrated that TPL-2 signalling regulates gene expression in LPS stimulated macrophages via ERK1/2 and non-ERK1/2 pathways (unpublished data). Such experiments would significantly increase our understanding of how TPL-2 regulates innate immune responses.

As well as determining the biological relevance of novel TPL-2 substrates in BMDM, it will be important to confirm these in *ex vivo* macrophage populations like peritoneal macrophages after intra-peritoneal injection of LPS. It would also be interesting to extend this to establish how many novel substrates are common to other cell types or whether TPL-2 signalling is heavily dependent on the cell context. For example, could the novel TPL-2/MKK3/6/p38γ/δ pathway found here control the ERK1/2-independent, TPL-2-mediated regulation of IL-1β in bone marrow-derived dendritic cells described by Mielke et al. (2009)? In the same way, whether these substrates are involved in TPL-2-dependent responses to other ligands such as TNFα and IL-1. To facilitate such experiments it would be necessary to generate phospho-specific antibodies against the TPL-2 target sites so that phosphorylation can easily be monitored across different conditions.

Since only LPS-stimulated samples were analysed, it is not possible to establish whether TPL-2-dependent phosphorylations detected were present in unstimulated cells. However, earlier data from the Ley laboratory has demonstrated TPL-2 in macrophages has very little activity towards MEK1 without LPS stimulation, making this unlikely. Nevertheless, this will be important to determine this directly by MS analysis of unstimulated BMDM. An extension of this will be to determine whether TPL-2 regulates other substrates at earlier or later time points before degradation, as this study has looked at only one stimulation time-point. Cross-referencing the phosphorylated targets from phosphoproteomics experiments us-

ing different time-points may make it clearer which pathways are being activated by tracing them from upstream components to downstream ones through the time-course.

7.3 Concluding remarks

This study has extended our understanding of TPL-2 signalling which will lead to a clearer picture of how TPL-2 controls the biological outcomes that contribute to innate immune responses. Furthermore, this dataset will augment future studies of TPL-2 signalling, such as the search for upstream regulators, as new information gives context to a larger proportion of the list of regulated proteins.

References

Abe, M. K., W.-L. Kuo, M. B. Hershenson, and M. R. Rosner: 1999, 'Extracellular signal-regulated kinase 7 (ERK7), a novel ERK with a C-terminal domain that regulates its activity, its cellular localization, and cell growth'. *Molecular and Cellular Biology* **19**(2), 1301–1312.

Abell, A. N., J. A. Rivera-Perez, B. D. Cuevas, M. T. Uhlik, S. Sather, N. L. Johnson, S. K. Minton, J. M. Lauder, A. M. Winter-Vann, K. Nakamura, T. Magnuson, R. R. Vaillancourt, L. E. Heasley, and G. L. Johnson: 2005, 'Ablation of MEKK4 Kinase Activity Causes Neurulation and Skeletal Patterning Defects in the Mouse Embryo'. *Molecular and Cellular Biology* **25**(20), 8948–8959.

Adams, J. A.: 2001, 'Kinetic and Catalytic Mechanisms of Protein Kinases'. *Chemical Reviews* **101**(8), 2271–2290.

Aggeli, I.-K. S., C. Gaitanaki, A. Lazou, and I. Beis: 2002, 'Hyperosmotic and thermal stresses activate p38-MAPK in the perfused amphibian heart'. *Journal of Experimental Biology* **205**(4), 443–454.

Alexopoulou, L., M. Pasparakis, and G. Kollias: 1997, 'A murine transmembrane tumor necrosis factor (TNF) transgene induces arthritis by cooperative p55/p75 TNF receptor signaling'. *European Journal of Immunology* **27**(10), 2588–2592.

Aoki, M., F. Hamada, T. Sugimoto, S. Sumida, T. Akiyama, and K. Toyoshima: 1993, 'The human cot proto-oncogene encodes two protein serine/threonine kinases with different transforming activities by alternative initiation of translation'. *The Journal of Biological Chemistry* **268**(30), 22723–32.

Apostolaki, M., M. Armaka, P. Victoratos, and G. Kollias: 2010, 'Cellular mechanisms of TNF function in models of inflammation and autoimmunity'. *Curr Dir Autoimmun* **11**, 1–26.

Aravalli, R. N.: 2013, 'Role of innate immunity in the development of hepatocellular carcinoma'. *World Journal of Gastroenterology* **19**(43), 7500.

Arthur, J. S. and S. C. Ley: 2013, 'Mitogen-activated protein kinases in innate immunity'. *Nature Reviews. Immunology* **13**(9), 679–92.

Ashburner, M., C. A. Ball, J. A. Blake, D. Botstein, H. Butler, J. M. Cherry, A. P. Davis, K. Dolinski, S. S. Dwight, J. T. Eppig, and others: 2000, 'Gene Ontology: tool for the unification of biology'. *Nature Genetics* **25**(1), 25–29.

Babu, G., M. Waterfield, M. Chang, X. Wu, and S. C. Sun: 2006a, 'Deregulated activation of oncoprotein kinase Tpl2/Cot in HTLV-I-transformed T cells'. *The Journal of Biological Chemistry* **281**(20), 14041–7.

Babu, G. R., W. Jin, L. Norman, M. Waterfield, M. Chang, X. Wu, M. Zhang, and S. C. Sun: 2006b, 'Phosphorylation of NF-κB1/p105 by oncoprotein kinase Tpl2: implications for a novel mechanism of Tpl2 regulation'. *Biochimica et Biophysica Acta* **1763**(2), 174–81.

Bain, J., L. Plater, M. Elliott, N. Shpiro, C. J. Hastie, H. McLauchlan, I. Klevernic, J. S. C. Arthur, D. R. Alessi, and P. Cohen: 2007, 'The selectivity of protein kinase inhibitors: a further update'. *Biochemical Journal* **408**(3), 297.

Bandow, K., J. Kusuyama, M. Shamoto, K. Kakimoto, T. Ohnishi, and T. Matsuguchi: 2012, 'LPS-induced chemokine expression in both MyD88-dependent and -independent manners is regulated by Cot/Tpl2-ERK axis in macrophages'. *FEBS Letters* **586**(10), 1540–6.

Barrett, S. D., A. J. Bridges, D. T. Dudley, A. R. Saltiel, J. H. Fergus, C. M. Flamme, A. M. Delaney, M. Kaufman, S. LePage, W. R. Leopold, S. A. Przybranowski, J. Sebolt-Leopold, K. Van Becelaere, A. M. Doherty, R. M. Kennedy, D. Marston, W. A. Howard, Y. Smith, J. S. Warmus, and H. Tecle: 2008, 'The discovery of the benzhydroxamate MEK inhibitors CI-1040 and PD 0325901'. *Bioorganic & Medicinal Chemistry Letters* **18**(24), 6501–6504.

Beinke, S., J. Deka, V. Lang, M. P. Belich, P. A. Walker, S. Howell, S. J. Smerdon, S. J. Gamblin, and S. C. Ley: 2003, 'NF-κB1 p105 negatively regulates TPL-2 MEK kinase activity'. *Molecular and Cellular Biology* **23**(14), 4739–52.

Beinke, S., M. J. Robinson, M. Hugunin, and S. C. Ley: 2004, 'Lipopolysaccharide activation of the TPL-2/MEK/extracellular signal-regulated kinase mitogen-activated protein kinase cascade is regulated by IκB kinase-induced proteolysis of NF-κB1 p105'. *Molecular and Cellular Biology* **24**(21), 9658–67.

Belich, M. P., A. Salmerón, L. H. Johnston, and S. C. Ley: 1999, 'TPL-2 kinase regulates the proteolysis of the NF-κB-inhibitory protein NF-κB1 p105'. *Nature* **397**(6717), 363–8.

Ben-Addi, A., A. Mambole-Dema, C. Brender, S. R. Martin, J. Janzen, S. Kjaer, S. J. Smerdon, and S. C. Ley: 2014, 'IκB kinase-induced interaction of TPL-2 kinase with 14-3-3 is essential for Toll-like receptor activation of ERK-1 and -2 MAP kinases'. *Proceedings of the National Academy of Sciences* **111**(23), E2394–E2403.

Black, R. A., C. T. Rauch, C. J. Kozlosky, J. J. Peschon, J. L. Slack, M. F. Wolfson, B. J. Castner, K. L. Stocking, P. Reddy, S. Srinivasan, N. Nelson, N. Boiani, K. A. Schooley, M. Gerhart, R. Davis, J. N. Fitzner, R. S. Johnson, R. J. Paxton, C. J. March, and D. P. Cerretti: 1997, 'A metalloproteinase disintegrin that releases tumour-necrosis factor-[alpha] from cells'. *Nature* **385**(6618), 729–733.

Black, T. M., C. L. Andrews, G. Kilili, M. Ivan, P. N. Tsichlis, and P. Vouros: 2007, 'Characterization of phosphorylation sites on Tpl2 using IMAC enrichment and a linear ion trap mass spectrometer'. *Journal of Proteome Research* **6**(6), 2269–76.

Bluml, S., C. Scheinecker, J. S. Smolen, and K. Redlich: 2012, 'Targeting TNF receptors in rheumatoid arthritis'. *International Immunology* **24**(5), 275–281.

Bodenmiller, B., L. N. Mueller, M. Mueller, B. Domon, and R. Aebersold: 2007, 'Reproducible isolation of distinct, overlapping segments of the phosphoproteome'. *Nature Methods* **4**(3), 231–7.

Boekhorst, J., P. J. Boersema, B. B. J. Tops, B. van Breukelen, A. J. R. Heck, and B. Snel: 2011, 'Evaluating Experimental Bias and Completeness in Comparative Phosphoproteomics Analysis'. *PLoS ONE* **6**(8), e23276.

Bogoyevitch, M. A. and B. Kobe: 2006, 'Uses for JNK: the many and varied substrates of the c-Jun N-terminal kinases'. *Microbiology and Molecular Biology Reviews* **70**(4), 1061–95.

Brancho, D., N. Tanaka, A. Jaeschke, J. Ventura, N. Kelkar, Y. Tanaka, M. Kyuuma, T. Takeshita, R. A. Flavell, and R. J. Davis: 2003, 'Mechanism of p38 MAP kinase activation in vivo'. *Genes & Development* **17**(16), 1969–1978.

Cao, Wei and Liu, Yong-Jun: 2006, 'Opn: key regulator of pDC interferon production'. *Nature Immunology* **7**(5), 441–443.

Cargnello, M. and P. P. Roux: 2011, 'Activation and function of the MAPKs and their substrates, the MAPK-activated protein kinases'. *Microbiology and Molecular Biology Reviews* **75**(1), 50–83.

Carlberg, U., A. Nilsson, and O. Nygård: 1990, 'Functional properties of phosphorylated elongation factor 2'. *European Journal of Biochemistry* **191**(3), 639–645.

Carlson, S. M., C. R. Chouinard, A. Labadorf, C. J. Lam, K. Schmelzle, E. Fraenkel, and F. M. White: 2011, 'Large-scale discovery of ERK2 substrates identifies ERK-mediated transcriptional regulation by ETV3'. *Science Signaling* **4**(196), rs11.

Casar, B., V. Sanz-Moreno, M. N. Yazicioglu, J. Rodríguez, M. T. Berciano, M. Lafarga, M. H. Cobb, and P. Crespo: 2007, 'Mxi2 promotes stimulus-independent ERK nuclear translocation'. *The EMBO J\textbackslashournal* **26**(3), 635–646.

Caunt, C. J. and S. M. Keyse: 2013, 'Dual-specificity MAP kinase phosphatases (MKPs): Shaping the outcome of MAP kinase signalling'. *FEBS Journal* **280**(2), 489–504.

Ceci, J. D., C. P. Patriotis, C. Tsatsanis, A. M. Makris, R. Kovatch, D. A. Swing, N. A. Jenkins, P. N. Tsichlis, and N. G. Copeland: 1997, 'Tpl-2 is an oncogenic kinase that is activated by carboxy-terminal truncation'. *Genes & Development* **11**(6), 688–700.

Cekaite, L., G. Furset, E. Hovig, and M. Sioud: 2007, 'Gene Expression Analysis in Blood Cells in Response to Unmodified and 2′-Modified siRNAs Reveals TLR-dependent and Independent Effects'. *Journal of Molecular Biology* **365**(1), 90–108.

Chen, R. E. and J. Thorner: 2007, 'Function and regulation in MAPK signaling pathways: lessons learned from the yeast Saccharomyces cerevisiae'. *Biochimica et Biophysica Acta (BBA)-Molecular Cell Research* **1773**(8), 1311–1340.

Cheung, P. C., D. G. Campbell, A. R. Nebreda, and P. Cohen: 2003, 'Feedback control of the protein kinase TAK1 by SAPK2a/p38α'. *The EMBO journal* **22**(21), 5793–5805.

Chiariello, M., M. J. Marinissen, and J. S. Gutkind: 2000, 'Multiple mitogen-activated protein kinase signaling pathways connect the COT oncoprotein to the c-jun promoter and to cellular transformation'. *Molecular and Cellular Biology* **20**(5), 1747–1758.

Cho, J., M. Melnick, G. P. Solidakis, and P. N. Tsichlis: 2005, 'Tpl2 (tumor progression locus 2) phosphorylation at Thr290 is induced by lipopolysaccharide via an Iκ-B Kinase-β-dependent pathway and is required for Tpl2 activation by external signals'. *The Journal of Biological Chemistry* **280**(21), 20442–8.

Cho, J. and P. N. Tsichlis: 2005, 'Phosphorylation at Thr-290 regulates Tpl2 binding to NF-κB1/p105 and Tpl2 activation and degradation by lipopolysaccharide'. *Proceedings of the National Academy of Sciences of the United States of America* **102**(7), 2350–5.

Choi, H. S., B. S. Kang, J. H. Shim, Y. Y. Cho, B. Y. Choi, A. M. Bode, and Z. Dong: 2008, 'Cot, a novel kinase of histone H3, induces cellular transformation through up-regulation of c-fos transcriptional activity'. *The FASEB journal : official publication of the Federation of American Societies for Experimental Biology* **22**(1), 113–26.

Christoforidou, A. V., H. A. Papadaki, A. N. Margioris, G. D. Eliopoulos, and C. Tsatsanis: 2004, 'Expression of the Tpl2/Cot oncogene in human T-cell neoplasias'. *Mol Cancer* **3**(1), 34.

Clark, A. M., S. H. Reynolds, M. Anderson, and J. S. Wiest: 2004, 'Mutational activation of the MAP3K8 protooncogene in lung cancer'. *Genes, Chromosomes and Cancer* **41**(2), 99–108.

Clark, K., K. F. Mackenzie, K. Petkevicius, Y. Kristariyanto, J. Zhang, H. G. Choi, M. Peggie, L. Plater, P. G. Pedrioli, E. McIver, N. S. Gray, J. S. Arthur, and P. Cohen: 2012, 'Phosphorylation of CRTC3 by the salt-inducible kinases controls the interconversion of classically activated and regulatory macrophages'. *Proceedings of the National Academy of Sciences of the United States of America* **109**(42), 16986–16991.

Clark, K., M. Peggie, L. Plater, Ronald J. Sorcek, E. R. R. Young, J. B. Madwed, J. Hough, E. G. McIver, and P. Cohen: 2011, 'Novel cross-talk within the IKK family controls innate immunity'. *Biochemical Journal* **434**(1), 93–104.

Cohen, P.: 2000, 'The regulation of protein function by multisite phosphorylation - a 25 year update'. *Trends in Biochemical Sciences* **25**(12), 596–601.

Cohen, P.: 2002, 'Protein kinases — the major drug targets of the twenty-first century?'. *Nature Reviews Drug Discovery* **1**, 309–315.

Cohen, P.: 2009, 'Targeting protein kinases for the development of anti-inflammatory drugs'. *Current Opinion in Cell Biology* **21**(2), 317–24.

Cohen, P. and A. Knebel: 2006, 'KESTREL: a powerful method for identifying the physiological substrates of protein kinases'. *The Biochemical Journal* **393**(Pt 1), 1–6.

Cong, L., F. A. Ran, D. Cox, S. Lin, R. Barretto, N. Habib, P. D. Hsu, X. Wu, W. Jiang, L. A. Marraffini, and F. Zhang: 2013, 'Multiplex Genome Engineering Using CRISPR/Cas Systems'. *Science* **339**(6121), 819–823.

Consortium, T. U.: 2015, 'UniProt: a hub for protein information'. *Nucleic Acids Research* **43**(D1), D204–D212.

Conze, D. B., C.-J. Wu, J. A. Thomas, A. Landstrom, and J. D. Ashwell: 2008, 'Lys63-Linked Polyubiquitination of IRAK-1 Is Required for Interleukin-1 Receptor- and Toll-Like Receptor-Mediated NF- B Activation'. *Molecular and Cellular Biology* **28**(10), 3538–3547.

Coulombe, P. and S. Meloche: 2007, 'Atypical mitogen-activated protein kinases: Structure, regulation and functions'. *Biochimica et Biophysica Acta (BBA) - Molecular Cell Research* **1773**(8), 1376–1387.

Coulthard, L. R., D. E. White, D. L. Jones, M. F. McDermott, and S. A. Burchill: 2009, 'p38MAPK: stress responses from molecular mechanisms to therapeutics'. *Trends in Molecular Medicine* **15**(8), 369–379.

Courcelles, M., C. Fremin, L. Voisin, S. Lemieux, S. Meloche, and P. Thibault: 2013, 'Phosphoproteome dynamics reveal novel ERK1/2 MAP kinase substrates with broad spectrum of functions'. *Molecular systems biology* **9**, 669.

Cox, J. and M. Mann: 2008, 'MaxQuant enables high peptide identification rates, individualized p.p.b.-range mass accuracies and proteome-wide protein quantification'. *Nature Biotechnology* **26**(12), 1367–72.

Cox, J. and M. Mann: 2012, '1D and 2D annotation enrichment: a statistical method integrating quantitative proteomics with complementary high-throughput data'. *BMC Bioinformatics* **13 Suppl 16**, S12.

Criado, G., A. Risco, D. Alsina-Beauchamp, M. J. Pérez-Lorenzo, A. Escós, and A. Cuenda: 2014, 'Alternative p38 MAPKs Are Essential for Collagen-Induced Arthritis: p38γ and p38δ in Arthritis'. *Arthritis & Rheumatology* **66**(5), 1208–1217.

Cuadrado, A. and A. R. Nebreda: 2010, 'Mechanisms and functions of p38 MAPK signalling'. *The Biochemical Journal* **429**(3), 403–17.

Cuenda, A., P. Cohen, V. Buée-Scherrer, and M. Goedert: 1997, 'Activation of stress-activated protein kinase-3 (SAPK3) by cytokines and cellular stresses is mediated via SAPKK3 (MKK6); comparison of the specificities of SAPK3 and SAPK2 (RK/p38)'. *The EMBO Journal* **16**(2), 295–305.

Cuenda, A. and S. Rousseau: 2007, 'p38 MAP-Kinases pathway regulation, function and role in human diseases'. *Biochimica et Biophysica Acta (BBA) - Molecular Cell Research* **1773**(8), 1358–1375.

Cusson-Hermance, N.: 2005, 'Rip1 Mediates the Trif-dependent Toll-like Receptor 3- and 4-induced NF- B Activation but Does Not Contribute to Interferon Regulatory Factor 3 Activation'. *Journal of Biological Chemistry* **280**(44), 36560–36566.

Das, S., J. Cho, I. Lambertz, M. A. Kelliher, A. G. Eliopoulos, K. Du, and P. N. Tsichlis: 2005, 'Tpl2/cot signals activate ERK, JNK, and NF-κB in a cell-type and stimulus-specific manner'. *The Journal of biological chemistry* **280**(25), 23748–57.

Davies, H., G. R. Bignell, C. Cox, P. Stephens, S. Edkins, S. Clegg, J. Teague, H. Woffendin, M. J. Garnett, W. Bottomley, and others: 2002, 'Mutations of the BRAF gene in human cancer'. *Nature* **417**(6892), 949–954.

Davis, R. J.: 2000, 'Signal transduction by the JNK group of MAP kinases'. *Cell* **103**(2), 239–252.

DeCicco-Skinner, K. L., E. L. Trovato, J. K. Simmons, P. K. Lepage, and J. S. Wiest: 2011, 'Loss of tumor progression locus 2 (tpl2) enhances tumorigenesis and inflammation in two-stage skin carcinogenesis'. *Oncogene* **30**(4), 389–397.

del Reino, P., D. Alsina-Beauchamp, A. Escos, M. I. Cerezo-Guisado, A. Risco, N. Aparicio, R. Zur, M. Fernandez-Estevez, E. Collantes, J. Montans, and A. Cuenda: 2014, 'Pro-Oncogenic Role of Alternative p38 Mitogen-Activated Protein Kinases p38g and p38d, Linking Inflammation and Cancer in Colitis-Associated Colon Cancer'. *Cancer Research* **74**(21), 6150–6160.

Deleris, P., M. Trost, I. Topisirovic, P.-L. Tanguay, K. L. B. Borden, P. Thibault, and S. Meloche: 2011, 'Activation Loop Phosphorylation of ERK3/ERK4 by Group I p21-activated Kinases (PAKs) Defines a Novel PAK-ERK3/4-MAPK-activated Protein Kinase 5 Signaling Pathway'. *Journal of Biological Chemistry* **286**(8), 6470–6478.

Dinasarapu, A. R., S. Gupta, M. Ram Maurya, E. Fahy, J. Min, M. Sud, M. J. Gersten, C. K. Glass, and S. Subramaniam: 2013, 'A combined omics study on activated macrophages–enhanced role of STATs in apoptosis, immunity and lipid metabolism'. *Bioinformatics* **29**(21), 2735–2743.

Ding, L., M. J. Ellis, S. Li, D. E. Larson, K. Chen, J. W. Wallis, C. C. Harris, M. D. McLellan, R. S. Fulton, L. L. Fulton, R. M. Abbott, J. Hoog, D. J. Dooling, D. C. Koboldt, H. Schmidt, J. Kalicki, Q. Zhang, L. Chen, L. Lin, M. C. Wendl, J. F. McMichael, V. J. Magrini, L. Cook, S. D. McGrath, T. L. Vickery, E. Appelbaum, K. DeSchryver, S. Davies, T. Guintoli, L. Lin, R. Crowder, Y. Tao, J. E. Snider, S. M. Smith, A. F. Dukes, G. E. Sanderson, C. S. Pohl, K. D. Delehaunty, C. C. Fronick, K. A. Pape, J. S. Reed, J. S. Robinson, J. S. Hodges, W. Schierding, N. D. Dees, D. Shen, D. P. Locke, M. E. Wiechert, J. M. Eldred, J. B. Peck, B. J. Oberkfell, J. T. Lolofie, F. Du, A. E. Hawkins, M. D. O'Laughlin, K. E. Bernard, M. Cunningham, G. Elliott, M. D. Mason, D. M. Thompson Jr, J. L. Ivanovich, P. J. Goodfellow, C. M. Perou, G. M. Weinstock, R. Aft, M. Watson, T. J. Ley, R. K. Wilson, and E. R. Mardis: 2010, 'Genome remodelling in a basal-like breast cancer metastasis and xenograft'. *Nature* **464**(7291), 999–1005.

Dolado, I. and A. R. Nebreda: 2008, 'Regulation of Tumorigenesis by p38α MAP

Kinase'. In: F. Posas and A. R. Nebreda (eds.): *Stress-Activated Protein Kinases*, Vol. 20. Berlin, Heidelberg: Springer Berlin Heidelberg, pp. 99–128.

Doza, Y. N., A. Cuenda, G. M. Thomas, P. Cohen, and A. R. Nebreda: 1995, 'Activation of the MAP kinase homologue RK requires the phosphorylation of Thr-180 and Tyr-182 and both residues are phosphorylated in chemically stressed KB cells'. *FEBS Letters* **364**(2), 223–228.

Dérijard, B., J. Raingeaud, T. Barrett, I.-H. Wu, J. Han, R. J. Ulevitch, and R. J. Davis: 1995, 'Independent human MAP-kinase signal transduction pathways defined by MEK and MKK isoforms'. *Science* **267**(5198), 682–685.

Dumitru, C. D., J. D. Ceci, C. Tsatsanis, D. Kontoyiannis, K. Stamatakis, J. H. Lin, C. Patriotis, N. A. Jenkins, N. G. Copeland, G. Kollias, and P. N. Tsichlis: 2000, 'TNF-α induction by LPS is regulated posttranscriptionally via a Tpl2/ERK-dependent pathway'. *Cell* **103**(7), 1071–83.

Duong-Ly, K. C. and J. R. Peterson: 2013, 'The Human Kinome and Kinase Inhibition'. In: S. Enna, M. Williams, J. F. Barret, J. W. Ferkany, T. Kenakin, and R. D. Porsolt (eds.): *Current Protocols in Pharmacology*. Hoboken, NJ, USA: John Wiley & Sons, Inc.

Ebach, D. R., T. E. Riehl, and W. F. Stenson: 2005, 'Opposing effects of tumor necrosis factor receptor 1 and 2 in sepsis due to cecal ligation and puncture.'. *Shock* **23**(4), 311–318.

Eliopoulos, A. G., C. Davies, S. S. M. Blake, P. Murray, S. Najafipour, P. N. Tsichlis, and L. S. Young: 2002a, 'The Oncogenic Protein Kinase Tpl-2/Cot Contributes to Epstein-Barr Virus-Encoded Latent Infection Membrane Protein 1-Induced NF-kB Signaling Downstream of TRAF2'. *Journal of Virology* **76**(9), 4567–4579.

Eliopoulos, A. G., C. D. Dumitru, C. C. Wang, J. Cho, and P. N. Tsichlis: 2002b, 'Induction of COX-2 by LPS in macrophages is regulated by Tpl2-dependent CREB activation signals'. *The EMBO Journal* **21**(18), 4831–40.

Eliopoulos, A. G., C. C. Wang, C. D. Dumitru, and P. N. Tsichlis: 2003, 'Tpl2 transduces CD40 and TNF signals that activate ERK and regulates IgE induction by CD40'. *The EMBO Journal* **22**(15), 3855–64.

Elphick, L. M., S. E. Lee, V. Gouverneur, and D. J. Mann: 2007, 'Using Chemical Genetics and ATP Analogues To Dissect Protein Kinase Function'. *ACS Chemical Biology* **2**(5), 299–314.

Emoto, N. and M. Yanagisawa: 1995, 'Endothelin-converting enzyme-2 is a membrane-bound, phosphoramidon-sensitive metalloprotease with acidic pH optimum.'. *Journal of Biological Chemistry* **270**(25), 15262–15268.

Epelman, S., K. J. Lavine, and G. J. Randolph: 2014, 'Origin and Functions of Tissue Macrophages'. *Immunity* **41**(1), 21–35.

Ermolaeva, M. A., M.-C. Michallet, N. Papadopoulou, O. Utermöhlen, K. Kranidioti, G. Kollias, J. Tschopp, and M. Pasparakis: 2008, 'Function of TRADD in tumor necrosis factor receptor 1 signaling and in TRIF-dependent inflammatory responses'. *Nature Immunology* **9**(9), 1037–1046.

Fernández, M., R. Manso, F. Bernáldez, P. López, A. Martín-Duce, and S. Alemany: 2011, 'Involvement of Cot activity in the proliferation of ALCL lymphoma cells'. *Biochemical and Biophysical Research Communications* **411**(4), 655–660.

Fleming, Y., C. Armstrong, N. Morrice, A. Paterson, M. Goedert, and P. Cohen: 2000, 'Synergistic activation of stress-activated protein kinase 1/c-Jun N-terminal kinase (SAPK1/JNK) isoforms by mitogen-activated protein kinase kinase 4 (MKK4) and MKK7'. *Biochem. J* **352**, 145–154.

Forbes, S. A., D. Beare, P. Gunasekaran, K. Leung, N. Bindal, H. Boutselakis, M. Ding, S. Bamford, C. Cole, S. Ward, C. Y. Kok, M. Jia, T. De, J. W. Teague, M. R. Stratton, U. McDermott, and P. J. Campbell: 2015, 'COSMIC: exploring the world's knowledge of somatic mutations in human cancer'. *Nucleic Acids Research* **43**(D1), D805–D811.

Gantke, T., S. Boussouf, J. Janzen, N. A. Morrice, S. Howell, E. Muhlberger, and S. C. Ley: 2013, 'Ebola virus VP35 induces high-level production of recombinant TPL-2-ABIN-2-NF-kappaB1 p105 complex in co-transfected HEK-293 cells'. *The Biochemical journal* **452**(2), 359–65.

Gantke, T., S. Sriskantharajah, and S. C. Ley: 2011, 'Regulation and function of TPL-2, an IκB kinase-regulated MAP kinase kinase kinase'. *Cell research* **21**(1), 131–45.

Gantke, T., S. Sriskantharajah, M. Sadowski, and S. C. Ley: 2012, 'IκB kinase regulation of the TPL-2/ERK MAPK pathway'. *Immunological Reviews* **246**, 168–182.

Gauci, S., A. O. Helbig, M. Slijper, J. Krijgsveld, A. J. R. Heck, and S. Mohammed: 2009, 'Lys-N and Trypsin Cover Complementary Parts of the Phosphoproteome in a Refined SCX-Based Approach'. *Analytical Chemistry* **81**(11), 4493–4501.

Ge, B., H. Gram, F. Di Padova, B. Huang, L. New, R. J. Ulevitch, Y. Luo, and J. Han: 2002, 'MAPKK-Independent Activation of p38alpha Mediated by TAB1-Dependent Autophosphorylation of p38alpha'. *Science* **295**(5558), 1291–1294.

Geiger, T., J. Cox, P. Ostasiewicz, J. R. Wisniewski, and M. Mann: 2010, 'Super-SILAC mix for quantitative proteomics of human tumor tissue'. *Nature methods* **7**(5), 383–5.

Geiger, T., J. R. Wisniewski, J. Cox, S. Zanivan, M. Kruger, Y. Ishihama, and M. Mann: 2011, 'Use of stable isotope labeling by amino acids in cell culture as a spike-in standard in quantitative proteomics'. *Nature protocols* **6**(2), 147–57.

George, D., M. Friedman, H. Allen, M. Argiriadi, C. Barberis, A. Bischoff, A. Clabbers, K. Cusack, R. Dixon, S. Fix-Stenzel, T. Gordon, B. Janssen, Y. Jia, M. Moskey, C. Quinn, J.-A. Salmeron, N. Wishart, K. Woller, and Z. Yu: 2008, 'Discovery of thieno[2,3-c]pyridines as potent COT inhibitors'. *Bioorganic & Medicinal Chemistry Letters* **18**(18), 4952–4955.

Gilroy, D. and R. De Maeyer: 2015, 'New insights into the resolution of inflammation'. *Seminars in Immunology* **Online ahead of print.**

Gkirtzimanaki, K., K. K. Gkouskou, U. Oleksiewicz, G. Nikolaidis, D. Vyrla, M. Liontos, V. Pelekanou, D. C. Kanellis, K. Evangelou, E. N. Stathopoulos, J. K. Field, P. N. Tsichlis, V. Gorgoulis, T. Liloglou, and A. G. Eliopoulos: 2013, 'TPL2 kinase is a suppressor of lung carcinogenesis'. *Proceedings of the National Academy of Sciences of the United States of America* **110**(16), E1470–9.

Gándara, M. L., P. Lopez, R. Hernando, J. G. Castano, and S. Alemany: 2003, 'The COOH-terminal domain of wild-type Cot regulates its stability and kinase specific activity'. *Molecular and Cellular Biology* **23**(20), 7377–90.

Goedert, M., A. Cuenda, M. Craxton, R. Jakes, and P. Cohen: 1997, 'Activation of the novel stress-activated protein kinase SAPK4 by cytokines and cellular stresses is mediated by SKK3 (MKK6); comparison of its substrate specificity with that of other SAP kinases'. *The EMBO Journal* **16**(12), 3563–3571.

Goh, E. T. H., J. S. C. Arthur, P. C. F. Cheung, S. Akira, R. Toth, and P. Cohen: 2012, 'Identification of the protein kinases that activate the E3 ubiquitin ligase Pellino 1 in the innate immune system'. *Biochemical Journal* **441**(1), 339–346.

González-Terán, B., J. R. Cortés, E. Manieri, N. Matesanz, A. Verdugo, M. E. Rodríguez, A. González-Rodríguez, A. Valverde, P. Martín, R. J. Davis, and G. Sabio: 2013, 'Eukaryotic elongation factor 2 controls TNF-α translation in LPS-induced hepatitis'. *Journal of Clinical Investigation* **123**(1), 164–178.

Green, N., Y. Hu, K. Janz, H. Q. Li, N. Kaila, S. Guler, J. Thomason, D. Joseph-McCarthy, S. Y. Tam, R. Hotchandani, J. Wu, A. Huang, Q. Wang, L. Leung, J. Pelker, S. Marusic, S. Hsu, J. B. Telliez, J. P. Hall, J. W. Cuozzo, and L. L.

Lin: 2007, ‘Inhibitors of tumor progression loci-2 (Tpl2) kinase and tumor necrosis factor alpha (TNF-alpha) production: selectivity and in vivo antiinflammatory activity of novel 8-substituted-4-anilino-6-aminoquinoline-3-carbonitriles’. *Journal of Medicinal Chemistry* **50**(19), 4728–45.

Grell, M., E. Douni, H. Wajant, M. Löhden, M. Clauss, B. Maxeiner, S. Georgopoulos, W. Lesslauer, G. Kollias, K. Pfizenmaier, and P. Scheurich: 1995, ‘The transmembrane form of tumor necrosis factor is the prime activating ligand of the 80 kDa tumor necrosis factor receptor’. *Cell* **83**(5), 793–802.

Gronborg, M.: 2002, ‘A Mass Spectrometry-based Proteomic Approach for Identification of Serine/Threonine-phosphorylated Proteins by Enrichment with Phospho-specific Antibodies: Identification of a Novel Protein, Frigg, as a Protein Kinase A Substrate’. *Molecular & Cellular Proteomics* **1**(7), 517–527.

Guma, M., D. Hammaker, K. Topolewski, M. Corr, D. L. Boyle, M. Karin, and G. S. Firestein: 2012, ‘Antiinflammatory functions of p38 in mouse models of rheumatoid arthritis: Advantages of targeting upstream kinases MKK-3 or MKK-6’. *Arthritis & Rheumatism* **64**(9), 2887–2895.

Guo, H., Z. Mi, D. E. Bowles, S. D. Bhattacharya, and P. C. Kuo: 2010, ‘Osteopontin and Protein Kinase C Regulate PDLIM2 Activation and STAT1 Ubiquitination in LPS-treated Murine Macrophages’. *Journal of Biological Chemistry* **285**(48), 37787–37796.

Gutmann, S., A. Hinniger, G. Fendrich, P. Drueckes, S. Antz, H. Mattes, H. Moebitz, S. Ofner, N. Schmiedeberg, A. Stojanovic, S. Rieffel, A. Strauss, T. Troxler, R. Glatthar, and H. Sparrer: 2015, ‘The Crystal Structure of Cancer Osaka Thyroid Kinase Reveals an Unexpected Kinase Domain Fold’. *Journal of Biological Chemistry* **290**(24), 15210–15218.

Hagar, J. A., D. A. Powell, Y. Aachoui, R. K. Ernst, and E. A. Miao: 2013, ‘Cytoplasmic LPS activates caspase-11: implications in TLR4-independent endotoxic shock’. *Science* **341**(6151), 1250–3.

Hall, J. P., Y. Kurdi, S. Hsu, J. Cuozzo, J. Liu, J. B. Telliez, K. J. Seidl, A. Winkler, Y. Hu, N. Green, G. R. Askew, S. Tam, J. D. Clark, and L. L. Lin: 2007, ‘Pharmacologic inhibition of tpl2 blocks inflammatory responses in primary human monocytes, synoviocytes, and blood’. *The Journal of Biological Chemistry* **282**(46), 33295–304.

Han, M. S., D. Y. Jung, C. Morel, S. A. Lakhani, J. K. Kim, R. A. Flavell, and R. J. Davis: 2013, ‘JNK expression by macrophages promotes obesity-induced insulin resistance and inflammation’. *Science* **339**(6116), 218–22.

Hasegawa, M., A. Cuenda, M. Grazia Spillantini, G. M. Thomas, V. Buée-Scherrer, P. Cohen, and M. Goedert: 1999, 'Stress-activated Protein Kinase-3 Interacts with the PDZ Domain of alpha1-Syntrophin'. *The Journal of Biological Chemistry* **274**(18), 12626–12631.

Hatziapostolou, M., G. Koukos, C. Polytarchou, F. Kottakis, O. Serebrennikova, A. Kuliopulos, and P. N. Tsichlis: 2011, 'Tumor progression locus 2 mediates signal-induced increases in cytoplasmic calcium and cell migration'. *Science signaling* **4**(187), ra55.

Häcker, H., V. Redecke, B. Blagoev, I. Kratchmarova, L.-C. Hsu, G. G. Wang, M. P. Kamps, E. Raz, H. Wagner, G. Häcker, M. Mann, and M. Karin: 2006, 'Specificity in Toll-like receptor signalling through distinct effector functions of TRAF3 and TRAF6'. *Nature* **439**(7073), 204–207.

Heissmeyer, V., D. Krappmann, E. N. Hatada, and C. Scheidereit: 2001, 'Shared pathways of IκB kinase-induced SCF(βTrCP)-mediated ubiquitination and degradation for the NF-κB precursor p105 and IκBα'. *Molecular and Cellular Biology* **21**(4), 1024–35.

Hinsley, E. E., S. Hunt, K. D. Hunter, S. A. Whawell, and D. W. Lambert: 2012, 'Endothelin-1 stimulates motility of head and neck squamous carcinoma cells by promoting stromal-epithelial interactions'. *International Journal of Cancer* **130**(1), 40–47.

Hope, C., S. J. Ollar, E. Heninger, E. Hebron, J. L. Jensen, J. Kim, I. Maroulakou, S. Miyamoto, C. Leith, D. T. Yang, N. Callander, P. Hematti, M. Chesi, P. L. Bergsagel, and F. Asimakopoulos: 2014, 'TPL2 kinase regulates the inflammatory milieu of the myeloma niche'. *Blood* **123**(21), 3305–15.

Horiuchi, K., T. Kimura, T. Miyamoto, H. Takaishi, Y. Okada, Y. Toyama, and C. P. Blobel: 2007, 'Cutting Edge: TNF- -Converting Enzyme (TACE/ADAM17) Inactivation in Mouse Myeloid Cells Prevents Lethality from Endotoxin Shock'. *The Journal of Immunology* **179**(5), 2686–2689.

Hornbeck, P. V., J. M. Kornhauser, S. Tkachev, B. Zhang, E. Skrzypek, B. Murray, V. Latham, and M. Sullivan: 2012, 'PhosphoSitePlus: a comprehensive resource for investigating the structure and function of experimentally determined post-translational modifications in man and mouse'. *Nucleic Acids Research* **40**(D1), D261–D270.

Hu, Y., D. Cole, R. A. Denny, D. R. Anderson, M. Ipek, Y. Ni, X. Wang, S. Thaisrivongs, T. Chamberlain, J. P. Hall, J. Liu, M. Luong, L.-L. Lin, J.-B. Telliez, and A. Gopalsamy: 2011, 'Discovery of indazoles as inhibitors of Tpl2 kinase'. *Bioorganic & Medicinal Chemistry Letters* **21**(16), 4758–4761.

Huang, D. W., B. T. Sherman, and R. A. Lempicki: 2008, 'Systematic and integrative analysis of large gene lists using DAVID bioinformatics resources'. *Nature Protocols* **4**(1), 44–57.

Huang, D. W., B. T. Sherman, and R. A. Lempicki: 2009, 'Bioinformatics enrichment tools: paths toward the comprehensive functional analysis of large gene lists'. *Nucleic Acids Research* **37**(1), 1–13.

Hunter, T. and B. M. Sefton: 1980, 'Transforming gene product of Rous sarcoma virus phosphorylatestyrosine'. *Proceedings of the National Academy of Sciences* **77**(3), 1311–1315.

Imami, K., N. Sugiyama, M. Tomita, and Y. Ishihama: 2010, 'Quantitative proteome and phosphoproteome analyses of cultured cells based on SILAC labeling without requirement of serum dialysis'. *Molecular BioSystems* **6**, 594–602.

Iwasaki, A. and R. Medzhitov: 2015, 'Control of adaptive immunity by the innate immune system'. *Nature Immunology* **16**(4), 343–353.

Jacque, E., E. Schweighoffer, V. L. J. Tybulewicz, and S. C. Ley: 2015, 'BAFF activation of the ERK5 MAP kinase pathway regulates B cell survival'. *Journal of Experimental Medicine* **212**(6), 883–892.

Jensen, S. S. and M. R. Larsen: 2007, 'Evaluation of the impact of some experimental procedures on different phosphopeptide enrichment techniques'. *Rapid Communications in Mass Spectrometry* **21**(22), 3635–45.

Jia, Y., C. M. Quinn, N. J. Bump, K. M. Clark, A. Clabbers, J. Hardman, A. Gagnon, J. Kamens, M. J. Tomlinson, N. Wishart, and H. Allen: 2005, 'Purification and kinetic characterization of recombinant human mitogen-activated protein kinase kinase kinase COT and the complexes with its cellular partner NF-κB1 p105'. *Archives of Biochemistry and Biophysics* **441**(1), 64–74.

Jiang, H. and A. M. English: 2002, 'Quantitative analysis of the yeast proteome by incorporation of isotopically labeled leucine.'. *Journal of Proteome Research* **1**(4), 345–350.

Johannessen, C. M., J. S. Boehm, S. Y. Kim, S. R. Thomas, L. Wardwell, L. A. Johnson, C. M. Emery, N. Stransky, A. P. Cogdill, J. Barretina, G. Caponigro, H. Hieronymus, R. R. Murray, K. Salehi-Ashtiani, D. E. Hill, M. Vidal, J. J. Zhao, X. Yang, O. Alkan, S. Kim, J. L. Harris, C. J. Wilson, V. E. Myer, P. M. Finan, D. E. Root, T. M. Roberts, T. Golub, K. T. Flaherty, R. Dummer, B. L. Weber, W. R. Sellers, R. Schlegel, J. A. Wargo, W. C. Hahn, and L. A. Garraway: 2010, 'COT

drives resistance to RAF inhibition through MAP kinase pathway reactivation'. *Nature* **468**(7326), 968–72.

Jostins, L., S. Ripke, R. K. Weersma, R. H. Duerr, D. P. McGovern, K. Y. Hui, J. C. Lee, L. P. Schumm, Y. Sharma, C. A. Anderson, J. Essers, M. Mitrovic, K. Ning, I. Cleynen, E. Theatre, S. L. Spain, S. Raychaudhuri, P. Goyette, Z. Wei, C. Abraham, J. P. Achkar, T. Ahmad, L. Amininejad, A. N. Ananthakrishnan, V. Andersen, J. M. Andrews, L. Baidoo, T. Balschun, P. A. Bampton, A. Bitton, G. Boucher, S. Brand, C. Buning, A. Cohain, S. Cichon, M. D'Amato, D. De Jong, K. L. Devaney, M. Dubinsky, C. Edwards, D. Ellinghaus, L. R. Ferguson, D. Franchimont, K. Fransen, R. Gearry, M. Georges, C. Gieger, J. Glas, T. Haritunians, A. Hart, C. Hawkey, M. Hedl, X. Hu, T. H. Karlsen, L. Kupcinskas, S. Kugathasan, A. Latiano, D. Laukens, I. C. Lawrance, C. W. Lees, E. Louis, G. Mahy, J. Mansfield, A. R. Morgan, C. Mowat, W. Newman, O. Palmieri, C. Y. Ponsioen, U. Potocnik, N. J. Prescott, M. Regueiro, J. I. Rotter, R. K. Russell, J. D. Sanderson, M. Sans, J. Satsangi, S. Schreiber, L. A. Simms, J. Sventoraityte, S. R. Targan, K. D. Taylor, M. Tremelling, H. W. Verspaget, M. De Vos, C. Wijmenga, D. C. Wilson, J. Winkelmann, R. J. Xavier, S. Zeissig, B. Zhang, C. K. Zhang, H. Zhao, M. S. Silverberg, V. Annese, H. Hakonarson, S. R. Brant, G. Radford-Smith, C. G. Mathew, J. D. Rioux, and E. E. Schadt: 2012, 'Host-microbe interactions have shaped the genetic architecture of inflammatory bowel disease'. *Nature* **491**(7422), 119–24.

Judge, A. D., V. Sood, J. R. Shaw, D. Fang, K. McClintock, and I. MacLachlan: 2005, 'Sequence-dependent stimulation of the mammalian innate immune response by synthetic siRNA'. *Nature Biotechnology* **23**(4), 457–462.

Kaiser, F., D. Cook, S. Papoutsopoulou, R. Rajsbaum, X. Wu, H. T. Yang, S. Grant, P. Ricciardi-Castagnoli, P. N. Tsichlis, S. C. Ley, and A. O'Garra: 2009, 'TPL-2 negatively regulates interferon-beta production in macrophages and myeloid dendritic cells'. *The Journal of Experimental Medicine* **206**(9), 1863–71.

Kakimoto, K., T. Musikacharoen, N. Chiba, K. Bandow, T. Ohnishi, and T. Matsuguchi: 2010, 'Cot/Tpl2 regulates IL-23 p19 expression in LPS-stimulated macrophages through ERK activation'. *Journal of Physiology and Biochemistry* **66**(1), 47–53.

Kanei-Ishii, C., J. Ninomiya-Tsuji, J. Tanikawa, T. Nomura, T. Ishitani, S. Kishida, K. Kokura, T. Kurahashi, E. Ichikawa-Iwata, Y. Kim, K. Matsumoto, and S. Ishii: 2004, 'Wnt-1 signal induces phosphorylation and degradation of c-Myb protein via TAK1, HIPK2, and NLK'. *Genes & Development* **18**(7), 816–829.

Kanellis, D. C., S. Bursac, P. N. Tsichlis, S. Volarevic, and A. G. Eliopoulos: 2014,

‘Physical and functional interaction of the TPL2 kinase with nucleophosmin’. *Oncogene* **34**, 2516–2526.

Kawagoe, T., S. Sato, K. Matsushita, H. Kato, K. Matsui, Y. Kumagai, T. Saitoh, T. Kawai, O. Takeuchi, and S. Akira: 2008, ‘Sequential control of Toll-like receptor–dependent responses by IRAK1 and IRAK2’. *Nature Immunology* **9**(6), 684–691.

Kawai, T. and S. Akira: 2010, ‘The role of pattern-recognition receptors in innate immunity: update on Toll-like receptors’. *Nature Immunology* **11**(5), 373–384.

Kay, J. G., R. Z. Murray, J. K. Pagan, and J. L. Stow: 2006, ‘Cytokine Secretion via Cholesterol-rich Lipid Raft-associated SNAREs at the Phagocytic Cup’. *Journal of Biological Chemistry* **281**(17), 11949–11954.

Kim, G., P. Khanal, J. Y. Kim, H.-J. Yun, S.-C. Lim, J.-H. Shim, and H. S. Choi: 2015, ‘COT phosphorylates prolyl-isomerase Pin1 to promote tumorigenesis in breast cancer: COT upregulates Pin1 activity’. *Molecular Carcinogenesis* **54**(6), 440–448.

Knebel, A., N. Morrice, and P. Cohen: 2001, ‘A novel method to identify protein kinase substrates: eEF2 kinase is phosphorylated and inhibited by SAPK4/p38delta.’. *The EMBO Journal* **20**(16), 4360–4369.

Kojima, H., T. Sasaki, T. Ishitani, S.-i. Iemura, H. Zhao, S. Kaneko, H. Kunimoto, T. Natsume, K. Matsumoto, and K. Nakajima: 2005, ‘STAT3 regulates Nemo-like kinase by mediating its interaction with IL-6-stimulated TGFβ-activated kinase 1 for STAT3 Ser-727 phosphorylation’. *Proceedings of the National Academy of Sciences of the United States of America* **102**(12), 4524–4529.

Kolaczkowska, E. and P. Kubes: 2013, ‘Neutrophil recruitment and function in health and inflammation’. *Nature Reviews Immunology* **13**(3), 159–175.

Koliaraki, V., M. Roulis, and G. Kollias: 2012, ‘Tpl2 regulates intestinal myofibroblast HGF release to suppress colitis-associated tumorigenesis’. *The Journal of clinical investigation* **122**(11), 4231–42.

Kontoyiannis, D., G. Boulougouris, M. Manoloukos, M. Armaka, M. Apostolaki, T. Pizarro, A. Kotlyarov, I. Forster, R. Flavell, M. Gaestel, P. Tsichlis, F. Cominelli, and G. Kollias: 2002, ‘Genetic dissection of the cellular pathways and signaling mechanisms in modeled tumor necrosis factor-induced Crohn’s-like inflammatory bowel disease’. *The Journal of Experimental Medicine* **196**(12), 1563–74.

Kontoyiannis, D., M. Pasparakis, T. T. Pizarro, F. Cominelli, and G. Kollias: 1999, ‘Impaired on/off regulation of TNF biosynthesis in mice lacking TNF AU-rich ele-

ments: implications for joint and gut-associated immunopathologies'. *Immunity* **10**(3), 387–398.

Kornev, A. P., N. M. Haste, S. S. Taylor, and L. F. Ten Eyck: 2006, 'Surface comparison of active and inactive protein kinases identifies a conserved activation mechanism'. *Proceedings of the National Academy of Sciences* **103**(47), 17783–17788.

Kravtsova-Ivantsiv, Y., I. Shomer, V. Cohen-Kaplan, B. Snijder, G. Superti-Furga, H. Gonen, T. Sommer, T. Ziv, A. Admon, I. Naroditsky, M. Jbara, A. Brik, E. Pikarsky, Y. T. Kwon, I. Doweck, and A. Ciechanover: 2015, 'KPC1-Mediated Ubiquitination and Proteasomal Processing of NF-κB1 p105 to p50 Restricts Tumor Growth'. *Cell* **161**(2), 333–347.

Krishnan, R. K., H. Nolte, T. Sun, H. Kaur, K. Sreenivasan, M. Looso, S. Offermanns, M. Krüger, and J. M. Swiercz: 2015, 'Quantitative analysis of the TNF-α-induced phosphoproteome reveals AEG-1/MTDH/LYRIC as an IKKβ substrate'. *Nature Communications* **6**, 6658.

Lacaze, P., S. Raza, G. Sing, D. Page, T. Forster, P. Storm, M. Craigon, T. Awad, P. Ghazal, and T. C. Freeman: 2009, 'Combined genome-wide expression profiling and targeted RNA interference in primary mouse macrophages reveals perturbation of transcriptional networks associated with interferon signalling'. *BMC Genomics* **10**(1), 372.

Lamothe, B., A. Besse, A. D. Campos, W. K. Webster, H. Wu, and B. G. Darnay: 2006, 'Site-specific Lys-63-linked Tumor Necrosis Factor Receptor-associated Factor 6 Auto-ubiquitination Is a Critical Determinant of I B Kinase Activation'. *Journal of Biological Chemistry* **282**(6), 4102–4112.

Lancaster, G. I., G. M. Kowalski, E. Estevez, M. J. Kraakman, G. Grigoriadis, M. A. Febbraio, S. Gerondakis, and A. Banerjee: 2012, 'Tumor Progression Locus 2 (Tpl2) Deficiency Does Not Protect against Obesity-Induced Metabolic Disease'. *PLoS ONE* **7**(6), e39100.

Lang, V., J. Janzen, G. Z. Fischer, Y. Soneji, S. Beinke, A. Salmerón, H. Allen, R. T. Hay, Y. Ben-Neriah, and S. C. Ley: 2003, 'TrCP-Mediated Proteolysis of NF-κB1 p105 Requires Phosphorylation of p105 Serines 927 and 932'. *Molecular and Cellular Biology* **23**(1), 402–413.

Lang, V., A. Symons, S. J. Watton, J. Janzen, Y. Soneji, S. Beinke, S. Howell, and S. C. Ley: 2004, 'ABIN-2 forms a ternary complex with TPL-2 and NF-κB1 p105 and is essential for TPL-2 protein stability'. *Molecular and Cellular Biology* **24**(12), 5235–48.

Langeberg, L. K. and J. D. Scott: 2015, 'Signalling scaffolds and local organization of cellular behaviour'. *Nature Reviews Molecular Cell Biology* **16**(4), 232–244.

Lawler, S., Y. Fleming, M. Goedert, and P. Cohen: 1998, 'Synergistic activation of SAPK1/JNK1 by two MAP kinase kinases in vitro'. *Current Biology* **8**(25), 1387–1391.

Lee, H. W., K. M. Joo, J. E. Lim, H. J. Cho, M. C. Park, H. J. Seol, S. I. Seo, J. I. Lee, S. Kim, B. C. Jeong, and D. H. Nam: 2013, 'Tpl2 kinase impacts tumor growth and metastasis of clear cell renal cell carcinoma'. *Molecular Cancer Research* **11**(11), 1375–86.

Lee, J. C., J. T. Laydon, P. C. McDonnell, T. F. Gallagher, S. Kumar, D. Green, D. McNulty, M. J. Blumenthal, J. R. Heys, S. W. Landvatter, J. E. Strickler, M. M. McLaughlin, I. R. Siemens, S. M. Fisher, G. P. Livi, J. R. White, J. L. Adams, and P. R. Young: 1994, 'A protein kinase involved in the regulation of inflammatory cytokine biosynthesis'. *Nature* **372**, 739–746.

Levine, S. J.: 2008, 'Molecular Mechanisms of Soluble Cytokine Receptor Generation'. *Journal of Biological Chemistry* **283**(21), 14177–14181.

Li, N., J. Sun, Z. L. Benet, Z. Wang, S. Al-Khodor, S. P. John, B. Lin, M.-H. Sung, and I. D. C. Fraser: 2015, 'Development of a cell system for siRNA screening of pathogen responses in human and mouse macrophages'. *Scientific Reports* **5**, 9559.

Li, Q.-r., Z.-b. Ning, J.-s. Tang, S. Nie, and R. Zeng: 2009, 'Effect of Peptide-to-TiO2 Beads Ratio on Phosphopeptide Enrichment Selectivity'. *Journal of Proteome Research* **8**, 5375–5381.

Licona-Limón, P., L. K. Kim, N. W. Palm, and R. A. Flavell: 2013, 'TH2, allergy and group 2 innate lymphoid cells'. *Nature Immunology* **14**(6), 536–542.

Lin, A., A. Minden, H. Martinetto, F.-X. Claret, C. Lange-Carter, F. Mercurio, G. L. Johnson, and M. Karin: 1995, 'Identification of a Dual Specificity Kinase That Activates the Jun Kinases and p38-Mpk2'. *Science* **268**(5208), 286–290.

Lizcano, J. M., O. Göransson, R. Toth, M. Deak, N. A. Morrice, J. Boudeau, S. A. Hawley, L. Udd, T. P. Mäkelä, D. G. Hardie, and others: 2004, 'LKB1 is a master kinase that activates 13 kinases of the AMPK subfamily, including MARK/PAR-1'. *The EMBO Journal* **23**(4), 833–843.

Locksley, R. M.: 2009, 'Nine lives: plasticity among T helper cell subsets'. *Journal of Experimental Medicine* **206**(8), 1643–1646.

Lopez-Pelaez, M., I. Soria-Castro, L. Bosca, M. Fernandez, and S. Alemany: 2011, 'Cot/tpl2 activity is required for TLR-induced activation of the Akt p70 S6k pathway in macrophages: Implications for NO synthase 2 expression'. *European Journal of Immunology* **41**(6), 1733–41.

Luciano, B. S., S. Hsu, P. L. Channavajhala, L. L. Lin, and J. W. Cuozzo: 2004, 'Phosphorylation of threonine 290 in the activation loop of Tpl2/Cot is necessary but not sufficient for kinase activity'. *The Journal of Biological Chemistry* **279**(50), 52117–23.

MacBeath, G. and S. L. Schreiber: 2000, 'Printing Proteins as Microarrays for High-Throughput Function Determination'. *Science* **289**(5485), 1760–1763.

MacEwan, D. J.: 2002, 'TNF receptor subtype signalling: differences and cellular consequences'. *Cellular signalling* **14**(6), 477–492.

Magrane, M. and U. Consortium: 2011, 'UniProt Knowledgebase: a hub of integrated protein data'. *Database* **2011**, 1–13.

Mali, P., L. Yang, K. M. Esvelt, J. Aach, M. Guell, J. E. DiCarlo, J. E. Norville, and G. M. Church: 2013, 'RNA-Guided Human Genome Engineering via Cas9'. *Science* **339**(6121), 823–826.

Mann, M.: 2006, 'Functional and quantitative proteomics using SILAC'. *Nature Reviews. Molecular Cell Biology* **7**(12), 952–8.

Mann, M. and O. N. Jensen: 2003, 'Proteomic analysis of post-translational modifications'. *Nature Biotechnology* **21**(3), 255–261.

Marquis, M., S. Boulet, S. Mathien, J. Rousseau, P. Thébault, J.-F. Daudelin, J. Rooney, B. Turgeon, C. Beauchamp, S. Meloche, and N. Labrecque: 2014, 'The Non-Classical MAP Kinase ERK3 Controls T Cell Activation'. *PLoS ONE* **9**(1), e86681.

Matsuzawa, A., K. Saegusa, T. Noguchi, C. Sadamitsu, H. Nishitoh, S. Nagai, S. Koyasu, K. Matsumoto, K. Takeda, and H. Ichijo: 2005, 'ROS-dependent activation of the TRAF6-ASK1-p38 pathway is selectively required for TLR4-mediated innate immunity'. *Nature Immunology* **6**(6), 587–592.

McNab, F. W., J. Ewbank, R. Rajsbaum, E. Stavropoulos, A. Martirosyan, P. S. Redford, X. Wu, C. M. Graham, M. Saraiva, P. Tsichlis, D. Chaussabel, S. C. Ley, and A. O'Garra: 2013, 'TPL-2-ERK1/2 Signaling Promotes Host Resistance against Intracellular Bacterial Infection by Negative Regulation of Type I IFN Production'. *Journal of immunology* **191**(4), 1732–43.

Meylan, E., J. Tschopp, and M. Karin: 2006, 'Intracellular pattern recognition receptors in the host response'. *Nature* **442**(7098), 39–44.

Mielke, L. A., K. L. Elkins, L. Wei, R. Starr, P. N. Tsichlis, J. J. O'Shea, and W. T. Watford: 2009, 'Tumor progression locus 2 (Map3k8) is critical for host defense against Listeria monocytogenes and IL-1β production'. *Journal of Immunology* **183**(12), 7984–93.

Mieulet, V., L. Yan, C. Choisy, K. Sully, J. Procter, A. Kouroumalis, S. Krywawych, M. Pende, S. C. Ley, C. Moinard, and R. F. Lamb: 2010, 'TPL-2-mediated activation of MAPK downstream of TLR4 signaling is coupled to arginine availability'. *Science Signaling* **3**(135), ra61.

Miyoshi, J., T. Higashi, H. Mukai, T. Ohuchi, and T. Kakunaga: 1991, 'Structure and transforming potential of the human cot oncogene encoding a putative protein kinase.'. *Molecular and cellular biology* **11**(8), 4088–4096.

Monetti, M., N. Nagaraj, K. Sharma, and M. Mann: 2011, 'Large-scale phosphosite quantification in tissues by a spike-in SILAC method'. *Nature methods* **8**(8), 655–8.

Monsma, D. J., D. M. Cherba, E. E. Eugster, D. L. Dylewski, P. T. Davidson, C. A. Peterson, A. S. Borgman, M. E. Winn, K. J. Dykema, C. P. Webb, and others: 2015, 'Melanoma patient derived xenografts acquire distinct Vemurafenib resistance mechanisms'. *American journal of cancer research* **5**(4), 1507.

Moss, M. L., S.-L. C. Jin, M. E. Milla, W. Burkhart, H. L. Carter, W.-J. Chen, W. C. Clay, J. R. Didsbury, D. Hassler, C. R. Hoffman, T. A. Kost, M. H. Lambert, M. A. Leesnitzer, P. McCauley, G. McGeehan, J. Mitchell, M. Moyer, G. Pahel, W. Rocque, L. K. Overton, F. Schoenen, T. Seaton, J.-L. Su, J. Warner, D. Willard, and J. D. Becherer: 1997, 'Cloning of a disintegrin metalloproteinase that processes precursor tumour-necrosis factor-[alpha]'. *Nature* **385**(6618), 733–736.

Mosser, D. M. and J. P. Edwards: 2008, 'Exploring the full spectrum of macrophage activation'. *Nature Reviews Immunology* **8**(12), 958–969.

Mukherjee, S., G. Keitany, Y. Li, Y. Wang, H. L. Ball, E. J. Goldsmith, and K. Orth: 2006, 'Yersinia YopJ Acetylates and Inhibits Kinase Activation by Blocking Phosphorylation'. *Science* **312**(5777), 1211–1214.

Municio, M. M., J. Lozano, P. Sánchez, J. Moscat, and M. T. Diaz-Meco: 1995, 'Identification of Heterogeneous Ribonucleoprotein A1 as a Novel Substrate for Protein Kinase C ζ'. *Journal of Biological Chemistry* **270**(26), 15884–15891.

Murphy, K., P. Travers, and M. Walport: 2008, *Janeway's Immunobiology*. New York: Garland Science, 7 edition.

Murray, P. J. and T. A. Wynn: 2011, 'Protective and pathogenic functions of macrophage subsets'. *Nature reviews. Immunology* **11**(11), 723–37.

Murray, R. Z. and J. L. Stow: 2014, 'Cytokine Secretion in Macrophages: SNAREs, Rabs, and Membrane Trafficking'. *Frontiers in Immunology* **5**, 538.

Nithianandarajah-Jones, G. N., B. Wilm, C. E. Goldring, J. Müller, and M. J. Cross: 2012, 'ERK5: Structure, regulation and function'. *Cellular Signalling* **24**(11), 2187–2196.

Nowak, M., G. C. Gaines, J. Rosenberg, R. Minter, F. R. Bahjat, J. Rectenwald, S. L. MacKay, C. K. Edwards, and L. L. Moldawer: 2000, 'LPS-induced liver injury ind-galactosamine-sensitized mice requires secreted TNF-α and the TNF-p55 receptor'. *American Journal of Physiology-Regulatory, Integrative and Comparative Physiology* **278**(5), R1202–R1209.

O'Callaghan, C., L. J. Fanning, and O. P. Barry: 2014, 'p38δ MAPK: Emerging Roles of a Neglected Isoform'. *International Journal of Cell Biology* **2014**, 1–12.

Oda, Y., T. Nagasu, and B. T. Chait: 2001, 'Enrichment analysis of phosphorylated proteins as a tool for probing the phosphoproteome'. *Nature Biotechnology* **19**(4), 379–382.

O'Donnell, A., Z. Odrowaz, and A. D. Sharrocks: 2012, 'Immediate-early gene activation by the MAPK pathways: what do and don't we know?'. *Biochemical Society Transactions* **40**(1), 58–66.

Oganesyan, G., S. K. Saha, B. Guo, J. Q. He, A. Shahangian, B. Zarnegar, A. Perry, and G. Cheng: 2006, 'Critical role of TRAF3 in the Toll-like receptor-dependent and -independent antiviral response'. *Nature* **439**(7073), 208–211.

Ohkawara, B., K. Shirakabe, J. Hyodo-Miura, R. Matsuo, N. Ueno, K. Matsumoto, and H. Shibuya: 2004, 'Role of the TAK1-NLK-STAT3 pathway in TGF-β-mediated mesoderm induction'. *Genes & Development* **18**(4), 381–386.

O'Keefe, S. J., J. S. Mudgett, S. Cupo, J. N. Parsons, N. A. Chartrain, C. Fitzgerald, S.-L. Chen, K. Lowitz, C. Rasa, D. Visco, S. Luell, E. Carballo-Jane, K. Owens, and D. M. Zaller: 2007, 'Chemical Genetics Define the Roles of p38α and p38β in Acute and Chronic Inflammation'. *Journal of Biological Chemistry* **282**(48), 34663–34671.

Olsen, J. V.: 2004, 'Trypsin Cleaves Exclusively C-terminal to Arginine and Lysine Residues'. *Molecular & Cellular Proteomics* **3**(6), 608–614.

Olsen, J. V., B. Macek, O. Lange, A. Makarov, S. Horning, and M. Mann: 2007, 'Higher-energy C-trap dissociation for peptide modification analysis'. *Nature methods* **4**(9), 709–12.

Ong, S.-E.: 2012, 'The expanding field of SILAC'. *Analytical and Bioanalytical Chemistry* **404**(4), 967–976.

Ong, S. E., B. Blagoev, I. Kratchmarova, D. B. Kristensen, H. Steen, A. Pandey, and M. Mann: 2002, 'Stable isotope labeling by amino acids in cell culture, SILAC, as a simple and accurate approach to expression proteomics'. *Molecular & Cellular Proteomics* **1**(5), 376–86.

Ong, S.-E., I. Kratchmarova, and M. Mann: 2003, 'Properties of 13C-Substituted Arginine in Stable Isotope Labeling by Amino Acids in Cell Culture (SILAC)'. *Journal of Proteome Research* **2**(2), 173–181.

Orian, A., H. Gonen, B. Bercovich, I. Fajerman, E. Eytan, A. Israël, F. Mercurio, K. Iwai, A. L. Schwartz, and A. Ciechanover: 2000, 'SCFβTrCP ubiquitin ligase-mediated processing of NF-κB p105 requires phosphorylation of its C-terminus by IκB kinase.'. *EMBO Journal* **19**(11), 2580–2591.

Ostuni, R. and G. Natoli: 2011, 'Transcriptional control of macrophage diversity and specialization'. *European Journal of Immunology* **41**(9), 2486–2490.

Palladino, M. A., F. R. Bahjat, E. A. Theodorakis, and L. L. Moldawer: 2003, 'Anti-TNF-α therapies: the next generation'. *Nature Reviews Drug Discovery* **2**(9), 736–746.

Palumbo, A. M., S. A. Smith, C. L. Kalcic, M. Dantus, P. M. Stemmer, and G. E. Reid: 2011, 'Tandem mass spectrometry strategies for phosphoproteome analysis'. *Mass spectrometry reviews* **30**(4), 600–25.

Papadakis, K. A. and S. R. Targan: 2000, 'Tumor necrosis factor: Biology and therapeutic inhibitors'. *Gastroenterology* **119**(4), 1148–1157.

Papoutsopoulou, S., A. Symons, T. Tharmalingham, M. P. Belich, F. Kaiser, D. Kioussis, A. O'Garra, V. Tybulewicz, and S. C. Ley: 2006, 'ABIN-2 is required for optimal activation of Erk MAP kinase in innate immune responses'. *Nature immunology* **7**(6), 606–15.

Parikh, K., S. H. Diks, J. H. Tuynman, A. Verhaar, M. Lowenberg, D. W. Hommes, J. Joore, A. Pandey, and M. P. Peppelenbosch: 2009, 'Comparison of peptide array substrate phosphorylation of c-Raf and mitogen activated protein kinase kinase kinase 8'. *PloS one* **4**(7), e6440.

Parker, C. G., J. Hunt, K. Diener, M. McGinley, B. Soriano, G. A. Keesler, J. Bray, Z. Yao, X. S. Wang, T. Kohno, and H. S. Lichenstein: 1998, 'Identification of Stathmin as a Novel Substrate for p38 Delta'. *Biochemical and Biophysical Research Communications* **249**, 791–796.

Parsons, D. W., S. Jones, X. Zhang, J. C.-H. Lin, R. J. Leary, P. Angenendt, P. Mankoo, H. Carter, I.-M. Siu, G. L. Gallia, and others: 2008, 'An integrated genomic analysis of human glioblastoma multiforme'. *Science* **321**(5897), 1807–1812.

Patriotis, C., A. Makris, S. E. Bear, and P. N. Tsichlis: 1993, 'Tumor progression locus 2 (Tpl-2) encodes a protein kinase involved in the progression of rodent T-cell lymphomas and in T-cell activation.'. *Proceedings of the National Academy of Sciences* **90**(6), 2251–2255.

Patriotis, C., M. G. Russeva, J. H. Lin, S. M. Srinivasula, D. Z. Markova, C. Tsatsanis, A. M. Makris, E. S. Alnemri, and P. Tsichlis: 2001, 'Tpl-2 Induces Apoptosis by Promoting the Assembly of Protein Complexes That Contain Caspase-9, the Adapter Protein Tvl-1, and Procaspase-3'. *Journal of Cellular Physiology* **187**, 176–187.

Peregrin, S., M. Jurado-Pueyo, P. M. Campos, V. Sanz-Moreno, A. Ruiz-Gomez, P. Crespo, F. Mayor, and C. Murga: 2006, 'Phosphorylation of p38 by GRK2 at the Docking Groove Unveils a Novel Mechanism for Inactivating p38MAPK'. *Current Biology* **16**(20), 2042–2047.

Perfield, J. W., Y. Lee, G. I. Shulman, V. T. Samuel, M. J. Jurczak, E. Chang, C. Xie, P. N. Tsichlis, M. S. Obin, and A. S. Greenberg: 2011, 'Tumor Progression Locus 2 (TPL2) Regulates Obesity-Associated Inflammation and Insulin Resistance'. *Diabetes* **60**(4), 1168–1176.

Pinkse, M. W. H., P. M. Uitto, M. J. Hilhorst, B. Ooms, and A. J. Heck: 2004, 'Selective Isolation at the Femtomole Level of Phosphopeptides from Proteolytic Digests Using 2D-NanoLC-ESI-MS/MS and Titanium Oxide Precolumns'. *Analytical Chemistry* **76**(14), 3935–3943.

Pobezinskaya, Y. L., Y.-S. Kim, S. Choksi, M. J. Morgan, T. Li, C. Liu, and Z. Liu: 2008, 'The function of TRADD in signaling through tumor necrosis factor receptor 1 and TRIF-dependent Toll-like receptors'. *Nature Immunology* **9**(9), 1047–1054.

Pollard, J. W.: 2009, 'Trophic macrophages in development and disease'. *Nature reviews. Immunology* **9**(4), 259–70.

Prowse, C. N., M. S. Deal, and J. Lew: 2001, 'The Complete Pathway for Catalytic Activation of the Mitogen-activated Protein Kinase, ERK2'. *Journal of Biological Chemistry* **276**(44), 40817–40823.

Raschke, W. C., S. Baird, P. Ralph, and I. Nakoinz: 1978, 'Functional Macrophage Cell Lines Transformed by Abelson Leukemia Virus'. *Cell* **15**, 261–267.

Remy, G., A. M. Risco, F. A. Iñesta-Vaquera, B. González-Terán, G. Sabio, R. J. Davis, and A. Cuenda: 2010, 'Differential activation of p38MAPK isoforms by MKK6 and MKK3'. *Cellular Signalling* **22**(4), 660–667.

Risco, A. and A. Cuenda: 2012, 'New Insights into the p38 γ and p38 δ MAPK Pathways'. *Journal of Signal Transduction* **2012**, 1–8.

Risco, A., C. D. Fresno, A. Mambole, D. Alsina-Beauchamp, K. F. MacKenzie, H. T. Yang, D. F. Barber, C. Morcelle, J. S. C. Arthur, S. C. Ley, C. Ardavin, and A. Cuenda: 2012, 'p38γ and p38δ kinases regulate the Toll-like receptor 4 (TLR4)-induced cytokine production by controlling ERK1/2 protein kinase pathway activation'. *Proceedings of the National Academy of Sciences of the United States of America* **109**(28), 11200–11205.

Robbins, D. J., E. Zhen, H. Owaki, C. A. Vanderbilt, D. Ebert, T. D. Geppert, and M. H. Cobb: 1993, 'Regulation and properties of extracellular signal-regulated protein kinases 1 and 2 in vitro.'. *Journal of Biological Chemistry* **268**(7), 5097–5106.

Robinson, M. J., S. Beinke, A. Kouroumalis, P. N. Tsichlis, and S. C. Ley: 2007, 'Phosphorylation of TPL-2 on serine 400 is essential for lipopolysaccharide activation of extracellular signal-regulated kinase in macrophages'. *Molecular and cellular biology* **27**(21), 7355–64.

Roche, P. A. and K. Furuta: 2015, 'The ins and outs of MHC class II-mediated antigen processing and presentation'. *Nature Reviews Immunology* **15**(4), 203–216.

Roget, K., A. Ben-Addi, A. Mambole-Dema, T. Gantke, H. T. Yang, J. Janzen, N. Morrice, D. Abbott, and S. C. Ley: 2012, 'IKK2 regulates TPL-2 activation of ERK-1/2 MAP kinases by direct phosphorylation of TPL-2 serine 400'. *Molecular and Cellular Biology* **32**(22), 4684–4690.

Ronkina, N., A. Kotlyarov, O. Dittrich-Breiholz, M. Kracht, E. Hitti, K. Milarski, R. Askew, S. Marusic, L.-L. Lin, M. Gaestel, and J.-B. Telliez: 2007, 'The Mitogen-Activated Protein Kinase (MAPK)-Activated Protein Kinases MK2 and MK3 Cooperate in Stimulation of Tumor Necrosis Factor Biosynthesis and Stabilization of p38 MAPK'. *Molecular and Cellular Biology* **27**(1), 170–181.

Rosette, C. and M. Karin: 1996, 'Ultraviolet light and osmotic stress: activation of the JNK cascade through multiple growth factor and cytokine receptors'. *Science* **274**(5290), 1194–1197.

Rousseau, S., M. Papoutsopoulou, A. Symons, D. Cook, J. M. Lucocq, A. R. Prescott, A. O'Garra, S. C. Ley, and P. Cohen: 2008, 'TPL2-mediated activation of ERK1 and ERK2 regulates the processing of pre-TNFα in LPS-stimulated macrophages'. *Journal of cell science* **121**(Pt 2), 149–54.

Roux, P. P. and J. Blenis: 2004, 'ERK and p38 MAPK-Activated Protein Kinases: a Family of Protein Kinases with Diverse Biological Functions'. *Microbiology and Molecular Biology Reviews* **68**(2), 320–344.

Rowley, S. M., T. Kuriakose, L. M. Dockery, T. Tran-Ngyuen, A. D. Gingerich, L. Wei, and W. T. Watford: 2014, 'Tumor Progression Locus 2 (Tpl2) Kinase Promotes Chemokine Receptor Expression and Macrophage Migration during Acute Inflammation'. *Journal of Biological Chemistry* **289**(22), 15788–15797.

Russell, F. D. and A. P. Davenport: 1999, 'Evidence for Intracellular Endothelin-Converting Enzyme-2 Expression in Cultured Human Vascular Endothelial Cells'. *Circulation Research* **84**, 891–896.

Ruuls, S. R., R. M. Hoek, V. N. Ngo, T. McNeil, L. A. Lucian, M. J. Janatpour, H. Körner, H. Scheerens, E. M. Hessel, J. G. Cyster, and others: 2001, 'Membrane-bound TNF supports secondary lymphoid organ structure but is subservient to secreted TNF in driving autoimmune inflammation'. *Immunity* **15**(4), 533–543.

Ryazanov, A. G., E. A. Shestakova, and P. G. Natapov: 1988, 'Phosphorylation of elongation factor 2 by EF-2 kinase affects rate of translation.'. *Nature* **334**, 170–173.

Sabio, G., J. S. C. Arthur, Y. Kuma, M. Peggie, J. Carr, V. Murray-Tait, F. Centeno, M. Goedert, N. A. Morrice, and A. Cuenda: 2005, 'p38γ regulates the localisation of SAP97 in the cytoskeleton by modulating its interaction with GKAP'. *The EMBO journal* **24**(6), 1134–1145.

Sabio, G., M. I. Cerezo-Guisado, P. del Reino, F. A. Inesta-Vaquera, S. Rousseau, J. S. C. Arthur, D. G. Campbell, F. Centeno, and A. Cuenda: 2010, 'p38 regulates interaction of nuclear PSF and RNA with the tumour-suppressor hDlg in response to osmotic shock'. *Journal of Cell Science* **123**(15), 2596–2604.

Sag, D., D. Carling, R. D. Stout, and J. Suttles: 2008, 'Adenosine 5'-Monophosphate-Activated Protein Kinase Promotes Macrophage Polarization to an Anti-Inflammatory Functional Phenotype'. *The Journal of Immunology* **181**(12), 8633–8641.

Sakurai, H.: 2012, 'Targeting of TAK1 in inflammatory disorders and cancer'. *Trends in Pharmacological Sciences* **33**(10), 522–530.

Salmerón, A., J. Janzen, Y. Soneji, N. Bump, J. Kamens, H. Allen, and S. C. Ley: 2001, 'Direct phosphorylation of NF-κB1 p105 by the IκB kinase complex on serine 927 is essential for signal-induced p105 proteolysis'. *The Journal of Biological Chemistry* **276**(25), 22215–22.

Salmeron, A., T. B. Ahmad, G. W. Carlile, D. Pappin, R. P. Narsimhan, and S. C. Ley: 1996, 'Activation of MEK-1 and SEK-1 by Tpl-2 proto-oncoprotein, a novel MAP kinase kinase kinase.'. *The EMBO Journal* **15**(4), 817–826.

Salvador, J. M., P. R. Mittelstadt, T. Guszczynski, T. D. Copeland, H. Yamaguchi, E. Appella, A. J. Fornace, and J. D. Ashwell: 2005, 'Alternative p38 activation pathway mediated by T cell receptor–proximal tyrosine kinases'. *Nature Immunology* **6**(4), 390–395.

Sano, A. and H. Nakamura: 2004, 'Chemo-affinity of titania for the column-switching HPLC analysis of phosphopeptides'. *Analytical Sciences* **20**, 565–566.

Sanz-Garcia, C., L. E. Nagy, M. A. Lasuncion, M. Fernandez, and S. Alemany: 2014, 'Cot/tpl2 participates in the activation of macrophages by adiponectin'. *Journal of leukocyte biology* **95**(6), 917–30.

Schulz, C., E. Gomez Perdiguero, L. Chorro, H. Szabo-Rogers, N. Cagnard, K. Kierdorf, M. Prinz, B. Wu, S. E. Jacobsen, J. W. Pollard, J. Frampton, K. J. Liu, and F. Geissmann: 2012, 'A lineage of myeloid cells independent of Myb and hematopoietic stem cells'. *Science* **336**(6077), 86–90.

Schwanhäusser, B., D. Busse, N. Li, G. Dittmar, J. Schuchhardt, J. Wolf, W. Chen, and M. Selbach: 2011, 'Global quantification of mammalian gene expression control'. *Nature* **473**(7347), 337–342.

Serebrennikova, O., C. Tsatsanis, C. Mao, E. Gounaris, W. Ren, L. D. Siracusa, A. G. Eliopoulos, K. Khazaie, and P. N. Tsichlis: 2012, 'Tpl2 ablation promotes intestinal inflammation and tumorigenesis in Apcmin mice by inhibiting IL-10 secretion and regulatory T-cell generation'. *Proceedings of the National Academy of Sciences of the United States of America* pp. E1082–E1091.

Sfikakis, P. P.: 2010, 'The first decade of biologic TNF antagonists in clinical practice: lessons learned, unresolved issues and future directions'. *Curr Dir Autoimmun* **11**(3), 180–210.

Shah, K., Y. Liu, C. Deirmengian, and K. M. Shokat: 1997, 'Engineering unnatural nucleotide specificity for Rous sarcoma virus tyrosine kinase to uniquely label its direct substrates'. *Proceedings of the National Academy of Sciences of the United States of America* **94**, 6.

Shalem, O., N. E. Sanjana, and F. Zhang: 2015, 'High-throughput functional genomics using CRISPR–Cas9'. *Nature Reviews Genetics* **16**(5), 299–311.

Shaw, R. J., M. Kosmatka, N. Bardeesy, R. L. Hurley, L. A. Witters, R. A. DePinho, and L. C. Cantley: 2004, 'The tumor suppressor LKB1 kinase directly activates AMP-activated kinase and regulates apoptosis in response to energy stress'. *Proceedings of the National Academy of Sciences of the United States of America* **101**(10), 3329–3335.

Shi, J., Y. Zhao, Y. Wang, W. Gao, J. Ding, P. Li, L. Hu, and F. Shao: 2014, 'Inflammatory caspases are innate immune receptors for intracellular LPS'. *Nature* **514**, 187–192.

Shinohara, M. L., L. Lu, J. Bu, M. B. F. Werneck, K. S. Kobayashi, L. H. Glimcher, and H. Cantor: 2006, 'Osteopontin expression is essential for interferon-α production by plasmacytoid dendritic cells'. *Nature Immunology* **7**(5), 498–506.

Silva, A. M., M. Whitmore, Z. Xu, Z. Jiang, X. Li, and B. R. G. Williams: 2004, 'Protein Kinase R (PKR) Interacts with and Activates Mitogen-activated Protein Kinase Kinase 6 (MKK6) in Response to Double-stranded RNA Stimulation'. *Journal of Biological Chemistry* **279**(36), 37670–37676.

Smith, S. M.: 2011, 'Strategies for the Purification of Membrane Proteins'. In: D. Walls and S. T. Loughran (eds.): *Protein Chromatography*, Vol. 681. Totowa, NJ: Humana Press, pp. 485–496.

Soond, S. M., B. Everson, D. W. Riches, and G. Murphy: 2005, 'ERK-mediated phosphorylation of Thr735 in TNFalpha-converting enzyme and its potential role in TACE protein trafficking'. *Journal of Cell Science* **118**(Pt 11), 2371–80.

Sourvinos, G., C. Tsatsanis, and D. A. Spandidos: 1999, 'Overexpression of the Tpl-2/Cot oncogene in human breast cancer'. *Oncogene* **18**(35), 4968–73.

Sriskantharajah, S., M. P. Belich, S. Papoutsopoulou, J. Janzen, V. Tybulewicz, B. Seddon, and S. C. Ley: 2009, 'Proteolysis of NF-κB1 p105 is essential for T cell antigen receptor-induced proliferation'. *Nature immunology* **10**(1), 38–47.

Sriskantharajah, S., E. Guckel, N. Tsakiri, K. Kierdorf, C. Brender, A. Ben-Addi, M. Veldhoen, P. N. Tsichlis, B. Stockinger, A. O'Garra, M. Prinz, G. Kollias, and S. C. Ley: 2014, 'Regulation of Experimental Autoimmune Encephalomyelitis by TPL-2 Kinase'. *Journal of Immunology* **192**(8), 3518–3529.

Stafford, M. J., N. A. Morrice, M. W. Peggie, and P. Cohen: 2006, 'Interleukin-1 stimulated activation of the COT catalytic subunit through the phosphorylation of Thr290 and Ser62'. *FEBS Letters* **580**(16), 4010–4.

Stanley, A. C., C. X. Wong, M. Micaroni, J. Venturato, T. Khromykh, J. L. Stow, and P. Lacy: 2014, 'The Rho GTPase Rac1 is required for recycling endosome-mediated secretion of TNF in macrophages'. *Immunology and Cell Biology* **92**(3), 275–86.

Takeuchi, O. and S. Akira: 2010, 'Pattern Recognition Receptors and Inflammation'. *Cell* **140**(6), 805–820.

Talbot, S., S. Tötemeyer, M. Yamamoto, S. Akira, K. Hughes, D. Gray, T. Barr, P. Mastroeni, D. J. Maskell, and C. E. Bryant: 2009, 'Toll-like receptor 4 signalling through MyD88 is essential to control Salmonella enterica serovar Typhimurium infection, but not for the initiation of bacterial clearance'. *Immunology* **128**(4), 472–483.

Tanaka, N., M. Kamanaka, H. Enslen, C. Dong, M. Wysk, R. J. Davis, and R. A. Flavell: 2002, 'Differential involvement of p38 mitogen-activated protein kinase kinases MKK3 and MKK6 in T-cell apoptosis'. *EMBO reports* **3**(8), 785–791.

Tanaka, T., M. J. Grusby, and T. Kaisho: 2007, 'PDLIM2-mediated termination of transcription factor NF-κB activation by intranuclear sequestration and degradation of the p65 subunit'. *Nature Immunology* **8**(6), 584–591.

Tellier, E., M. Canault, L. Rebsomen, B. Bonardo, I. Juhan-Vague, G. Nalbone, and F. Peiretti: 2006, 'The shedding activity of ADAM17 is sequestered in lipid rafts'. *Experimental Cell Research* **312**(20), 3969–3980.

Tian, Y., C. Pate, A. Andreolotti, L. Wang, E. Tuomanen, K. Boyd, E. Claro, and S. Jackowski: 2008, 'Cytokine secretion requires phosphatidylcholine synthesis'. *The Journal of Cell Biology* **181**(6), 945–957.

Tiedje, C., N. Ronkina, M. Tehrani, S. Dhamija, K. Laass, H. Holtmann, A. Kotlyarov, and M. Gaestel: 2012, 'The p38/MK2-Driven Exchange between Tristetraprolin and HuR Regulates AU–Rich Element–Dependent Translation'. *PLoS Genetics* **8**(9), e1002977.

Tortorella, L. L., C. B. Lin, and P. F. Pilch: 2003, 'ERK6 is expressed in a developmentally regulated manner in rodent skeletal muscle'. *Biochemical and Biophysical Research Communications* **306**(1), 163–168.

Tournier, C., C. Dong, T. K. Turner, S. N. Jones, R. A. Flavell, and R. J. Davis: 2001, 'MKK7 is an essential component of the JNK signal transduction path-

way activated by proinflammatory cytokines'. *Genes & development* **15**(11), 1419–1426.

Trosky, J. E., Y. Li, S. Mukherjee, G. Keitany, H. Ball, and K. Orth: 2007, 'VopA Inhibits ATP Binding by Acetylating the Catalytic Loop of MAPK Kinases'. *Journal of Biological Chemistry* **282**(47), 34299–34305.

Tsatsanis, C., K. Vaporidi, V. Zacharioudaki, A. Androulidaki, Y. Sykulev, A. N. Margioris, and P. N. Tsichlis: 2008, 'Tpl2 and ERK transduce antiproliferative T cell receptor signals and inhibit transformation of chronically stimulated T cells'. *Proceedings of the National Academy of Sciences of the United States of America* **105**(8), 2987–92.

Ubersax, J. A. and J. E. Ferrell Jr: 2007, 'Mechanisms of specificity in protein phosphorylation'. *Nature Reviews Molecular Cell Biology* **8**(7), 530–541.

Unterholzner, L.: 2013, 'The interferon response to intracellular DNA: Why so many receptors?'. *Immunobiology* **218**(11), 1312–1321.

Uren, A. G., J. Kool, A. Berns, and M. van Lohuizen: 2005, 'Retroviral insertional mutagenesis: past, present and future'. *Oncogene* **24**(52), 7656–72.

Villen, J. and S. P. Gygi: 2008, 'The SCX/IMAC enrichment approach for global phosphorylation analysis by mass spectrometry'. *Nature protocols* **3**(10), 1630–8.

Vougioukalaki, M., D. C. Kanellis, K. Gkouskou, and A. G. Eliopoulos: 2011, 'Tpl2 kinase signal transduction in inflammation and cancer'. *Cancer letters* **304**(2), 80–9.

Wabl, M. and C. Steinberg: 1996, 'Affinity maturation and class switching'. *Current Opinion in Immunology* **8**(1), 89–92.

Wagner, E. F. and A. R. Nebreda: 2009, 'Signal integration by JNK and p38 MAPK pathways in cancer development'. *Nature Reviews Cancer* **9**(8), 537–549.

Wajant, H., K. Pfizenmaier, and P. Scheurich: 2003, 'Tumor necrosis factor signaling'. *Cell Death & Differentiation* **10**(1), 45–65.

Wang, C., L. Deng, M. Hong, G. R. Akkaraju, J.-i. Inoue, and Z. J. Chen: 2001, 'TAK1 is a ubiquitin-dependent kinase of MKK and IKK'. *Nature* **412**(6844), 346–351.

Wang, G. G., K. R. Calvo, M. P. Pasillas, D. B. Sykes, H. Hacker, and M. P. Kamps: 2006, 'Quantitative production of macrophages or neutrophils ex vivo using conditional Hoxb8'. *Nature Methods* **3**(4), 287–293.

Wang, J. Y. J.: 1988, 'Antibodies for phosphotyrosine: Analytical and preparative tool for tyrosyl-phosphorylated proteins'. *Analytical Biochemistry* **172**(1), 1–7.

Wang, X., S. Pesakhov, J. S. Harrison, M. Kafka, M. Danilenko, and G. P. Studzinski: 2015, 'The MAPK ERK5, but not ERK1/2, inhibits the progression of monocytic phenotype to the functioning macrophage'. *Experimental Cell Research* **330**(1), 199–211.

Waterfield, M. R., M. Zhang, L. P. Norman, and S. C. Sun: 2003, 'NF-κ1/p105 regulates lipopolysaccharide-stimulated MAP kinase signaling by governing the stability and function of the Tpl2 kinase'. *Molecular cell* **11**(3), 685–94.

Watford, W. T., B. D. Hissong, L. R. Durant, H. Yamane, L. M. Muul, Y. Kanno, C. M. Tato, H. L. Ramos, A. E. Berger, L. Mielke, M. Pesu, B. Solomon, D. M. Frucht, W. E. Paul, A. Sher, D. Jankovic, P. N. Tsichlis, and J. J. O'Shea: 2008, 'Tpl2 kinase regulates T cell interferon-gamma production and host resistance to Toxoplasma gondii'. *The Journal of Experimental Medicine* **205**(12), 2803–12.

Weintz, G., J. V. Olsen, K. Fruhauf, M. Niedzielska, I. Amit, J. Jantsch, J. Mages, C. Frech, L. Dolken, M. Mann, and R. Lang: 2010, 'The phosphoproteome of toll-like receptor-activated macrophages'. *Molecular Systems Biology* **6**, 371.

Weischenfeldt, J. and B. Porse: 2008, 'Bone Marrow-Derived Macrophages (BMM): Isolation and Applications'. *Cold Spring Harbor Protocols* **3**(12), 1–6.

Wesche, H., W. J. Henzel, W. Shillinglaw, S. Li, and Z. Cao: 1997, 'MyD88: An Adapter That Recruits IRAK to the IL-1 Receptor Complex'. *Immunity* **7**(6), 837–847.

Wiese, S., K. A. Reidegeld, H. E. Meyer, and B. Warscheid: 2007, 'Protein labeling by iTRAQ: A new tool for quantitative mass spectrometry in proteome research'. *Proteomics* **7**(3), 340–350.

Wu, B., P. Jiang, Y. Mu, and R. C. Wilmouth: 2009, 'Cancer Osaka thyroid (Cot) phosphorylates Polo-like kinase (PLK1) at Ser137 but not at Thr210'. *Biological chemistry* **390**(12), 1271–7.

Wu, J., Q. Shakey, W. Liu, A. Schuller, and M. T. Follettie: 2007, 'Global Profiling of Phosphopeptides by Titania Affinity Enrichment'. *Journal of Proteome Research* **6**(12), 4684–4689.

Wynn, T. A., A. Chawla, and J. W. Pollard: 2013, 'Macrophage biology in development, homeostasis and disease'. *Nature* **496**(7446), 445–55.

Xue, J., S. V. Schmidt, J. Sander, A. Draffehn, W. Krebs, I. Quester, D. De Nardo, T. D. Gohel, M. Emde, L. Schmidleithner, H. Ganesan, A. Nino-Castro, M. R.

Mallmann, L. Labzin, H. Theis, M. Kraut, M. Beyer, E. Latz, T. C. Freeman, T. Ulas, and J. L. Schultze: 2014, 'Transcriptome-Based Network Analysis Reveals a Spectrum Model of Human Macrophage Activation'. *Immunity* **40**(2), 274–288.

Yagasaki, Y., T. Sudo, and H. Osada: 2004, 'Exip, a splicing variant of p38α, participates in interleukin-1 receptor proximal complex and downregulates NF-κB pathway'. *FEBS Letters* **575**(1-3), 136–140.

Yamamoto, M., S. Sato, K. Mori, K. Hoshino, O. Takeuchi, K. Takeda, and S. Akira: 2002, 'Cutting Edge: A Novel Toll/IL-1 Receptor Domain-Containing Adapter That Preferentially Activates the IFN- Promoter in the Toll-Like Receptor Signaling'. *The Journal of Immunology* **169**(12), 6668–6672.

Yang, H.-T., S. Papoutsopoulou, M. Belich, C. Brender, J. Janzen, T. Gantke, M. Handley, and S. C. Ley: 2012, 'Coordinate Regulation of TPL-2 and NF-B Signaling in Macrophages by NF- B1 p105'. *Molecular and Cellular Biology* **32**(17), 3438–3451.

Yang, H. T., Y. Wang, X. Zhao, E. Demissie, S. Papoutsopoulou, A. Mambole, A. O'Garra, M. F. Tomczak, S. E. Erdman, J. G. Fox, S. C. Ley, and B. H. Horwitz: 2011, 'NF-κB1 inhibits TLR-induced IFN-β production in macrophages through TPL-2-dependent ERK activation'. *Journal of immunology* **186**(4), 1989–96.

Yang, Z., B. B. Kahn, H. Shi, and B.-z. Xue: 2010, 'Macrophage alpha 1 AMP-activated Protein Kinase (alpha1AMPK) Antagonizes Fatty Acid-induced Inflammation through SIRT1'. *Journal of Biological Chemistry* **285**(25), 19051–19059.

Ye, X., B. Luke, T. Andresson, and J. Blonder: 2009, '18O Stable Isotope Labeling in MS-based Proteomics'. *Briefings in Functional Genomics and Proteomics* **8**(2), 136–144.

Yu, Y., S. O. Yoon, G. Poulogiannis, Q. Yang, X. M. Ma, J. Villen, N. Kubica, G. R. Hoffman, L. C. Cantley, S. P. Gygi, and J. Blenis: 2011, 'Phosphoproteomic analysis identifies Grb10 as an mTORC1 substrate that negatively regulates insulin signaling'. *Science* **332**(6035), 1322–6.

Zarei, M., A. Sprenger, F. Metzger, C. Gretzmeier, and J. Dengjel: 2011, 'Comparison of ERLIC-TiO2, HILIC-TiO2, and SCX-TiO2 for global phosphoproteomics approaches'. *Journal of proteome research* **10**(8), 3474–83.

Zhang, C., D. M. Kenski, J. L. Paulson, A. Bonshtien, G. Sessa, J. V. Cross, D. J. Templeton, and K. M. Shokat: 2005, 'A second-site suppressor strategy for chemical genetic analysis of diverse protein kinases'. *Nature methods* **2**(6), 435–41.

Zhang, J., B. Shen, and A. Lin: 2007, 'Novel strategies for inhibition of the p38 MAPK pathway'. *Trends in Pharmacological Sciences* **28**(6), 286–295.

Zhong, H., R. E. Voll, and S. Ghosh: 1998, 'Phosphorylation of NF-κB p65 by PKA Stimulates Transcriptional Activity by Promoting a Novel Bivalent Interaction with the Coactivator CBP/p300'. *Molecular Cell* **1**, 611–671.

Zhou, H., T. Y. Low, M. L. Hennrich, H. van der Toorn, T. Schwend, H. Zou, S. Mohammed, and A. J. Heck: 2011, 'Enhancing the Identification of Phosphopeptides from Putative Basophilic Kinase Substrates Using Ti (IV) Based IMAC Enrichment'. *Molecular & Cellular Proteomics : MCP* **10**(10), 1–14.

Zhu, H., M. Bilgin, R. Bangham, D. Hall, A. Casamayor, P. Bertone, N. Lan, R. Jansen, S. Bidlingmaier, T. Houfek, T. Mitchell, P. Miller, R. A. Dean, M. Gerstein, and M. Snyder: 2001, 'Global Analysis of Protein Activities Using Proteome Chips'. *Science* **293**(5537), 2101–2105.

Zhu, H., S. Pan, S. Gu, E. M. Bradbury, and X. Chen: 2002, 'Amino acid residue specific stable isotope labeling for quantitative proteomics.'. *Rapid communications in mass spectrometry : RCM* **16**(22), 2115–2123.

Appendices

A MAP kinase activation in SILAC-labelled BMDM lysates for phosphoproteomics.

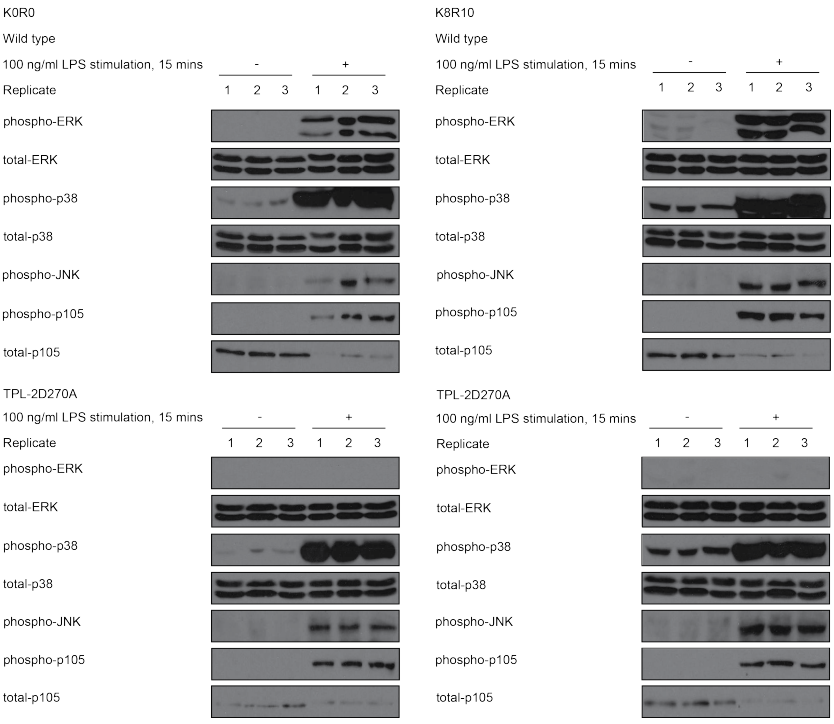

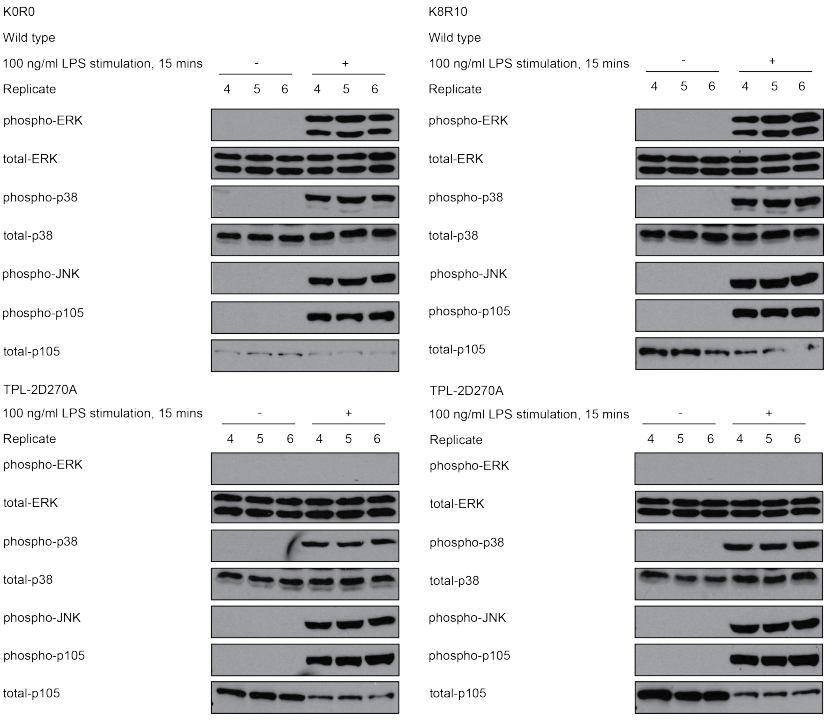

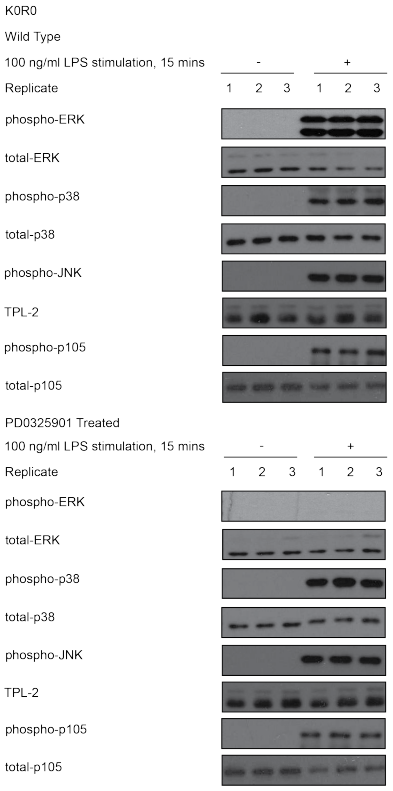
K0R0
Wild Type
100 ng/ml LPS stimulation, 15 mins
- +
Replicate
1 2 3 1 2 3
phospho-ERK
total-ERK
phospho-p38
total-p38
phospho-JNK
TPL-2
phospho-p105
total-p105
PD0325901 Treated
100 ng/ml LPS stimulation, 15 mins
- +
Replicate
1 2 3 1 2 3
phospho-ERK
total-ERK
phospho-p38
total-p38
phospho-JNK
TPL-2
phospho-p105
total-p105

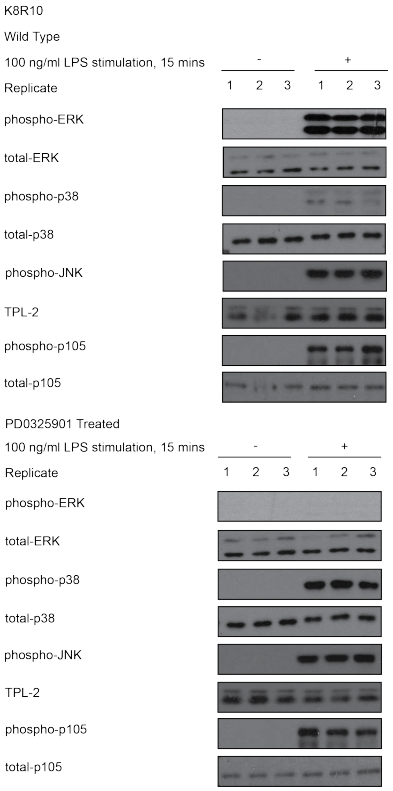
K8R10
Wild Type
100 ng/ml LPS stimulation, 15 mins
- +
Replicate
1 2 3 1 2 3
phospho-ERK
total-ERK
phospho-p38
total-p38
phospho-JNK
TPL-2
phospho-p105
total-p105
PD0325901 Treated
100 ng/ml LPS stimulation, 15 mins
- +
Replicate
1 2 3 1 2 3
phospho-ERK
total-ERK
phospho-p38
total-p38
phospho-JNK
TPL-2
phospho-p105
total-p105

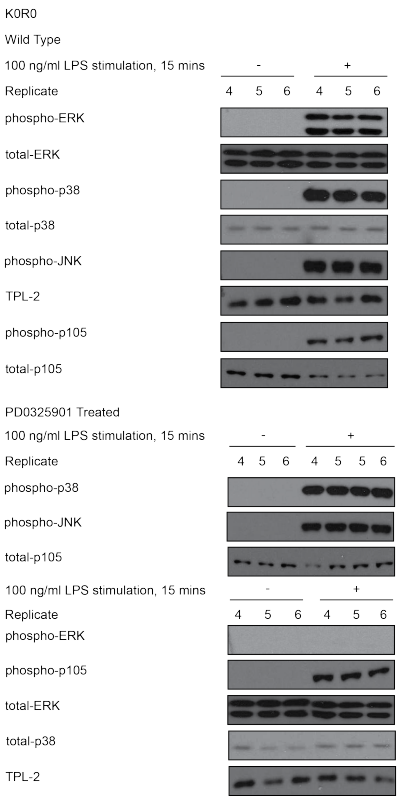
K0R0
Wild Type
100 ng/ml LPS stimulation, 15 mins
- +
Replicate
4 5 6 4 5 6
phospho-ERK
total-ERK
phospho-p38
total-p38
phospho-JNK
TPL-2
phospho-p105
total-p105
PD0325901 Treated
100 ng/ml LPS stimulation, 15 mins
- +
Replicate
4 5 6 4 5 5 6
phospho-p38
phospho-JNK
total-p105
100 ng/ml LPS stimulation, 15 mins
- +
Replicate
4 5 6 4 5 6
phospho-ERK
phospho-p105
total-ERK
total-p38
TPL-2

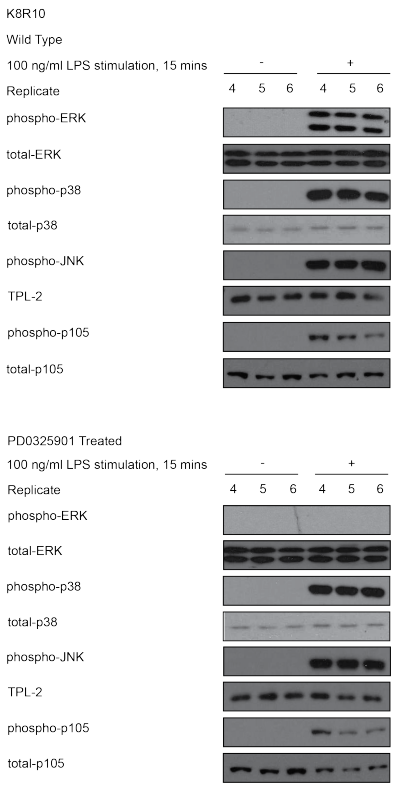
K8R10
Wild Type
100 ng/ml LPS stimulation, 15 mins
- +
Replicate
4 5 6 4 5 6
phospho-ERK
total-ERK
phospho-p38
total-p38
phospho-JNK
TPL-2
phospho-p105
total-p105
PD0325901 Treated
100 ng/ml LPS stimulation, 15 mins
- +
Replicate
4 5 6 4 5 6
phospho-ERK
total-ERK
phospho-p38
total-p38
phospho-JNK
TPL-2
phospho-p105
total-p105

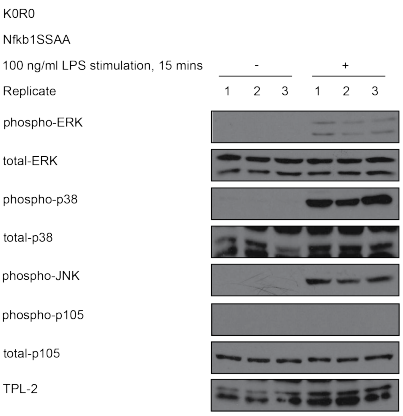
K0R0
Nfkb1SSAA
100 ng/ml LPS stimulation, 15 mins
-
+
Replicate
1 2 3 1 2 3
phospho-ERK
total-ERK
phospho-p38
total-p38
phospho-JNK
phospho-p105
total-p105
TPL-2

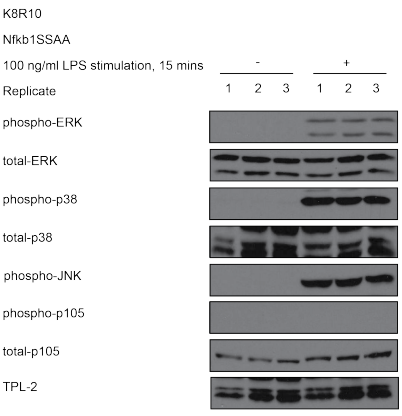
K8R10
Nfkb1SSAA
100 ng/ml LPS stimulation, 15 mins
-
+
Replicate
1 2 3 1 2 3
phospho-ERK
total-ERK
phospho-p38
total-p38
phospho-JNK
phospho-p105
total-p105
TPL-2

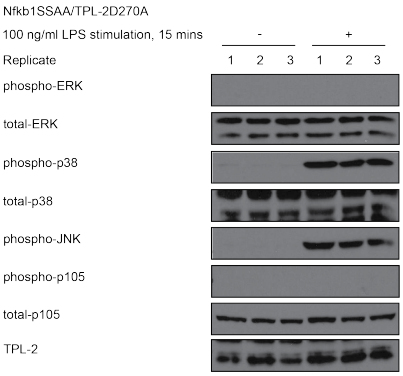
Nfkb1SSAA/TPL-2D270A
100 ng/ml LPS stimulation, 15 mins
-
+
Replicate
1 2 3 1 2 3
phospho-ERK
total-ERK
phospho-p38
total-p38
phospho-JNK
phospho-p105
total-p105
TPL-2

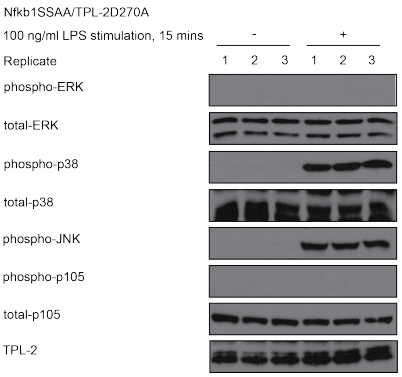
Nfkb1SSAA/TPL-2D270A
100 ng/ml LPS stimulation, 15 mins
-
+
Replicate
1 2 3 1 2 3
phospho-ERK
total-ERK
phospho-p38
total-p38
phospho-JNK
phospho-p105
total-p105
TPL-2

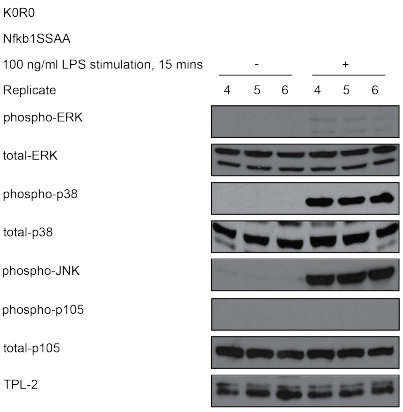
K0R0
Nfkb1SSAA
100 ng/ml LPS stimulation, 15 mins
-
+
Replicate
4 5 6 4 5 6
phospho-ERK
total-ERK
phospho-p38
total-p38
phospho-JNK
phospho-p105
total-p105
TPL-2

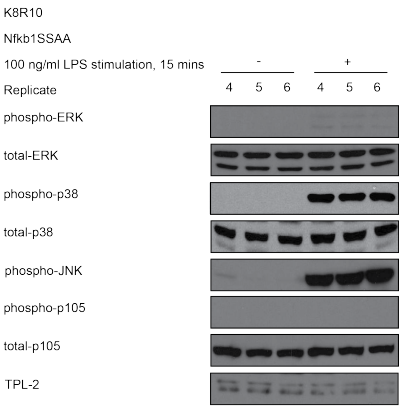
K8R10
Nfkb1SSAA
100 ng/ml LPS stimulation, 15 mins
-
+
Replicate
4 5 6 4 5 6
phospho-ERK
total-ERK
phospho-p38
total-p38
phospho-JNK
phospho-p105
total-p105
TPL-2

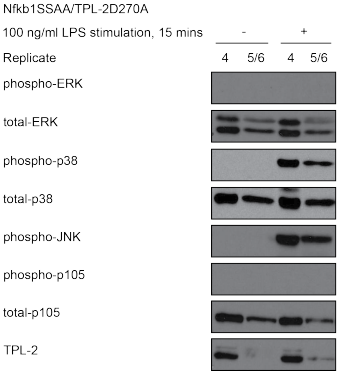
Nfkb1SSAA/TPL-2D270A
100 ng/ml LPS stimulation, 15 mins
-
+
Replicate
4 5/6 4 5/6
phospho-ERK
total-ERK
phospho-p38
total-p38
phospho-JNK
phospho-p105
total-p105
TPL-2

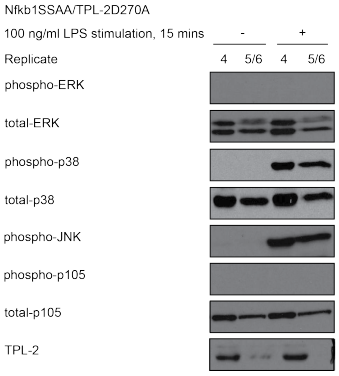
Nfkb1SSAA/TPL-2D270A
100 ng/ml LPS stimulation, 15 mins
-
+
Replicate
4 5/6 4 5/6
phospho-ERK
total-ERK
phospho-p38
total-p38
phospho-JNK
phospho-p105
total-p105
TPL-2

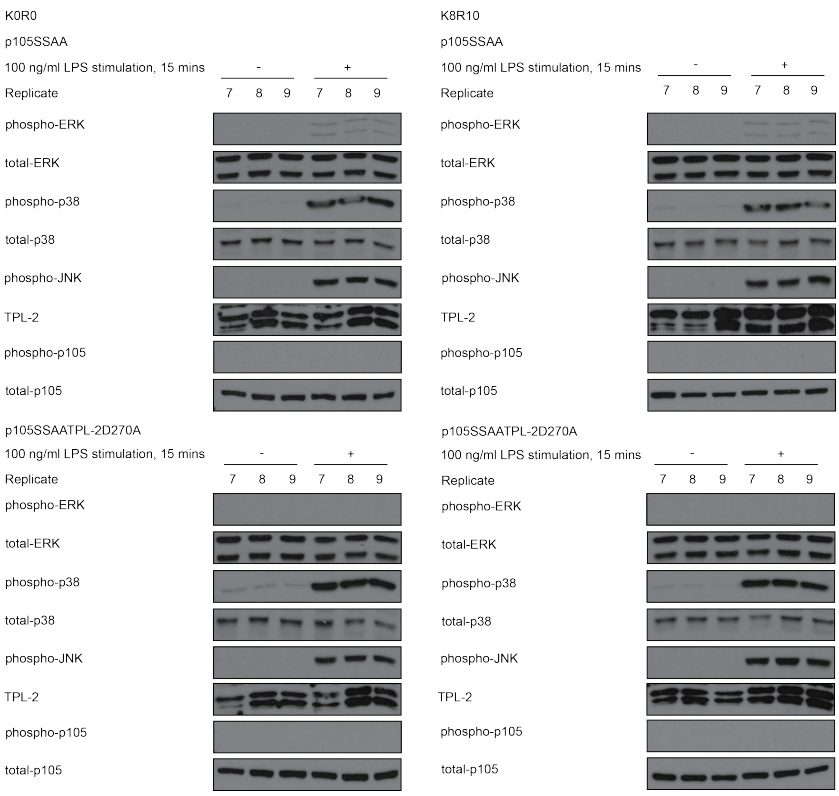
K0R0
p105SSAA
100 ng/ml LPS stimulation, 15 mins
-
+
Replicate
7 8 9 7 8 9
phospho-ERK
total-ERK
phospho-p38
total-p38
phospho-JNK
TPL-2
phospho-p105
total-p105
K8R10
p105SSAA
100 ng/ml LPS stimulation, 15 mins
-
+
Replicate
7 8 9 7 8 9
phospho-ERK
total-ERK
phospho-p38
total-p38
phospho-JNK
TPL-2
phospho-p105
total-p105
p105SSAATPL-2D270A
100 ng/ml LPS stimulation, 15 mins
-
+
Replicate
7 8 9 7 8 9
phospho-ERK
total-ERK
phospho-p38
total-p38
phospho-JNK
TPL-2
phospho-p105
total-p105
p105SSAATPL-2D270A
100 ng/ml LPS stimulation, 15 mins
-
+
Replicate
7 8 9 7 8 9
phospho-ERK
total-ERK
phospho-p38
total-p38
phospho-JNK
TPL-2
phospho-p105
total-p105

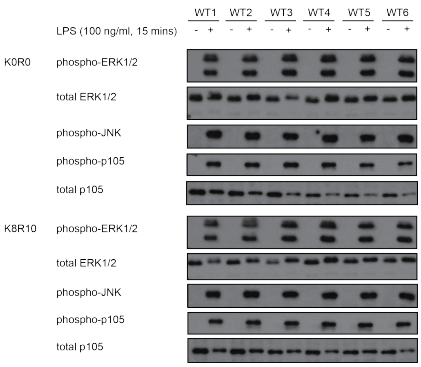
WT1 WT2 WT3 WT4 WT5 WT6
LPS (100 ng/ml, 15 mins)
- + - + - + - + - + - +
K0R0
phospho-ERK1/2
total ERK1/2
phospho-JNK
phospho-p105
total p105
K8R10
phospho-ERK1/2
total ERK1/2
phospho-JNK
phospho-p105
total p105

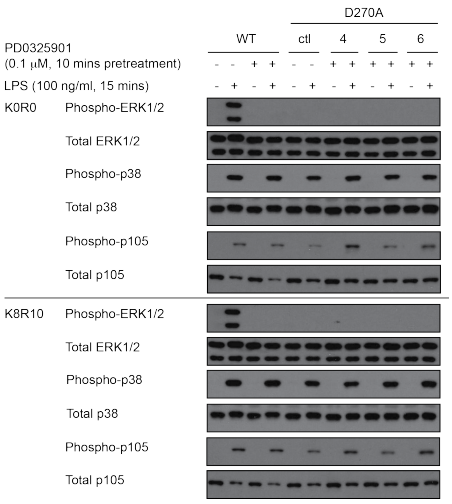
D270A
WT
ctl
4
5
6
PD0325901
(0.1 μM, 10 mins pretreatment)
- - + + - - + + + + + +
LPS (100 ng/ml, 15 mins)
- + - + - + - + - + - +
K0R0
Phospho-ERK1/2
Total ERK1/2
Phospho-p38
Total p38
Phospho-p105
Total p105
K8R10
Phospho-ERK1/2
Total ERK1/2
Phospho-p38
Total p38
Phospho-p105
Total p105

B Total protein levels of TPL-2 dependent phosphorylations.

Ratios have not been inverted for one of each label reversal pair, as they have for the presented phosphoproteomics data.

Arg1

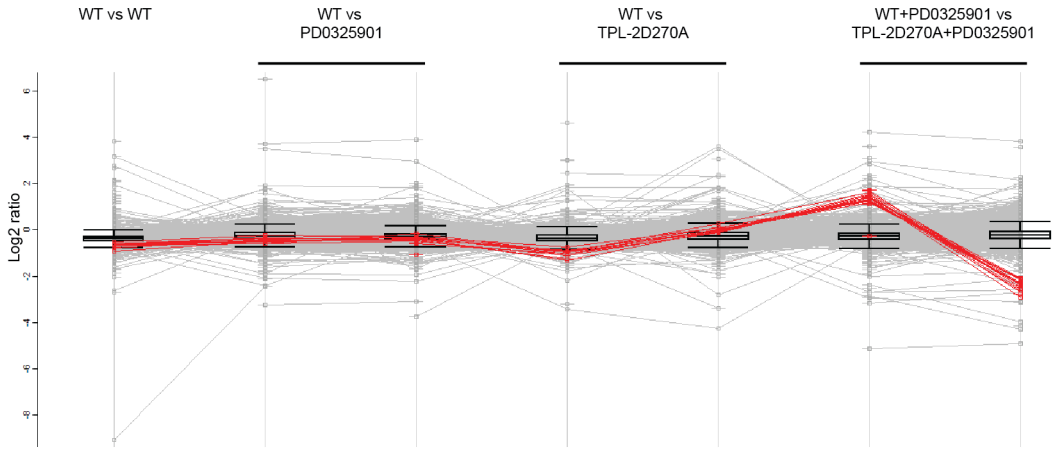

Hsp90b1

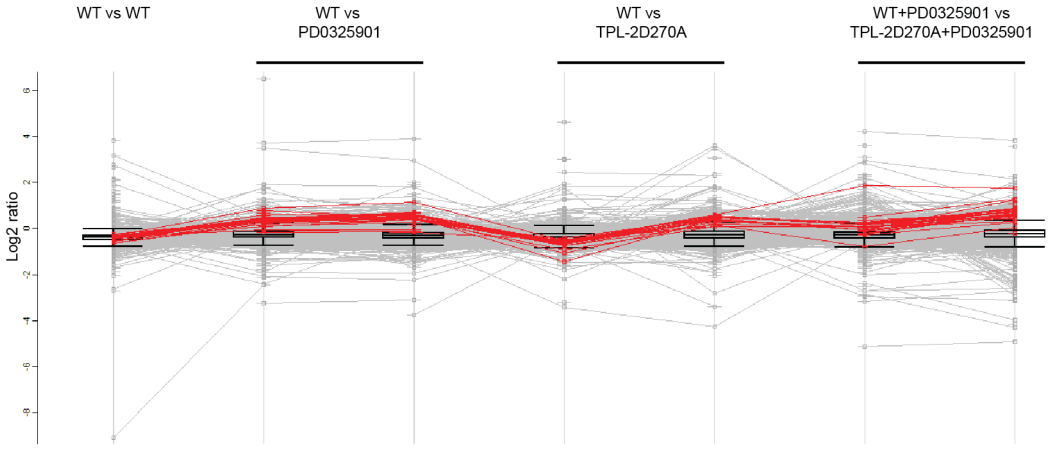

Fermt3, Hist1h1c, Luc7l2, Map2k1/2

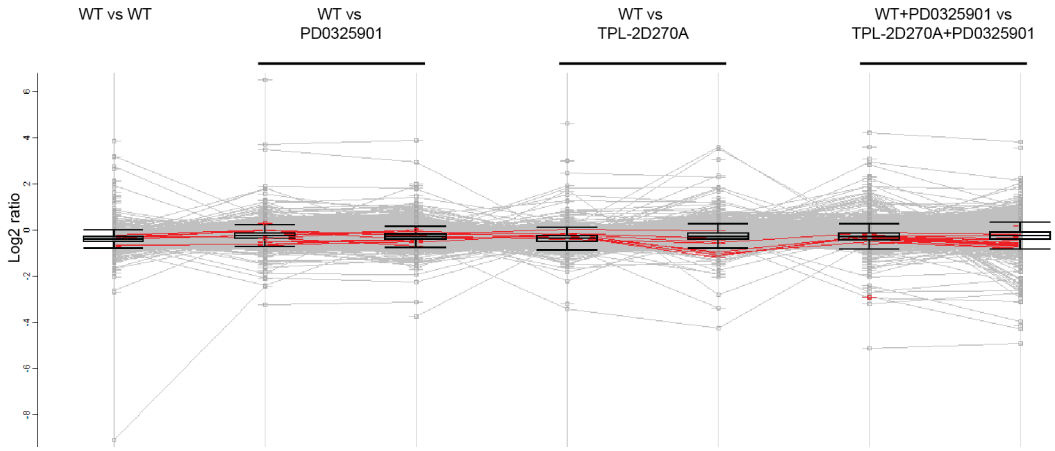

C TPL-2/ERK1/2 regulated phosphosites identified by phosphoproteomics.

Gene names	Position	Known ERK1/2 target	Ratio WT vs WT	Ratio WT vs PD0325901	Ratio WT vs PD0325901	Ratio WT vs D270A	Ratio WT vs D270A	Ratio WT+ PD0325901 vs D270A+ PD0325901	Ratio WT+ PD0325901 vs D270A+ PD0325901	Localization probabil-ity	PEP
2410018M08Rik	S45		-0.51	-0.83	-1.27	-1.01	-1.61	0.39	-0.28	1	1.11E-64
3110043O21Rik	S9		-0.36	2.64	1.77	3.32	2.29	0.90	0.33	1	5.15E-18
Add1	S12		-0.18	1.39	0.87	1.46	1.21	0.15	-0.28	1	5.92E-107
Agfg1	S167		-0.77	-0.91	-1.43	-1.58	-2.85	0.42	-0.29	0.99	3.90E-104
Ahnak	S4879	+	-0.22	2.12	1.19	1.88	1.52	0.53	-0.06	1	7.80E-97
Ahnak	S2985		-0.31	1.45	0.48	1.38	0.99	0.75	-0.03	1	6.66E-71
Ahnak	S5555		-0.33	-1.80	-2.20	-2.35	-2.83	0.27	-0.27	1	4.92E-55
Ahnak	S5557		NaN	-1.88	-2.32	-2.28	-2.85	0.46	-0.37	1	4.92E-55
Ahnak	T5590		-0.14	-0.61	-1.14	-1.46	-1.49	-0.25	-0.69	1	6.37E-07
Ahnak	S5099		-0.18	-0.60	-1.13	-0.65	-1.35	0.24	-0.13	0.99	7.87E-89
Ahnak	S5098		-0.40	-0.73	-1.14	-0.73	-1.34	0.21	-0.06	0.90	6.09E-14
Ahnak2	S1458		-0.40	1.82	0.72	1.89	1.12	0.62	-0.35	1	1.55E-15
Als2	S486		-0.50	-0.59	-0.85	-0.54	-1.11	0.31	-0.09	1	8.14E-190

Gene names	Position	Known ERK1/2 target	Ratio WT vs WT	Ratio WT vs PD0325901	Ratio WT vs PD0325901	Ratio WT vs D270A	Ratio WT vs D270A	Ratio WT+ PD0325901 vs D270A+ PD0325901	Ratio WT+ PD0325901 vs D270A+ PD0325901	Localization probabil-ity	PEP
Ankle2	S820		-0.19	1.94	1.61	2.28	1.96	NaN	NaN	1	3.19E-255
Anks1	S461		-0.33	1.66	0.91	1.99	1.34	0.70	0.19	1	2.11E-17
Ap3d1	S760		-0.63	-1.69	-2.06	-2.18	-3.44	0.21	-0.42	1	1.75E-293
Ap3d1	T758		-0.66	-1.71	-1.68	-2.21	-2.40	0.15	-0.29	1	9.70E-142
Apbb1ip	S532		-0.24	1.69	0.61	1.40	1.19	0.58	-0.07	1	4.04E-236
Apbb1ip	S537		-0.46	-1.16	-1.53	-1.14	-1.84	0.44	-0.34	1	5.64E-182
Arfgap3	S458		0.02	2.93	2.12	NaN	2.40	NaN	NaN	0.88	2.28E-131
Arhgap10	S719		NaN	2.58	1.06	NaN	NaN	0.26	-0.32	0.67	3.16E-07
Arhgap17	S700		NaN	2.84	1.28	NaN	NaN	1.10	-0.34	0.90	2.13E-49
Arhgap25	S534		-0.12	2.78	1.95	1.60	2.10	0.29	-0.51	1	2.00E-143
Arhgap27	S195		-0.26	2.22	1.63	3.48	NaN	NaN	-0.07	1	7.46E-65
Arhgap30	S669		-0.58	1.74	0.74	2.02	1.15	0.71	-0.07	0.89	4.03E-79
Arhgap31	S1355		NaN	-0.47	-0.98	NaN	NaN	0.16	-0.50	1	4.31E-17

Gene names	Position	Known ERK1/2 target	Ratio WT vs WT	Ratio WT vs PD0325901	Ratio WT vs PD0325901	Ratio WT vs D270A	Ratio WT vs D270A	Ratio WT+ PD0325901 vs D270A+ PD0325901	Ratio WT+ PD0325901 vs D270A+ PD0325901	Localization probabil-ity	PEP
Arhgap31	S1359		NaN	-0.50	-0.98	NaN	NaN	0.24	-0.50	0.93	4.31E-17
Arhgap5	S1203		NaN	-1.46	-1.68	-2.18	-2.10	0.32	-0.20	1	1.01E-14
Arhgef6	S663		-0.15	2.34	1.33	2.51	2.12	0.61	-0.07	1	8.93E-23
Arhgef7	S673		-0.37	2.57	1.52	2.87	1.50	0.76	-0.08	1	8.06E-23
Aspscr1	S279		-0.34	2.58	1.83	2.50	2.02	0.84	0.01	1	2.35E-146
Atrx	T1218		NaN	-0.54	-3.65	NaN	NaN	0.19	-0.47	0.86	3.93E-09
Atxn1	S62		-0.21	3.00	2.27	3.24	2.65	0.59	0.08	1	5.71E-52
Atxn2	S593		NaN	-0.85	-1.14	NaN	NaN	0.22	-0.29	1	4.24E-35
Bad	S111		-0.52	1.61	0.72	1.51	1.26	NaN	NaN	0.69	2.63E-60
Bcl3	S362		0.02	1.97	1.74	2.61	2.47	NaN	NaN	0.89	9.24E-117
Bmp2k	S908		-0.20	1.33	0.85	1.59	1.57	0.21	-0.05	1	1.39E-145
Braf	S134		-0.34	1.66	0.87	1.73	0.87	0.64	-0.15	1	6.00E-43
Brd8	S268		-0.30	1.29	0.56	1.50	0.90	-0.03	-0.44	1	1.42E-10

Gene names	Position	Known ERK1/2 target	Ratio WT vs WT	Ratio WT vs PD0325901	Ratio WT vs PD0325901	Ratio WT vs D270A	Ratio WT vs D270A	Ratio WT+ PD0325901 vs D270A+ PD0325901	Ratio WT+ PD0325901 vs D270A+ PD0325901	Localization probabil-ity	PEP
Bsn	S2858		-0.60	-0.84	-1.40	-0.89	NaN	0.28	-0.16	0.88	3.93E-61
Bsn	S2860		-0.44	-0.59	-1.84	-0.88	-1.82	0.32	0.03	1	3.93E-61
Cast	S466		-0.46	1.78	0.94	1.75	1.09	0.64	-0.27	0.74	5.64E-25
Cast	T467		-0.27	1.53	0.68	1.91	1.08	0.62	-0.12	0.98	1.06E-24
Cbx3	93		-0.49	1.44	0.46	1.50	1.14	NaN	NaN	1	1.80E-76
Ccdc88b	S1354		-0.11	-0.63	-1.13	-1.41	NaN	-0.22	-0.61	1	9.02E-72
Cdc42ep3	S100		-0.06	2.09	0.97	2.12	NaN	0.64	-0.47	1	1.76E-211
Cep170	S1260		-0.05	1.42	0.69	1.58	1.83	0.73	0.19	1	2.06E-43
Chn2	S181		-0.28	2.55	1.51	3.08	1.45	1.09	0.20	1	3.77E-59
Cic	S2284		-0.91	-2.94	-3.88	-3.48	-4.34	0.21	-0.73	0.98	1.18E-36
Cic	S1644		-0.17	2.28	1.63	2.48	1.92	0.30	-0.15	1	3.67E-26
Cic	T1489		-0.26	2.77	1.62	1.74	1.79	NaN	NaN	0.97	1.88E-23
Cux1	S1212		NaN	-1.46	-1.67	-1.67	NaN	0.34	-0.56	0.99	3.12E-24

Gene names	Position	Known ERK1/2 target	Ratio WT vs WT	Ratio WT vs PD0325901	Ratio WT vs PD0325901	Ratio WT vs D270A	Ratio WT vs D270A	Ratio WT+ PD0325901 vs D270A+ PD0325901	Ratio WT+ PD0325901 vs D270A+ PD0325901	Localization probabil-ity	PEP
Dab2	S325		-0.16	1.31	0.57	1.27	1.19	-0.31	0.21	1	1.86E-58
Dab2	S759		-0.44	1.79	0.58	1.80	1.10	0.60	-0.28	1	8.95E-55
Dab2	S32		-0.55	3.47	1.72	4.00	1.95	NaN	NaN	1	1.20E-37
Dbndd2	S117		NaN	-0.70	-1.28	NaN	-2.31	0.10	-0.44	1	1.39E-24
Ddi2	S194		-0.14	3.67	1.76	3.66	3.24	0.75	0.25	1	2.69E-95
Dennd1b	S494		-0.47	1.68	0.79	NaN	NaN	NaN	NaN	1	0
Dennd4a	S1282		-0.20	1.99	1.31	2.21	NaN	NaN	NaN	0.85	2.66E-08
Dennd4c	S1289		-0.23	1.68	1.17	1.85	1.47	0.32	-0.02	1	1.07E-285
Dennd4c	S1310		-0.29	1.33	0.68	1.31	1.07	0.42	-0.29	1	3.80E-23
Dennd4c	S1107		NaN	2.01	1.11	NaN	NaN	0.44	-0.79	0.99	3.15E-125
Dido1	S657		-0.15	2.15	1.00	1.91	1.50	0.68	-0.73	1	1.00E-26
Dnajc12	S166		-0.35	2.09	1.23	NaN	1.17	0.41	NaN	1	5.44E-36
Dock7	S2119		-0.60	-0.64	-1.21	-0.68	-1.27	0.39	-0.34	1	1.82E-47

Gene names	Position	Known ERK1/2 target	Ratio WT vs WT	Ratio WT vs PD0325901	Ratio WT vs PD0325901	Ratio WT vs D270A	Ratio WT vs D270A	Ratio WT+ PD0325901 vs D270A+ PD0325901	Ratio WT+ PD0325901 vs D270A+ PD0325901	Localization probabil-ity	PEP
Dopey2	S719		-0.07	1.70	1.30	1.80	1.44	0.46	-0.08	0.98	4.02E-12
Dr1	S105		NaN	2.13	1.40	NaN	NaN	0.62	-0.61	1	9.05E-16
Dync1i2	S81	+	-0.35	3.64	0.81	2.15	1.32	0.82	0.07	1	1.16E-110
Dync1i2	S15		-0.29	1.60	0.92	2.11	1.28	0.78	0.06	1	4.64E-10
Dync1li1	S412		-0.02	1.63	0.64	3.06	2.34	0.83	0.17	1	1.40E-154
Dync1li2	S203		-0.45	2.29	1.72	2.52	NaN	NaN	NaN	0.76	3.61E-30
Eef2k	S469		-0.58	2.10	0.90	2.32	NaN	0.80	-0.38	1	4.43E-54
Eif4b	S422		-0.35	2.18	1.19	2.25	1.33	0.61	-0.28	1	4.58E-281
Eif4b	S424		-0.24	1.93	1.29	1.99	1.53	NaN	NaN	0.98	1.47E-157
Eif4g2	S394		-0.40	-0.66	-0.90	-0.68	-1.44	0.30	-0.37	1	3.79E-252
Eif4g2	T384		-0.72	-0.46	-1.24	-0.47	-1.88	0.51	-0.45	0.94	9.24E-42
Etv3	S139	+	-0.06	1.97	0.83	1.53	1.67	0.62	-0.08	1	3.00E-44
Etv3	S132		-0.81	3.88	2.67	NaN	NaN	NaN	NaN	0.89	4.66E-44

Gene names	Position	Known ERK1/2 target	Ratio WT vs WT	Ratio WT vs PD0325901	Ratio WT vs PD0325901	Ratio WT vs D270A	Ratio WT vs D270A	Ratio WT+ PD0325901 vs D270A+ PD0325901	Ratio WT+ PD0325901 vs D270A+ PD0325901	Localization probabil-ity	PEP
Etv3	S133		-0.81	3.88	2.67	NaN	NaN	NaN	NaN	0.85	4.66E-44
Exoc7	S250		-0.41	-0.81	-1.10	-0.68	-1.62	0.49	-0.21	1	2.05E-36
Eya3	S210		-0.32	1.96	1.04	2.19	1.82	0.56	-0.61	1	7.00E-81
Eya3	S215		-0.23	2.29	1.20	2.22	1.74	NaN	NaN	1	1.84E-29
Fam129a	S581		-0.44	-0.78	-1.11	-0.76	-1.36	0.41	0.00	1	2.24E-190
Fam129a	S580		-0.24	-0.63	-1.12	-0.74	-1.03	0.34	-0.08	0.93	7.16E-124
Fam193a	S648		-0.27	2.50	1.90	3.02	2.69	0.68	0.38	1	3.38E-26
Fam21	S1137		-0.18	3.12	2.01	2.37	1.63	0.89	0.26	0.90	5.56E-153
Fam21	S866		-0.41	2.42	1.73	1.96	3.89	NaN	0.21	0.84	1.01E-143
Fam21	S867		-0.33	4.19	3.12	4.57	NaN	1.05	NaN	0.95	1.01E-143
Fam21	S1305		-0.05	4.27	1.58	1.85	4.94	NaN	NaN	1	7.37E-109
Fam21	S284		-0.23	2.44	1.11	2.73	1.87	0.49	-0.35	1	1.21E-27
Fam21	S832		-0.18	2.93	2.21	3.41	2.83	0.58	0.28	0.94	5.22E-277

Gene names	Position	Known ERK1/2 target	Ratio WT vs WT	Ratio WT vs PD0325901	Ratio WT vs PD0325901	Ratio WT vs D270A	Ratio WT vs D270A	Ratio WT+ PD0325901 vs D270A+ PD0325901	Ratio WT+ PD0325901 vs D270A+ PD0325901	Localization probabil-ity	PEP
Fam21	T833		-0.34	2.10	1.92	3.60	2.58	0.43	0.04	0.83	5.22E-277
Fam63a	S103		-0.48	1.78	0.73	1.88	1.28	0.56	-0.17	1	6.05E-57
FLJ45252	S115		-0.27	2.14	1.18	2.44	1.79	0.67	-0.33	1	9.43E-114
Fyb	S665		-0.22	4.18	3.02	4.06	3.81	0.99	0.45	0.98	2.48E-178
Fyb	S663		-0.15	2.70	2.70	4.02	2.08	1.01	0.54	1	2.96E-80
Gab2	S532		-0.27	2.40	1.86	2.53	1.99	0.60	0.10	1	6.88E-150
Gab2	S613		-0.48	-0.49	-1.03	-0.65	-1.44	0.46	-0.63	1	3.81E-89
Gab2	S142		0.10	2.56	1.39	2.21	1.62	0.82	-0.16	1	7.11E-77
Gab2	S143		-0.42	2.26	1.31	2.21	1.15	0.59	-0.045	1	7.11E-77
Gab2	S615		-0.46	-0.57	-1.12	-0.62	-1.45	0.32	0.03	0.99	2.13E-08
Gas7	S92		-0.34	1.93	1.22	1.92	1.78	0.41	-0.37	1	1.79E-201
Gatad2b	S339		-0.07	1.44	0.98	1.61	1.77	0.10	0.09	1	3.16E-216
Gch1	S51		-0.00	1.80	1.17	2.15	2.18	1.07	0.53	1	6.08E-25

Gene names	Position	Known ERK1/2 target	Ratio WT vs WT	Ratio WT vs PD0325901	Ratio WT vs PD0325901	Ratio WT vs D270A	Ratio WT vs D270A	Ratio WT+ PD0325901 vs D270A+ PD0325901	Ratio WT+ PD0325901 vs D270A+ PD0325901	Localization probabil-ity	PEP
Gga2	S414		-0.45	1.87	1.57	2.17	1.64	0.11	-0.28	1	1.76E-125
Gga2	S418		-0.28	3.22	3.71	4.83	3.54	0.27	-0.33	1	1.23E-57
Gigyf2	S30	+	-0.29	2.18	1.23	1.79	1.31	0.39	-0.27	1	1.67E-104
Gmip	S479		-0.41	-0.41	-1.05	-0.70	-1.50	0.69	-0.48	1	9.48E-93
Gmip	S365		-0.23	1.40	0.89	2.21	1.62	0.68	NaN	1	2.94E-07
Haus6	S405		-0.49	1.95	0.76	1.95	1.04	0.47	-0.27	1	1.78E-31
Hdgfrp2	S450		-0.39	1.69	0.60	1.77	1.26	0.43	-0.42	1	5.23E-36
Hirip3	S85		-0.44	1.65	0.67	1.57	1.02	NaN	2.78	1	8.58E-06
Hmha1	S875		-0.33	3.99	3.04	3.12	2.78	0.63	-0.06	1	2.46E-131
Hmha1	S591		-0.32	-1.43	-1.94	-1.17	-1.59	0.19	-0.54	1	2.03E-103
Hn1l	S97		-0.32	-0.39	-1.10	-0.45	-0.91	0.41	-0.28	1	3.86E-75
Hnrnpc	S115	+	-0.32	2.67	2.36	3.09	1.90	NaN	NaN	0.97	1.65E-64
Ifit3	S327		0.17	1.83	1.16	2.24	1.84	0.33	-0.27	1	7.24E-262

Gene names	Position	Known ERK1/2 target	Ratio WT vs WT	Ratio WT vs PD0325901	Ratio WT vs PD0325901	Ratio WT vs D270A	Ratio WT vs D270A	Ratio WT+ PD0325901 vs D270A+ PD0325901	Ratio WT+ PD0325901 vs D270A+ PD0325901	Localization probabil-ity	PEP
Ik	S402		0.06	2.79	2.34	3.63	NaN	NaN	NaN	1	7.71E-08
Il16	S838		-0.09	2.57	2.25	3.68	1.02	1.03	0.32	0.84	4.60E-60
Il16	S839		-0.16	3.53	2.28	3.25	2.76	1.04	0.38	0.98	8.85E-08
Iqsec1	S92		-0.20	1.49	1.12	1.67	1.42	0.80	0.52	1	1.16E-108
Irf2bp2	S226		-0.29	2.85	1.90	3.17	2.52	0.75	0.03	1	2.14E-127
Irf2bpl	S69		-0.32	1.99	1.24	1.74	1.69	0.55	-0.36	1	6.84E-20
Itpkb	S28		-0.37	2.53	1.80	3.92	NaN	NaN	NaN	0.99	1.27E-68
Itpkb	S42		-0.54	-1.45	-1.82	-1.66	-2.26	0.03	-0.36	1	7.36E-44
Itpkb	S48		-0.20	2.83	1.94	3.01	2.64	0.54	-0.43	1	7.36E-44
Itpkb	S70		0.23	2.15	1.31	NaN	NaN	0.24	-0.54	1	3.98E-38
Itsn1	S974		-0.33	3.19	1.80	3.14	NaN	0.91	-0.21	0.90	8.21E-196
Kiaa1671	S259		NaN	1.80	1.25	1.92	NaN	-0.05	-0.76	1	3.78E-25
Kiaa1671	S262		NaN	1.80	1.25	1.92	NaN	0.14	-0.50	1	6.32E-10

Gene names	Position	Known ERK1/2 target	Ratio WT vs WT	Ratio WT vs PD0325901	Ratio WT vs PD0325901	Ratio WT vs D270A	Ratio WT vs D270A	Ratio WT+ PD0325901 vs D270A+ PD0325901	Ratio WT+ PD0325901 vs D270A+ PD0325901	Localization probabil-ity	PEP
L3mbtl3	T609		-0.34	1.62	0.87	1.49	1.26	0.38	-0.14	0.99	4.27E-17
Larp1	T278	+	0.01	1.81	1.31	1.71	NaN	0.24	-0.77	1	3.38E-13
Larp4b	S570		-0.24	1.29	0.54	1.55	1.14	0.63	0.01	1	1.26E-261
Lasp1	T104		-0.61	-0.81	-1.22	-1.15	-1.88	0.30	-0.35	1	1.30E-72
Lbh	S63		-0.18	2.55	1.55	3.41	2.41	0.88	-0.72	1	6.06E-124
Lcp1	S5		-0.47	3.20	1.85	3.15	2.07	0.94	0.08	1	0
Lmnb2	S15		-0.07	1.80	0.71	1.83	1.56	-0.00	-0.78	1	4.48E-132
Lrch1	S522		-0.25	1.23	0.64	1.56	1.24	0.38	-0.24	1	2.38E-43
Lrrc16a	T1286		-0.26	2.75	1.44	NaN	NaN	NaN	NaN	1	4.28E-56
Lrrc16a	S1281		-0.12	2.62	1.62	NaN	NaN	0.49	-0.86	0.90	2.85E-44
Lrrc41	S276		-0.34	1.87	1.16	2.01	1.56	NaN	NaN	1	1.28E-82
Lrrfip1	S302		-0.22	1.99	1.09	2.60	2.01	0.74	-0.02	1	1.63E-42
Lrrfip1	S84		-0.02	-0.99	-1.38	-0.77	-1.43	0.19	-0.36	0.97	1.12E-250

Gene names	Position	Known ERK1/2 target	Ratio WT vs WT	Ratio WT vs PD0325901	Ratio WT vs PD0325901	Ratio WT vs D270A	Ratio WT vs D270A	Ratio WT+ PD0325901 vs D270A+ PD0325901	Ratio WT+ PD0325901 vs D270A+ PD0325901	Localization probabil-ity	PEP
Lsp1	S162		-0.93	-1.96	-1.53	-3.10	-4.44	-0.39	-0.79	1	7.29E-217
Lsp1	S168		-0.93	-1.96	-1.53	-3.10	-4.44	-0.39	-0.79	1	7.29E-217
Lsp1	T160		-0.75	-1.99	-1.53	-3.10	-4.24	-0.45	-0.78	1	1.00E-190
Lsp1	T186		NaN	-0.58	-1.93	NaN	NaN	NaN	-0.01	0.76	9.33E-42
Luzp1	S982		-0.20	1.61	0.74	1.99	1.53	0.37	-0.32	1	1.49E-37
Macf1	S1376		-0.12	2.91	2.52	2.86	NaN	0.46	0.17	1	3.81E-127
Mafb	S70		NaN	-1.11	-1.54	NaN	NaN	0.49	-0.01	0.89	2.00E-15
Map3k3	S337		-0.24	1.44	0.64	1.87	1.36	0.93	0.36	1	1.20E-199
Mapk1	Y185	+	-0.23	4.08	2.59	4.66	4.03	0.40	NaN	1	6.62E-25
Mapk1	T183	+	-0.28	3.66	3.10	2.85	3.64	NaN	NaN	1	1.04E-21
Mapk3	T203	+	-0.40	2.85	1.14	4.03	3.24	NaN	NaN	1	1.01E-31
Marcks	S138		-0.12	1.47	0.57	1.53	1.22	0.39	-0.14	1	3.62E-128
Marcks	S112		-0.29	1.77	0.81	1.64	1.59	0.65	0.00	0.86	5.79E-91

Gene names	Position	Known ERK1/2 target	Ratio WT vs WT	Ratio WT vs PD0325901	Ratio WT vs PD0325901	Ratio WT vs D270A	Ratio WT vs D270A	Ratio WT+ PD0325901 vs D270A+ PD0325901	Ratio WT+ PD0325901 vs D270A+ PD0325901	Localization probabil-ity	PEP
Marcks	S113		-0.16	1.84	0.81	1.69	1.57	0.68	-0.01	0.99	5.79E-91
Marcks	T143		-0.32	-0.47	-1.11	-0.76	-1.19	0.19	-0.49	1	1.36E-88
Mark2	S40		-0.27	1.77	1.03	2.07	1.76	0.82	0.19	1	3.82E-61
Mast3	S61		NaN	-2.10	-2.30	-2.02	NaN	0.53	-0.16	0.87	2.20E-09
Mast3	T63		NaN	-2.10	-2.38	NaN	NaN	0.78	-0.16	0.72	2.20E-09
Mast3	S1229		-0.53	-0.87	-1.49	-0.42	-1.31	0.44	-0.11	1	1.29E-07
Matr3	S612		-0.37	-0.79	-1.41	NaN	NaN	0.09	-0.64	1	2.79E-38
Mcrs1	T90		-0.25	2.03	0.94	1.95	1.53	0.33	-0.38	0.98	1.80E-79
Med1	S588		-0.24	1.76	1.02	2.49	1.84	0.23	-0.36	1	4.92E-09
Med1	S596		NaN	1.88	1.13	NaN	NaN	0.23	-0.32	0.98	1.88E-06
Mesdc1	S15		-0.31	2.61	1.01	2.48	1.87	NaN	NaN	1	8.92E-107
Micall2	S733		-0.13	3.00	1.95	3.44	NaN	0.80	NaN	0.95	6.47E-35
Mkl1	S32		-0.36	2.59	1.30	2.12	1.60	0.55	-0.42	1	5.05E-210

Gene names	Position	Known ERK1/2 target	Ratio WT vs WT	Ratio WT vs PD0325901	Ratio WT vs PD0325901	Ratio WT vs D270A	Ratio WT vs D270A	Ratio WT+ PD0325901 vs D270A+ PD0325901	Ratio WT+ PD0325901 vs D270A+ PD0325901	Localization probabil-ity	PEP
Mkl1	S41		-0.37	2.40	1.38	1.99	1.59	0.63	-0.29	1	7.43E-78
Mkl1	S492		-0.68	-0.69	-1.41	-1.40	-2.12	0.36	-0.12	1	7.20E-83
Mkl1	T485		-0.65	-0.85	-1.40	-1.03	-2.30	0.35	-0.13	0.82	7.20E-83
Mkl1	T488		-0.71	-0.69	-1.44	-1.40	-2.03	0.35	-0.11	1	3.79E-68
Mkl2	S77		-0.47	2.77	1.78	2.97	2.33	0.72	-0.32	1	9.94E-20
Mllt4	S1802		-0.17	2.38	1.60	2.00	1.61	0.40	-0.28	1	1.28E-58
Morc2a	S741		-0.68	-1.20	-1.42	-1.55	-2.25	0.24	-0.27	1	3.07E-198
Mtmr1	S47		-0.36	2.39	0.94	1.70	0.99	0.18	-0.21	1	6.47E-19
Nab2	S367		-0.16	3.74	0.99	NaN	3.79	-0.19	-0.46	1	2.49E-13
Nav1	T32		NaN	-1.60	-1.83	-2.07	NaN	0.19	-0.17	1	3.74E-11
Ncbp1	S22		-0.39	2.40	1.54	2.54	1.64	0.53	-0.15	1	4.59E-34
Nck1	S91		NaN	-1.49	-2.42	-1.70	-2.40	0.76	-0.39	1	2.82E-39
Ncor2	S1781		NaN	-1.13	-1.14	NaN	-1.55	0.05	-0.29	0.91	3.64E-153

Gene names	Position	Known ERK1/2 target	Ratio WT vs WT	Ratio WT vs PD0325901	Ratio WT vs PD0325901	Ratio WT vs D270A	Ratio WT vs D270A	Ratio WT+ PD0325901 vs D270A+ PD0325901	Ratio WT+ PD0325901 vs D270A+ PD0325901	Localization probabil-ity	PEP
Nfatc2	S270		-0.76	-0.95	-1.57	-0.52	-1.53	0.60	-0.28	1	2.72E-52
Nfatc2	S274		-0.49	-0.87	-1.61	-0.41	-1.49	0.57	0.08	1	6.45E-20
Nop56	T546		-0.29	2.02	0.51	1.77	1.15	0.38	-0.14	1	1.55E-203
Numa1	S1974		-0.17	1.54	1.17	1.95	1.60	-0.24	-0.21	1	9.14E-70
Nup153	S339		-0.16	1.70	0.82	1.32	1.37	0.48	-0.16	1	1.42E-102
Oxr1	S194		-0.40	1.61	0.72	1.84	1.29	0.93	0.21	1	0
Oxr1	S195		-0.44	2.26	1.44	2.71	1.81	1.08	0.51	1	9.83E-191
Oxsr1	S359		-0.21	1.94	1.05	1.40	1.47	0.70	-0.02	1	1.27E-07
Palld	S901		-0.38	2.38	1.66	2.96	NaN	NaN	0.02	1	8.13E-53
Parp4	S1266		-0.26	3.35	2.39	2.99	2.50	0.86	0.12	1	7.43E-20
Parp4	S1683		-0.05	1.29	0.66	1.36	1.53	0.25	-0.24	1	4.94E-06
Parp9	S42		-0.29	2.25	1.77	2.45	2.14	0.91	0.54	1	5.12E-19
Pcm1	S1332		-0.11	2.01	1.56	1.85	1.14	-0.08	-0.19	1	3.15E-27

Gene names	Position	Known ERK1/2 target	Ratio WT vs WT	Ratio WT vs PD0325901	Ratio WT vs PD0325901	Ratio WT vs D270A	Ratio WT vs D270A	Ratio WT+ PD0325901 vs D270A+ PD0325901	Ratio WT+ PD0325901 vs D270A+ PD0325901	Localization probabil-ity	PEP
Pdcd4	S76		-0.33	2.29	1.58	1.19	1.76	NaN	NaN	1	2.58E-142
Pds5a	S1274		-0.22	2.49	1.86	NaN	2.08	0.48	-0.26	1	1.23E-44
Phf2	S622		-0.32	2.25	1.40	2.60	2.11	0.25	-0.28	1	1.01E-06
Phf2	S899		NaN	2.54	1.45	NaN	NaN	0.11	-0.66	1	3.63E-57
Phf3	S1127		NaN	2.09	1.77	2.32	NaN	0.21	-0.47	0.99	2.22E-66
Phf3	S1909		-0.37	1.92	1.30	1.82	1.31	0.22	-0.06	1	1.89E-08
Phf6	S225		-0.33	2.92	1.71	2.59	0.91	NaN	NaN	1	8.49E-17
Phip	S674		0.05	2.54	0.69	2.57	3.29	0.07	-0.28	1	3.11E-64
Pi4ka	T197		NaN	-1.11	-1.93	NaN	NaN	0.43	NaN	0.99	1.74E-59
Pi4ka	S201		-0.26	1.74	0.77	1.37	NaN	0.49	NaN	0.99	5.08E-56
Pi4ka	S198		NaN	-1.13	-1.47	NaN	NaN	0.44	-0.45	1	1.86E-45
Pi4ka	S202		-0.14	1.53	0.80	2.19	1.06	0.48	-0.33	0.99	6.48E-38
Pid1	S202		-0.31	1.56	0.75	NaN	NaN	0.40	-0.07	0.97	0

Gene names	Position	Known ERK1/2 target	Ratio WT vs WT	Ratio WT vs PD0325901	Ratio WT vs PD0325901	Ratio WT vs D270A	Ratio WT vs D270A	Ratio WT+ PD0325901 vs D270A+ PD0325901	Ratio WT+ PD0325901 vs D270A+ PD0325901	Localization probabil-ity	PEP
Pik3c2a	S261		-0.15	1.62	1.23	1.65	1.54	0.59	0.38	1	5.07E-22
Pip4k2b	S17		0.06	2.68	1.85	2.76	2.25	-0.08	-0.28	0.96	3.46E-08
Plec	S4481		-0.53	-0.95	-1.17	-0.87	-1.62	0.46	-0.39	0.99	8.58E-161
Plec	S4477		NaN	-0.69	-1.19	NaN	-1.76	0.11	0.04	0.99	3.45E-160
Plec	S4472		-0.37	-0.85	-1.20	-0.77	-1.60	0.35	-0.25	1	5.15E-137
Plec	T4482		-0.63	-0.66	-1.51	-0.72	-1.74	NaN	-0.49	0.94	5.15E-137
Plec	T4261		-0.32	2.42	2.07	NaN	NaN	NaN	NaN	0.88	2.12E-110
Plec	Y4471		-0.42	-0.55	-1.49	-1.22	-1.69	NaN	-0.44	0.92	5.87E-107
Plec	S4479		-0.42	-0.66	-1.64	NaN	NaN	0.43	NaN	0.95	2.93E-21
Plekhg3	S1134		-0.14	2.18	1.45	2.21	NaN	0.57	0.06	1	1.25E-27
Plekhg3	S1136		-0.18	2.19	1.45	2.32	1.87	NaN	0.01	1	3.42E-10
Plekhm1	S433		-0.61	-1.73	-1.89	-2.72	-3.62	-0.12	-0.26	1	6.63E-23
Plekhm1	S436		-0.34	1.41	0.82	1.39	1.11	0.27	0.03	1	6.63E-23

Gene names	Position	Known ERK1/2 target	Ratio WT vs WT	Ratio WT vs PD0325901	Ratio WT vs PD0325901	Ratio WT vs D270A	Ratio WT vs D270A	Ratio WT+ PD0325901 vs D270A+ PD0325901	Ratio WT+ PD0325901 vs D270A+ PD0325901	Localization probabil-ity	PEP
Ppfibp1	S37		-0.17	-1.06	-1.51	-1.78	-1.87	0.31	-0.16	1	4.04E-89
Ppfibp1	S40		-0.09	3.05	2.00	NaN	NaN	NaN	NaN	1	1.16E-17
Ppp1r12a	S507		-0.24	1.57	0.72	1.77	1.91	0.36	-0.03	1	9.54E-115
Ppp1r12a	T508		-0.20	1.58	0.86	1.69	2.21	0.18	-0.22	0.94	2.01E-78
Ppp6r1	S739		-0.34	1.39	0.57	1.70	1.19	0.71	-0.08	0.99	5.10E-75
Prkag2	S157		NaN	-1.29	-2.10	NaN	NaN	0.37	-0.51	0.99	3.41E-35
Prkag2	S161		NaN	-2.42	-2.21	NaN	NaN	-0.47	-0.52	0.93	3.41E-35
Prrc2a	S454		-0.30	2.98	1.50	3.49	2.57	0.91	-0.17	1	6.37E-51
Prrc2c	S102		-0.30	1.74	0.71	1.98	1.58	0.76	NaN	1	4.39E-17
Psd4	S244		-0.26	1.93	1.24	1.59	1.21	0.27	-0.16	1	8.03E-56
Pstpip1	S318		-0.53	-0.88	-0.96	-1.03	-1.68	0.48	0.16	1	2.95E-08
Pum2	S587		-0.04	1.58	0.50	1.78	1.58	0.48	-0.31	1	0
Pyhin1	S176		0.01	1.86	0.74	1.63	2.11	0.28	0.38	1	7.70E-73

Gene names	Position	Known ERK1/2 target	Ratio WT vs WT	Ratio WT vs PD0325901	Ratio WT vs PD0325901	Ratio WT vs D270A	Ratio WT vs D270A	Ratio WT+ PD0325901 vs D270A+ PD0325901	Ratio WT+ PD0325901 vs D270A+ PD0325901	Localization probabil-ity	PEP
Rab11fip5	S1348		-0.04	2.04	1.28	2.70	2.43	0.11	-0.09	1	2.87E-75
Rab11fip5	S1247		NaN	3.27	2.00	3.15	3.14	0.69	0.17	0.96	4.31E-48
Rab11fip5	S515		NaN	-0.77	-1.23	NaN	-1.53	-0.09	-0.55	0.99	2.30E-37
Rab3gap1	S536		-0.36	2.81	1.37	2.73	2.85	1.07	0.48	0.99	1.66E-132
Rab3gap1	T541		NaN	2.32	1.86	NaN	NaN	NaN	-0.46	0.62	1.90E-06
Rai14	S281		NaN	-1.69	-2.30	NaN	-2.82	0.89	-0.44	1	3.10E-21
Rai14	S293		-0.31	2.03	1.36	1.76	1.20	0.79	-0.12	1	1.64E-10
Rai14	T297		-0.29	1.95	1.36	1.76	1.08	0.78	-0.25	1	1.64E-10
Raph1	T195		-0.39	-1.32	-2.03	NaN	NaN	0.16	-0.10	1	1.50E-17
Rbm17	S169		-0.21	1.61	0.94	2.13	1.73	0.26	-0.35	1	6.43E-12
Rbm27	S1020		-0.22	2.14	1.99	3.57	2.71	0.62	0.42	1	3.07E-78
Rbm6	S743		NaN	2.16	1.68	NaN	NaN	-0.01	-0.07	1	7.65E-08
Rcsd1	S135		-0.50	2.58	1.57	2.53	1.65	NaN	NaN	0.97	8.68E-18

Gene names	Position	Known ERK1/2 target	Ratio WT vs WT	Ratio WT vs PD0325901	Ratio WT vs PD0325901	Ratio WT vs D270A	Ratio WT vs D270A	Ratio WT+ PD0325901 vs D270A+ PD0325901	Ratio WT+ PD0325901 vs D270A+ PD0325901	Localization probabil-ity	PEP
Ripk1	S415		-0.14	1.50	0.56	1.47	1.21	0.72	-0.17	1	1.24E-30
Rpp30	S251		-0.57	2.87	1.16	3.11	1.47	0.88	-0.71	1	3.90E-45
Rps6ka1	S386	+	-0.07	1.68	0.88	1.96	1.62	0.69	-0.03	1	7.98E-155
Rps6ka1	T390		NaN	1.72	0.88	1.74	NaN	0.63	-0.13	0.54	1.75E-15
Rps6ka3	S354	+	-0.26	1.36	0.54	1.70	1.10	0.73	0.12	1	1.07E-84
Rps6ka3	T545		-0.19	3.61	3.00	3.27	2.41	NaN	NaN	1	3.15E-73
Rps6ka3	T333		-0.66	-2.09	-2.43	-2.13	-2.79	NaN	NaN	1	7.35E-93
Samd4b	T599		0.03	1.57	0.78	1.32	1.47	0.17	-0.39	1	3.09E-58
Scrib	S1209		-0.48	1.92	1.23	NaN	NaN	NaN	NaN	1	9.72E-22
Scrib	S1212		-0.48	1.95	1.23	NaN	NaN	NaN	NaN	1	9.72E-22
Sipa1	T143		-0.48	-0.76	-1.67	-1.09	-1.99	0.33	-0.48	1	1.12E-47
Skap2	S5		-0.10	3.49	2.13	3.62	2.76	1.05	0.54	1	3.49E-131
Skap2	S9		-0.58	-1.40	-2.03	-1.30	-1.79	0.43	-0.02	1	3.49E-131

Gene names	Position	Known ERK1/2 target	Ratio WT vs WT	Ratio WT vs PD0325901	Ratio WT vs PD0325901	Ratio WT vs D270A	Ratio WT vs D270A	Ratio WT+ PD0325901 vs D270A+ PD0325901	Ratio WT+ PD0325901 vs D270A+ PD0325901	Localization probabil-ity	PEP
Skil	S487		0.34	3.41	3.23	3.11	1.25	NaN	-0.21	1	4.95E-24
Smarcad1	S79		-0.20	1.96	1.20	2.05	1.97	0.22	-0.33	1	1.68E-41
Snx7	S8		-0.52	2.43	1.55	2.33	1.37	0.26	-0.49	1	1.99E-143
Socs6	S69		0.23	2.30	2.09	1.60	2.34	0.54	NaN	0.99	3.96E-09
Sos1	S1120		-0.26	1.76	1.25	2.24	1.65	0.36	-0.05	1	8.78E-32
Sp110	S177		-0.07	1.59	0.55	1.80	1.61	0.63	-0.03	1	2.03E-220
Spag9	S691		-0.10	1.92	1.54	2.29	1.86	0.58	0.20	1	8.65E-35
Specc1l	S385		-0.44	1.60	1.28	2.20	1.35	0.46	0.05	1	3.20E-240
Srpk2	S490		-0.15	2.48	1.65	2.63	2.43	NaN	NaN	0.94	2.01E-54
Srrt	S136		-0.25	1.59	0.75	2.21	1.55	0.28	-0.24	1	1.08E-36
Srsf11	S235		-0.14	1.36	0.69	1.65	1.34	0.19	-0.21	1	7.76E-81
Stk17b	S10		0.10	2.60	1.92	4.84	4.07	0.51	NaN	1	4.04E-85
Stmn1	S16		-0.28	-0.59	-1.38	-0.90	-1.10	0.03	-0.58	1	2.28E-132

Gene names	Position	Known ERK1/2 target	Ratio WT vs WT	Ratio WT vs PD0325901	Ratio WT vs PD0325901	Ratio WT vs D270A	Ratio WT vs D270A	Ratio WT+ PD0325901 vs D270A+ PD0325901	Ratio WT+ PD0325901 vs D270A+ PD0325901	Localization probabil-ity	PEP
Stmn1	S25	+	-0.18	2.20	1.20	1.65	1.87	0.68	-0.06	1	3.38E-132
Svil	S248		-0.36	2.23	1.05	2.32	NaN	NaN	NaN	0.99	2.97E-30
Synj1	S1478		-0.21	3.35	2.10	2.70	2.12	0.57	-0.15	1	5.52E-10
Tacc1	S378		-0.51	1.92	2.03	1.40	2.20	0.70	0.09	1	2.26E-53
Tacc1	S284		-0.02	2.82	2.24	2.74	2.27	0.40	0.13	1	6.20E-11
Tbc1d14	S112		-0.39	1.80	0.61	1.41	0.94	0.75	-0.18	1	1.92E-40
Tbc1d14	S460		-0.32	2.40	1.16	NaN	NaN	NaN	NaN	0.87	6.26E-232
Tbc1d14	S462		-0.26	2.20	1.25	NaN	1.89	NaN	NaN	0.84	6.26E-232
Tbc1d2	S10		NaN	3.66	1.87	NaN	NaN	0.68	-0.31	0.99	5.58E-18
Tbrg1	T13		-0.17	1.46	0.88	1.53	1.49	-0.21	-0.40	1	9.51E-208
Tln1	S1248		-0.20	1.66	0.69	2.08	1.52	0.28	-0.17	1	4.83E-124
Tmpo	S411		0.15	1.64	1.52	2.13	2.27	NaN	NaN	1	7.86E-36
Tom1	T164		-0.47	3.73	0.69	2.21	1.15	NaN	NaN	1	7.41E-41

Gene names	Position	Known ERK1/2 target	Ratio WT vs WT	Ratio WT vs PD0325901	Ratio WT vs PD0325901	Ratio WT vs D270A	Ratio WT vs D270A	Ratio WT+ PD0325901 vs D270A+ PD0325901	Ratio WT+ PD0325901 vs D270A+ PD0325901	Localization probabil-ity	PEP
Top2b	T1280		0.05	2.57	1.31	3.35	NaN	NaN	NaN	0.99	6.12E-08
Tor1aip1	S94		-0.41	3.55	2.56	3.18	2.29	0.45	NaN	1	3.83E-06
Tpd52	S170		-0.23	3.33	2.12	3.35	2.48	0.66	-0.05	1	1.33E-66
Tpr	S2224	+	-0.26	1.33	0.47	1.50	1.18	0.30	-0.40	1	6.09E-65
Tpr	T2215		-0.29	1.41	0.45	1.47	1.08	0.39	-0.36	1	2.84E-94
Triobp	S1603		-0.56	-0.41	-1.04	-0.47	-1.47	0.61	-0.05	0.83	2.43E-71
Triobp	S1604		-0.21	-0.46	-1.13	-0.46	-1.50	0.64	-0.25	0.99	2.43E-71
Tsc22d4	T223		-0.57	-0.68	-1.09	-0.91	-2.02	0.39	-0.23	1	2.63E-99
Tsc22d4	S254		-0.55	-1.50	-2.07	-1.13	-1.89	0.30	-0.33	0.99	8.63E-12
Tsc22d4	S258		-0.53	-1.46	-2.07	-1.13	-1.87	0.12	-0.58	1	8.63E-12
Twistnb	S318		-0.47	1.42	0.70	1.72	1.14	0.39	-0.27	1	2.61E-27
Ube4b	S36		-0.02	-1.15	-1.25	-1.19	-1.52	0.32	-0.20	1	2.23E-117
Ubxn6	S36		-0.72	-0.89	-1.17	-0.99	-1.93	0.26	-0.05	1	4.37E-13

Gene names	Position	Known ERK1/2 target	Ratio WT vs WT	Ratio WT vs PD0325901	Ratio WT vs PD0325901	Ratio WT vs D270A	Ratio WT vs D270A	Ratio WT+ PD0325901 vs D270A+ PD0325901	Ratio WT+ PD0325901 vs D270A+ PD0325901	Localization probabil-ity	PEP
Ulk1	S620		-0.05	2.63	1.90	2.10	2.25	0.30	-0.21	1	7.53E-11
Wdfy3	S970		-0.42	2.95	2.06	3.01	1.87	0.75	0.08	1	1.94E-27
Wdr3	S333		-0.30	1.88	1.01	2.09	1.28	0.16	-0.15	1	1.20E-37
Wdr81	S1570		-0.49	1.94	1.17	1.83	1.02	0.78	-0.30	1	2.74E-82
Ybx1	S100		-0.26	2.75	3.00	4.38	3.11	0.85	0.30	1	0
Ybx1	T106		-0.31	4.36	2.99	NaN	3.33	NaN	NaN	0.86	8.43E-12
Ythdc2	S1216		-0.02	2.99	1.83	3.88	3.18	1.07	0.52	0.63	5.28E-107
Ythdc2	T1217		-0.02	2.99	1.83	3.89	3.18	1.07	0.27	0.81	5.28E-107
Zc3hc1	S393		-0.28	1.33	0.82	1.66	1.08	0.24	-0.57	0.98	5.11E-57
Zc3hc1	S394		-0.30	1.51	0.76	1.41	1.01	0.25	-0.57	1	4.22E-30
Zcchc6	S132		-0.10	2.03	0.65	1.97	1.88	0.99	-0.18	1	1.77E-11
Zcchc8	S411		-0.08	1.67	1.08	2.37	2.07	-0.01	-0.29	1	0
Zfml	S381		-0.19	1.97	2.85	4.03	1.56	NaN	NaN	1	4.28E-08

Gene names	Position	Known ERK1/2 target	Ratio WT vs WT	Ratio WT vs PD0325901	Ratio WT vs PD0325901	Ratio WT vs D270A	Ratio WT vs D270A	Ratio WT+ PD0325901 vs D270A+ PD0325901	Ratio WT+ PD0325901 vs D270A+ PD0325901	Localization probabil-ity	PEP
Zfp161	T253		-0.19	2.82	2.11	2.59	NaN	NaN	NaN	1	1.19E-102
Zfp36	T249		NaN	2.88	1.63	NaN	NaN	0.55	-0.21	0.74	1.77E-06
Zfp36	T250		NaN	2.88	1.63	NaN	NaN	0.55	-0.21	0.63	1.77E-06
Zfp36	S248		NaN	2.88	1.63	NaN	NaN	0.55	-0.21	0.80	1.77E-06
Zmiz2	S395		-0.30	1.86	1.83	2.20	2.06	0.43	-0.35	1	1.85E-30
Zyx	S144		-0.10	2.03	1.39	2.09	1.73	0.49	-0.45	1	9.63E-58